

Coordination Chemistry with the P<sub>2</sub> Ligand Complex  
[Cp<sub>2</sub>Mo<sub>2</sub>(CO)<sub>4</sub>(μ,η<sup>2:2</sup>-P<sub>2</sub>)], Ag(I) and Cu(I) Salts with Weakly  
Coordinating Anions and Pyridine-Based Organic Linkers

**DISSERTATION**

Zur Erlangung eines

DOKTORGRADES DER NATURWISSENSCHAFTEN

(Dr. rer. Nat.)

an der Naturwissenschaftlichen Fakultät IV – Chemie und Pharmazie

der Universität Regensburg



vorgelegt von

**Andrea Schreiner**

aus Deggendorf

im Jahr 2020



Diese Arbeit wurde angeleitet von Prof. Dr. Manfred Scheer.

Promotionsgesuch eingereicht am: 29. Juni 2020

Tag der mündlichen Prüfung: 31. Juli 2020

Vorsitzender: Prof. Dr. Rainer Müller

Prüfungsausschuss: Prof. Dr. Manfred Scheer

Prof. Dr. Henri Brunner

Prof. Dr. Oliver Tepner



Universität Regensburg

## Eidesstattliche Erklärung

Ich erkläre hiermit an Eides statt, dass ich die vorliegende Arbeit ohne unzulässige Hilfe Dritter und ohne Benutzung anderer als der angegebenen Hilfsmittel angefertigt habe; die aus anderen Quellen direkt oder indirekt übernommenen Daten und Konzepte sind unter Angabe des Literaturzitats gekennzeichnet.

---

Andrea Schreiner

This thesis was elaborated within the period from **January 2016** until **June 2020** in the Institute of Inorganic Chemistry at the University of Regensburg under the supervision of Prof. Dr. Manfred Scheer. Parts of this work have already been published.

**List of publications:**

Mehdi Elsayed Moussa, Martin Piesch, Martin Fleischmann, Andrea Schreiner, Michael Seidl and Manfred Scheer

*'Highly soluble Cu(I)-acetonitrile salts as building blocks for novel phosphorus-rich organometallic-inorganic compounds'*

*Dalton Trans.* **2018**, 47, 16031-16035.

Jana Schiller,<sup>‡</sup> Andrea Schreiner,<sup>‡</sup> Gábor Balázs, Michael Seidl and Manfred Scheer

*'Linking of Cu(I) units by tetrahedral Mo<sub>2</sub>E<sub>2</sub> complexes (E = P, As)'*

‡ These authors contributed equally to this work.

*Chem. Eur. J.* 10.1002/chem.202003133 (accepted manuscript)



*To my family*





Without imagination,  
nothing really new will ever be created.

– Jostein Gaarder, *'Sophie's World'*

## **Preface**

At the beginning of each chapter, a list of authors is given and the individual contribution of each author is described. Also, on the first page of each chapter, if some of the results have already been discussed in other theses, it is stated.

Each chapter includes an own short introduction. However, a general introduction and the research objectives are given in the beginning of this thesis. In the end of this manuscript, a comprehensive conclusion of this work is presented. To ensure uniform design of this thesis, all chapters are subdivided into 'Abstract', 'Introduction', 'Results and Discussion', 'Conclusion', 'Supporting Information' and 'References'. Furthermore, all chapters have the same text settings and the numeration of compounds, schemes and figures begins anew.

## Table of Contents

<b>1</b>	<b>Introduction .....</b>	<b>1</b>
1.1	<i>The Origin of Life, Self-Organisation and Supramolecular Chemistry .....</i>	1
1.2	<i>Supramolecular Chemistry – Coordination Polymers (CPs), Metal-Organic Frameworks (MOFs) and Weakly Coordinating Anions (WCAs).....</i>	2
1.2.1	<i>Coordination Polymers (CPs) – A Classification .....</i>	2
1.2.2	<i>Metal-Organic Frameworks (MOFs) and their Applications .....</i>	3
1.2.3	<i>Weakly Coordinating Anions and their Significance for Coordination Chemistry .....</i>	3
1.3	<i>P<sub>n</sub> Ligand Complexes, their Coordination Behaviour and Use in Supramolecular Coordination Chemistry.....</i>	6
1.3.1	<i>Phosphorus – An Excursus .....</i>	6
1.3.2	<i>P<sub>n</sub> Ligand Complexes and their Coordination Behaviour .....</i>	8
1.3.3	<i>The P<sub>2</sub> Ligand Complex [Cp<sub>2</sub>Mo<sub>2</sub>(CO)<sub>4</sub>(μ,η<sup>2:2</sup>-P<sub>2</sub>)] as Building Block in Supramolecular Coordination Chemistry .....</i>	10
1.4	<i>References .....</i>	14
<b>2</b>	<b>Research Objectives .....</b>	<b>19</b>
<b>3</b>	<b>Influence of organic linker and weakly coordinating anion in the synthesis of one- and two-dimensional organometallic-organic coordination polymers with the P<sub>2</sub> ligand complex [Cp<sub>2</sub>Mo<sub>2</sub>(CO)<sub>4</sub>(μ,η<sup>2:2</sup>-P<sub>2</sub>)] and Cu(I) salts.....</b>	<b>21</b>
3.1	<i>Abstract .....</i>	21
3.2	<i>Introduction.....</i>	22
3.4	<i>Conclusion .....</i>	32
3.5	<i>Supporting Information.....</i>	33
3.6	<i>References.....</i>	43
<b>4</b>	<b>The weakly coordinating anion [Al{OC(CF<sub>3</sub>)<sub>3</sub>}<sub>4</sub>]<sup>-</sup> in the selective, crystallisation method dependent synthesis of 1D and 2D coordination polymers with the P<sub>2</sub> ligand complex [Cp<sub>2</sub>Mo<sub>2</sub>(CO)<sub>4</sub>(μ,η<sup>2:2</sup>-P<sub>2</sub>)] and organic linkers .....</b>	<b>45</b>
4.1	<i>Abstract .....</i>	45
4.2	<i>Introduction.....</i>	46
4.3	<i>Results and Discussion.....</i>	47
4.4	<i>Conclusion .....</i>	55
4.5	<i>Supporting Information.....</i>	56
4.6	<i>References.....</i>	66

<b>5</b>	<b>The weakly coordinating anion [FAl{O(C<sub>6</sub>F<sub>10</sub>)(C<sub>6</sub>F<sub>5</sub>)<sub>3</sub>}]<sup>-</sup> in the synthesis of novel phosphorus rich precursors for organometallic-organic coordination polymers .....</b>	<b>69</b>
5.1	<i>Abstract .....</i>	70
5.2	<i>Introduction.....</i>	70
5.3	<i>Results and Discussion.....</i>	72
5.4	<i>Conclusion .....</i>	77
5.5	<i>Supporting Information.....</i>	78
5.6	<i>References.....</i>	87
<b>6</b>	<b>Linking of Cu(I) units by tetrahedral Mo<sub>2</sub>E<sub>2</sub> complexes (E = P, As).....</b>	<b>89</b>
6.1	<i>Abstract .....</i>	90
6.2	<i>Introduction.....</i>	90
6.3	<i>Results and Discussion.....</i>	91
6.4	<i>Conclusion .....</i>	96
6.5	<i>Supporting Information.....</i>	97
6.6	<i>References.....</i>	121
<b>7</b>	<b>Conclusion.....</b>	<b>123</b>
<b>8</b>	<b>Thesis Treasury.....</b>	<b>131</b>
8.1	<i>Discussion.....</i>	131
8.2	<i>Crystallographic Data.....</i>	145
8.3	<i>References.....</i>	150
<b>9</b>	<b>Appendix.....</b>	<b>151</b>
9.1	<i>Thematic List of Abbreviations.....</i>	151
9.2	<i>Acknowledgements.....</i>	152

# 1 Introduction

## 1.1 The Origin of Life, Self-Organisation and Supramolecular Chemistry

*'In the beginning the Universe was created. This has made a lot of people very angry and been widely regarded as a bad move.'*

The first sentence of Douglas Adams' novel *'The Restaurant at the End of the Universe'* makes the beginning of life sound trivial, but the processes occurring during the early universe are still not fully uncovered and probably never will. Considering the Big Bang has already occurred, solar systems have formed (cf. **Figure 1.1-1**),

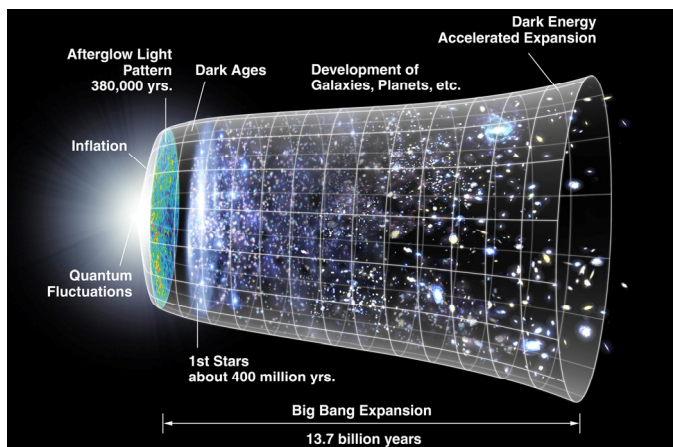


**Figure 1.1-1.** Infographic of the Big Bang and the Expansion of the Universe. Image credit: Courtesy NASA/JPL-Caltech, <https://www.jpl.nasa.gov/infographics/infographic.view.php?id=10824>, 17/06/20.

and there is a planet capable of supporting life, the question of how exactly life started remains unanswered and the origin of life (OOL) problem is one of the more challenging and intriguing scientific questions of all time.<sup>[1]</sup> Although there are different approaches to explain the emergence of life ('replication first' or 'metabolism first'),<sup>[2]</sup> there are some things that are agreed upon, like that the interaction of small molecules was a central factor<sup>[3]</sup> and some kind of autocatalytic chemical system must have been involved. Also, some driving force was necessary to stabilise huge assemblies like DNA strands.<sup>[1]</sup> A plausible explanation for this and – in the broadest sense – the physiochemical basis for abiogenesis, which is the chemical process by which simple life emerged from inanimate beginnings, is *dynamic kinetic stability (DKS)*.<sup>[1]</sup> This concept states that 'all stable (persistent) replicating systems will tend to evolve over time towards systems of greater stability' and is 'generally found to be enhanced by increasing complexation, [...] thereby offering an explanation for the emergence of life's extraordinary complexity'.<sup>[1]</sup> Essential is however how the transformation of inanimate into animate matter was performed. The link between inorganic ('dead') and organic ('living') matter was established by Friedrich Wöhler, who in 1828 synthesised urea from ammonium cyanate.<sup>[4]</sup> Concerning the concept of self-organisation, or self-assembly, of huge biomolecules like DNA, RNA, sugars, and proteins from their building blocks, the work of Jean-Marie Lehn must be mentioned.<sup>[5]</sup> Lehn was awarded the Nobel Prize in Chemistry in 1987 for the '*development and use of molecules with structure-specific interactions of high selectivity*',<sup>[6]</sup> defined supramolecular chemistry as '*chemistry beyond the molecule*',<sup>[7]</sup> and laid the foundation for a whole new field of chemistry. Artificial supramolecules have shown the ability to mimic enzyme activity,<sup>[8]</sup> show host-guest interactions,<sup>[9]</sup> virus-like particles are studied,<sup>[10]</sup> and the field is constantly developed further.

## 1.2 Supramolecular Chemistry – Coordination Polymers (CPs), Metal-Organic Frameworks (MOFs) and Weakly Coordinating Anions (WCAs)

### 1.2.1 Coordination Polymers (CPs) – A Classification

The first purely synthetic coordination polymer was Prussian Blue,  $\text{Fe}_4[\text{Fe}(\text{CN})_6]_3 \cdot x\text{H}_2\text{O}$  ( $x = 14-16$ ), also known as ‘Berlin blue’, ‘Parisian blue’ or ‘Turnbull’s blue’. Although the pigment has been known since the early 18<sup>th</sup> century<sup>[11]</sup> and used by painters including the famous Vincent van Gogh and Katsushika Hokusai (Figure 1.2-1),<sup>[12]</sup> its crystal structure has not been fully uncovered until 1977.<sup>[13]</sup> The term ‘coordination polymer’, however, is very general, as it only describes structures that are



**Figure 1.2-1.** Vincent Van-Gogh’s famous painting ‘The Starry Night’, oil on canvas, 1889, and ‘The Great Wave of Kanagawa’ by Katsushika Hokusai, colour woodblock, 1829-1833. Image credits: <https://commons.wikimedia.org/w/index.php?curid=25498286> and <https://commons.wikimedia.org/w/index.php?curid=2798407>, 22/06/2020.

extended into one, two or three dimensions by bridging ligands (Figure 1.2-2) and even the term ‘polymer’ itself is flawed.<sup>[14]</sup> Further, a distinction between 1D CPs and 2D/3D CPs is made and 2D and 3D CPs are generally considered Metal-Organic Frameworks (MOFs). Because of the rapid development in both research areas (CP and MOF) in the last 20 years, the terminology is not entirely clear and despite of the IUPAC guidelines,<sup>[15]</sup> it is argued that there are no strict rules for naming CPs.<sup>[15]</sup> Still, coordination polymers as described in literature possess a huge variety of intriguing properties, such as (photo)luminescence,<sup>[16, 17]</sup> (electro-/photo)-catalytic activity,<sup>[18, 19, 20]</sup> and magnetic properties.<sup>[21]</sup> CPs are also investigated in terms of anticancer drug,<sup>[22]</sup> can act as absorbent of a carcinogenic dye,<sup>[23]</sup> and selective trap and sense perrhenate/pertechnetate.<sup>[24]</sup>

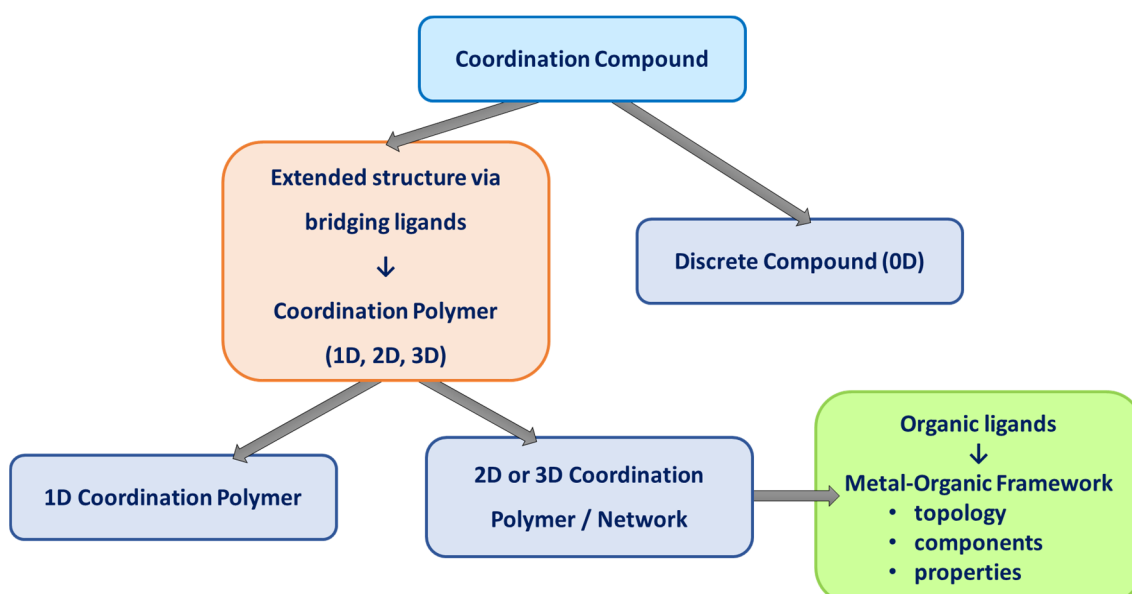


**Figure 1.2-2.** Tentative hierarchy of coordination compounds, CPs and MOFs. The scheme was inspired by ‘Coordination polymers, metal-organic frameworks and the need for terminology guidelines’.<sup>[15]</sup>

## 1.2.2 Metal-Organic Frameworks (MOFs) and their Applications

Metal-organic frameworks (MOFs, **Figure 1.2-3**) are 2D/3D CPs and are defined by their topology, their components, and properties. In general, MOFs are designed with the goal of acting as storage units for small molecules or substrates and therefore are usually porous with a large internal surface area. Like CPs, they stand out with wide ranging possibilities in their design,<sup>[25]</sup> so it can be chosen from a large variety of starting materials and reaction conditions to design the desired metal-organic framework.

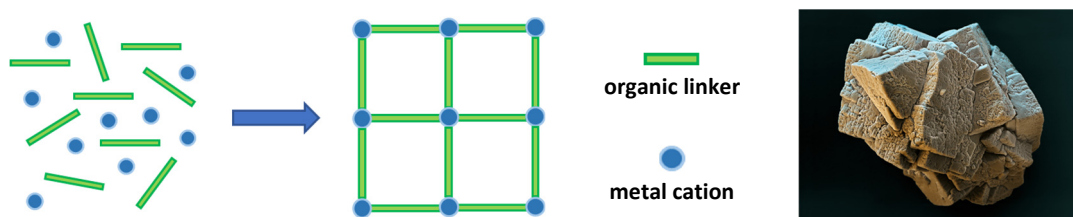


**Figure 1.2-3.** Schematic self-assembly of metal and organic linker forming a 2D network (left) and MOF under scanning electron microscope (SEM, right), 660:1 (when 15 cm wide). The picture was reprinted with the kind permission of Oliver Meckes from eye of science, Nicole Ottawa & Oliver Meckes GbR, [www.eyeofscience.de](http://www.eyeofscience.de) (MOF).

The possible applications of MOFs seem endless.<sup>[26]</sup> They have already shown to be able to fixate CO<sub>2</sub> and capture and release singlet oxygen.<sup>[27]</sup> MOFs are also promising to act as drug carriers and are investigated for anticancer treatment.<sup>[28]</sup> As hydrogen is considered a possible future energy source, MOFs are tested for storing and releasing hydrogen.<sup>[29]</sup> Also chemical purification<sup>[30]</sup> is an important research area, as the removal of gaseous pollutants is desirable for nature and humans alike.<sup>[31]</sup> The field of chemical sensors, which are already used for a number of important applications, *e.g.* in medicine, could also profit from the development of MOFs. The mentioned versatile possibilities MOFs offer and their intriguing physical properties like photoluminescence<sup>[32]</sup> and fluorescence<sup>[33]</sup> could lead to many more exciting developments in that area.<sup>[34]</sup> Further, the concept of charge separation introduced by Stang *et al.*<sup>[35]</sup> into the design of MOFs turned out to be a suitable tool for the selective coordination-driven self-assembly, opening the door for many further applications.<sup>[36]</sup>

However, the coordination polymers addressed in this thesis cannot be classified as MOFs and are better described as metal-organometallic-organic coordination polymers (**Figure 1.2-4**).

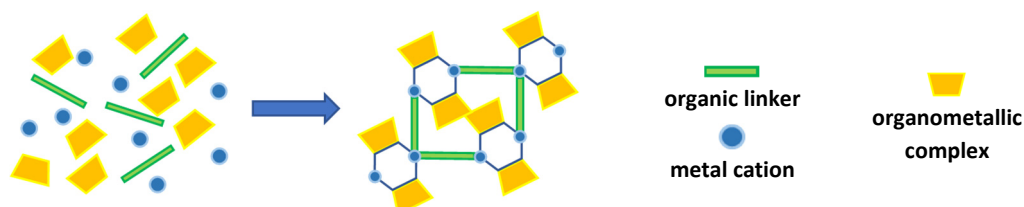


**Figure 1.2-4.** Schematic of self-assembly of metal, organic linker and organometallic complex forming a metal-organometallic-organic coordination polymer.

In addition to metal cations and organic linkers, those CPs consist of organometallic complexes containing phosphorus as donor atoms. Whereas for MOFs, classical coordination complexes as

moieties are forming the nodes to which the linkers are coordinating, in the metal-organometallic-organic coordination polymers the nodes are motives formed by the organometallic complex and the metal ions. Instead of 'one-pot'-reactions, the organometallic complex and the metal ion can in some cases be used to synthesise a precursor, *i.e.* a discrete, 0D coordination compound, which is *in situ* reacted with the organic linker. However, the concept of coordination-driven self-assembly is the same.

### 1.2.3 Weakly Coordinating Anions and their Significance for Coordination Chemistry

Weakly coordinating anions (WCAs) have been known for decades, as has the myth of the existence of a 'non-coordinating anion'.<sup>[37]</sup> From the present point of view this is impossible,<sup>[38,39]</sup> and a complete cation-anion charge separation is physically forbidden by the Coulomb Equation (1), which describes the force between two charged particles in relation to the distance between them. However, the charge separation provided by modern WCAs comes very close to non-coordination.<sup>[40]</sup> As the Coulomb force depends on the ionic charges and the distance between the charges, a good WCA exhibits a relatively low negative charge, ideally -1, which is delocalised over as many atoms as possible. Also, fluorination of the anion is an effective way to keep the electron shell from being polarised easily, which could in turn lead to coordination of the anion.<sup>[41]</sup>

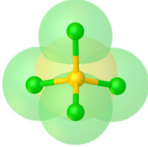
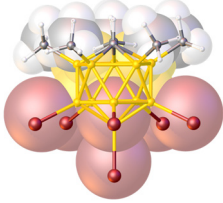
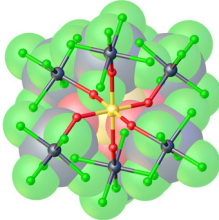
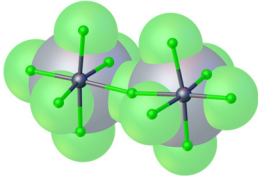
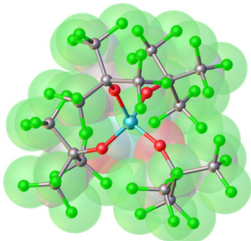
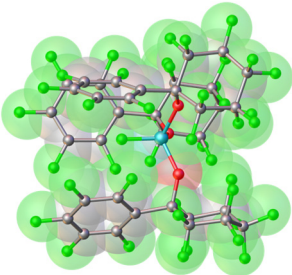
$$F = \frac{1}{4\pi\epsilon_0} \cdot \frac{q_1 \cdot q_2}{r^2} = \frac{1}{4\pi\epsilon_0} \cdot \frac{z_1 \cdot z_2 \cdot e^2}{r^2} \quad (1)$$

$q_1, q_2$  = point charges;  $z_1, z_2$  = ionic charges;  $e$  = elementary charge;  $r$  = distance between charges;  $\epsilon_0$  = dielectric constant.

WCAs can be divided into five different classes (**Table 1.2-1**).<sup>[42]</sup> They can be borate-based like  $[\text{B}(\text{CF}_3)_3]^-$  or  $[(\text{C}_6\text{F}_5)_3\text{B}(\mu\text{-CN})\text{B}(\text{C}_6\text{F}_5)_3]^-$  or carborane-based like  $[1\text{-H-CB}_{11}\text{Me}_5\text{Br}_6]^-$ .<sup>[43]</sup> Also, teflates, *e.g.*  $[\text{As}(\text{OTeF}_5)_6]^-$ ,<sup>[44]</sup> and anions derived from Lewis-acids, *e.g.*  $[\text{Sb}_4\text{F}_{21}]^-$  exist. Two important examples for alkoxy- and aryl-metallates are  $[\text{Al}\{\text{OC}(\text{CF}_3)_3\}_4]^-$ <sup>[45,46]</sup> and  $[\text{Al}\{\text{O}(\text{C}_6\text{F}_{10})(\text{C}_6\text{F}_5)\}_3]^-$ ,<sup>[46,47]</sup> which were also used in this thesis.



**Table 1.2-1.** Different classes of WCAs and selected examples.<sup>[42]</sup>

Borate-based	Carborane-based	Teflates	Anions from Lewis-acids
$[\text{B}(\text{CF}_3)_3]^-$ $[\text{B}(\text{R})_4]^-$ (R = F, CH <sub>3</sub> , C <sub>6</sub> F <sub>5</sub> , C <sub>6</sub> H <sub>3</sub> (CF <sub>3</sub> ) <sub>2</sub> ) <sub>4</sub> ) $[(\text{C}_6\text{F}_5)_3\text{B}(\mu\text{-CN})\text{B}(\text{C}_6\text{F}_5)_3]^-$	$[\text{CB}_{11}\text{H}_6\text{Cl}_6]^-$ $[1\text{-H-CB}_{11}\text{Me}_5\text{Br}_6]^-$ $[1\text{-Et-CB}_{11}\text{F}_{12}]^-$	$[\text{B}(\text{OTeF}_5)_4]^-$ $[\text{M}(\text{OTeF}_5)_6]^-$ (M = As, Sb, Bi, Nb)	$[\text{Sb}_2\text{F}_{11}]^-$ <i>trans</i> - $[\text{Sb}_3\text{F}_{16}]^-$ <i>cis</i> - $[\text{Sb}_3\text{F}_{16}]^-$ $[\text{Sb}_4\text{F}_{21}]^-$
			
Alkoxy- and aryl-metallates			
$[\text{Nb}(\text{OC}_6\text{F}_5)_6]^-$ $[\text{Al}\{\text{OC}(\text{CF}_3)_3\}_4]^-$ $[\text{Al}\{\text{O}(\text{C}_6\text{F}_{10})(\text{C}_6\text{F}_5)\}_3]^-$			

The structure determination and synthesis of some cationic species has been enabled by using WCAs. The  $\text{Xe}_2^+$  cation, which has been reported by Stein *et al.* in 1980,<sup>[48]</sup> could not be characterised by X-ray analysis until almost 20 years later, when Seppelt *et al.* treated yellow  $[\text{XeF}][\text{Sb}_2\text{F}_{11}]$  with the ‘magic’ acid  $\text{HF}/\text{SbF}_5$  and obtained dark-green crystals by cooling to  $-30\text{ }^\circ\text{C}$ .<sup>[49]</sup> The  $\text{Xe}_2^{2+}$  cation has a Xe-Xe bond length of 308.7(1) pm, rendering the bond rather weak, and remains the longest atom-atom bond of the main group elements up to this date. Krossing *et al.*, whose work with WCAs is exemplary,<sup>[50]</sup> reported the first homoleptic metal phosphorus cation,  $[\text{Ag}(\text{P}_4)_2]^+$  (**Figure 1.2-5**, left),<sup>[51]</sup> and recently the first homoleptic metal( $\text{P}_4\text{Se}_3$ ) and metal( $\text{As}_4\text{S}_3$ ) complexes (**Figure 1.2-5**, right) by reacting  $\text{P}_4$ ,  $\text{P}_4\text{Se}_3$  or  $\text{As}_4\text{S}_3$ , respectively, with  $\text{Ag}\{\text{Al}\{\text{OC}(\text{CF}_3)_3\}_4\}$ .<sup>[52]</sup>

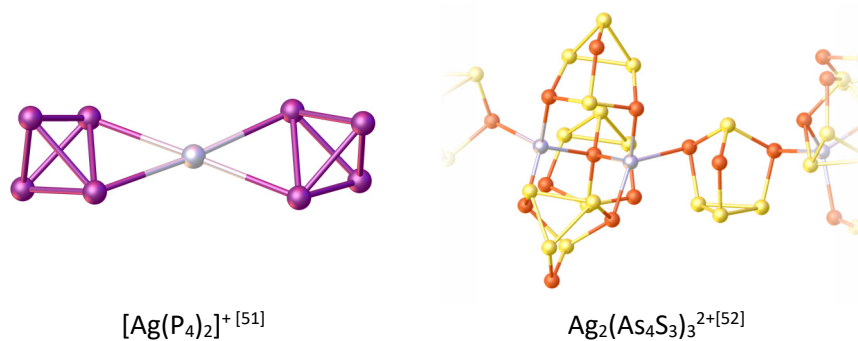


**Figure 1.2-5.** The first homoleptic metal phosphorus cation  $[\text{Ag}(\text{P}_4)_2]^+^{[51]}$  and section of the first homoleptic metal( $\text{As}_4\text{S}_3$ ) complex  $\text{Ag}_2(\text{As}_4\text{S}_3)_3^{2+}$ ,<sup>[52]</sup> both by Krossing *et al.* Anions and solvent molecules are omitted for clarity.

## 1.3 P<sub>n</sub> Ligand Complexes, their Coordination Behaviour and Use in Supramolecular Coordination Chemistry

### 1.3.1 Phosphorus – An Excursus

Elemental phosphorus has evidently been *in situ* produced by the supernova of the star Cassiopeia A (Cas A, **Figure 1.3-1**), as a group of astrophysicists reported in 2013.<sup>[53]</sup> On earth, phosphorus is only found in derivatives of phosphates due to its high affinity to oxygen, which is why white phosphorus (P<sub>4</sub>) is synthesised technically from fluorine-rich apatite Ca<sub>5</sub>(PO<sub>4</sub>)<sub>3</sub>(OH, F, Cl). P<sub>4</sub> is the most reactive modification of phosphorus and highly toxic. Possibilities to activate,<sup>[54]</sup> as well as to store and release P<sub>4</sub> in a safe and facile way are therefore exceptionally preferable.<sup>[55]</sup> Besides a huge variety of peaceful applications like fertilisers, phosphorus and its compounds have also been used for the extremely unpleasant purposes of chemical warfare, *e.g.* incendiary bombs containing white phosphorus or different neurotoxic agents. Neurotoxic agents, also called ‘nerve agents’ or ‘nerve gases’, are inhibitors of the enzyme acetylcholinesterase (AChE), which is found in neurons and glial cells of the human brain and acts mainly in the central and peripheral nervous system.<sup>[56]</sup> Here, it catalytically hydrolyses the neurotransmitter acetylcholine (ACh), whose purpose is the process of the transmission of the nerve impulse in the brain. ACh is assumingly also involved in cell proliferation and further biological processes,<sup>[57]</sup> and is also linked to Alzheimer disease, in which the cognitive and neuromuscular functions are deteriorating.<sup>[58]</sup> Three of the four most important nerve agents are Tabun, Sarin and Soman (**Figure 1.3-2**). Tabun was accidentally discovered in the process of finding a new insecticide which was a project of the German conglomerate Farbenindustrie. Tabun was found out to be highly toxic and thus unsuitable for this purpose, as was Sarin, which was discovered in 1937. Although Tabun, Sarin and the nerve agent Soman, which was specifically synthesised for the purpose of warfare, were never used against the Allies in World War II, Sarin was confirmed to have been used during the Iran-Iraq war in the 1980s and appeared in the news again in 2013, when the Ghouta chemical attack in Syria occurred.<sup>[59]</sup>



**Figure 1.3-1.** False-colour image of the scattered remains of the exploded star Cassiopeia A taken with an Instrument Infrared Array Camera (IRAC).

Image credit: Courtesy NASA/JPL-Caltech, <https://www.jpl.nasa.gov/spaceimages/details.php?id=PIA01903>, 09/06/2020.

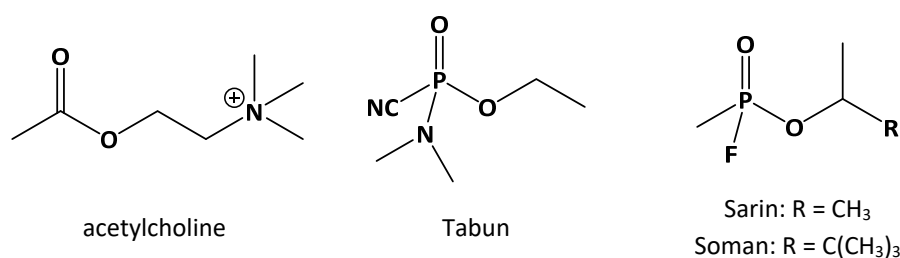


**Figure 1.3-2.** Acetylcholine and Acetylcholinesterase inhibitors Tabun, Sarin and Soman.<sup>[59]</sup>

A less reactive modification of phosphorus is the amorphous red phosphorus (**Figure 1.3-3**), which is obtained by heating  $P_4$  to 200-400 °C. Though not pyrophoric, it is still used in smoke materials or as igniter in the military<sup>[60]</sup> and paradoxically also as flame inhibitor.<sup>[61]</sup> Red phosphorus is probably most associated with matches (**Figure 1.3-3**). Originally containing small amounts of white phosphorus, the friction alone was sufficient to ignite a match. Nowadays, due to the invention of 'safety matches', red phosphorus is no longer located at the head of the match but on the outside of the package. Black phosphorus, which is denser than  $P_4$ , can be synthesised by heating  $P_4$  to 200 °C under high pressure (12.000 bar) and consists of parallel double layers (**Figure 1.3-4**). In the rhombohedral high-pressure (80.000 bar) modification, the layers are not aligned parallel but lie transversal underneath each other leading to a structure analogous to grey arsenic. A further known modification is fibrous phosphorus, which was discovered in 2005 and is structurally similar to violet phosphorus, or 'Hittorf's phosphorus', which was discovered by the German physicist and chemist Johann Wilhelm Hittorf already in 1865.<sup>[62]</sup> Both modifications consist of pentagonal tubes of  $P_8$  and  $P_9$  cages with bridging  $P_2$  groups in-between, and only differ in the arrangement of the tubes.



**Figure 1.4.1-3.** Matches. Photo credit: Tanja Wenzel, Graphic & Motion Design, www.gramotic.de.

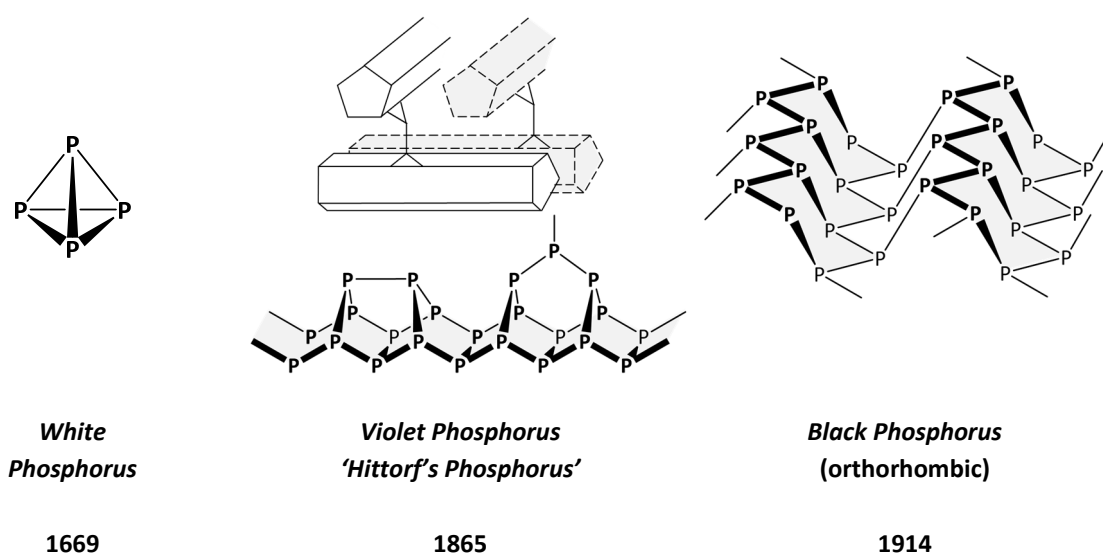


**Figure 1.3-4.** Modifications of phosphorus from left to right with date of discovery: White phosphorus  $P_4$ , violet phosphorus or 'Hittorf's Phosphorus' and orthorhombic black phosphorus.<sup>[63]</sup>

### 1.3.2 P<sub>n</sub> Ligand Complexes and their Coordination Behaviour

P<sub>n</sub> ligand complexes are basically complexes bearing 'naked', *i.e.* substituent-free, phosphorus atoms that are only bonded to other phosphorus atoms and transition metals.<sup>[64]</sup> The pioneer work in this field was performed in the early 1970s (**Figure 1.3-5**). The rhodium complex by Ginsberg *et al.*<sup>[65]</sup> as well as the cobalt complex by Dahl *et al.*<sup>[66]</sup> were both synthesised by treatment of the complexes L<sub>3</sub>RhCl (L = PPh<sub>3</sub>, AsPh<sub>3</sub>, P(*m*-CH<sub>3</sub>C<sub>6</sub>H<sub>4</sub>)<sub>3</sub>, P(*p*-CH<sub>3</sub>C<sub>6</sub>H<sub>4</sub>)<sub>3</sub>) and [CoCp(CO)<sub>2</sub>], respectively, with white phosphorus (P<sub>4</sub>). The reaction of Na[Co(CO)<sub>4</sub>] with PX<sub>3</sub> (X = Cl or Br) yielded the P<sub>2</sub> complex [Co<sub>2</sub>(CO)<sub>6</sub>P<sub>2</sub>] of Markó *et al.*,<sup>[67]</sup> which was regarded as the first metal-carbonyl-stabilised derivative of the P<sub>2</sub> molecule. Also the works of L. Sacconi *et al.*, who synthesised the first *cyclo*-triphosphoryl complex in 1979,<sup>[68]</sup> and G. Huttner *et al.*, who presented the dinuclear Fe-complex [{CpMn(CO)<sub>2</sub>}(μ<sub>3</sub>-P<sub>2</sub>){Fe<sub>2</sub>(CO)<sub>6</sub>}] in 1983,<sup>[69]</sup> are important milestones in the history of P<sub>n</sub> ligand complexes.

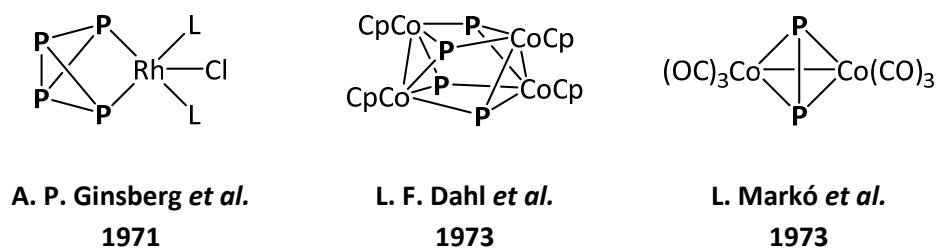


**Figure 1.3-5.** First examples of P<sub>n</sub> ligand complexes. L = PPh<sub>3</sub>, AsPh<sub>3</sub>, P(*m*-CH<sub>3</sub>C<sub>6</sub>H<sub>4</sub>)<sub>3</sub>, P(*p*-CH<sub>3</sub>C<sub>6</sub>H<sub>4</sub>)<sub>3</sub>.

The field of P<sub>n</sub> ligand complexes continued to grow and in 1985, Scherer *et al.* discovered the first P<sub>n</sub> ligand complex with n > 4, the triple-decker sandwich complex [{Cp\*Mo}<sub>2</sub>(μ,η<sup>6:6</sup>-P<sub>6</sub>)].<sup>[70]</sup> After *cyclo*-P<sub>5</sub> could be stabilised in the triple-decker complex [(Cp\*Cr)<sub>2</sub>P<sub>5</sub>] one year later,<sup>[71]</sup> it was also possible to synthesise pentamethyl-pentaphosphaferrocene [Cp\*FeP<sub>5</sub>] (Cp\* = C<sub>5</sub>(CH<sub>3</sub>)<sub>5</sub>) by thermolysis of the Fe complex [(Cp\*Fe(CO)<sub>2</sub>)<sub>2</sub>] with P<sub>4</sub> in 1987.<sup>[72]</sup> Nowadays, a huge range of P<sub>n</sub> ligand complexes with n = 2-6 (**Table 1.3-1**) with different transition metals and ligands are known and have been focus of various studies. These include investigations regarding their redox chemistry,<sup>[73]</sup> their behaviour towards nucleophiles,<sup>[74]</sup> and their coordination behaviour.<sup>[75]</sup>

**Table 1.3-1.** Examples for P<sub>n</sub> (n = 2-6) ligand complexes.

P <sub>2</sub>	P <sub>3</sub>	P <sub>4</sub>	P <sub>5</sub>	P <sub>6</sub>
<i>e.g.</i> Cp <sub>2</sub> Mo <sub>2</sub> (CO) <sub>4</sub> P <sub>2</sub>	<i>e.g.</i> (CO) <sub>3</sub> CoP <sub>3</sub>	<i>e.g.</i> Cp'''CoP <sub>4</sub>	<i>e.g.</i> Cp*FeP <sub>5</sub>	<i>e.g.</i> (Cp*Mo) <sub>2</sub> P <sub>6</sub>

The P<sub>5</sub> ligand complex [Cp\*Fe(μ,η<sup>5</sup>-P<sub>5</sub>)], which has been used in the synthesis of various organometallic-organic coordination polymers,<sup>[76]</sup> has received particular attention as building block in the design of spherical supramolecules.<sup>[77]</sup> Here, different compounds containing templates, *e.g.* [Cp\*FeP<sub>5</sub>], Cp<sub>2</sub>Fe or [(CpCr)<sub>2</sub>As<sub>6</sub>], nano-sized capsules,<sup>[78]</sup> and nano-bowls<sup>[79]</sup> have been realised so far (**Figure 1.3-6**). Also the design and chemistry of homologues with bigger Cp-derivatives are a present research field.<sup>[80]</sup>

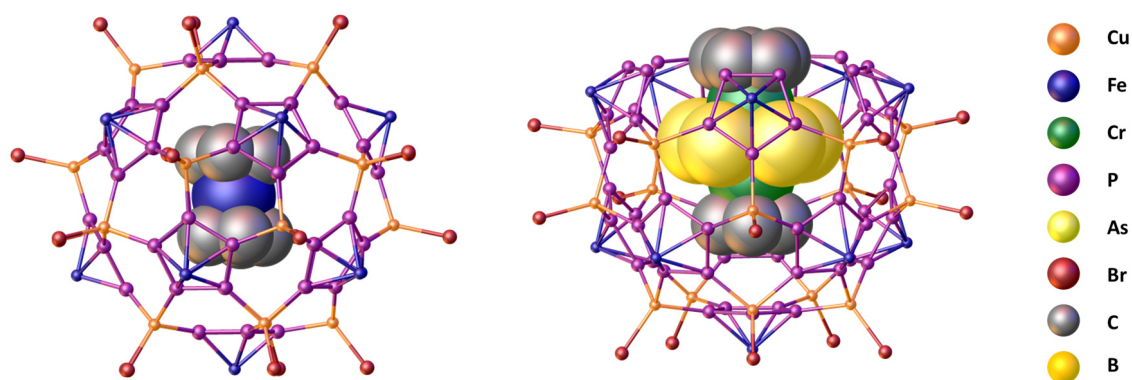


**Figure 1.3-6.** Selected examples for supramolecular aggregates containing the P<sub>5</sub> ligand complex [Cp\*FeP<sub>5</sub>]. Thermal ellipsoids are shown at 50 % probability level. Hydrogen atoms, Cp- and CO-ligands, anions and solvent molecules are omitted for clarity. The templates are depicted in space-filling model including Cp-ligands. Left: Nano-sized capsule with Cp<sub>2</sub>Fe as template, [Cp<sub>2</sub>Fe]@[{Cp\*Fe(η<sup>5</sup>-P<sub>5</sub>)<sub>12</sub>(CuBr)<sub>17.3</sub>].<sup>[78a]</sup> Right: Nano-bowl containing complex [(CpCr)<sub>2</sub>(μ,η<sup>6:6</sup>-As<sub>6</sub>)] as template, [{CpCr)<sub>2</sub>(μ,η<sup>5</sup>-As<sub>5</sub>)]@[{Cp\*Fe(η<sup>5</sup>-P<sub>5</sub>)<sub>12</sub>(CuCl)<sub>20</sub>].<sup>[79]</sup>

Besides the coordination chemistry of complex [Cp<sub>2</sub>Mo<sub>2</sub>(CO)<sub>4</sub>(μ,η<sup>2:2</sup>-P<sub>2</sub>)], which will be discussed in the next chapter, the P<sub>2</sub> ligand complex as well as the analogous E<sub>2</sub> (E = As, Sb, Bi) ligand complexes of the higher homologues of the pnictogen group have been studied regarding their oxidation chemistry (**Figure 1.3-7**). The reactions yielded either E<sub>4</sub> chains (E = P, As) or E<sub>4</sub> butterfly units (E = Sb, Bi).<sup>[81]</sup>

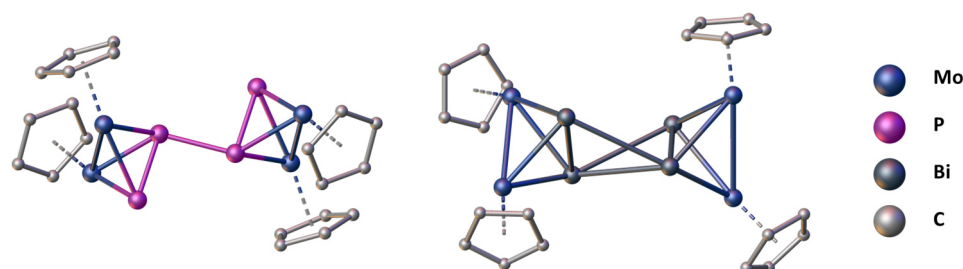


**Figure 1.3-7.** Solid-state structures of cationic E<sub>4</sub> complexes [{CpMo(CO)<sub>2</sub>]<sub>4</sub>(μ<sub>4</sub>,η<sup>2:2:2:2</sup>-E<sub>4</sub>)] [TEF]<sub>2</sub> (E = P, Bi) obtained by oxidation of the respective [Cp<sub>2</sub>Mo<sub>2</sub>(CO)<sub>4</sub>(μ,η<sup>2:2</sup>-E<sub>2</sub>)] complexes. Thermal ellipsoids are shown at 50 % probability level. Hydrogen atoms, CO-ligands, anions, and solvent molecules are omitted for clarity.<sup>[81]</sup>

### 1.3.3 The P<sub>2</sub> Ligand Complex [Cp<sub>2</sub>Mo<sub>2</sub>(CO)<sub>4</sub>(μ,η<sup>2:2</sup>-P<sub>2</sub>)] as Building Block in Supramolecular Coordination Chemistry

The P<sub>2</sub> ligand complex [Cp<sub>2</sub>Mo<sub>2</sub>(CO)<sub>4</sub>(μ,η<sup>2:2</sup>-P<sub>2</sub>)] was first synthesised in 1984 by Scherer *et. al.* in 20 % yield by thermolysis of the molybdenum complex [Cp<sub>2</sub>Mo<sub>2</sub>(CO)<sub>4</sub>] in presence of white phosphorus (P<sub>4</sub>).<sup>[82]</sup> Like other P<sub>n</sub> ligand complexes, [Cp<sub>2</sub>Mo<sub>2</sub>(CO)<sub>4</sub>(μ,η<sup>2:2</sup>-P<sub>2</sub>)] has been used in supramolecular chemistry and is the most common used of the P<sub>2</sub> ligand complexes in this field so far. Up to now, the Mo<sub>2</sub>P<sub>2</sub> complex has exhibited three different kinds of coordination modes (I-III) and two further ones (IV, V) might be possible (Figure 1.3-8).

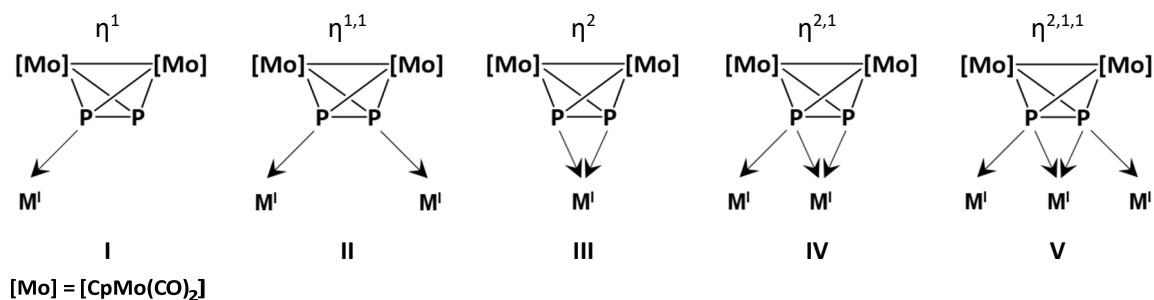
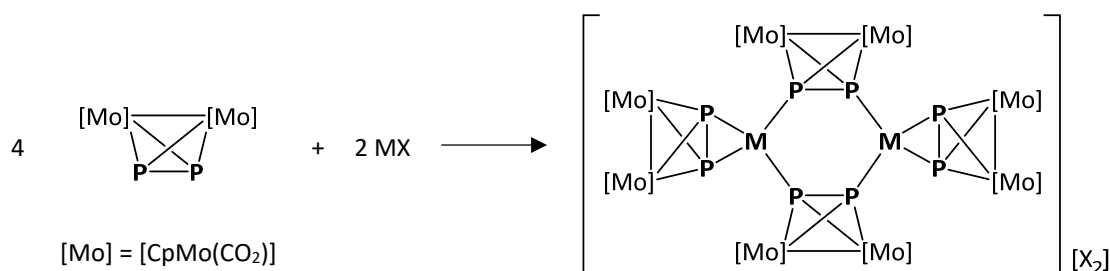


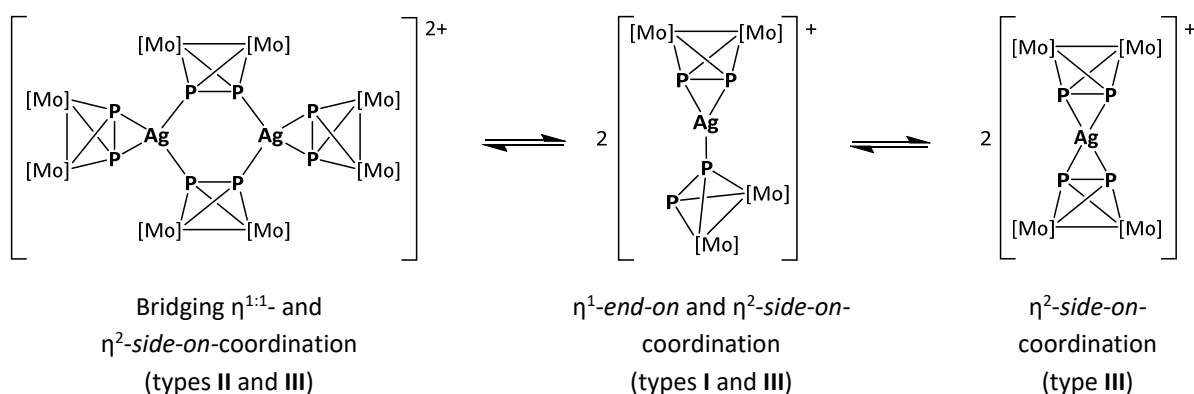
Figure 1.3-8. Exhibited (I, II and III) and possible (IV and V) coordination types of Mo<sub>2</sub>P<sub>2</sub>.<sup>[83]</sup>

Types II and III are present in the dicationic coordination complexes [M<sub>2</sub>{Cp<sub>2</sub>Mo<sub>2</sub>(CO)<sub>4</sub>(μ,η<sup>2:2:1:1</sup>-P<sub>2</sub>)}<sub>2</sub>{Cp<sub>2</sub>Mo<sub>2</sub>(CO)<sub>4</sub>(μ,η<sup>2:2:2</sup>-P<sub>2</sub>)}] (M = Cu, Ag, Au) obtained by the reaction of the Mo<sub>2</sub>P<sub>2</sub> complex with coinage metal WCA salts in a 2:1-ratio (Scheme 1.3-1).<sup>[84]</sup> The η<sup>1:1</sup>-coordination mode of two units of Mo<sub>2</sub>P<sub>2</sub> results in the formation of a six-membered M<sub>2</sub>P<sub>4</sub>-ring (M = Cu, Ag, Au).



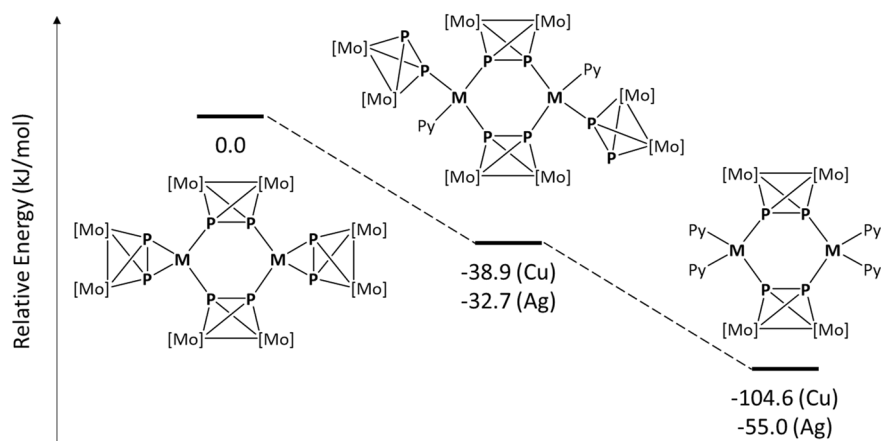
Scheme 1.3-1. Reaction of the P<sub>2</sub> ligand complex [Cp<sub>2</sub>Mo<sub>2</sub>(CO)<sub>4</sub>(μ,η<sup>2:2</sup>-P<sub>2</sub>)] with different metal salts MX. (MX = CuPF<sub>6</sub>, AgBF<sub>4</sub>, AgClO<sub>4</sub>, AgPF<sub>6</sub>, AgSbF<sub>6</sub>, AgAl{OC(CF<sub>3</sub>)<sub>3</sub>}<sub>4</sub>, AuPF<sub>6</sub>, [Cu(CH<sub>3</sub>CN)<sub>4</sub>][BF<sub>4</sub>], [Cu(o-DFB)][Al{OC(CF<sub>3</sub>)<sub>3</sub>}<sub>4</sub>], [Cu(CH<sub>3</sub>CN<sub>4</sub>)<sub>3.5</sub>][FAl{O(C<sub>6</sub>F<sub>10</sub>)(C<sub>6</sub>F<sub>5</sub>)<sub>3</sub>}] and AgFAl{O(C<sub>6</sub>F<sub>10</sub>)(C<sub>6</sub>F<sub>5</sub>)<sub>3</sub>}).<sup>[84,85,86,87]</sup>

Furthermore, DFT (Density Functional Theory) calculations regarding the dissociation of the metal dimer in solution have been performed for the complex obtained from the reaction of Mo<sub>2</sub>P<sub>2</sub> and the Ag(I) salt Ag[Al{OC(CF<sub>3</sub>)<sub>3</sub>}<sub>4</sub>].<sup>[84]</sup> It could be shown that the energy barrier for the transformation of the coordination mode of the Mo<sub>2</sub>P<sub>2</sub> unit from η<sup>2</sup>-side-on to η<sup>1</sup>-end-on is as small as 9 kJ/mol (Scheme 1.3-2). The unsaturated metal centre of the monomeric complex exhibiting Mo<sub>2</sub>P<sub>2</sub> in coordination mode I makes it accessible for the coordination of organic linkers.



**Scheme 1.3-2.** Suggested equilibrium in solution between the  $[\text{Ag}_2(\text{Mo}_2\text{P}_2)_4]^{2+}$  dimer and the  $[\text{Ag}(\text{Mo}_2\text{P}_2)_2]^+$  monomers.<sup>[84]</sup>

DFT calculations were performed for the cationic dimers containing  $\text{Ag}^{[88]}$  or  $\text{Cu}^{[89]}$  as metal centre, respectively. It was revealed that the substitution of the peripheral units of  $\text{Mo}_2\text{P}_2$  against pyridine is energetically favoured (**Scheme 1.3-3**). After the first substitution, both the peripheral units of  $\text{Mo}_2\text{P}_2$  and the pyridine ligands are  $\eta^1$ -coordinated to the metal centres. After coordination of a second pair of pyridine ligands, the peripheral  $\text{Mo}_2\text{P}_2$  units are removed from the complex and only the bridging  $\eta^{1:1}$ -coordinated  $\text{Mo}_2\text{P}_2$  units and the four pyridine ligands remain attached to the metal centres.



**Scheme 1.3-3.** Structures of metal dimers by step-wise substitution of the  $\eta^2$ -side-on-coordinated  $\text{Mo}_2\text{P}_2$  units against pyridine as obtained by DFT calculations.<sup>[88,89]</sup>

The reaction of  $\text{Mo}_2\text{P}_2$  with the Ag(I) WCA salt  $\text{Ag}[\text{FAl}\{\text{OC}(\text{CF}_3)_3\}_4]$  and the pyridine-based linker trans-1,2-di(pyridine-4-yl)-ethene yielded, depending on the stoichiometry, a zero-dimensional coordination compound and one- to three-dimensional coordination polymers exhibiting different coordination modes of  $\text{Mo}_2\text{P}_2$ .<sup>[90,91]</sup> In the 1D CP (**Figure 1.3-9a**),  $\text{Mo}_2\text{P}_2$  is  $\eta^{1:1}$ -coordinated (type II) to form the six-membered  $\text{Mo}_2\text{P}_4$ -ring and  $\eta^1$ -end-on-coordinated (type I). The structure is also an example for the incomplete substitution of the peripheral  $\text{Mo}_2\text{P}_2$ -units (**Scheme 1.3-3**, middle). Coordination type II is also visualised in a 2D CP (**Figure 1.3-9b**). However, no six-membered  $\text{Ag}_2\text{P}_4$ -ring exists and the

tetrahedral coordination sphere of the Ag(I) centres is saturated by three linker molecules. Type III, which is present in the dimeric complexes (**Figure 1.3-1**), also occurs in a further 2D CP obtained from the same components as the previously described 2D CP. To each Ag(I) centre, one unit of Mo<sub>2</sub>P<sub>2</sub> in an η<sup>2</sup>-side-on-coordination mode and three molecules of linker are attached. The network consists of interlaced layers (**Figure 1.3-9c**, left) of two 2D networks (**Figure 1.3-9c**, middle).

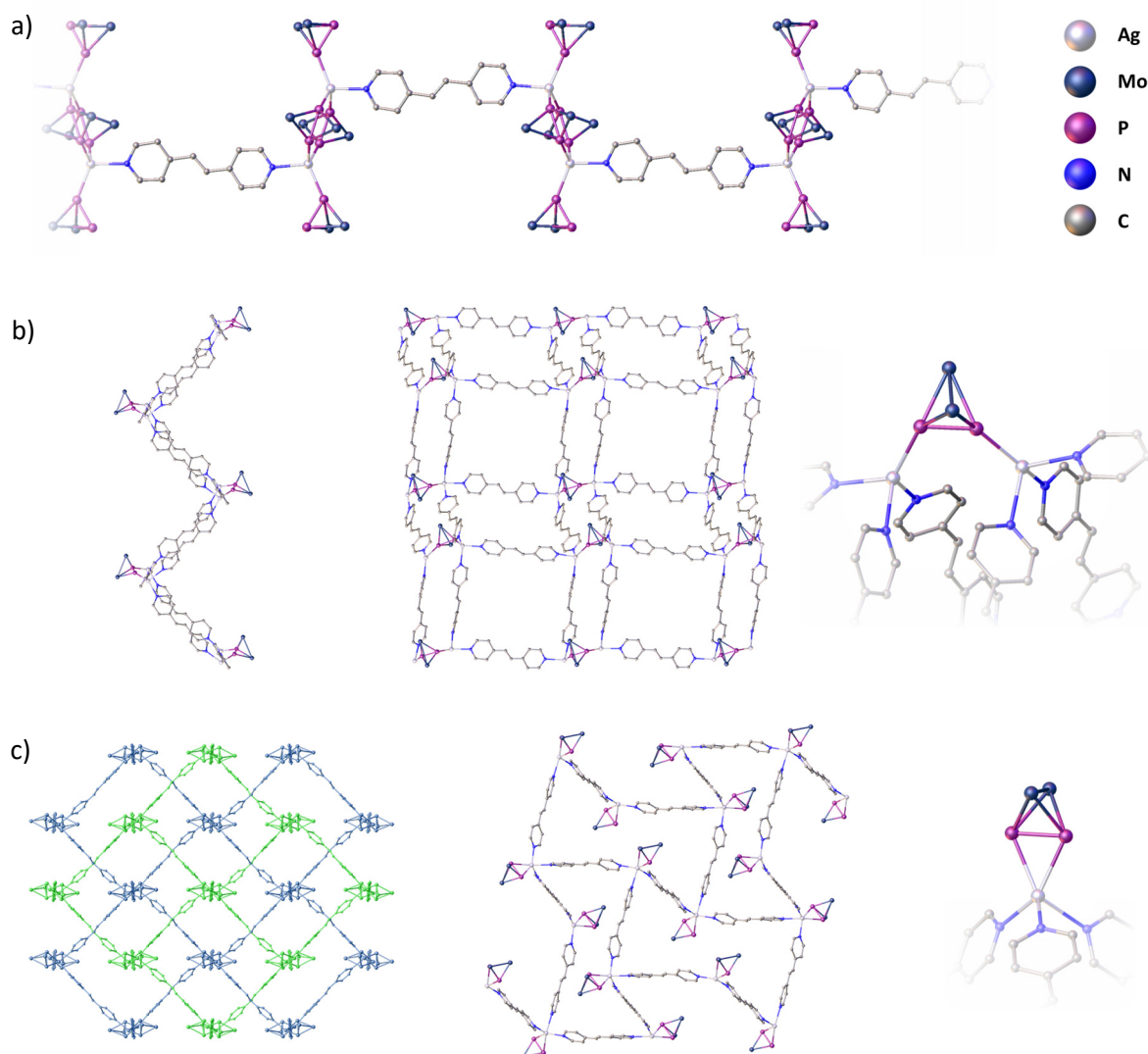


**Figure 1.3-9.** Examples for compounds exhibiting coordination types I, II and III of the Mo<sub>2</sub>P<sub>2</sub> complex. Thermal ellipsoids are shown at 50 % probability level. Hydrogen atoms, Cp- and CO-ligands, anions and solvent molecules are omitted for clarity. a) 1D CP obtained by reaction of Mo<sub>2</sub>P<sub>2</sub> with the Ag(I) salt AgAl{OC(CF<sub>3</sub>)<sub>3</sub>}<sub>4</sub> and the organic linker trans-1,2-di(pyridine-4-yl)-ethene.<sup>[90]</sup> b) 2D CP containing Mo<sub>2</sub>P<sub>2</sub> in η<sup>1,1</sup>-coordination mode (type II), view along the a and b -axis and detail view on the Cu<sub>2</sub>-node.<sup>[91]</sup> c) Interwoven 2D CP containing Mo<sub>2</sub>P<sub>2</sub> in η<sup>2</sup>-side-on-coordination (type III).<sup>[91]</sup>

By reacting the Mo<sub>2</sub>P<sub>2</sub> complex with AgNO<sub>3</sub> and Cu(I) halides, respectively, neutral 1D CPs could be obtained with the anion functioning as bridging unit between two metal centres (**Figure 1.3-10**). Besides Mo<sub>2</sub>P<sub>2</sub>, other tetrahedral M<sub>2</sub>P<sub>2</sub> complexes with M = Cr<sup>[92]</sup> and M = W<sup>[93]</sup> have been subject of investigations regarding their reactivity towards CuX (X = Cl, Br, I; **Figure 1.3-10**). Like in the case of



$\text{Mo}_2\text{P}_2$ ,<sup>[84,94]</sup> the reactions yield neutral 1D CPs exhibiting six-membered  $\text{Cu}_2\text{P}_4$ -rings connected by bridging halides.

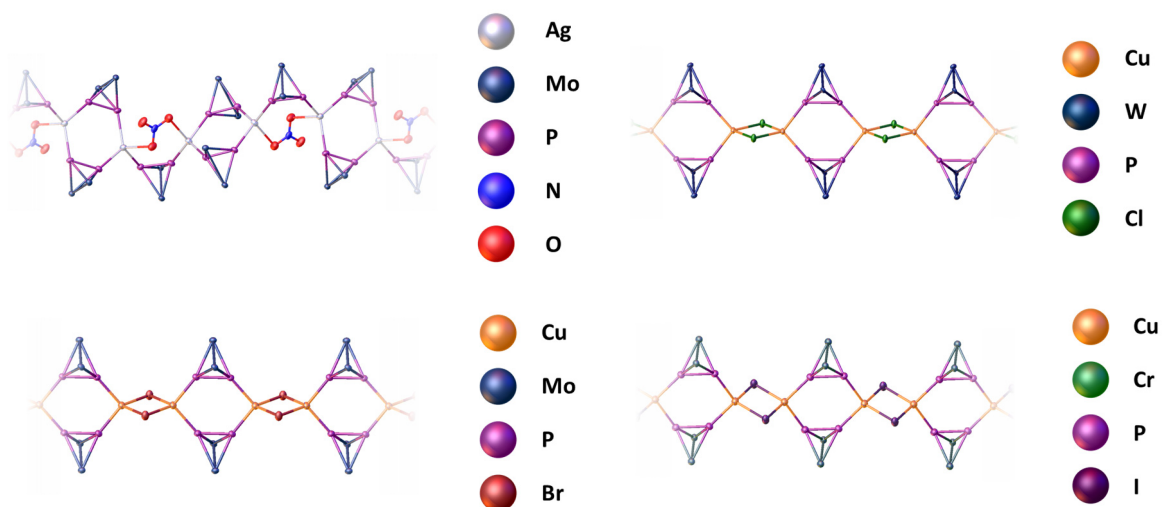


**Figure 1.3-10.** Solid-state structures of neutral 1D CPs obtained from the reaction of  $\text{M}_2\text{P}_2$  with  $\text{AgNO}_3$  and  $\text{CuX}$ , respectively, with  $\text{M} = \text{Mo}, \text{W}, \text{Cr}$  and  $\text{X} = \text{Cl}, \text{Br}, \text{I}$ . Thermal ellipsoids are shown at 50 % probability level. Hydrogen atoms, Cp- and CO-ligands and solvent molecules are omitted for clarity.<sup>[83,84,95,96,97]</sup>

Also other complexes containing higher homologues of the pnictogen group in mixed tetrahedral  $\text{Mo}_2\text{PE}$  ( $\text{E} = \text{As}, \text{Sb}$ ) complexes<sup>[95]</sup> have been studied. The  $\text{Mo}_2\text{PE}$  ( $\text{E} = \text{As}, \text{Sb}$ ) complexes have exhibited a so far for  $\text{Mo}_2\text{P}_2$  unknown coordination mode. The reaction of  $[\text{Cp}_2\text{Mo}_2(\text{CO})_4(\mu, \eta^{2:2}\text{-PSb})]$  with  $\text{Cu(I)}$  bromide yielded the neutral coordination complex  $[\{\text{Cp}_2\text{Mo}_2(\text{CO})_4\}\{\mu_4, \eta^{2:2:2:1}\text{-PSb}\}]_4[\{\text{CuBr}\}\{\text{Cu}(\mu\text{-Br})\}]_2$  (**Figure 1.3-11**).<sup>[95]</sup> The  $\text{Mo}_2\text{PSb}$ -unit is present in a  $\eta^{2:1}$ -coordination mode (type **IV**). Considering the P atom coordinating to two  $\text{Cu(I)}$  centres it might as well be possible for the  $\text{Mo}_2\text{P}_2$  complex to coordinate in this type.

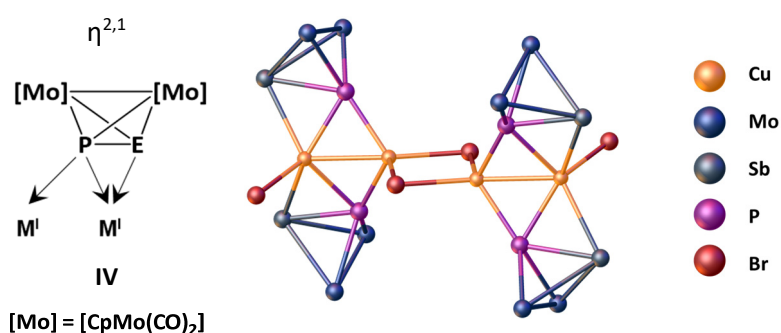


**Figure 1.3-11.** For  $\text{Mo}_2\text{PE}$  ( $\text{E} = \text{As}, \text{Sb}$ ) additionally known coordination mode **IV** (left) and the solid-state structure of the coordination complex  $[\{\text{Cp}_2\text{Mo}_2(\text{CO})_4\}\{\mu_4, \eta^{2:2:2:1}\text{-PSb}\}]_4[\{\text{CuBr}\}\{\text{Cu}(\mu\text{-Br})\}]_2$  obtained from the reaction of the complex  $[\text{Cp}_2\text{Mo}_2(\text{CO})_4(\mu, \eta^{2:2}\text{-PSb})]$  with  $\text{CuBr}$  (right). Thermal ellipsoids are shown at 50 % probability level. Hydrogen atoms, Cp- and CO-ligands, anions and solvent molecules are omitted for clarity.<sup>[95]</sup>

## 1.4 References

- [1] A. Pross, R. Pascal, *Open Biol* **2013**, *3*, 120190.
- [2] P. G. Higgs, N. Lehman *Nat Rev Genet* **2015**, *16*, 7-17.
- [3] R. Shapiro, *The Quarterly Review of Biology* **2006**, *81*, 105-126.
- [4] F. Wöhler, *Ann. Phys. Chem.* **1828**, *2*, 253-256.
- [5] a) J.-M. Lehn, *Science* **1985**, *227*, 849-856; b) J.-M. Lehn, *PNAS* **2002**, *99*, 4763-4768; c) J.-M. Lehn, *Isr. J. Chem.* **2018**, *58*, 136-141.
- [6] The Nobel Prize in Chemistry 1987. NobelPrize.org. Nobel Media AB 2020. Tue. 3 Mar 2020. <<https://www.nobelprize.org/prizes/chemistry/1987/summary/>>
- [7] J.-M. Lehn, *Angew. Chem. Int. Ed. Engl.* **1988**, *27*, 89-112.
- [8] Y. Zhao, B. Lei, M. Wang, S. Wu, W. Qi, R. Su, Z. He *J. Mater. Chem. B*, **2018**, *6*, 2444.
- [9] X. Yan, T. R. Cook, J. B. Pollock, P. Wei, Y. Zhang Y. Yu, F. Huang, P. J. Stang, *J. Am. Chem. Soc.* **2014**, *136*, 4460-4463.
- [10] a) P. Pushko, I. Tretyakova *Viruses* **2020**, *12*, 518; b) A. J. Olson, Y. H. E. Hu, E. Keinan, *Proc. Natl. Acad. Sci. U.S.A.* **2007**, *104*, 20731-20736.
- [11] A. Kraft, *Bull. Hist. Chem.* **2008**, *33*, 61-67.
- [12] P. McCouat, 'Prussian Blue and its Partner in Crime' *Journal of Art in Society*, [www.artinsociety.com](http://www.artinsociety.com), accessed 22/06/2020.
- [13] H. J. Buser, D. Schwarzenbach, W. Petter, A. Ludi, *Inorg. Chem.* **1977**, *16*, 2704-2710.
- [14] R. Batten, N. R. Champness, X.-M. Chen, J. Garcia-Martinez, S. Kitagawa, L. Öhrström, M. O'Keeffe, M. Paik Suh, J. Reedijk *CrystEngComm*, **2012**, *14*, 3001 and *Pure Appl. Chem.* **2013**, *85*, 1715-1724.
- [15] N. G. Connelly, T. Damhus, R. M. Hartshorn, A. T. Hutton, 'Nomenclature of Inorganic Chemistry: IUPAC Recommendations' **2005**, RSC Publishing.
- [16] a) X.-Y. Dong, C.-D. Si, Y. Fan, D.-C. Hu, X.-Q. Yao, Y.-X. Yang, J.-C. Liu *Cryst. Growth Des.* **2016**, *16*, 2062-2073; b) W.-Q. Kan, J. Yang, Y.-Y. Liu, J.-F. Ma, *CrystEngComm*, **2012**, *14*, 6271-6281.
- [17] a) T. Yoneda, C. Kasai, Yo Manabe, M. Tsurui, Y. Kitagawa, Y. Hasegawa, P. Sarkar, Y. Inokuma *Chem Asian J.* **2020**, *15*, 601-605; b) S.-C. Chen, X.-X. Cai, Z.-H. Zhang, Q. Yan, M.-Y. He, F. Tian, J. Gao and Q. Chen *Z. Anorg. Allg. Chem.* **2013**, *639*, 1726-1730; c) L. Y. Jin, M. M. Li, D. B. Dang, Y. Bai, Y. N. Zheng, *Z. Naturforsch.* **2013**, *68b*, 284-288; d) J. F. Lu, Y. H. Xu, P. A. Li, L. X. Jin, C. B. Zhao, X. H. Guo and H. G. Ge *Crystallography Reports* **2017**, *62*, 1046-1050; e) S. Miao, Z. Li, C. Xu, D. Deng, B. Ji, *Crystals* **2019**, *9*, 592; f) K. Banerjee, S. Roy, M. Kotal, K. Biradha *Cryst. Growth Des.* **2015**, *15*, 5604-5613.
- [18] Y. Hu, S. hen, Y. Han, H. Chen, Q. Wang, Z. Nie, Y. Huang and S. Yao, *Chem. Commun.* **2015**, *51*, 17611-17614.
- [19] a) T. Wen, D.-X. Zhang, J. Zhang *Inorg. Chem.* **2013**, *52*, 12-14; b) J. Guo, D. Sun, L. Zhang, Q. Yang, X. Zhao, D. Sun, *Cryst. Growth Des.* **2012**, *12*, 5649-5654.
- [20] N.-X. Zhu, C.-W. Zhao, J. Yang, X.-R. Wang, J.-P. Ma, Y.-B. Dong *RSC Adv.* **2016**, *6*, 108645-108653.
- [21] E. Coronado, J. R. Galán-Mascarós, C. J. Gómez-García, J. M. Martínez-Agudo, *Inorg. Chem.* **2001**, *40*, 113-120.
- [22] R.-S. Wang, J. Feng, Y.-Z. Lei, D.-M. Chen and M.-L. Lian *Cryst. Res. Technol.* **2018**, *53*, 1800065.
- [23] C.-P. Li, H. Zhou, S. Wang, H.-H. Yuan, S.-Z. Zhang and M. Du *Chem. Commun.* **2017**, *53*, 4767-4770.
- [24] C.-P. Li, H. Zhou, J. Chen, J.-J. Wang, M. Du, W. Zhou *ACS Appl. Mater. Interfaces* **2020**, *12*, 15246-15254.
- [25] W. L. Leong, J. J. Vittal *Chem. Rev.* **2011**, *111*, 688-764.
- [26] T. R. Cook, Y.-R. Zheng, P. J. Stang *Chem. Rev.* **2013**, *113*, 734-777.
- [27] Y.-Q. He, W. Fudickar, J.-H. Tang, H. Wang, X. Li, J. Han, Z. Wang, M. Liu, Y.-W. Zhong, T. Linker, P. J. Stang *J. Am. Chem. Soc.* **2020**, *142*, 2601-2608.
- [28] a) M.-X. Wu, Y.-W. Yang, *Adv. Mater.* **2017**, *29*, 1606134; b) I. Abánades Lázaro, S. Abanades Lázaro, R. S. Forgan, *Chem. Commun.* **2018**, *54*, 2792-2795.
- [29] M. P. Suh, H. J. Park, T. K. Prasad, D.-W. Lim, *Chem. Rev.* **2012**, *112*, 782.
- [30] J.-R. Li, J. Sculley, H.-C. Zhou, *Chem. Rev.* **2012**, *112*, 869.

- [31] Y. Huang, W. Su, R. Wang, T. Zhao, *Aerosol Air Qual. Res.* **2019**, *19*, 2130-2150.
- [32] a) X. Zhao, X. Wang, S. Wang, J. Dou, P. Cui, Z. hen Chen, D. Sun, X. Wang, D. Sun *Cryst. Growth Des.* **2012**, *12*, 2736-2739; b) S.-C. Chen, X.-X. Cai, Z.-H. Zhang, Q. Yan, M.-Y. He, F. Tian, J. Gao and Q. Chen *Z. Anorg. Allg. Chem.* **2013**, *639*, 1726-1730.
- [33] L. Wen, Z. Lu, J. Lin, Z. Tian, H. Zhu, Q. Meng, *Cryst. Growth Des.* **2007**, *7*, 93-99.
- [34] L. E. Kreno, K. Leong, O. K. Farha, M. Allendorf, R. P. Van Duyne, J. T. Hupp, *Chem. Rev.* **2012**, *112*, 1105.
- [35] a) T. R. Cook, P. J. Stang, *Chem. Rev.* **2015**, *115*, 7001-7045; b) R. Chakrabarty, P. S. Mukherjee, P. J. Stang, *Chem. Rev.* **2011**, *111*, 6810-6918; c) Y.-R. Zheng, P. J. Stang, *J. Am. Chem. Soc.* **2009**, *131*, 3487-3489; d) Y. Sun, C. Chen, J. Liu, P. J. Stang, *Chem. Rev.* **2013**, *113*, 734-777.
- [36] Y.-R. Zheng, Z. Zhao, M. Wang, K. Ghosh, J. B. Pollock, T. R. Cook, P. J. Stang *J. Am. Chem. Soc.* **2010**, *132*, 16873-16882.
- [37] M. R. Rosenthal, *J. Chem. Educ.* **1973**, *50*, 331.
- [38] M. Bochmann, *Angew. Chem. Int. Ed.* **1992**, *31*, 1182-1183; *Angew. Chem.* **1992**, *104*, 1206.
- [39] K. Seppelt *Angew. Chem. Int. Ed.* **1993**, *32*, 1025-1027; *Angew. Chem.* **1993**, *105*, 1074.
- [40] S. H. Strauss *Chem. Rev.* **1993**, *93*, 927-942.
- [41] H. Plenio *Chem. Rev.* **1997**, *97*, 3363-3384.
- [42] I. Krossing, I. Rabe *Angew. Chem. Int. Ed.* **2004**, *43*, 2066-2090; *Angew. Chem.* **2004**, *116*, 2116-2142.
- [43] D. Stasko, C. A. Reed, *J. Am. Chem. Soc.* **2002**, *124*, 1148.
- [44] H. P. A. Mercier, J. C. P. Saunders, G. T. Schrobilgen, *J. Am. Chem. Soc.* **1994**, *116*, 2921.
- [45] I. Krossing, *Chem. Eur. J.* **2001**, *7*, 490-502.
- [46] M. E. Moussa, M. Piesch, M. Fleischmann, A. Schreiner, M. Seidl, M. Scheer *Dalton Trans.* **2018**, *47*, 16031-16035.
- [47] T. Köchner, N. Trapp, T. A. Engesser, A. J. Lehner, C. Röhr, S. Riedel, C. Knapp, H. Scherer, I. Krossing, *Angew. Chem. Int. Ed.* **2011**, *50*, 11253-11256; *Angew. Chem.* **2011**, *123*, 11449-11452.
- [48] L. Stein, W. W. Henderson *J. Am. Chem. Soc.* **1980**, *102*, 8, 2856-2857.
- [49] T. Drews, K. Seppelt *Angew. Chem. Int. Ed.* **1997**, *109*, 273-274; *Angew. Chem.* **1997**, *36*, 264-265.
- [50] a) I. M. Riddlestone, A. Kraft, J. Schaefer, I. Krossing *Angew. Chem. Int. Ed.* **2018**, *57*, 13982-14024; b) J. Bohnenberger, W. Feuerstein, D. Himmel, M. Daub, F. Breher, I. Krossing *Nat Commun* **2019**, *10*, 624.
- [51] I. Krossing, *J. Am. Chem. Soc.* **2001**, *123*, 4603-4604.
- [52] P. Weis, C. Hettich, D. Kratzert, I. Krossing *Eur. J. Inorg. Chem.* **2019**, 1657-1668.
- [53] B.-C. Koo, Y.-H. Lee, D.-S. Moon, S.-C. Yoon, J. C. Raymond *Science* **2013**, *342*, 1346-1348.
- [54] a) M. Caporali, L. Gonsalvi, A. Rossin, M. Peruzzini, *Chem. Rev.* **2010**, *110*, 4178-4235; b) B. M. Cossairt, N. A. Piro, C. C. Cummins, *Chem. Rev.* **2010**, *110*, 4164-4177; c)
- [55] A. E. Seitz, F. Hippauf, W. Kremer, S. Kaskel, M. Scheer *Nature Communications* **2018**, *9*, 361.
- [56] a) D. M. Quinn, *Chem. Rev.* **1987**, *87*, 955; b) P. Taylor, *J. Biol. Chem.* **1991**, *266*, 4025; c) E. Giacobini, *Pharmacol. Res.* **2004**, *50*, 433.
- [57] Z.-X. Shen, *Med. Hypotheses* **2008**, *70*, 43.
- [58] a) H. Soreq, S. Seidman, *Nat. Rev. Neurosci.* **2001**, *2*, 294; b) C. I. Wright, C. Geula, M. M. Mesulam, *Ann. Neurol.* **1993**, *34*, 373-384.
- [59] R. T. Delfino, T. S. Ribeiro, J. D. Figueroa-Villar *J. Braz. Chem. Soc.* **2009**, *20*, 407-428.
- [60] E.-C. Koch, *Propellants Explos. Pyrotech.* **2008**, *33*, 165-176.
- [61] a) U. Braun, B. Schartel, *Macromol. Chem. Phys.* **2004**, *205*, 2185-2196; b) B. Schartel *Materials* **2010**, *3*, 4710-4745.
- [62] J. W. Hittorf, *Ann. Phys.* **1865**, *202*, 193-228.
- [63] N. Wiberg, A. F. Hollemann *Hollemann, Wiberg – Lehrbuch der Anorganischen Chemie* **2007**, 102<sup>nd</sup> Edition: de Gruyter Berlin.
- [64] O. J. Scherer, *Chem. unserer Zeit* **2000**, *34*, 374-381; O. J. Scherer, *Acc. Chem. Res.* **1999**, *32*, 751-762; O. J. Scherer, *Angew. Chem. Int. Ed. Engl.* **1990**, *29*, 1104-1122; *Angew. Chem.* **1990**, *102*, 1137-1155.

- [65] a) A. P. Ginsberg, W. E. Lindsell, *J. Am. Chem. Soc.* **1971**, *93*, 2082-2084; b) A. P. Ginsberg, W. E. Lindsell, K. J. McCullough, C. R. Sprinkle, A. J. Welch, *J. Am. Chem. Soc.* **1986**, *108*, 403-416.
- [66] G. L. Simon, L. F. Dahl, *J. Am. Chem. Soc.* **1973**, *95*, 2175-2183.
- [67] A. Vizi-Orosz, G. Pályi, L. Markó, *J. Organomet. Chem.* **1973**, *60*, C25-C26.
- [68] S. Midollini, A. Orlandini, L. Sacconi *Angew. Chem.* **1979**, *91*, 93.
- [69] H. Lang, L. Zsolnai, G. Huttner, *Angew. Chem. Int. Ed. Engl.* **1983**, *22*, 976; *Angew. Chem.* **1983**, *95*, 1016.
- [70] O. J. Scherer, H. Sitzmann und G. Wolmershäuser, *Angew. Chem.* **1985**, *97*, 358.
- [71] O. J. Scherer, J. Schwalb, G. Wolmershäuser W. Kaim, R. Groß, *Angew. Chem. Int. Ed. Engl.* **1986**, *25*, 363; *Angew. Chem.* **1986**, *98*, 349.
- [72] O. J. Scherer, T. Brück, *Angew. Chem.* **1987**, *99*, 59.
- [73] M. Fleischmann, F. Dielmann, L. J. Gregoriades, E. V. Peresyphkina, A. V. Virovets, S. Huber, A. Y. Timoshkin, G. Balázs, M. Scheer *Angew. Chem.* **2015**, *127*, 13303-13308; *Angew. Chem. Int. Ed.* **2015**, *54*, 13110-13115.
- [74] E. Mädl, G. Balázs, E. V. Peresyphkina, M. Scheer *Angew. Chem. Int. Ed.* **2016**, *55*, 7702-7707; *Angew. Chem.* **2016**, *128*, 7833-7838.
- [75] a) S. Welsch, L. J. Gregoriades, M. Sierka, M. Zabel, A. V. Virovets, M. Scheer *Angew. Chem. Int. Ed.* **2007**, *46*, 9323-9326; b) L. J. Gregoriades, B. K. Wegley, M. Sierka, E. Brunner, C. Gröger, E. V. Peresyphkina, A. V. Virovets, M. Zabel, M. Scheer *Chem. Asian J.* **2009**, *4*, 1578-1587; c) M. Fleischmann, S. Welsch, E. V. Peresyphkina, A. V. Virovets, M. Scheer, *Chem. Eur. J.* **2015**, *21*, 14332-14336; d) C. Heindl, E. V. Peresyphkina, D. Lüdeker, G. Brunklaus, A. V. Virovets, M. Scheer, *Chem. Eur. J.* **2016**, *22*, 2599-2604; e) M. Scheer, L. J. Gregoriades, A. V. Virovets, W. Kunz, R. Neueder, I. Krossing *Angew. Chem. Int. Ed.* **2006**, *45*, 5689-5693; *Angew. Chem.* **2006**, *118*, 5818-5822; f) M. Scheer, *Dalton Trans.* **2008**, 4372-4386; g) E. Peresyphkina, A. Virovets, M. Scheer *Cryst. Growth Des.* **2016**, *16*, 2335-2341; h) C. Heindl, E. V. Peresyphkina, A. V. Virovets, G. Balázs, M. Scheer *Chem. Eur. J.* **2016**, *22*, 1944-1948; i) C. Heindl, S. Reisinger, C. Schwarzmaier, L. Rummel, A. V. Virovets, E. V. Peresyphkina, M. Scheer *Eur. J. Inorg. Chem.* **2016**, 743-753; j) Claudia Heindl, Eugenia Peresyphkina, Alexander V. Virovets, Ivan S. Bushmarinov, M. G. Medvedev, B. Krämer, B. Dittrich M. Scheer *Angew. Chem.* **2017**, *129*, 13420-13426; k) M. E. Moussa, S. Welsch, L. Dütsch, M. Piesch, S. Reichl, M. Seidl, M. Scheer *Molecules* **2019**, *24*, 325.
- [76] a) M. E. Moussa, S. Welsch, M. Lochner, E. V. Peresyphkina, A. V. Virovets, M. Scheer *Eur. J. Inorg. Chem.* **2018**, 2689-2694; b) A. V. Virovets, E. V. Peresyphkina, G. Brunklaus, H. Eckert, M. Scheer, *Chem. Eur. J.* **2012**, *18*, 1168-1179.
- [77] Selected publications: a) J. Bai, A. V. Virovets, M. Scheer *Science* **2003**, *300*, 781-783; b) M. Scheer, J. Bai, B. P. Johnson, R. Merkle, A. V. Virovets, C. E. Anson, *Eur. J. Inorg. Chem.* **2005**, 4023-4026; c) M. Scheer, A. Schindler, R. Merkle, B. P. Johnson, M. Linseis, R. Winter, C. E. Anson, A. V. Virovets, *J. Am. Chem. Soc.* **2007**, *129*, 13386-13387; d) F. Dielmann, C. Heindl, F. Hastreiter, E. V. Peresyphkina, A. V. Virovets, R. M. Gschwind, M. Scheer *Angew. Chem. Int. Ed.* **2014**, *53*, 13605-13608; *Angew. Chem.* **2014**, *126*, 13823-13827; e) F. Dielmann, M. Fleischmann, C. Heindl, E. V. Peresyphkina, A. V. Virovets, R. M. Gschwind, Manfred Scheer *Chem. Eur. J.* **2015**, *21*, 6208-6214; f) C. Heindl, E. V. Peresyphkina, A. V. Virovets, W. Kremer, M. Scheer *J. Am. Chem. Soc.* **2015**, *137*, 10938-10941; g) F. Dielmann, E. V. Peresyphkina, B. Krämer, F. Hastreiter, B. P. Johnson, M. Zabel, C. Heindl, M. Scheer *Angew. Chem.* **2016**, *128*, 15053-15058; h) E. V. Peresyphkina, C. Heindl, A. V. Virovets, M. Scheer, *Struct. Bond.* **2016**, *174*, 321-374; i) Heindl, E. Peresyphkina, A. V. Virovets, I. S. Bushmarinov, M. G. Medvedev, B. Krämer, B. Dittrich, M. Scheer *Angew. Chem. Int. Ed.* **2017**, *56*, 13237-13243.
- [78] a) E. Peresyphkina, C. Heindl, A. Virovets, H. Brake, E. Mädl, M. Scheer *Chem. Eur. J.* **2018**, *24*, 2503-2508; b) S. Welsch, C. Gröger, M. Sierka, M. Scheer *Angew. Chem. Int. Ed.* **2011**, *50*, 1435-1438.
- [79] H. Brake, E. Peresyphkina, C. Heindl, A. V. Virovets, W. Kremer, Manfred Scheer *Chem. Sci.* **2019**, *10*, 2940-2944.

- [80] a) J. Müller, S. Heinl, C. Schwarzmaier, G. Balázs, M. Keilwerth, K. Meyer, M. Scheer *Angew. Chem. Int. Ed.* **2017**, *56*, 7312-7317; *Angew. Chem.* **2017**, *129*, 7418-7423. b) S. Heinl, A. Y. Timoshkin, J. Müller, M. Scheer *Chem. Commun.* **2018**, *54*, 2244-2247.
- [81] L. Dütsch, M. Fleischmann, S. Welsch, G. Balázs, W. Kremer, M. Scheer *Angew. Chem. Int. Ed.* **2018**, *57*, 3256-3261; *Angew. Chem.* **2018**, *130*, 3311-3317.
- [82] O. J. Scherer, H. Sitzmann, G. Wolmershäuser *J. Organomet. Chem.* **1984**, *268*, C9-C12.
- [83] J. Bai, E. Leiner, M. Scheer *Angew. Chem.* **2002**, *114*, 820-823; *Angew. Chem. Int. Ed.* **2002**, *41*, 783-786.
- [84] M. Scheer, L. J. Gregoriades, M. Zabel, J. Bai, I. Krossing, G. Brunklaus, H. Eckert *Chem. Eur. J.* **2008**, *14*, 282-295.
- [85] M. Fleischmann, S. Welsch, E. V. Peresypkina, A. V. Virovets, M. Scheer, *Chem. Eur. J.* **2015**, *21*, 14332-14336.
- [86] M. E. Moussa, M. Piesch, M. Fleischmann, A. Schreiner, M. Seidl, M. Scheer *Dalton Trans.* **2018**, *47*, 16031-16035.
- [87] M. E. Moussa, M. Fleischmann, E. V. Peresypkina, L. Dütsch, M. Seidl, G. Balázs, M. Scheer *Eur. J. Inorg. Chem.* **2017**, 3222-3226.
- [88] M. E. Moussa, M. Seidl, G. Balázs, M. Zabel, A. V. Virovets, B. Attenberger, A. Schreiner, M. Scheer *Chem. Eur. J.* **2017**, *23*, 16199-16203.
- [89] M. E. Moussa, B. Attenberger, E. V. Peresypkina, M. Fleischmann, G. Balázs, M. Scheer *Chem. Commun.* **2016**, *52*, 10004-10007.
- [90] B. Attenberger, S. Welsch, M. Zabel, E. Peresypkina, M. Scheer *Angew. Chem. Int. Ed.* **2011**, *50*, 11516-11519; *Angew. Chem.* **2011**, *123*, 11718-11722.
- [91] B. Attenberger, E. V. Peresypkina, M. Scheer *Inorg. Chem.* **2015**, *54*, 7021-7029.
- [92] M. Scheer, L. J. Gregoriades, M. Zabel, M. Sierka, L. Zhang, H. Eckert *Eur. J. Inorg. Chem.* **2007**, 2775-2782.
- [93] M. E. Moussa, P. A. Shelyganov, B. Wegley, M. Seidl, M. Scheer *Eur. J. Inorg. Chem.* **2019**, 4241-4248.
- [94] M. Scheer, L. Gregoriades, J. Bai, M. Sierka, G. Brunklaus, H. Eckert *Chem. Eur. J.* **2005**, *11*, 2163-2169.
- [95] M. E. Moussa, M. Seidl, G. Balázs, M. Hautmann, M. Scheer *Angew. Chem.* **2019**, *131*, 13035-13039.



## 2 Research Objectives

This thesis focuses on investigations regarding the reaction of the P<sub>2</sub> ligand complex [Cp<sub>2</sub>Mo<sub>2</sub>(CO)<sub>4</sub>(μ,η<sup>2:2</sup>-P<sub>2</sub>)] (**A**) with the Cu(I) and Ag(I) metal salts [Cu(CH<sub>3</sub>CN)<sub>4</sub>][BF<sub>4</sub>], [Cu(CH<sub>3</sub>CN)<sub>3.5</sub>][FAl{O(C<sub>6</sub>F<sub>10</sub>)(C<sub>6</sub>F<sub>5</sub>)<sub>3</sub>}<sub>3</sub>], [Cu(CH<sub>3</sub>CN)<sub>4</sub>][Al{OC(CF<sub>3</sub>)<sub>3</sub>}<sub>4</sub>], Ag[Al{OC(CF<sub>3</sub>)<sub>3</sub>}<sub>4</sub>] and Ag[FAl{O(C<sub>6</sub>F<sub>10</sub>)(C<sub>6</sub>F<sub>5</sub>)<sub>3</sub>}<sub>3</sub>], respectively, and selected pyridine-based organic linker as a third reaction compound (**Figure 2-1**).

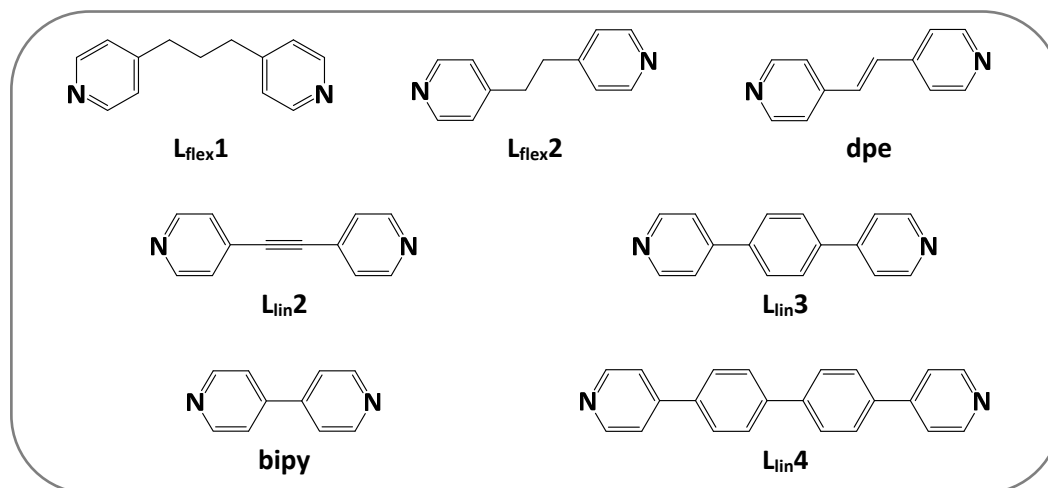


**Figure 2-1.** Organic pyridine-based linker 1,3-di(4-pyridyl)propane (**L<sub>flex1</sub>**), 1,2-di(4-pyridyl)ethane (**L<sub>flex2</sub>**), 1,2-di(4-pyridyl)ethylene (**dpe**), 4,4'-bipyridyl (**bipy**), 1,2-di(pyridin-4-yl)ethyne (**L<sub>lin2</sub>**), 1,4-di(4-pyridyl)benzene (**L<sub>lin3</sub>**) and 4,4'-di(4-pyridyl)biphenyl (**L<sub>lin4</sub>**).

The goal of those investigations was to determine the best reaction parameters needed for the selective synthesis of one desired product in preferable high yields, as the directed synthesis of organometallic-organic coordination polymers faces some challenges. The slightest changes in the parameters of the reaction, *e.g.* concentration of the reaction mixture, temperature, reaction time, and crystallisation method, can have an influence on the isolated product. Additionally, often more than one compound crystallises, which makes it even more complicated for selective syntheses. It can therefore be difficult to reproduce certain products as well as selectively synthesise one specific product. However, this is also the advantage of this chemistry, as there are many possibilities to push the reaction in the desired direction. The different approaches used in this thesis are the following:

- nature of the linker
- type of metal
- the Weakly Coordinating Anion
- influence of the reaction parameters, *e.g.* solvents and crystallisation methods

Another goal was the design of new phosphorus-rich precursors from the P<sub>2</sub> ligand complex [Cp<sub>2</sub>Mo<sub>2</sub>(CO)<sub>4</sub>(μ,η<sup>2:2</sup>-P<sub>2</sub>)] (**A**) and above-mentioned coinage metal salts for subsequent coordination chemistry. The use of suitable precursors could be a way for a more directed and selective synthesis of desired products.





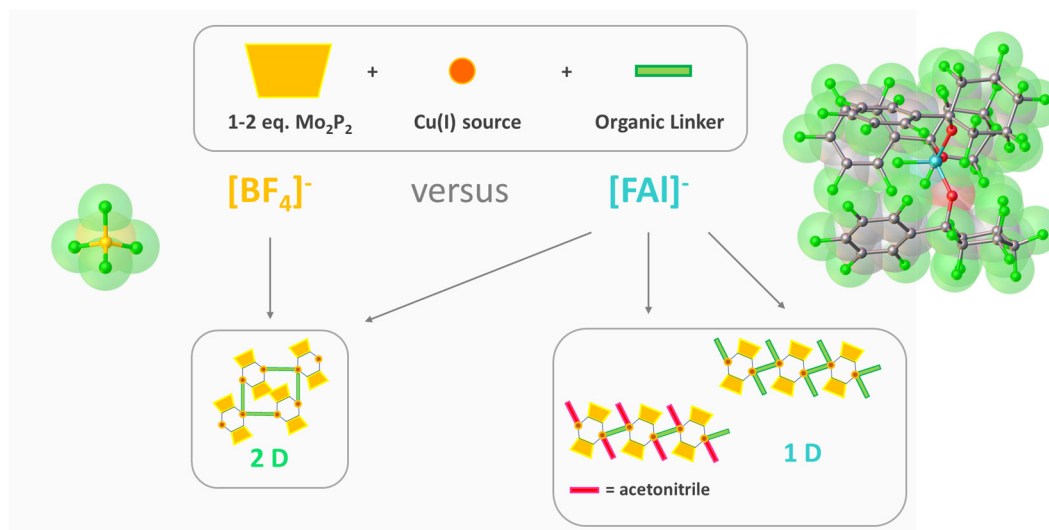
### 3 Influence of organic linker and weakly coordinating anion in the synthesis of one- and two-dimensional organometallic-organic coordination polymers with the P<sub>2</sub> ligand complex [Cp<sub>2</sub>Mo<sub>2</sub>(CO)<sub>4</sub>(μ,η<sup>2:2</sup>-P<sub>2</sub>)] and Cu(I) salts

#### Author contribution

Andrea Schreiner: Preparation of the manuscript, synthesis, and characterisation of compounds **3-1** to **3-7**

Michael Seidl: Refinement of the solid-state structures, support of the X-ray diffraction measurements and revision of the manuscript

Manfred Scheer: Supervision of the research and revision of the manuscript

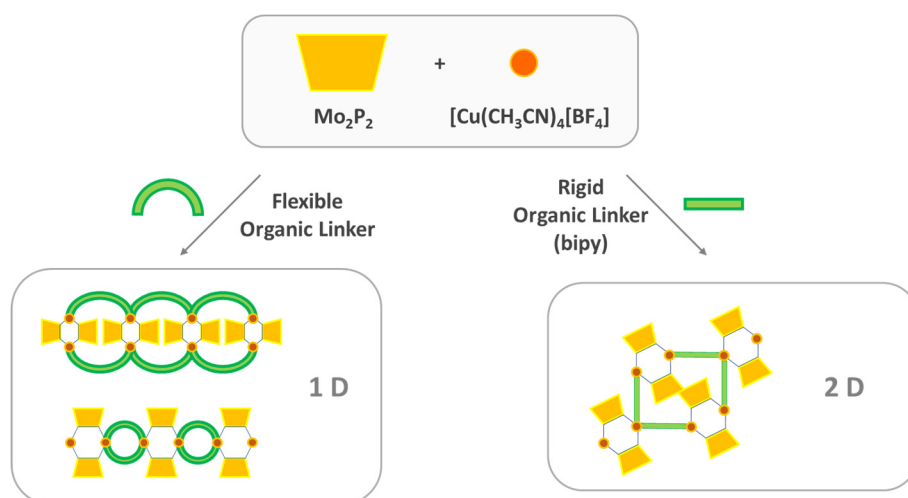


#### 3.1 Abstract

The P<sub>2</sub> ligand complex [Cp<sub>2</sub>Mo<sub>2</sub>(CO)<sub>4</sub>(μ,η<sup>2:2</sup>-P<sub>2</sub>)] (**A**) was used as a building block for supramolecular coordination chemistry. **A** was reacted with the Cu(I) salt [Cu(CH<sub>3</sub>CN)<sub>4</sub>][BF<sub>4</sub>] (**B**) or [Cu(CH<sub>3</sub>CN)<sub>3.5</sub>][FAl{O(C<sub>6</sub>F<sub>10</sub>)(C<sub>6</sub>F<sub>5</sub>)<sub>3</sub>}] (**C**) and the pyridine-based linker 4,4'-bipyridine (**bipy**), 1,2-di(4-pyridyl)ethane (**L<sub>flex2</sub>**), 1,2-di(pyridin-4-yl)ethyne (**L<sub>lin2</sub>**), 1,4-di(pyridyl)benzene (**L<sub>lin3</sub>**) and 4,4'-di(4-pyridyl)biphenyl (**L<sub>lin4</sub>**), respectively. The study focused on the influence of the linker and the anion on the formation of 1D or 2D organometallic organic coordination polymers. Seven new compounds with the general formulas [Cu<sub>2</sub>{Cp<sub>2</sub>Mo<sub>2</sub>(CO)<sub>4</sub>(μ<sub>4</sub>,η<sup>2:2:1:1</sup>-P<sub>2</sub>)}<sub>2</sub>(μ,η<sup>1:1</sup>-L)<sub>2</sub>][X]<sub>2n</sub> (L = **L<sub>lin2</sub>**, **L<sub>lin3</sub>**, **L<sub>lin4</sub>** and **L<sub>flex2</sub>**), [Cu<sub>2</sub>{Cp<sub>2</sub>Mo<sub>2</sub>(CO)<sub>4</sub>(μ<sub>4</sub>,η<sup>2:2:2:1</sup>-P<sub>2</sub>)}<sub>2</sub>(μ,η<sup>1:1</sup>-L<sub>lin4</sub>)(CH<sub>3</sub>CN)<sub>n</sub>][FAl]<sub>2n</sub> and [Cu<sub>2</sub>{Cp<sub>2</sub>Mo<sub>2</sub>(CO)<sub>4</sub>(μ,η<sup>2:2:1:1</sup>-P<sub>2</sub>)}<sub>2</sub>(μ,η<sup>1:1</sup>-bipy)(bipy)<sub>n</sub>][BF<sub>4</sub>]<sub>2n</sub> were obtained and characterised by X-ray structure analysis, elemental analysis, IR spectroscopy, NMR spectroscopy and mass spectrometry.

## 3.2 Introduction

The research field of coordination polymers (CPs) has extremely expanded,<sup>[1]</sup> which is not only due to their properties like luminescence,<sup>[2]</sup> redox behaviour<sup>[3]</sup> and magnetic properties<sup>[4]</sup> but also because they exhibit interesting structural topologies.<sup>[5]</sup> CPs containing Cu(I) moieties are especially of interest due to the biochemical significance of copper.<sup>[6]</sup> Cu(I) coordination polymers<sup>[7]</sup> display luminescence<sup>[8]</sup> and even catalytic<sup>[9]</sup> and photocatalytic properties.<sup>[10]</sup> Cu(I) halides have been shown to react with the P<sub>2</sub> ligand complex [Cp<sub>2</sub>Mo<sub>2</sub>(CO)<sub>4</sub>(μ,η<sup>2:2</sup>-P<sub>2</sub>)] (**A**) to form one-dimensional coordination polymers, where the Cu(I) halide is the bridging unit between the organometallic units.<sup>[11]</sup> The same behaviour could be observed for [Cp<sub>2</sub>M<sub>2</sub>(CO)<sub>4</sub>(μ,η<sup>2:2</sup>-P<sub>2</sub>)] with M = Cr<sup>[12]</sup>, W<sup>[13]</sup> and even [Cp<sub>2</sub>M<sub>2</sub>(CO)<sub>4</sub>(μ,η<sup>2:2</sup>-PE)] (E = As, Sb).<sup>[14]</sup> The P<sub>2</sub> ligand complex **A** has further been studied using Cu(I) salts with weakly coordinating anions (WCAs) as counterion for the purpose of designing novel coordination polymers with the anions being separated from the Cu(I) building blocks. This led to the discovery of discrete, zero-dimensional coordination complexes of the type [Cu<sub>2</sub>(Cp<sub>2</sub>Mo<sub>2</sub>(CO)<sub>4</sub>(μ,η<sup>2:2:1:1</sup>-P<sub>2</sub>)<sub>2</sub>(Cp<sub>2</sub>Mo<sub>2</sub>(CO)<sub>4</sub>(μ,η<sup>2:2:1</sup>-P<sub>2</sub>)<sub>2</sub>)] [X<sub>2</sub>] (X = PF<sub>6</sub>,<sup>[11b]</sup> BF<sub>4</sub>,<sup>[15]</sup> FA)<sup>[16]</sup>. Furthermore, the P<sub>2</sub> ligand complex **A** was combined with Cu(I) WCA salts and pyridine-based organic linkers which yielded zero-dimensional coordination compounds<sup>[17]</sup> as well as one-<sup>[17,18]</sup> and two-dimensional<sup>[17,19]</sup> coordination polymers. However, selectivity remains a problem in this delicate chemistry. The reaction outcome is easily influenced by slight changes in the reaction parameters, such as the choice of educts but also the procedure, stoichiometry, solvent system, reaction temperature and crystallisation techniques can influence the formation of the final product. Often even small differences in the nature of the linker, like a missing CH<sub>2</sub>-group or a different anion of the metal salt, as well as the amount of solvent can influence the outcome of a reaction.<sup>[20]</sup> Recently, the reaction of the P<sub>2</sub> ligand complex **A** with the Cu(I) source [Cu(CH<sub>3</sub>CN)<sub>4</sub>][BF<sub>4</sub>] (**B**) and flexible pyridine-based organic linkers were reported (**Scheme 3-1**), being the first example of selective formation of 1D organometallic-organic CPs in very good yields.<sup>[21]</sup> These results were promising in regard to finding out more about the dominating factors that lead to a specific product and making the selective synthesis of desired products more facile. Further, the reaction of **A** and **B** with the organic linker 4,4'-bipyridine (**bipy**) resulted in the formation of a two-dimensional network (**Scheme 3-1**).<sup>[22]</sup>

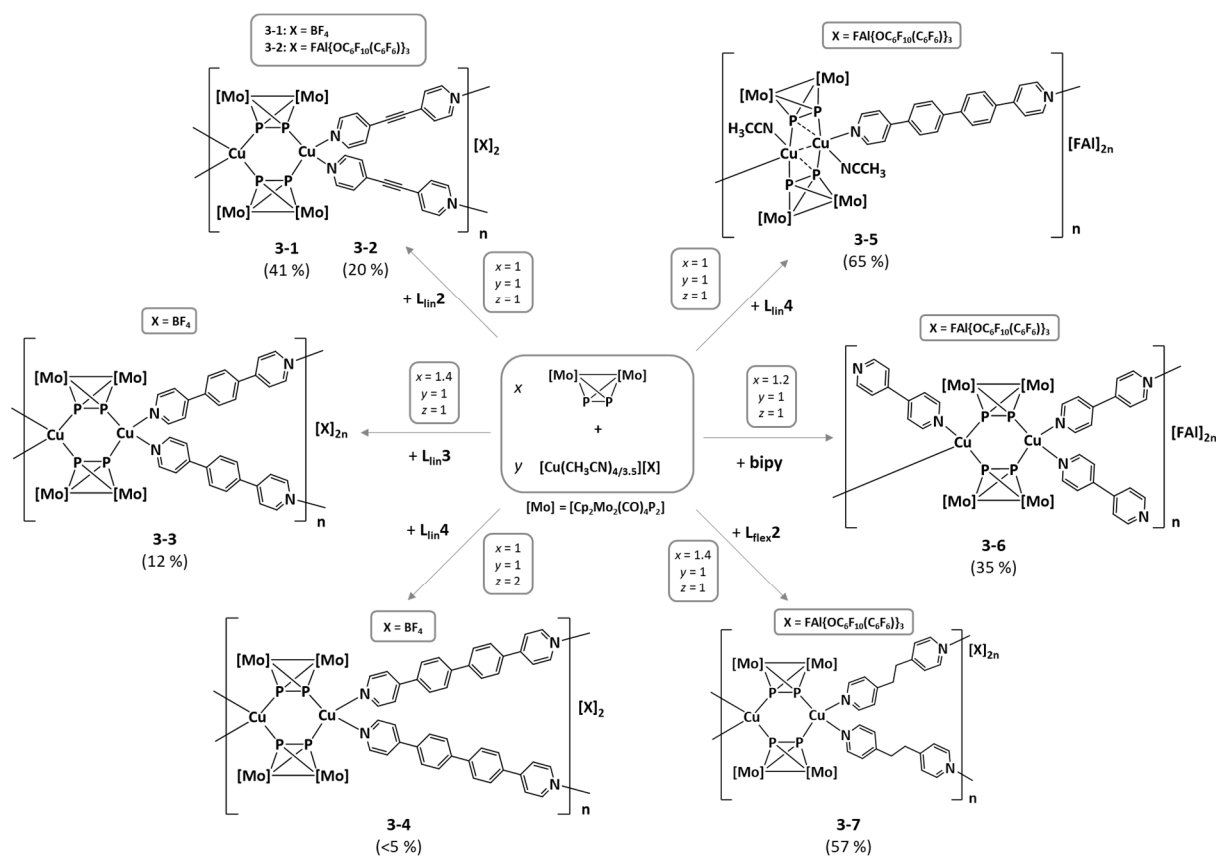


**Scheme 3-1.** Reported reactions of the P<sub>2</sub> ligand complex [Cp<sub>2</sub>Mo<sub>2</sub>(CO)<sub>4</sub>(μ,η<sup>2:2</sup>-P<sub>2</sub>)] (**A**) with [Cu(CH<sub>3</sub>CN)<sub>4</sub>][BF<sub>4</sub>] (**B**) and flexible linkers, e.g. 1,3-di(4-pyridyl)propane (**L<sub>flex1</sub>**) and 1,2-di(4-pyridyl)ethane (**L<sub>flex2</sub>**), and the rigid linker 4,4'-bipyridine (**bipy**).<sup>[21,22]</sup>

The formation of similar 1D CPs like in the reactions with **L<sub>flex</sub>1** and **L<sub>flex</sub>2** are not possible in the case of **bipy**, as the linker molecules cannot arrange in the same way due to the lack of flexible CH<sub>2</sub> groups. In general, rigid linkers like **bipy** have less conformational freedom, which limits the possibilities of structural arrangements, *e.g.* a pair of rigid, unbendable linkers like **bipy** cannot coordinate to the same two metal centres. The question arises if it is possible to synthesise similar 2D CPs by reacting the P<sub>2</sub> ligand complex **A** with the Cu(I) source **B** and other rigid organic linkers with increased length. Therefore, linear organic linkers containing pyridine and benzene rings as well as triple bonds to limit the conformational freedom were chosen. Herein, the reactions of the P<sub>2</sub> ligand complex [Cp<sub>2</sub>Mo<sub>2</sub>(CO)<sub>4</sub>(μ,η<sup>2-2</sup>-P<sub>2</sub>)] (**A**) with the Cu(I) salt [Cu(CH<sub>3</sub>CN)<sub>4</sub>][BF<sub>4</sub>] (**B**) and the rigid pyridine-based organic linker 1,2-di(pyridin-4-yl)ethyne (**L<sub>lin</sub>2**), 1,4-di(pyridyl)benzene (**L<sub>lin</sub>3**) and 4,4'-di(4-pyridyl)biphenyl (**L<sub>lin</sub>4**) are reported. Further, the influence of the weakly coordinating anion (WCA) on the system was investigated. Therefore the Cu(I) source **B** was exchanged for a Cu(I) source with a much larger WCA, [Cu(CH<sub>3</sub>CN)<sub>3.5</sub>][FAI] (**C**, FAI = FAI{O(C<sub>6</sub>F<sub>10</sub>)(C<sub>6</sub>F<sub>5</sub>)<sub>3</sub>}).<sup>[16]</sup> The Cu(I) salt **C** was reacted with the P<sub>2</sub> ligand complex **A** and the rigid organic linkers **L<sub>lin</sub>2**, **L<sub>lin</sub>4** and **bipy**. In a final type of experiment, the rigid linkers were in turn exchanged for the flexible linker **L<sub>flex</sub>2** to find out if the nature of the linker or the WCA is the decisive parameter concerning this system.

### 3.3 Results and Discussion

Complex  $[\text{Cp}_2\text{Mo}_2(\text{CO})_4(\mu, \eta^{2,2}\text{-P}_2)]$  (**A**) was reacted with the Cu(I) source  $[\text{Cu}(\text{CH}_3\text{CN})_4][\text{BF}_4]$  (**B**) or  $[\text{Cu}(\text{CH}_3\text{CN})_{3.5}][\text{FAI}]$  ( $\text{FAI} = \text{FAI}\{\text{O}(\text{C}_6\text{F}_{10})(\text{C}_6\text{F}_5)\}_3$ , **C**) and the organic pyridine-based linkers  $\text{L}_{\text{lin}}2$ ,  $\text{L}_{\text{lin}}3$ ,  $\text{L}_{\text{lin}}4$ , **bipy** and  $\text{L}_{\text{flex}}2$ , respectively (**Scheme 3-2**). All reactions were performed using a mixture of dichloromethane and acetonitrile as solvent and the crude reaction mixture were layered using either *n*-pentane, a 1:1-mixture of *n*-pentane and dichloromethane or in the case of **3-3**, toluene.



**Scheme 3-2.** Summary of the reactions of the  $\text{P}_2$  ligand complex **A** with the Cu(I) salts  $[\text{Cu}(\text{CH}_3\text{CN})_4][\text{BF}_4]$  (**B**) and  $[\text{Cu}(\text{CH}_3\text{CN})_{3.5}][\text{FAI}]$  (**C**,  $\text{FAI} = \text{FAI}\{\text{O}(\text{C}_6\text{F}_{10})(\text{C}_6\text{F}_5)\}_3$ ) and the pyridine-based organic linker  $\text{L}_{\text{lin}}2$ ,  $\text{L}_{\text{lin}}3$ ,  $\text{L}_{\text{lin}}4$ , **bipy** and  $\text{L}_{\text{flex}}2$ . Isolated yields of single crystals are given in parenthesis.

In the first part of the investigations, **A** was reacted with the Cu(I) salt  $[\text{Cu}(\text{CH}_3\text{CN})_4][\text{BF}_4]$  (**B**) and the linear organic linkers **L<sub>lin2</sub>**, **L<sub>lin3</sub>** and **L<sub>lin4</sub>** (**Figure 3-1**), respectively, using a ratio of 1-2:1:1. The reactions yielded three new 2D CP with the general formula  $[\text{Cu}_2\{\text{Cp}_2\text{Mo}_2(\text{CO})_4(\mu, \eta^{2:2:1:1}\text{-P}_2)\}_2(\mu, \eta^{1:1}\text{-L})_2]_n[\text{BF}_4]_{2n}$  (**3-1**: **L** = **L<sub>lin2</sub>**, **3-2**: **L** = **L<sub>lin3</sub>**, **3-3**: **L** = **L<sub>lin4</sub>**), whose structures were determined by single crystal X-ray analysis. Crystals of compounds **3-1** to **3-3** were obtained after in day in 41 %, 12 % and < 5 % yield.

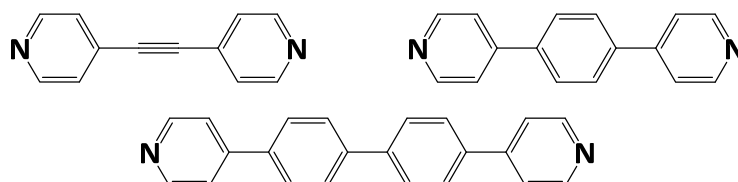


**Figure 3-1.** Organic pyridine-based linker 1,2-di(pyridin-4-yl)ethyne (**L<sub>lin2</sub>**), 1,2-di(pyridin-4-yl)ethyne (**L<sub>lin3</sub>**) and 4,4'-di(4-pyridyl)biphenyl (**L<sub>lin4</sub>**).

The cationic 2D networks of **3-1** (**Figure 3-4**), **3-2** (**Figure 3-4**) and **3-4** (**Figure 3-4**) contain the educts in a ratio of 1:1:1 and feature a six-membered  $\text{Cu}_2\text{P}_4$ -ring, consisting of two Cu(I) centres and two units of **A**, which serves as a node. Those nodes are connected to each other via linker molecules (**L<sub>lin2</sub>**, **L<sub>lin3</sub>** or **L<sub>lin4</sub>**, respectively). Each Cu(I) is tetracoordinated and every linker is connected to two different nodes. The cavities formed this way are up to 2.2 nm (**3-1** and **3-2**) and 3.1 nm (**3-3**) in diameter (*cf.* **Table 3-2**) between the Cu(I) centres of two opposing nodes.<sup>\*[23]</sup> The Cu-P, P-P and Cu-N distances as well as the angles around the Cu and P atoms are comparable to the dimeric complex  $[\text{Cu}_2(\text{Cp}_2\text{Mo}_2(\text{CO})_4(\mu, \eta^{2:2:1:1}\text{-P}_2))_2(\text{Cp}_2\text{Mo}_2(\text{CO})_4(\mu, \eta^{2:2:1:1}\text{-P}_2))_2]^{2+}$  (**D**)<sup>[11b,15,16]</sup> and other related coordination polymers.<sup>[17,18,19]</sup>

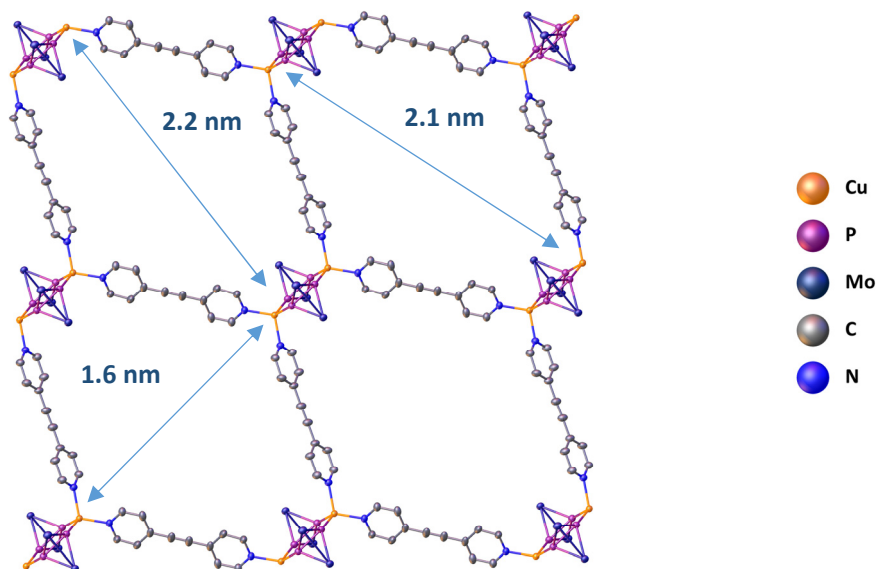


**Figure 3-2.** Section of the molecular structure of the cationic network of **3-1a** in the solid-state. Hydrogen atoms, Cp- and CO-ligands, anions and solvent molecules are omitted for clarity. Thermal ellipsoids are shown at 50 % probability level. Selected bond lengths [Å] and angles [°]: Cu1-P1 2.2745(7), Cu1-P2 2.2760(7), Cu1-N1 2.045(2),

\* The cavity sizes of the CPs are calculated by taking the Cu-Cu distances obtained from the X-ray experiment and abstracting the sum of the *van-der-Waals*-radii of copper (1.7 Å).<sup>[23]</sup>

Cu1-N2 2.010(2), P2-P1 2.0839(9), P1-Cu1-P2 109.54(3), N1-Cu1-P2 103.57(7), N1-Cu1-P1 109.49(7), N2-Cu1-P2 115.18(7), N2-Cu1-P1 108.83(7), N2-Cu1-N1 110.06(9).<sup>[23]</sup>

Single crystal X-ray structure analysis revealed that **3-1** crystallises as orange (**3-1a**) or clear orange (**3-1b**) blocks in the triclinic space group  $P\bar{1}$ . Both structures have been measured at 123 K using a  $\text{CuK}\alpha$  source with a radiation wavelength of 1.54184 Å. The unit cells contain 1.46  $\text{CH}_3\text{CN}$  and 0.47  $\text{CH}_2\text{Cl}_2$  solvent molecules in the case of **3-1a** and 1.85  $\text{CH}_2\text{Cl}_2$  solvent molecules in the case of **3-1b**. Apart from the angles ( $\alpha$ ,  $\beta$ ,  $\gamma$ ), the cell parameters ( $a$ ,  $b$ ,  $c$  and  $V$ ) are very similar (Table 3-1). There are no significant differences in the bond lengths and angles (*cf.* SI), which is why no further differentiations between **3-1a** and **3-1b** will be made. **3-2** crystallises as orange blocks in the triclinic space group  $P\bar{1}$  and **3-3** crystallises as clear orange blocks in the monoclinic space group  $P2_1/n$ .

**Table 3-1.** Comparison of the parameters from the X-ray measurements of **3-1a** and **3-1b**.

Compound	3-1a		3-1b	
Formula	$\text{C}_{29.4}\text{H}_{23.3}\text{BCl}_{0.9}\text{CuF}_4\text{Mo}_2\text{N}_{3.5}\text{O}_4\text{P}_2$		$\text{C}_{27.85}\text{H}_{21.7}\text{BCl}_{3.7}\text{CuF}_4\text{Mo}_2\text{N}_2\text{O}_4\text{P}_2$	
Formula Weight	915.20 <sup>g</sup> /mol		983.71 <sup>g</sup> /mol	
Cell Parameters	$a = 11.4132(2)$ Å	$\alpha = 65.022(2)$ °	$a = 11.4691(3)$ Å	$\alpha = 115.044(3)$ °
	$b = 12.7811(2)$ Å	$\beta = 73.4420(10)$ °	$b = 12.7088(4)$ Å	$\beta = 100.979(2)$ °
	$c = 14.4918(2)$ Å	$\gamma = 88.0010(10)$ °	$c = 14.2889(4)$ Å	$\gamma = 91.093(2)$ °
	$V = 1827.88(6)$ Å <sup>3</sup>		$V = 1840.71(10)$ Å <sup>3</sup>	

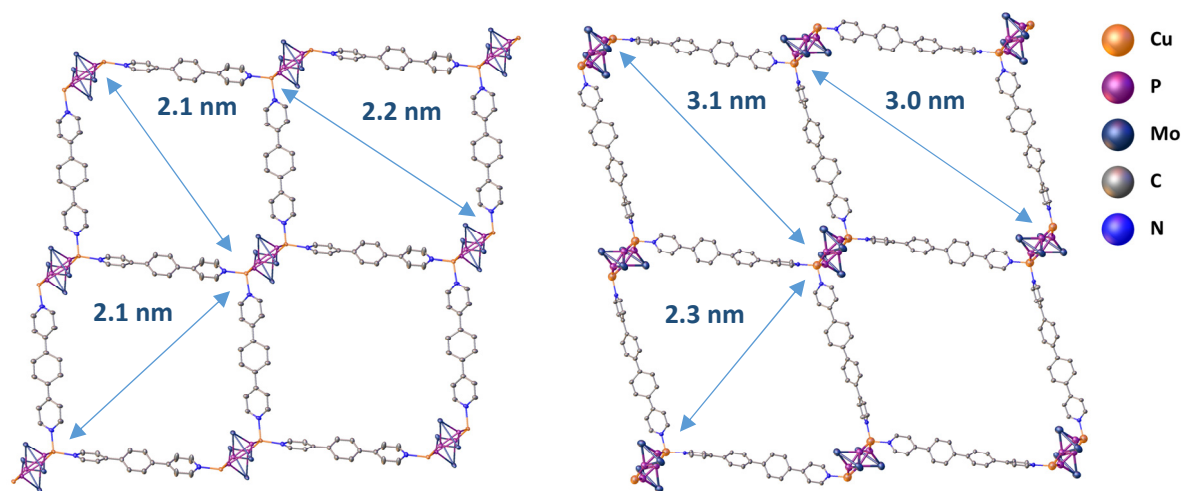


**Figure 3-3.** Section of the molecular structure of the cationic networks of **3-2** (left) and **3-3** (right) in the solid-state. Hydrogen atoms, Cp- and CO-ligands, anions and solvent molecules are omitted for clarity. Thermal ellipsoids are shown at 50 % probability level. Selected bond lengths [Å] and angles [°] for compound **3-2**: Cu1-P2 2.239(1), Cu1-P4 2.291(1), Cu1-N1 2.022(3), Cu1-N3 2.033(3), Cu2-P1 2.285(1), Cu2-P3 2.244(1), Cu2-N2 2.029(3), Cu2-N4 2.037(3), P1-P2 2.080(1), P3-P4 2.083(1), P2-Cu1-P4 112.93(4), N1-Cu1-P2 115.0(1), N1-Cu1-P4 109.9(1), N1-Cu1-N3 104.6(1), N3-Cu1-P2 109.9(1), N3-Cu1-P4 103.6(1), P3-Cu2-P1 113.60(4), N2-Cu2-P1 111.0(1), N2-Cu2-P3 115.4(1), N2-Cu2-N4 104.0(1), N4-Cu2-P1 99.4(1), N4-Cu2-P3 112.0(1). Selected bond lengths [Å] and angles [°] for compound **3-3**: Cu1-P1 2.305(1), Cu1-P2 2.2376(9), Cu1-N1 2.045(3), Cu1-N2 2.025(3), P2-P1 2.083(1), P2-Cu1-P1 108.93(4), N1-Cu1-P1 97.55(8), N2-Cu1-P1 112.98(9), N1-Cu1-P2 114.65(9), N2-Cu1-P2 115.28(9), N2-Cu1-N1 106.2(1).<sup>[23]</sup>

To evaluate the influence of the WCA on the system of **A**, Cu(I) and linear linkers, similar reactions using the Cu(I) source  $[\text{Cu}(\text{CH}_3\text{CN})_{3.5}][\text{FAI}]$  ( $\text{FAI} = [\text{FAI}(\text{O}(\text{C}_6\text{F}_{10})(\text{C}_6\text{F}_5)_3]$ , **C**) were performed using a ratio of 1-1.2:1:1 of the educts. The FAI anion is a significantly bigger WCA than  $[\text{BF}_4]^-$ , so some differences in the reaction outcome could be anticipated. Still, in both cases the formation of 1D CPs, as obtained for the system of **A**, **B** and flexible linkers, is sterically impossible. Linker **L<sub>lin2</sub>** was chosen for a first reaction with **A** and **C** which was performed using a 1:1:1-ratio of the educts. Crystals of **3-4** were obtained in 40 % yield after one week. Compound **3-4** crystallises as orange blocks in the monoclinic space group  $P2_1/c$ . Single crystal X-ray analysis further revealed the formation of a 2D CP (**Figure 3-4**) with a to compounds **3-1**, **3-2** and **3-3** similar structure. The Cu-P, Cu-N and P-P bond lengths (**Table 3-2**) are also very similar and comparable to values found in the dimeric complex **D**.<sup>[11,15]</sup> Compared to compound **3-1**, which also possesses **L<sub>lin2</sub>** as linker units, the P-Cu-P and N-Cu-N angles in **3-4** are larger and the P-Cu-N angles are shorter. Furthermore, the size of the cavities within the network are different. Due to the bigger N-Cu-N angles in **3-4**, the network is compressed, leading to rather diamond-shaped cavities with different distances between the Cu(I) centres.

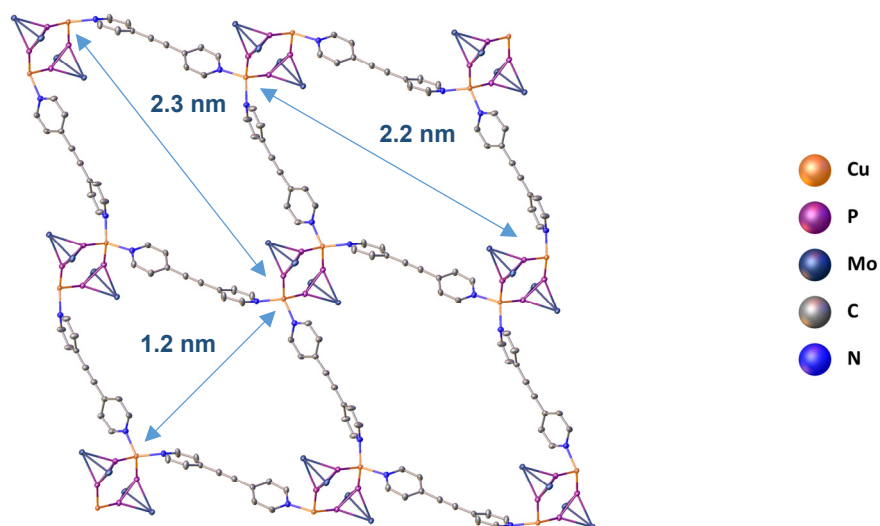


**Figure 3-4.** Molecular structure of the two-dimensional network of **3-4** in the solid-state, view along the a-axis. Thermal ellipsoids are shown at 50 % probability level. Hydrogen atoms, Cp- and CO-ligands, anions and solvent molecules are omitted for clarity. Average of selected bond lengths [ $\text{\AA}$ ] and angles [ $^\circ$ ]: Cu1-P1 2.2957(6), Cu1-P2 2.2858(6), Cu1-N1 2.019(2), Cu1-N2 2.023(2), P1-P2 2.0844(8), P2Cu1P1 116.06(2), N1-Cu1-P1 111.59(6), N2-Cu1-P1 99.37(6), N1-Cu1-P2 107.16(6), N2-Cu1-P2 109.96(6), N1-Cu1-N2 112.72(8).<sup>[23]</sup>

To find out if one could obtain a similar result using the longest linker **L<sub>lin4</sub>**, the reaction of **A** with **C** and **L<sub>lin4</sub>** was performed and yielded a 1D CP. Crystals of compound **3-5** formed in 65 % yield within the following day. By performing single crystal X-ray structure analysis of the clear orange plates of **3-5**, which crystallise in the triclinic space group  $P\bar{1}$ , a novel and compared to compounds **3-1** to **3-4** very different structure was obtained (**Figure 3-5**). The ratio of **A**:**C**:**L<sub>lin4</sub>** in the CP is not, as in the previously discussed compound, 1:1:1, but 2:2:1. The nodes, which also consist of a six-membered  $\text{Cu}_2\text{P}_4$ -ring, are connected to each other via one linker molecule instead of two. The Cu(I) centres are tetra-coordinated and the coordination sphere is completed by one acetonitrile molecule per Cu(I) centre. The node itself is strongly squeezed. The two units of the  $\text{P}_2$  ligand complex **A** in the node are connected to the two Cu(I) centres in a  $\eta^2:\eta^1$ -coordination mode (compounds **3-1-3-4**:  $\eta^1:\eta^1$ ). The distance between the Cu

atoms within the node is 2.5927(4) Å and thus not below the sum of the covalent radii of copper (112 pm).<sup>[24]</sup> The short Cu-Cu distance in the Cu<sub>2</sub>P<sub>4</sub> fragment in **3-5** has influence on the other bond lengths in the compound. Compared to complex **D**,<sup>[11b]</sup> the Cu-P bonds in **3-5** are longer (2.3978(5) and 2.3708(5) Å compared to 2.259(2)-2.378(2) Å), pointing in the direction of weak interaction between the Cu(I) centres causing the weakening of the Cu-P bonds. The Cu1-P1' distance is only 2.7075(5) Å, but still too long to be considered a bond. The P-P and Cu-N bond lengths (2.1198(6) Å and 2.011(2) and 2.044(1) Å, respectively) and the values for the P-Cu-P and N-Cu-N angles are comparable to the values found in **D**<sup>[11b,15,16]</sup> and similar coordination polymers.<sup>[17,18,19]</sup> Due to symmetry generation, the angles of the Cu-Cu-P and Cu-P-P planes to each other are exactly 180°. The twist and fold angles of the pyridine and benzene rings in **L<sub>lin</sub>4** are 27.8927(10) and 3.06013(11)°, respectively. The twist and fold angles between the two pyridine and the two benzene rings are close to zero.

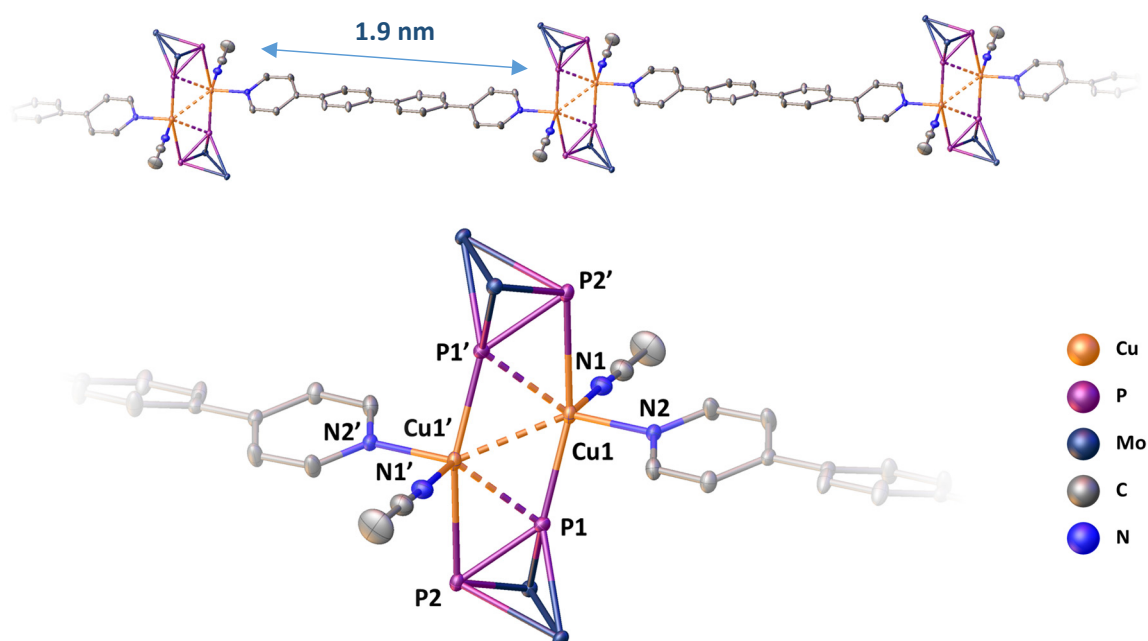


**Figure 3-5.** Molecular structure of the cation of **3-5** in the solid-state, view along the *a*-axis. Thermal ellipsoids are shown at 50 % probability level. Hydrogen atoms, Cp- and CO-ligands, anions and solvent molecules are omitted for clarity. Average of selected bond lengths [Å] and angles [°]: Cu1-Cu1' 2.5927(4), Cu1-P1' 2.3978(5), Cu1-P1 2.3708(5), Cu1-P2' 2.7075(5), Cu1-N1 2.011(2), Cu1-N2 2.044(1), P1-P2 2.1198(6), P1'-Cu1-Cu1' 56.57(1), Cu1'-Cu1-P2' 104.61(2), P1-Cu1-P1' 114.13(1), P1-Cu1-P2' 160.9(2), P1'-Cu1-P2' 48.60(1), N1-Cu1-Cu1' 123.75(5), N2-Cu1-Cu1' 128.43(4), N1-Cu1-P1' 115.18(5), N2-Cu1-P1' 123.57(4), N1-Cu1-P2' 95.92(5), N2-Cu1-P2' 89.37(4), N1-Cu1-P1 100.20(5), N2-Cu1-P1 96.92(4), N1-Cu1-N2 103.07(6).<sup>[23]</sup>

As explained in the introduction, the reaction of the P<sub>2</sub> ligand complex **A** with the Cu(I) salt [Cu(CH<sub>3</sub>CN)<sub>4</sub>][BF<sub>4</sub>] (**B**) and the organic linker 4,4'-di(4-pyridyl)biphenyl (**bipy**, **Figure 3-6**) yielded a two-dimensional CP which is a structural analogue to compounds **3-1** to **3-4**.<sup>[18,22]</sup> To find out of this can also be applied to the system with FAI as WCA, the P<sub>2</sub> ligand complex **A** was reacted with **C** and **bipy**.

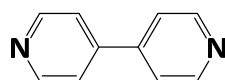


**Figure 3-6.** Organic pyridine-based linker 4,4'-bipyridine (**bipy**).



Crystals of a further 1D CP were formed within the following day. Compound **3-6**, which was obtained in 35 % yield crystallises as orange blocks in the monoclinic space group  $P2_1/n$  was analysed by single crystal X-ray analysis to determine its solid-state structure (**Figure 3-7**). The ratio of the starting materials in the network is 2:2:3. Again, a  $\text{Cu}_2\text{P}_4$  fragment serves as node and the Cu(I) centres are tetra-coordinated. The nodes are connected to each other by one molecule of linker, forming a one-dimensional CP. The coordination sphere of the Cu(I) centres is saturated by one additional linker molecule, which is not connected to any other node. The resulting ratio of the starting material of the network is therefore 2:2:3. This non-connecting **bipy** molecule has a fold angle of  $175.7(1)^\circ$  and a twist angle of  $37.1(1)^\circ$ , whereas the connecting **bipy** linker has a twist angle of  $24.4(1)^\circ$  and fold angle of  $176.3(1)^\circ$ . As in all previous structures, the tetrahedral coordination sphere of the Cu(I) centres is slightly distorted (P-Cu-P:  $112.83(2)^\circ$ , P-Cu-N:  $106.87(5)$ - $108.3(4)^\circ$ , N-Cu-N  $112.4(5)^\circ$ ). The Cu-P ( $2.2785(5)$  and  $2.2967(5)$  Å), Cu-N ( $2.0334(15)$  and  $2.069(13)$  Å) and P-P ( $2.0815(6)$  Å) bond lengths are in accordance to comparable compounds<sup>[17,18,19]</sup> and the free  $\text{P}_2$  ligand complex **A**.<sup>[25]</sup>

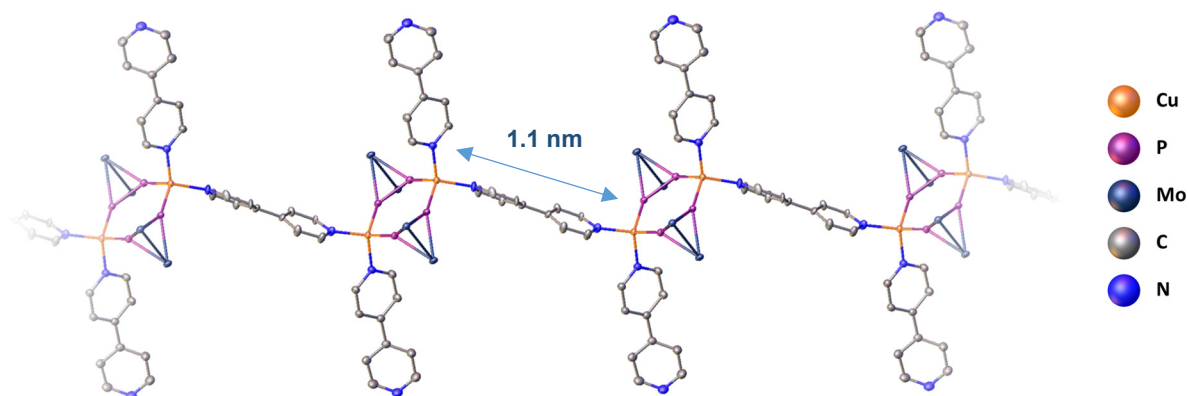


**Figure 3-7.** Molecular structure of the cation of **3-6** in the solid-state, view along the *a*-axis. Thermal ellipsoids are shown at 50 % probability level. Hydrogen atoms, Cp- and CO-ligands, anions and solvent molecules are omitted for clarity. Selected bond length [Å] and angles [°]: Cu1-P1 2.2785(5), Cu1-P2 2.2967(5), Cu1-N1 2.033(2), Cu1-N3 2.07(1), P1-P2 2.0815(6), P1-Cu1-P2 112.83(2), N1-Cu1-P1 106.87(5), N1-Cu1-P2 108.21(5), N3-Cu1-P1 108.2(3), N1-Cu1-N3 112.4(5), N3-Cu1-P2 108.3(4).<sup>[23]</sup>

To further investigate the influence of the WCA on the reaction of **A** with a Cu(I) source and organic linkers, a reaction using **C** and the flexible linker 1,2-bis(4-pyridyl)ethane (**L<sub>flex</sub>2**, **Figure 3-8**) was performed. The analogous reaction using the WCA  $[\text{BF}_4]^-$  and **L<sub>flex</sub>2** selectively yielded 1D CPs, as a former study showed.<sup>[21]</sup> Also other, similar flexible linkers were used in this study with the same result. It was therefore of great interest to perform a similar reaction using the larger WCA  $[\text{FAI}\{\text{O}(\text{C}_6\text{F}_{10})(\text{C}_6\text{F}_5)\}_3]^-$  to examine the influence of the size of the WCA on the system. Therefore, a reaction of **A**, **C** and **L<sub>flex</sub>2** in a ratio of 1.4:1:1 was performed.

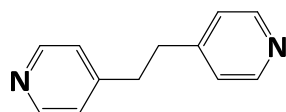


**Figure 3-8.** Organic pyridine-based linker 1,2-bis(4-pyridyl)ethane (**L<sub>flex</sub>2**).

Crystals of compound **3-7** were obtained in 57 % yield as orange blocks. The solid-state structure of **3-7** (**Figure 3-9**), which crystallises in the triclinic space group  $P\bar{1}$ , was determined by single crystal X-ray analysis. Unlike the expected 1D CP, the reaction yielded a 2D CP which possesses structural similarities to compounds **3-1** to **3-4**. Therefore, it can be concluded that the FAI anion, which is significantly bigger compared to  $[\text{BF}_4]^-$ , is the reason for this result. Like in compounds **3-1** to **3-6**, a  $\text{Cu}_2\text{P}_4$  unit serves as node, which are connected to each other via linker molecules. The Cu(I) centres are tetra-coordinated. The size of the cavities of **3-7** (1.5-2.0 nm) are comparable to compounds **3-1** to **3-2**, as the organic linkers  $\text{L}_{\text{lin}}\mathbf{2}$ ,  $\text{L}_{\text{lin}}\mathbf{3}$  and  $\text{L}_{\text{flex}}\mathbf{2}$  have roughly the same length. The Cu-P (2.2619(9)-2.2832(8)Å), Cu-N (2.015(3)- 2.039(3) Å) and P-P (2.079(1), 2.087(1) Å) bond lengths and P-Cu-P (112.22(4), 113.12(3) °) and P-Cu-N (103.3(1), 105.5(1) °) angles are in the expected range (**Table 3-2**) and comparable to compounds **3-1** to **3-2** and other compounds known from literature.<sup>[17,18,19]</sup>

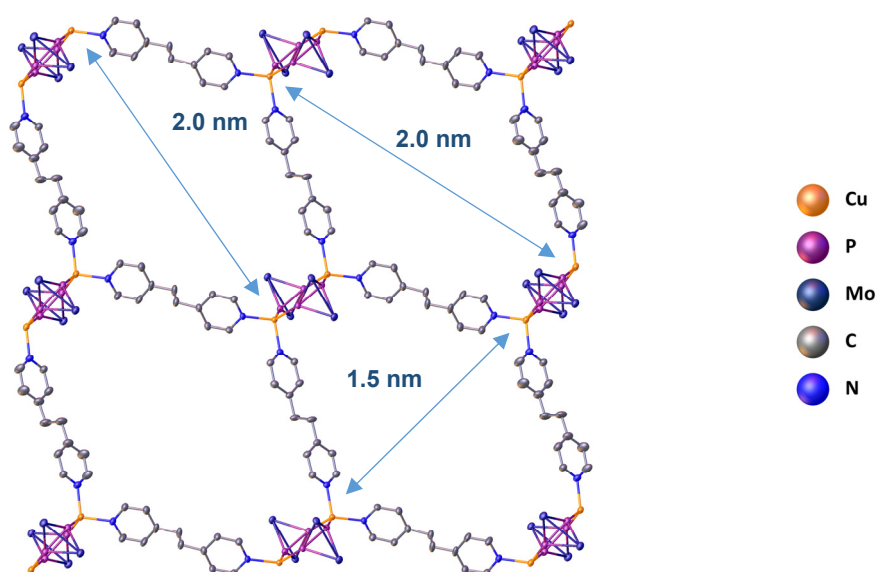
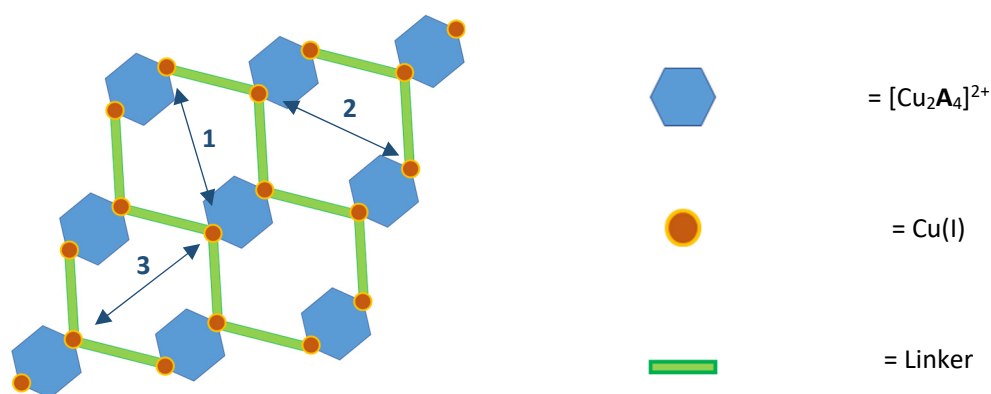


**Figure 3-9.** Molecular structure of the cation of **3-7** in the solid-state, view along the a-axis. Thermal ellipsoids are shown at 50 % probability level. Hydrogen atoms, Cp- and CO-ligands, anions and solvent molecules are omitted for clarity. Average of selected bond lengths [Å] and angles [°]: Cu1-P1 2.2817(8), Cu1-P2 2.2832(8), Cu1-N1 2.024(2), Cu1-N2 2.039(3), Cu2-P3 2.2619(9), Cu2-P4 2.2714(9), Cu2-N3 2.028(3), Cu2-N4 2.015(3), P1-P2 2.087(1), P3-P4 2.079(1), P1-Cu1-P2 113.12(3), P3-Cu2-P4 112.22(4), N1-Cu1-P1 120.01(8), N2-Cu1-P1 103.12(7), N1-Cu1-P2 104.95(8), N2-Cu1-P2 109.69(8), N3-Cu2-P3 110.91(9), N4-Cu2-P3 112.90(9), N4-Cu2-P4 110.11(9), N3-Cu2-P4 106.88(9), N1-Cu1-N2 105.5(1), N4-Cu2-N3 103.3(1).<sup>[23]</sup>

Compound **3-1** to **3-7** are well soluble in acetonitrile, although under dissociation, and insoluble in other common solvents like dichloromethane, tetrahydrofuran, toluene, and *n*-pentane. In the  $^1\text{H}$  NMR spectra (acetonitrile- $d_3$ , r.t.) of **3-1**, **3-2**, **3-3**, **3-6** and **3-7**, the chemical shifts of the Cp protons are similar to the one of the free  $\text{P}_2$  ligand complex **A**. In the  $^{13}\text{C}\{^1\text{H}\}$  NMR spectra, signals which can be assigned to the Cp and CO ligand of **A** and the organic linker can be observed. The  $^{31}\text{P}$  NMR shows signals in the range from -42.26 to -49.58 ppm. As the free  $\text{P}_2$  complex **A** shows a chemical shift of -42.9 ppm in the  $^{31}\text{P}\{^1\text{H}\}$  NMR spectrum,<sup>[24]</sup> it can be concluded from the  $^{31}\text{P}$  NMR chemical shifts of the CPs that there is at least a partial dissociation in solution. In the  $^{19}\text{F}$  NMR spectra (acetonitrile- $d_3$ , r.t.) of compounds **3-1**, **3-2** and **3-3**, the signal for the  $[\text{BF}_4]^-$  anion and in the spectra for **3-4**, **3-5** and **3-7**, the signals for the FAI anion are observed. For compounds **3-1**, **3-2** and **3-3**, the signal for the  $[\text{BF}_4]^-$  anion is observed in the  $^{11}\text{B}$  NMR. In the positive ion ESI-MS spectra ( $\text{CH}_3\text{CN}$ , r.t.) of compound **3-1** to

**3-7**, peaks referring to fragments containing Cu ( $[\text{Cu}(\text{CH}_3\text{CN})]^+$ ,  $[\text{Cu}(\text{CH}_3\text{CN})_2]^+$ ) and the  $\text{P}_2$  ligand complex **A** ( $[\text{Cu}(\text{CH}_3\text{CN})\{\text{Cp}_2\text{Mo}_2(\text{CO})_4\text{P}_2\}]^+$ ,  $[\text{Cu}\{\text{Cp}_2\text{Mo}_2(\text{CO})_4\text{P}_2\}_2]^+$ ) are detected. The mass spectrometric analyses were performed using a solution of the compounds dissolved in acetonitrile. It was therefore expected to only be able to detect fragments of the compounds, which undermines the conclusion drawn from the  $^{31}\text{P}$  NMR results in solution. Additionally to fragments containing Cu and **A**, fragments containing the organic linker can be detected in the positive ion ESI-MS spectra of **3-4** to **3-7**. For **3-4**, **3-6** and **3-5**, the peaks for  $[\text{L}_{\text{lin}}\mathbf{2}]^+$ ,  $[\text{bipy}]^+$  and  $[\text{L}_{\text{lin}}\mathbf{4}]^+$ , respectively, are detected. In the spectra of **3-2** and **3-7** the peak for  $[\text{Cu}(\text{CH}_3\text{CN})(\text{L}_{\text{lin}}\mathbf{3})]^+$  and  $[\text{Cu}(\text{CH}_3\text{CN})(\text{L}_{\text{flex}}\mathbf{2})]^+$ , respectively, are detected. In the spectra of **3-3**, the peaks for  $[\text{L}_{\text{lin}}\mathbf{4}]^+$  and  $[\text{Cu}(\text{L}_{\text{lin}}\mathbf{4})\{\text{Cp}_2\text{Mo}_2(\text{CO})_4\text{P}_2\}]^+$  are detected. The negative ion ESI-MS ( $\text{CH}_3\text{CN}$ , r.t.) shows the peak for the  $[\text{BF}_4]^-$  or  $[\text{FAl}\{\text{O}(\text{C}_6\text{F}_{10})(\text{C}_6\text{F}_5)_3\}]^-$  anion, respectively.

**Table 3-2.** Comparison of the cavity sizes of compounds **3-1-3-4** and **3-7** [nm], as well as Cu-P, Cu-N and P-P bond lengths [ $\text{\AA}$ ] and P-Cu-P and N-Cu-N angles [ $^\circ$ ].<sup>[23]</sup>



Compound	<b>3-1</b>	<b>3-2</b>	<b>3-3</b>	<b>3-4</b>	<b>3-7</b>
Linker	$\text{L}_{\text{lin}}\mathbf{2}$	$\text{L}_{\text{lin}}\mathbf{3}$	$\text{L}_{\text{lin}}\mathbf{4}$	$\text{L}_{\text{lin}}\mathbf{2}$	$\text{L}_{\text{flex}}\mathbf{2}$
Anion	$\text{BF}_4$	$\text{BF}_4$	$\text{BF}_4$	FAl	FAl
1	2.2	2.1	3.1	2.3	2.0
2	2.1	2.2	3.0	2.2	2.0
3	1.6	2.1	2.3	1.2	1.5
Cu-P	2.2745(7), 2.2760(7)	2.239(1)- 2.291(1)	2.2376(9), 2.305(1)	2.2858(6), 2.2957(6)	2.2619(9)- 2.2832(8)
Cu-N	2.010(2), 2.045(2)	2.022(3)- 2.037(3)	2.025(3), 2.045(3)	2.019(2), 2.023(2)	2.015(3)- 2.039(3)
P-P	2.0839(9)	2.080(1), 2.083(1)	2.083(1)	2.0844(8)	2.0787(13), 2.0866(11)
$\sphericalangle$ P-Cu-P	109.54(3)	112.93(4)	108.93(4)	116.06(2)	112.22(4), 113.12(3)
$\sphericalangle$ N-Cu-N	110.06(9)	104.0(1), 104.6(1)	106.2(1)	112.72(8)	103.30(12), 105.48(11)

### 3.4 Conclusion

The  $P_2$  ligand complex  $[\text{Cp}_2\text{Mo}_2(\text{CO})_4(\mu, \eta^{2:2}\text{-P}_2)]$  (**A**) was reacted with Cu(I) WCA salts and organic pyridine-based linkers to synthesise organometallic organic coordination polymers. The reactions of **A** with the Cu(I) salt  $[\text{Cu}(\text{CH}_3\text{CN})_4][\text{BF}_4]$  (**B**) and rigid linkers of varying lengths yielded three new similar 2D CPs with the general formula  $[\text{Cu}_2\{\text{Cp}_2\text{Mo}_2(\text{CO})_4(\mu_4, \eta^{2:2:1:1}\text{-P}_2)\}_2(\mu, \eta^{1:1}\text{-L})_2]_n[\text{BF}_4]_{2n}$  (**L** = **L<sub>lin</sub>2**, **L<sub>lin</sub>3**, **L<sub>lin</sub>4**). These results are in accordance with the expectations, as the formation of one-dimensional polymers is not possible assuming every node has four connecting linker molecules. To investigate the influence of the WCA on the formation of organometallic-organic CPs, similar reacting using a Cu(I) source with a much bigger WCA,  $[\text{Cu}(\text{CH}_3\text{CN})_{3.5}][\text{FAI}]$  (**C**,  $\text{FAI} = \text{FAI}\{\text{O}(\text{C}_6\text{F}_{10})(\text{C}_6\text{F}_5)\}_3$ ), were performed. The reaction with **L<sub>lin</sub>2** also leads to the formation of similar 2D CP, suggesting that the anion plays a minor role. However, the reactions using the longest linker **L<sub>lin</sub>4** and the short linker **bipy**, respectively, lead to very different results. Both reactions yielded novel 1D CPs. In the 1D CP containing **bipy** as linking unit, one of the **bipy** molecules connected to the Cu(I) centres are non-connecting. In the case of **L<sub>lin</sub>4**, also only one unit of linker connects the nodes and the tetragonal coordination sphere of the Cu(I) centres is saturated by acetonitrile. The  $P_2$  ligand complexes **A**, however, are attached to the two Cu(I) centres of the node in a  $\eta^{2:1}$ -coordination mode. This results in a shortened Cu...Cu distance of 2.5927(4) Å as well as shortened Cu-P distances within the node. In those two cases, the choice of WCA has a huge influence on the formation of the final product. Considering the difference in size of the two WCAs  $[\text{BF}_4]^-$  and  $[\text{FAI}]^-$ , the influence on the packing within the unit cell are unsurprising. In a third type of experiment, the Cu(I) salt **C** was reacted with the  $P_2$  ligand complex **A** and the flexible linker **L<sub>flex</sub>2** to compare the influences the linker and the WCA have on the formation of 1D or 2D CPs. Surprisingly, the reaction using the WCA  $[\text{FAI}]^-$  afforded a new 2D CP with a to compounds **3-1** to **3-4** analogous structure. The results have shown that, regarding the system of **A**, Cu(I) and **L<sub>flex</sub>2**, the WCA is the decisive factor. The formation of a 1D CP might have been prevented due to reasons of steric, as  $[\text{FAI}]^-$  is significantly larger than  $[\text{BF}_4]^-$  and therefore too big to be packed within the cavities of a 1D CP.

## 3.5 Supporting Information

### General

All experiments were carried out in an inert atmosphere of nitrogen using standard Schlenk techniques. The nitrogen was dried and purified from traces of oxygen with a Cu/MgSO<sub>4</sub> catalyst, concentrated H<sub>2</sub>SO<sub>4</sub> and orange gel. Reactants were stored in a glovebox under argon atmosphere. All used solvents were taken from the solvent drying machine MB SPS-800 of the company MBRAUN.

### Chemicals

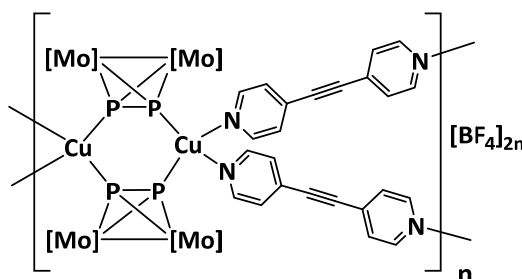
The organic linker 4,4'-bipyridine (**bipy**), 1,2-di(pyridin-4-yl)ethyne (**L<sub>lin</sub>2**), 1,4-di(4-pyridyl)benzene (**L<sub>lin</sub>3**), 4,4'-di(4-pyridyl)biphenyl (**L<sub>lin</sub>4**), 1,2-di(4-pyridyl)ethane (**L<sub>flex</sub>2**) and the copper salt [Cu(CH<sub>3</sub>CN)<sub>4</sub>][BF<sub>4</sub>] (**B**) were purchased from the companies Sigma Aldrich (now Merck) (**bipy**), TCI (**L<sub>lin</sub>3**, **L<sub>lin</sub>4**) and Ark Pharm (**L<sub>lin</sub>2**) and used without further purification. The precursor [Cp<sub>2</sub>Mo<sub>2</sub>(CO)<sub>4</sub>(μ,η<sup>2:2</sup>-P<sub>2</sub>)] (**A**) and the copper salt [Cu(CH<sub>3</sub>CN)<sub>3.5</sub>][FAl{O(C<sub>6</sub>F<sub>10</sub>)(C<sub>6</sub>F<sub>5</sub>)<sub>3</sub>}] (**C**) were prepared according to literature procedures.<sup>[25,16]</sup>

### Spectroscopic Methods

IR spectra were recorded as solids with an ATR-Ge disc on a varian FTS-800 spectrometer. Solution NMR spectra were recorded on a Bruker Avance III HD 400 spectrometer (<sup>1</sup>H: 400 MHz, <sup>31</sup>P: 161 MHz, <sup>13</sup>C: 100 MHz, <sup>19</sup>F: 376 MHz, <sup>11</sup>B: 128 MHz) with acetonitrile-d<sub>3</sub> as solvent at room temperature. The signals of tetramethylsilane (<sup>1</sup>H, <sup>13</sup>C), CFCl<sub>3</sub> (<sup>19</sup>F), Et<sub>2</sub>O x BF<sub>3</sub> (<sup>11</sup>B) and 85% H<sub>3</sub>PO<sub>4</sub> (<sup>31</sup>P) were used as reference for determining chemical shifts. The chemical shifts δ are presented in parts per million ppm and coupling constants *J* in Hz. The spectra were processed and analysed using the software Bruker TopSpin 3.0. Elemental analyses were performed on an Elementar vario MICRO cube apparatus. Mass spectra were recorded on an Agilent Q-TOF 6540 UHD mass spectrometer with acetonitrile as solvent.

### Experimental Procedures

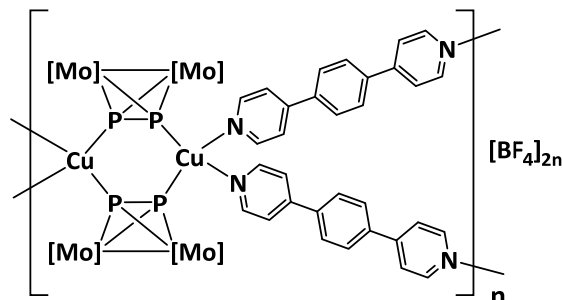
Synthesis of [Cu<sub>2</sub>{Cp<sub>2</sub>Mo<sub>2</sub>(CO)<sub>4</sub>(μ,η<sup>2:2:1:1</sup>-P<sub>2</sub>)<sub>2</sub>(η,μ<sup>1:1</sup>-C<sub>12</sub>H<sub>8</sub>N<sub>2</sub>)<sub>2</sub>]<sub>n</sub>[BF<sub>4</sub>]<sub>2n</sub> (**3-1**):



Compounds **A** (1 eq., 25 mg, 0.05 mmol), **B** (1 eq., 15.7 mg, 0.05 mmol) and **L<sub>lin</sub>2** (1 eq., 9.0 mg, 0.05 mmol) were dissolved in a mixture of dichloromethane (5 mL) and acetonitrile (1 mL). The reaction was stirred for 30 min, filtrated and layered with *n*-pentane/dichloromethane (1:1). After one day compound **3-1** can be obtained as orange blocks. The supernatant was decanted off, the remaining

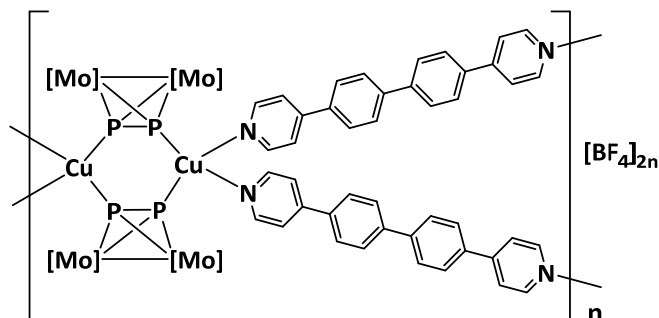
crystals washed with *n*-pentane and dried in vacuo. Crystalline Yield: 17 mg (41 %, related to **A**, **B** and **L<sub>in</sub>2** equally). <sup>1</sup>H NMR: δ[ppm] = 8.63 (dd, 4H, CH<sub>pyr</sub>), 7.49 (dd, 4H, CH<sub>arom</sub>), 5.31 (s, 10H, C<sub>5</sub>H<sub>5</sub>). <sup>31</sup>P NMR: δ[ppm] = -43.6 (s). <sup>13</sup>C{<sup>1</sup>H} NMR: δ[ppm] = 151.1 (s, CH<sub>pyr</sub>), 126.5 (s, CH<sub>pyr</sub>), 87.4 (s, C<sub>5</sub>H<sub>5</sub>). <sup>19</sup>F NMR: δ[ppm] = -150.7 (s). <sup>11</sup>B NMR: δ[ppm] = 0.56 (s). Positive ion ESI-MS (CH<sub>3</sub>CN, r.t.): *m/z* (%) = 599.77 (100) [Cu(CH<sub>3</sub>CN){Cp<sub>2</sub>Mo<sub>2</sub>(CO)<sub>4</sub>P<sub>2</sub>}]<sup>+</sup>, 1055.56 (43.3) [Cu{Cp<sub>2</sub>Mo<sub>2</sub>(CO)<sub>4</sub>P<sub>2</sub>}]<sup>+</sup>. IR (Ge-ATR):  $\tilde{\nu}$ /cm<sup>-1</sup>: 1966 (s), 1929 (s), 1905 (s). Elemental analysis calculated for C<sub>26</sub>H<sub>18</sub>BCuF<sub>4</sub>Mo<sub>2</sub>N<sub>2</sub>O<sub>4</sub>P<sub>2</sub> (826.6 g·mol<sup>-1</sup>): 37.78 %C, 2.19 %H, 3.39 %N; Found: 37.66 %C, 2.15 %H, 3.39 %N.

Synthesis of [Cu<sub>2</sub>{Cp<sub>2</sub>Mo<sub>2</sub>(CO)<sub>4</sub>(μ,η<sup>2:2:1:1</sup>-P<sub>2</sub>)<sub>2</sub>(μ,η<sup>1</sup>-C<sub>16</sub>H<sub>12</sub>N<sub>2</sub>)<sub>2</sub>]<sub>n</sub>[BF<sub>4</sub>]<sub>2n</sub> (**3-2**):



Compounds **A** (1.4 eq., 35 mg, 0.07 mmol), **B** (1 eq., 15.7 mg, 0.05 mmol) and **L<sub>in</sub>3** (1 eq., 11.6 mg, 0.05 mmol) were dissolved in a mixture of acetonitrile (1 mL) and dichloromethane (10 mL). Additional acetonitrile (1 mL) was added to clear the turbid solution and the reaction was stirred for 3h, filtrated and layered with *n*-pentane/dichloromethane (1:1). After one day, compound **3-2** was obtained as orange blocks. The supernatant was decanted off, the remaining crystals washed with *n*-pentane and dried in vacuo. Crystalline Yield: 5.1 mg (12 %, related to **A**, **B** and **L<sub>in</sub>3** equally). <sup>1</sup>H NMR δ[ppm] = 8.64 (dd, 4H, CH<sub>pyr</sub>), 7.91 (s, 4H, CH<sub>arom</sub>), 7.71 (dd, 4H, CH<sub>arom</sub>), 5.32 (s, 10H, C<sub>5</sub>H<sub>5</sub>). <sup>31</sup>P NMR δ[ppm] = -46.5 (s). <sup>13</sup>C{<sup>1</sup>H} NMR δ[ppm] = 226.7 (s, CO), 151.3 (s, C<sub>arom</sub>), 148.1 (s, CH<sub>pyr</sub>), 139.5 (s, C<sub>arom</sub>), 128.8 (s, CH<sub>arom</sub>), 122.6 (s, CH<sub>pyr</sub>), 87.5 (s, C<sub>5</sub>H<sub>5</sub>). <sup>19</sup>F NMR δ[ppm] = -150.68 (s). <sup>11</sup>B NMR δ[ppm] = 0.56 (s). Positive ion ESI-MS (CH<sub>3</sub>CN, r.t.): *m/z* (%) = 103.96 (100) [Cu(CH<sub>3</sub>CN)]<sup>+</sup>, 144.98 (199) [Cu(CH<sub>3</sub>CN)<sub>2</sub>]<sup>+</sup>, 336.06 (100) [Cu(CH<sub>3</sub>CN)(C<sub>16</sub>H<sub>12</sub>N<sub>2</sub>)]<sup>+</sup>, 599.77 (100) [Cu(CH<sub>3</sub>CN){Cp<sub>2</sub>Mo<sub>2</sub>(CO)<sub>4</sub>P<sub>2</sub>}]<sup>+</sup>, 1055.56 (56.2) [Cu{Cp<sub>2</sub>Mo<sub>2</sub>(CO)<sub>4</sub>P<sub>2</sub>}]<sup>+</sup>. Negative ion ESI-MS (CH<sub>3</sub>CN, r.t.): *m/z* (%) = 87.00 (100) [BF<sub>4</sub>]<sup>-</sup>. IR (Ge-ATR):  $\tilde{\nu}$ /cm<sup>-1</sup>: 1965 (s), 1940 (s), 1927 (s). Elemental analysis calculated for C<sub>30</sub>H<sub>22</sub>BCuF<sub>4</sub>Mo<sub>2</sub>N<sub>2</sub>O<sub>4</sub>P<sub>2</sub> (878.68 g·mol<sup>-1</sup>): 41.0 %C, 2.52 %H, 3.19 %N; Found: 40.83 %C, 2.50 %H, 3.34 %N.

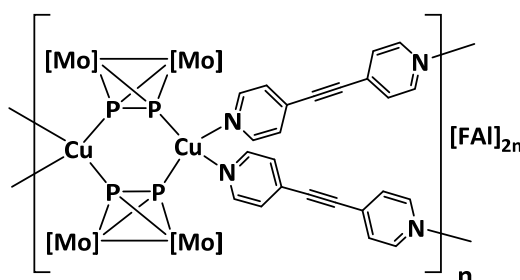
Synthesis of [Cu<sub>2</sub>{Cp<sub>2</sub>Mo<sub>2</sub>(CO)<sub>4</sub>(μ,η<sup>2:2:1:1</sup>-P<sub>2</sub>)<sub>2</sub>(μ,η<sup>1:1</sup>-C<sub>22</sub>H<sub>16</sub>N<sub>2</sub>)<sub>2</sub>]<sub>n</sub>[BF<sub>4</sub>]<sub>2</sub> (**3-3**):



Compounds **A** (2 eq., 50 mg, 0.1 mmol), **B** (1 eq., 15.7 mg, 0.05 mmol) and **L<sub>in</sub>4** (1 eq., 15.4 mg, 0.05 mmol) were dissolved in a mixture of acetonitrile (2 mL) and dichloromethane (10 mL). The reaction

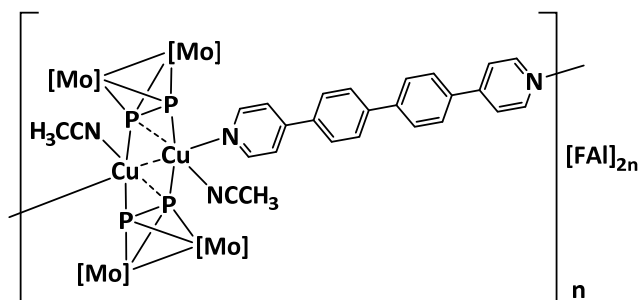
was stirred for 3 h, filtrated and layered with toluene. After one day, compound **3-3** was obtained as clear orange blocks. The supernatant was decanted off, the remaining crystals washed with *n*-pentane and dried in vacuo. Crystalline Yield: a few crystals (<5 %).  $^1\text{H}$  NMR  $\delta$ [ppm] = 8.64 (dd, 4H,  $\text{CH}_{\text{pyr}}$ ), 7.90 (s, 8H,  $\text{CH}_{\text{arom}}$ ), 7.75 (dd, 4H,  $\text{C}_{\text{H}_{\text{arom}}}$ ), 5.31 (s, 10 H,  $\text{C}_5\text{H}_5$ ).  $^{31}\text{P}$  NMR  $\delta$ [ppm] = -44.1 (s).  $^{13}\text{C}\{^1\text{H}\}$  NMR  $\delta$ [ppm] = 226.7 (s,  $\text{CO}$ ), 87.4 (s,  $\text{C}_5\text{H}_5$ ).  $^{19}\text{F}$  NMR  $\delta$ [ppm] = -150.6 (s).  $^{11}\text{B}$  NMR  $\delta$ [ppm] = 0.56 (s). Positive ion ESI-MS ( $\text{CH}_3\text{CN}$ , r.t.):  $m/z$  (%) = 103.96 (100)  $[\text{Cu}(\text{CH}_3\text{CN})]^+$ , 144.98 (100)  $[\text{Cu}(\text{CH}_3\text{CN})_2]^+$ , 309.14 (100)  $[\text{C}_{22}\text{H}_{17}\text{N}_2]^+$ , 599.77 (100)  $[\text{Cu}(\text{CH}_3\text{CN})\{\text{Cp}_2\text{Mo}_2(\text{CO})_4\text{P}_2\}]^+$ , 866.88 (55.5)  $[\text{Cu}(\text{C}_{22}\text{H}_{16}\text{N}_2)\{\text{Cp}_2\text{Mo}_2(\text{CO})_4\text{P}_2\}]^+$ , 1055.56 (56.2)  $[\text{Cu}\{\text{Cp}_2\text{Mo}_2(\text{CO})_4\text{P}_2\}]^+$ . Negative ion ESI-MS ( $\text{CH}_3\text{CN}$ , r.t.):  $m/z$  (%) = 87.00 (100)  $[\text{BF}_4]^-$ . IR (Ge-ATR):  $\tilde{\nu}/\text{cm}^{-1}$ : 1963 (s), 1941 (s), 1925 (s).

Synthesis of  $[\text{Cu}_2\{\text{Cp}_2\text{Mo}_2(\text{CO})_4(\mu, \eta^{2:2:1:1}\text{-P}_2)\}_2(\mu, \eta^{1:1}\text{-C}_{12}\text{H}_8\text{N}_2)_2]_n[\text{FAI}]_{2n}$  (**3-4**):



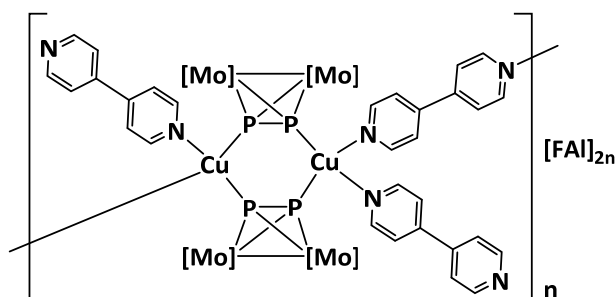
Compounds **A** (1 eq., 25 mg, 0.05 mmol), **C** (1 eq., 79.4 mg, 0.05 mmol) and **L<sub>in</sub>2** (1 eq., 9 mg, 0.05 mmol) were dissolved in a mixture of acetonitrile (1 mL) and dichloromethane (5 mL). The reaction was stirred for 30 min, filtrated, and layered with *n*-pentane. After one day, compound **3-4** was obtained as orange blocks. The supernatant was decanted off, the remaining crystals were washed with *n*-pentane and dried in vacuo. Crystalline Yield: 21.6 mg (20 %, related to **A**, **C** and **L<sub>in</sub>2** equally).  $^1\text{H}$  NMR  $\delta$ [ppm] = 8.62 (dd, 4H,  $\text{CH}_{\text{pyr}}$ ), 7.51 (dd, 4H,  $\text{CH}_{\text{arom}}$ ), 5.32 (s, 10 H,  $\text{C}_5\text{H}_5$ ).  $^{31}\text{P}$  NMR  $\delta$ [ppm] = -49.6 (s).  $^{13}\text{C}\{^1\text{H}\}$  NMR  $\delta$ [ppm] = 226.4 (s,  $\text{CO}$ ), 151.0 (s,  $\text{CH}_{\text{pyr}}$ ), 131.0 (s,  $\text{CH}_{\text{pyr}}$ ), 126.71 (s,  $\text{C}_{\text{arom}}$ ), 91.3 (s,  $\text{C}\equiv\text{C}$ ), 87.45 (s,  $\text{C}_5\text{H}_5$ ), 55.3 (s,  $\text{C}\equiv\text{C}$ ).  $^{19}\text{F}$  NMR  $\delta$ [ppm] = -111.7 (d,  $J_{\text{F-F}} = 275$  Hz,  $\text{CF}_2$ ), -116.1 (d,  $J_{\text{F-F}} = 279$  Hz,  $\text{CF}_2$ ), -121.1 (d,  $J_{\text{F-F}} = 277$  Hz,  $\text{CF}_2$ ), -127.9 (s,  $\text{CF}_2$ ), -130.0 (d,  $J_{\text{F-F}} = 275$  Hz,  $\text{CF}_2$ ), -136.5 (d,  $J_{\text{F-F}} = 276$  Hz,  $\text{CF}_2$ ), -140.8 (d,  $J_{\text{F-F}} = 277$ ,  $\text{CF}$ ), -154.0 (t,  $J_{\text{F-F}} = 22$  Hz,  $\text{CF}$ ), -164.7 (t,  $J_{\text{F-F}} = 18$  Hz,  $\text{CF}$ ), -170.7 (s,  $\text{AlF}$ ). Positive ion ESI-MS ( $\text{CH}_3\text{CN}$ , r.t.):  $m/z$  (%) = 181.08 (100)  $[\text{C}_{12}\text{H}_9\text{N}_2]^+$ , 599.77 (100)  $[\text{Cu}(\text{CH}_3\text{CN})\{\text{Cp}_2\text{Mo}_2(\text{CO})_4\text{P}_2\}]^+$ , 1056.56 (60.5)  $[\text{Cu}\{\text{Cp}_2\text{Mo}_2(\text{CO})_4\text{P}_2\}]^+$ . Negative ion ESI-MS ( $\text{CH}_3\text{CN}$ , r.t.):  $m/z$  (%) = 1380.9 (100)  $[\text{FAI}\{\text{O}(\text{C}_6\text{F}_{10})(\text{C}_6\text{F}_5)_3\}]^-$ . IR (Ge-ATR):  $\tilde{\nu}/\text{cm}^{-1}$ : 2002 (s), 1992 (s), 1953 (s), 1941 (s). Elemental analysis calculated for  $\text{C}_{62}\text{H}_{18}\text{AlCuF}_{46}\text{Mo}_2\text{N}_2\text{O}_7\text{P}_2$  (2121, 10  $\text{g}\cdot\text{mol}^{-1}$ ): 35.1 %C, 0.86 %H, 1.32 %N; Found: 34.95 %C, 0.85 %H, 1.32 %N.

Synthesis of  $[\text{Cu}_2\{\text{Cp}_2\text{Mo}_2(\text{CO})_4(\mu, \eta^{2:2:1:1}\text{-P}_2)\}_2(\text{CH}_3\text{CN})_2(\mu, \eta^{1:1}\text{-C}_{22}\text{H}_{16}\text{N}_2)]_n[\text{FAI}]_{2n}$  (**3-5**):



Compounds **A** (1 eq., 50 mg, 0.1 mmol), **C** (1 eq., 159 mg, 0.1 mmol) and **L<sub>lin</sub>4** (1 eq., 31 mg, 0.1 mmol) were dissolved in a 1:1-mixture of dichloromethane and acetonitrile (10 mL). The reaction was stirred for 3 h, filtrated and layered with *n*-pentane/dichloromethane (1:1) and another layer of pure *n*-pentane. After one day, compound **3-5** was obtained as clear orange blocks. The supernatant was decanted off, the remaining crystals washed with *n*-pentane and dried in vacuo. Crystalline Yield: 74 mg (65 %). Positive ion ESI-MS (CH<sub>3</sub>CN, r.t.): *m/z* (%) = 103.96 (100) [Cu(CH<sub>3</sub>CN)]<sup>+</sup>, 144.98 (100) [Cu(CH<sub>3</sub>CN)<sub>2</sub>]<sup>+</sup>, 309.14 (100) [C<sub>22</sub>H<sub>17</sub>N<sub>2</sub>]<sup>+</sup>, 599.77 (100) [Cu(CH<sub>3</sub>CN){Cp<sub>2</sub>Mo<sub>2</sub>(CO)<sub>4</sub>P<sub>2</sub>}]<sup>+</sup>, 1056.56 (60.5) [Cu{Cp<sub>2</sub>Mo<sub>2</sub>(CO)<sub>4</sub>P<sub>2</sub>}]<sup>+</sup>. Negative ion ESI-MS (CH<sub>3</sub>CN, r.t.): *m/z* (%) = 1380.9 (100) [FAI{O(C<sub>6</sub>F<sub>10</sub>)(C<sub>6</sub>F<sub>5</sub>)<sub>3</sub>}]<sup>-</sup>. IR (Ge-ATR):  $\tilde{\nu}/\text{cm}^{-1}$ : 1990 (vs), 1944 (vs). Elemental analysis calculated for C<sub>63</sub>H<sub>21</sub>AlCuF<sub>46</sub>Mo<sub>2</sub>N<sub>2</sub>O<sub>7</sub>P<sub>2</sub> · 0.92 CH<sub>3</sub>CN · 0.08 CH<sub>2</sub>Cl<sub>2</sub> (2183.19 g·mol<sup>-1</sup>): 2183.19 %C, 1.10 %H, 1.87 %N; Found: 35.83 %C, 0.95 %H, 1.69 %N.

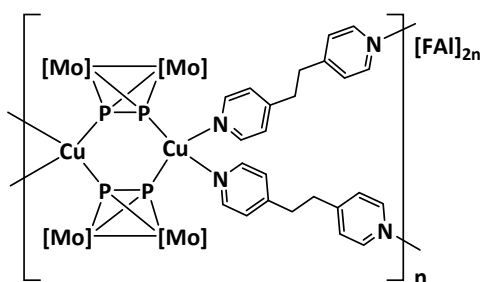
Synthesis of [Cu<sub>2</sub>{Cp<sub>2</sub>Mo<sub>2</sub>(CO)<sub>4</sub>(μ,η<sup>2:2:1:1</sup>-P<sub>2</sub>)<sub>2</sub>(C<sub>10</sub>H<sub>8</sub>N<sub>2</sub>)<sub>2</sub>(η<sup>1:1</sup>-C<sub>10</sub>H<sub>8</sub>N<sub>2</sub>)<sub>n</sub>][BF<sub>4</sub>]<sub>2n</sub> (**3-6**):



Compounds **A** (1.2 eq., 30 mg, 0.06 mmol), **C** (1 eq., 79.4 mg, 0.05 mmol) and **bipy** (1 eq., 7.8 mg, 0.05 mmol) were each dissolved in dichloromethane (5 mL). The solution of the Cu(I) salt **C** and the linker **bipy** were slowly given to the solution of **A** after one another and the reaction was stirred overnight. Acetonitrile (2.5 mL) was added to dissolve the light-brown precipitate and the reaction was further stirred for 2 h. After filtration, the mixture was layered with a layer of *n*-pentane/dichloromethane (1:1, 2 mL) and a further layer of pure hexane. After one day, compound **3-6** was obtained as orange blocks. The supernatant was decanted off, the remaining crystals washed with *n*-pentane and dried in vacuo. Crystalline Yield: 26 mg (35 %, related to **bipy**). <sup>1</sup>H NMR δ[ppm] = 8.70 (m, 4H, CH<sub>pyr</sub>), 7.68 (m, 4H, CH<sub>pyr</sub>), 5.31(s, 10H, C<sub>5</sub>H<sub>5</sub>). <sup>31</sup>P NMR δ[ppm] = -42.3 (s). <sup>13</sup>C{<sup>1</sup>H} NMR δ[ppm] = 151.6 (s, CH<sub>pyr</sub>), 122.4 (s, CH<sub>pyr</sub>), 87.4 (s, C<sub>5</sub>H<sub>5</sub>). <sup>19</sup>F NMR δ[ppm] = -111.7 (d, J<sub>F-F</sub> = 275 Hz, 2F), -116.1 (d, J<sub>F-F</sub> = 279 Hz, 2F), -121.1 (d, J<sub>F-F</sub> = 277 Hz, 2F), -127.9 (s, 2F), -129.7 (d, J<sub>F-F</sub> = 275 Hz, 2F), -136.5 (d, J<sub>F-F</sub> = 276 Hz, 2F), -140.8 (d, J<sub>F-F</sub> = 277, 1F), -154.0 (t, J<sub>F-F</sub> = 22 Hz, 1F), -164.7 (t, J<sub>F-F</sub> = 18 Hz, 1F), -170.7 (s, AlF). Positive ion ESI-MS (CH<sub>3</sub>CN, r.t.): *m/z* (%) = 103.96 (100) [Cu(CH<sub>3</sub>CN)]<sup>+</sup>, 144.98 (100) [Cu(CH<sub>3</sub>CN)<sub>2</sub>]<sup>+</sup>, 157.07 (10.8) [C<sub>10</sub>H<sub>8</sub>N<sub>2</sub>]<sup>+</sup>, 599.77 (100) [Cu(CH<sub>3</sub>CN){Cp<sub>2</sub>Mo<sub>2</sub>(CO)<sub>4</sub>P<sub>2</sub>}]<sup>+</sup>, 1056.56 (60.5) [Cu{Cp<sub>2</sub>Mo<sub>2</sub>(CO)<sub>4</sub>P<sub>2</sub>}]<sup>+</sup>. Negative ion ESI-MS (CH<sub>3</sub>CN, r.t.): *m/z* (%) = 1380.9 (100) [FAI{O(C<sub>6</sub>F<sub>10</sub>)(C<sub>6</sub>F<sub>5</sub>)<sub>3</sub>}]<sup>-</sup>. IR (Ge-ATR):  $\tilde{\nu}/\text{cm}^{-1}$ : 1992 (ws), 1950 (ws), 1935 (ws). Elemental analysis calculated for AlC<sub>65</sub>CuF<sub>46</sub>H<sub>22</sub>Mo<sub>2</sub>N<sub>3</sub>O<sub>7</sub>P<sub>2</sub> (2177,74 g·mol<sup>-1</sup>): 35.82 %C, 1.02 %H, 1.93 %N; Found: 35.61 %C, 0.79 %H, 1.86 %N.



Synthesis of  $[\text{Cu}_2\{\text{Cp}_2\text{Mo}_2(\text{CO})_4(\mu, \eta^{2:2:1:1}\text{-P}_2)_2(\mu, \eta^1\text{-C}_{12}\text{H}_{12}\text{N}_2)_2\}]_n[\text{FAI}]_{2n}$  (**3-7**):



Compounds **A** (1.4 eq., 35 mg, 0.07 mmol), **C** (1 eq., 79.4 mg, 0.05 mmol) and **L<sub>flex</sub>2** (1 eq., 9.2 mg, 0.05 mmol) were dissolved in a mixture of acetonitrile (1 mL) and dichloromethane (10 mL). Additional acetonitrile (2 mL) was added to clear the turbid mixture and the reaction was stirred for 3 h. After filtration, the mixture was layered with *n*-pentane/dichloromethane (1:1). After one day, compound **3-7** was obtained as orange blocks. The supernatant was decanted off, the remaining crystals washed with *n*-pentane and dried in vacuo. Crystalline Yield: 59 mg (57 %, related to **CuFAI**).  $^1\text{H}$  NMR  $\delta$ [ppm] = 8.42 (d, 4H,  $\text{CH}_{\text{pyr}}$ ), 7.19 (d, 4H,  $\text{CH}_{\text{pyr}}$ ), 5.31 (s, 10H,  $\text{C}_5\text{H}_5$ ), 2.97 (s, 4H,  $\text{CH}_2$ ).  $^{31}\text{P}$  NMR  $\delta$ [ppm] = -43.5 (s).  $^{13}\text{C}\{^1\text{H}\}$  NMR  $\delta$ [ppm] = 226.8 (s,  $\text{CO}$ ), 150.6 (s,  $\text{CH}_{\text{pyr}}$ ), 125.0 (s,  $\text{CH}_{\text{pyr}}$ ), 87.4 (s,  $\text{C}_5\text{H}_5$ ), 35.9 (s,  $\text{CH}_2$ ).  $^{19}\text{F}$  NMR  $\delta$ [ppm] = -111.6 (d,  $J_{\text{F-F}} = 275$  Hz,  $\text{CF}_2$ ), -116.1 (d,  $J_{\text{F-F}} = 279$  Hz,  $\text{CF}_2$ ), -121.1 (d,  $J_{\text{F-F}} = 277$  Hz,  $\text{CF}_2$ ), -127.8 (s,  $\text{CF}_2$ ), -129.6 (d,  $J_{\text{F-F}} = 275$  Hz,  $\text{CF}_2$ ), -136.5 (d,  $J_{\text{F-F}} = 276$  Hz,  $\text{CF}_2$ ), -140.8 (d,  $J_{\text{F-F}} = 277$ ,  $\text{CF}$ ), -154.0 (t,  $J_{\text{F-F}} = 22$  Hz,  $\text{CF}$ ), -164.7 (t,  $J_{\text{F-F}} = 18$  Hz,  $\text{CF}$ ), -170.6 (s,  $\text{AlF}$ ). Positive ion ESI-MS ( $\text{CH}_3\text{CN}$ , r.t.):  $m/z$  (%) = 103.96 (100)  $[\text{Cu}(\text{CH}_3\text{CN})]^+$ , 144.98 (100)  $[\text{Cu}(\text{CH}_3\text{CN})_2]^+$ , 288.06 (100)  $[\text{Cu}(\text{C}_{12}\text{H}_{12}\text{N}_2)(\text{CH}_3\text{CN})]^+$ , 599.77 (100)  $[\text{Cu}(\text{CH}_3\text{CN})\{\text{Cp}_2\text{Mo}_2(\text{CO})_4\text{P}_2\}]^+$ , 1056.56 (60.5)  $[\text{Cu}\{\text{Cp}_2\text{Mo}_2(\text{CO})_4\text{P}_2\}_2]^+$ . Negative ion ESI-MS ( $\text{CH}_3\text{CN}$ , r.t.):  $m/z$  (%) = 1380.89 (100)  $[\text{FAI}\{\text{O}(\text{C}_6\text{F}_{10})(\text{C}_6\text{F}_5)_3\}_3]^-$ . IR (Ge-ATR):  $\tilde{\nu}/\text{cm}^{-1}$ : 1995 (ws), 1945 (ws). Elemental analysis calculated for  $\text{C}_{124}\text{H}_{44}\text{Al}_2\text{Cu}_2\text{F}_{92}\text{Mo}_4\text{N}_4\text{O}_{14}\text{P}_4 \cdot 2 \text{CH}_3\text{CN}$  ( $4337.53 \text{ g}\cdot\text{mol}^{-1}$ ): 35.91 %C, 1.10 %H, 1.62 %N; Found: 35.67 %C, 1.11 %H, 1.49 %N.

## Crystallographic Details

**Crystal Structure Analysis:** The crystals were selected and mounted on a suitable support on a Gemini Ultra diffractometer equipped with an Atlas S2 CCD detector (**3-1b**, **3-3**, **3-4**, **3-5**, **3-6**) or on a GV50 diffractometer equipped with a Titan S2 CCD detector (**3-1a**, **3-2**, **3-7**), respectively. The crystals were kept at  $T = 123(1)$  K during data collection. Data collection and reduction were performed with **CrysAlisPro** [Version 171.39.37b, 2017 (**3-1a**, **3-1b**, **3-6**), 171.40.14a, 2018 (**3-2**, **3-4**, **3-5**, **3-7**), 171.41.21a, 2019 (**3-3**)].<sup>[26]</sup> For the compounds **3-1b**, **3-3**, **3-4**, **3-5** and **3-6** an analytical numeric absorption correction using a multifaceted crystal model based on expressions derived by R.C. Clark & J.S. Reid<sup>[27]</sup> and an empirical absorption correction using spherical harmonics as implemented in SCALE3 ABSPACK were applied. For the compounds **3-1a**, **3-2** and **3-7**, a numerical absorption correction based on gaussian integration over a multifaceted crystal model and an empirical absorption correction using spherical harmonics as implemented in SCALE3 ABSPACK were applied. Using **Olex2**,<sup>[28]</sup> the structures were solved with **ShelXT**<sup>[29]</sup> and a least-square refinement on  $F^2$  was carried out with **ShelXL**.<sup>[30]</sup> All non-hydrogen atoms were refined anisotropically. Hydrogen atoms at the carbon atoms were located in idealised positions and refined isotropically according to the riding model.

**Compound 3-1a:** The asymmetric unit contains 0.47  $\text{CH}_2\text{Cl}_2$  and 1.46  $\text{CH}_3\text{CN}$  solvent molecules. The two solvent positions are respectively occupied with a  $\text{CH}_2\text{Cl}_2$  molecule and an over two positions disordered  $\text{CH}_3\text{CN}$  molecule (40:39:21; 7:72:14). Further, the asymmetric unit contains a  $\text{BF}_4$  anion, half the complex  $[\text{Cu}_2(\eta^{1:1}\text{-A})_2]$  and two times half the linker **L<sub>lin</sub>2**. To model the solvent molecules the restraints DFIX, SADI, SIMU and RIGU were applied.

**Compound 3-1b:** The asymmetric unit contains 1.85  $\text{CH}_2\text{Cl}_2$  solvent molecules. For one of these  $\text{CH}_2\text{Cl}_2$  molecules a Cl atom is disordered over two positions (52:48). Further, the asymmetric unit contains a  $\text{BF}_4$  anion, half the complex  $[\text{Cu}_2(\eta^{1:1}\text{-A})_2]$  and two times half the linker **L<sub>lin</sub>2**. The SIMU restraint was used to model the disorder of the Cl atom.

**Compound 3-2:** The asymmetric unit contains 3.9  $\text{CH}_2\text{Cl}_2$  solvent molecules. It further contains two times half the complex  $[\text{Cu}_2(\eta^{1:1}\text{-A})_2]$ , two linker molecules **L<sub>lin</sub>3** and two  $\text{BF}_4$  molecules, which are located on three positions. One of these  $\text{BF}_4$  molecules is disordered over two position (63:37) and half a  $\text{BF}_4$  molecule is located near an inversion centre. The restraints DFIX, SADI, SIMU and RIGU were applied to model the disordered  $\text{BF}_4$  molecule as well as the partly occupied  $\text{BF}_4$  and  $\text{CH}_3\text{CN}$  molecules.

**Compound 3-3:** The asymmetric unit contains 3  $\text{CH}_2\text{Cl}_2$  solvent molecules. These  $\text{CH}_2\text{Cl}_2$  molecules are heavily disordered and therefore a solvent mask was calculated and 476.0 electrons were found in a volume of  $1604.0\text{\AA}^3$  in one void. This is consistent with the presence of three  $\text{CH}_2\text{Cl}_2$  molecules per formula unit, which account for 504.0 electrons. Further the asymmetric unit contains one  $\text{BF}_4$  molecule, half the complex  $[\text{Cu}_2(\eta^{1:1}\text{-A})_2]$  and one linker molecule **L<sub>lin</sub>4**. The  $\text{BF}_4$  molecule is disordered over two positions (61:39). To describe this disorder the restraints SADI and SIMU were applied.

**Compound 3-4:** The asymmetric unit contains 1  $\text{CH}_2\text{Cl}_2$  solvent molecules, which is disordered over two positions (70:30). Additionally, the asymmetric unit contains the  $[\text{FAl}\{\text{O}(\text{C}_6\text{F}_{10})(\text{C}_6\text{F}_5)\}_3]$  anion, half the complex  $[\text{Cu}_2(\eta^{1:1}\text{-A})_2]$  and the linker **L<sub>lin</sub>2**. The restraints SADI and SIMU were used to describe the disorder of the  $\text{CH}_2\text{Cl}_2$  molecule.

**Compound 3-5:** The asymmetric unit contains 0.08  $\text{CH}_2\text{Cl}_2$  and 1.92  $\text{CH}_3\text{CN}$  molecules, one  $\text{CH}_3\text{CN}$  molecule share the same position as a  $\text{CH}_2\text{Cl}_2$  molecule (92:8). The second  $\text{CH}_3\text{CN}$  molecule is coordinated to a Cu(I) atom. Further, the asymmetric unit contains a  $[\text{FAl}\{\text{O}(\text{C}_6\text{F}_{10})(\text{C}_6\text{F}_5)\}_3]$  anion, half

the complex  $[\text{Cu}_2(\eta^{1:1}\text{-A})_2]$  and half a linker molecule  $\text{L}_{\text{lin}}\mathbf{4}$ . The restraints DFIX, SADI and SIMU were used to model the  $\text{CH}_2\text{Cl}_2$  molecule.

Compound **3-6**: The asymmetric unit contains 1.7  $\text{CH}_2\text{Cl}_2$  solvent molecules. One  $\text{CH}_2\text{Cl}_2$  molecules was heavily disordered. Therefore, a solvent mask was calculated and 112 electrons were found in a volume of  $524\text{\AA}^3$  in one void. This is consistent with the presence of 0.7  $\text{CH}_2\text{Cl}_2$  per formula unit, which account for 117.6 electrons. Additionally, the asymmetric unit contains the  $[\text{FAl}\{\text{O}(\text{C}_6\text{F}_{10})(\text{C}_6\text{F}_5)\}_3]$  anion, half the complex  $[\text{Cu}_2(\eta^{1:1}\text{-A})_2]$  and the linker **bipy**.

Compound **3-7**: The asymmetric unit contains 5.6  $\text{CH}_2\text{Cl}_2$  and 2  $\text{CH}_3\text{CN}$  solvent molecules. Four of the  $\text{CH}_2\text{Cl}_2$  molecules and the two  $\text{CH}_3\text{CN}$  molecules were heavily disordered. Therefore, a solvent mask was calculated and 440.0 electrons were found in a volume of  $1471\text{\AA}^3$  in one void. This is consistent with the presence of 4  $\text{CH}_2\text{Cl}_2$  and 2  $\text{CH}_3\text{CN}$  molecules per formula unit, which account for 424.0 electrons. The asymmetric unit further contains two times half the complex  $[\text{Cu}_2(\eta^{1:1}\text{-A})_2]$ , two  $[\text{FAl}\{\text{O}(\text{C}_6\text{F}_{10})(\text{C}_6\text{F}_5)\}_3]$  anions and two linker molecules  $\text{L}_{\text{flex}}\mathbf{2}$ . For one  $[\text{FAl}\{\text{O}(\text{C}_6\text{F}_{10})(\text{C}_6\text{F}_5)\}_3]$  anion a  $\text{C}_6\text{F}_5$  group is disordered over two positions (70:30) and for the other  $[\text{FAl}\{\text{O}(\text{C}_6\text{F}_{10})(\text{C}_6\text{F}_5)\}_3]$  anion a  $\{\text{O}(\text{C}_6\text{F}_{10})(\text{C}_6\text{F}_5)\}$  group and a  $(\text{C}_6\text{F}_{10})$  group are disordered over two positions (51:49;60:40). To describe these disorders the restraints DFIX, SIMU and RIGU were applied.

**Table 3-3.** Crystallographic data and details of diffraction experiments for compounds **3-1a-3-3**.

Compound	<b>3-1a</b> · 1.46 CH <sub>3</sub> CN · 0.47 CH <sub>2</sub> Cl <sub>2</sub>	<b>3-1b</b> · 1.85 CH <sub>2</sub> Cl <sub>2</sub>	<b>3-2</b> · 3.9 CH <sub>3</sub> CN	<b>3-3</b> · 3 CH <sub>2</sub> Cl <sub>2</sub>
Data set (internal naming)	abs150	abs454a	abs425c	abs462a
Formula	C <sub>29.4</sub> H <sub>23.3</sub> BCl <sub>0.9</sub> CuF <sub>4</sub> Mo <sub>2</sub> N <sub>3.5</sub> O <sub>4</sub> P <sub>2</sub>	C <sub>27.85</sub> H <sub>21.7</sub> BCl <sub>3.7</sub> CuF <sub>4</sub> Mo <sub>2</sub> N <sub>2</sub> O <sub>4</sub> P <sub>2</sub>	C <sub>67.82</sub> H <sub>55.73</sub> B <sub>2</sub> Cu <sub>2</sub> F <sub>8</sub> Mo <sub>4</sub> N <sub>7.91</sub> O <sub>8</sub> P <sub>4</sub>	C <sub>39</sub> H <sub>32</sub> BCl <sub>6</sub> CuF <sub>4</sub> Mo <sub>2</sub> N <sub>2</sub> O <sub>4</sub> P <sub>2</sub>
<i>D</i> <sub>calc.</sub> / g · cm <sup>-3</sup>	1.663	1.775	1.500	1.321
$\mu$ /mm <sup>-1</sup>	8.215	9.956	6.540	5.771
Formula Weight	915.20	983.71	1917.84	954.76
Colour	orange	clear orange	orange	clear orange
Shape	block	block	block	block
Size/mm <sup>3</sup>	0.38×0.33×0.27	0.23×0.18×0.10	0.18×0.11×0.10	0.46×0.26×0.19
<i>T</i> /K	123.01(10)	123(1)	123.00(10)	123.15
Crystal System	triclinic	triclinic	triclinic	monoclinic
Space Group	<i>P</i> $\bar{1}$	<i>P</i> $\bar{1}$	<i>P</i> $\bar{1}$	<i>P</i> <sub>2</sub> <sub>1</sub> / <i>n</i>
<i>a</i> /Å	11.4132(2)	11.4691(3)	14.0029(2)	11.2799(3)
<i>b</i> /Å	12.7811(2)	12.7088(4)	17.2519(3)	30.2290(7)
<i>c</i> /Å	14.4918(2)	14.2889(4)	19.0613(2)	14.5789(4)
$\alpha$ /°	65.022(2)	115.044(3)	94.2020(10)	90
$\beta$ /°	73.4420(10)	100.979(2)	99.0750(10)	104.985(3)
$\gamma$ /°	88.0010(10)	91.093(2)	109.524(2)	90
<i>V</i> /Å <sup>3</sup>	1827.88(6)	1840.71(10)	4246.22(12)	4802.1(2)
<i>Z</i>	2	2	2	4
<i>Z'</i>	1	1	1	1
Wavelength/Å	1.54184	1.54184	1.54184	1.54184
Radiation type	Cu K $\alpha$	Cu K $\alpha$	Cu K $\alpha$	Cu K $\alpha$
<i>Q</i> <sub>min</sub> /°	3.374	3.499	3.374	3.462
<i>Q</i> <sub>max</sub> /°	74.316	72.942	73.545	72.710
Measured Refl.	32141	16331	39557	21624
Independent Refl.	7321	6999	16403	9181
Reflections with <i>I</i> > 2( <i>I</i> )	7199	6572	13434	8372
<i>R</i> <sub>int</sub>	0.0353	0.0368	0.0544	0.0318
Parameters	543	443	1013	515
Restraints	174	18	243	148
Largest Peak	0.630	0.864	1.692	0.844
Deepest Hole	-0.939	-0.726	-1.693	-0.777
GooF	1.094	1.034	1.024	1.049
<i>wR</i> <sub>2</sub> (all data)	0.0858	0.0937	0.1535	0.0978
<i>wR</i> <sub>2</sub>	0.0855	0.0915	0.1437	0.0956
<i>R</i> <sub>1</sub> (all data)	0.0314	0.0367	0.0602	0.0402
<i>R</i> <sub>1</sub>	0.0309	0.0347	0.0504	0.0371

**Table 3-4.** Crystallographic data and details of diffraction experiments for compounds **3-4-3-7**.

<b>Compound</b>	<b>3-4</b> · CH <sub>2</sub> Cl <sub>2</sub>	<b>3-5</b> · 0.92 CH <sub>3</sub> CN · 0.08 CH <sub>2</sub> Cl <sub>2</sub>	<b>3-6</b> · 3.9 CH <sub>3</sub> CN	<b>3-7</b> · 2 CH <sub>3</sub> CN · 5.61 CH <sub>2</sub> Cl <sub>2</sub>
Data set (internal naming)	abs454c	abs421e	abs425c	abs439c
Formula	C <sub>63</sub> H <sub>20</sub> AlCl <sub>2</sub> CuF <sub>46</sub> Mo <sub>2</sub> N <sub>2</sub> O <sub>7</sub> P <sub>2</sub>	C <sub>64.92</sub> H <sub>23.92</sub> AlCl <sub>0.16</sub> Cu F <sub>46</sub> Mo <sub>2</sub> N <sub>2.92</sub> O <sub>7</sub> P <sub>2</sub>	C <sub>67.82</sub> H <sub>55.73</sub> B <sub>2</sub> Cu <sub>2</sub> F <sub>8</sub> Mo <sub>4</sub> N <sub>7.91</sub> O <sub>8</sub> P <sub>4</sub>	Al <sub>2</sub> C <sub>133.6</sub> Cl <sub>11.2</sub> Cu <sub>2</sub> F <sub>92</sub> H <sub>61.2</sub> Mo <sub>4</sub> N <sub>6</sub> O <sub>14</sub> P <sub>4</sub>
<i>D</i> <sub>calc.</sub> / g · cm <sup>-3</sup>	1.928	1.997	1.500	1.857
μ/mm <sup>-1</sup>	5.696	0.869	6.540	6.101
Formula Weight	2206.05	2180.72	1917.84	4808.00
Colour	orange	clear orange	orange	orange
Shape	block	plate	block	block
Size/mm <sup>3</sup>	0.22×0.19×0.06	0.57×0.24×0.09	0.18×0.11×0.10	0.31×0.23×0.16
<i>T</i> /K	123.15	123.15	123.00(10)	123.01(10)
Crystal System	monoclinic	triclinic	triclinic	triclinic
Space Group	<i>P</i> 2 <sub>1</sub> / <i>c</i>	<i>P</i> $\bar{1}$	<i>P</i> $\bar{1}$	<i>P</i> $\bar{1}$
<i>a</i> /Å	16.40340(10)	13.6508(3)	14.0029(2)	15.8320(2)
<i>b</i> /Å	19.58240(10)	14.6790(4)	17.2519(3)	21.4196(2)
<i>c</i> /Å	24.6552(2)	19.2552(5)	19.0613(2)	26.7207(4)
α/°	90	72.118(2)	94.2020(10)	80.7420(10)
β/°	106.3820(10)	84.817(2)	99.0750(10)	80.6180(10)
γ/°	90	81.391(2)	109.524(2)	75.8780(10)
<i>V</i> /Å <sup>3</sup>	7598.17(9)	3626.55(16)	4246.22(12)	8600.27(19)
<i>Z</i>	4	2	2	2
<i>Z'</i>	1	1	1	1
Wavelength/Å	1.54184	0.71073	1.54184	1.54184
Radiation type	Cu K <sub>α</sub>	Mo K <sub>α</sub>	Cu K <sub>α</sub>	Cu K <sub>α</sub>
<i>Q</i> <sub>min</sub> /°	3.603	3.339	3.374	3.543
<i>Q</i> <sub>max</sub> /°	72.725	32.436	73.545	74.299
Measured Refl.	36001	55685	39557	132269
Independent Refl.	14624	23380	16403	34605
Reflections with <i>I</i> > 2( <i>I</i> )	13142	18688	13434	31345
<i>R</i> <sub>int</sub>	0.0241	0.0259	0.0544	0.0680
Parameters	1162	1173	1013	2782
Restraints	49	21	243	1209
Largest Peak	0.810	0.492	1.692	1.258
Deepest Hole	-0.593	-0.386	-1.693	-1.594
GooF	1.036	1.027	1.024	1.026
<i>wR</i> <sub>2</sub> (all data)	0.0786	0.0689	0.1535	0.1410
<i>wR</i> <sub>2</sub>	0.0756	0.0632	0.1437	0.1372
<i>R</i> <sub>1</sub> (all data)	0.0350	0.0492	0.0602	0.0582
<i>R</i> <sub>1</sub>	0.0305	0.0329	0.0504	0.0540

**Table 3-5.** Comparison of bond lengths and angles of compounds **3-1a** and **3-1b**.

<b>Bond lengths [Å]</b>	<b>3-1a</b>	<b>3-1b</b>
<b>Cu-P</b>	2.2760(7), 2.2745(7)	2.2778(9), 2.2863(8)
<b>Cu-N</b>	2.045(2), 2.010(2)	2.051(3), 2.019(3)
<b>P-P</b>	2.0839(9)	2.0870(10)
<b>P-Mo</b>	2.4590(7), 2.5352(6), 2.5367(7), 2.4539(7)	2.4540(7), 2.5383(7), 2.5457(8), 2.4581(8)
<b>Mo-Mo</b>	3.0253(3)	3.0285(3)

<b>Bond angles [°]</b>	<b>3-1a</b>	<b>3-1b</b>
<b>P-Cu-P</b>	109.54(3)	109.65(3)
<b>P-Cu-N</b>	103.57(7), 109.49(7), 115.18(7), 108.83(7)	104.67(8), 109.38(8), 116.10(9), 108.38(8)
<b>N-Cu-N</b>	110.06(9)	108.48(11)

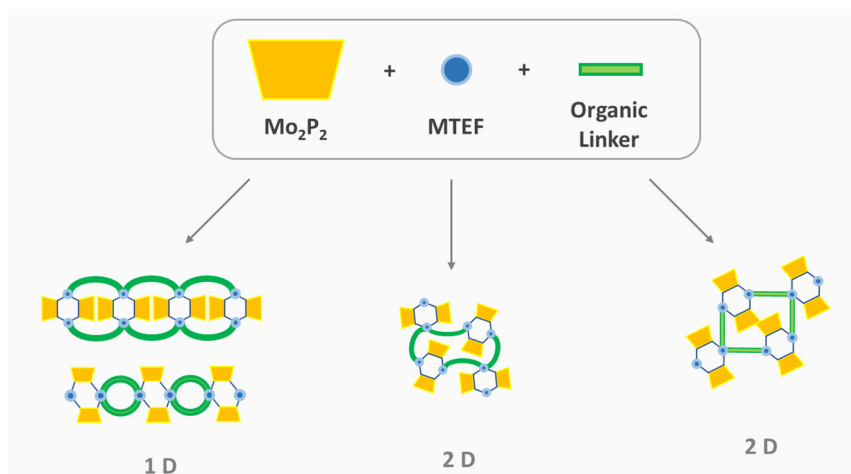
### 3.6 References

- [1] a) T. R. Cook, P. J. Stang *Chem. Rev.* **2015**, *115*, 7001-7045; b) T. R. Cook, Y.-R. Zheng, P. J. Stang *Chem. Rev.* **2013**, *113*, 734-777; c) W. L. Leong, J. J. Vittal *Chem. Rev.* **2011**, *111*, 688-764; d) R. Chakrabarty, P. S. Mukherjee, P. J. Stang *Chem. Rev.* **2011**, *111*, 6810-6918; e) A. J. Olson, Y. H. E. Hu, E. Keinan, *Proc. Natl. Acad. Sci. U.S.A.* **2007**, *104*, 20731-20736; f) Y.-R. Zheng, P. J. Stang, *J. Am. Chem. Soc.* **2009**, *131*, 3487-3489.
- [2] a) S. Miao, Z. Li, C. Xu, D. Deng, B. Ji, *Crystals* **2019**, *9*, 592; b) J. Guo, D. Sun, L. Zhang, Q. Yang, X. Zhao, D. Sun, *Cryst. Growth Des.* **2012**, *12*, 5649-5654; c) W.-Q. Kan, J. Yang, Y.-Y. Liu, J.-F. Ma, *CrystEngComm*, **2012**, *14*, 6271-6281; d) J. Guo, D. Sun, L. Zhang, Q. Yang, X. Zhao, D. Sun, *Cryst. Growth Des.* **2012**, *12*, 5649-5654.
- [3] K. Banerjee, S. Roy, M. Kotal, K. Biradha *Cryst. Growth Des.* **2015**, *15*, 5604-5613.
- [4] X.-Y. Dong, C.-D. Si, Y. Fan, D.-C. Hu, X.-Q. Yao, Y.-X. Yang, J.-C. Liu *Cryst. Growth Des.* **2016**, *16*, 2062-2073.
- [5] a) L. Carlucci, G. Ciani, D. M. Proserpio, T. G. Mitina, V. A. Blatov, *Chem. Rev.* **2014**, *114*, 7557-7580; b) R. Haldar, T. K. Maji, Z. *Anorg. Allg. Chem.* **2014**, *640*, 1102-1108.
- [6] a) M. C. Linder, *Biochemistry of Copper*; Plenum Press: New York, **1991**; b) M. C. Linder, M. Hazegh-Azam, *Am. J. Clin. Nutr. Suppl.* **1996**, *63*, 797S-811S; c) M. C. Linder, *Mutat. Res.* **2001**, *475*, 141-152; d) M. Pellei, G. G. Lobbia, C. Santini, R. Spagna, M. Camalli, D. Fedelic, G. Falcioni *Dalton Trans.* **2004**, 2822-2828.
- [7] X.-Q. Liang, R. K. Gupta, Y.-W. Li, H.-Y. Ma, L.-N. Gao, C.-H. Tung, D. Sun *Inorg. Chem.* **2020**, *59*, 2680-2688.
- [8] T. Yoneda, C. Kasai, Yo Manabe, M. Tsurui, Y. Kitagawa, Y. Hasegawa, P. Sarkar, Y. Inokuma *Chem Asian J.* **2020**, *15*, 601- 605.
- [9] N.-X. Zhu, C.-W. Zhao, J. Yang, X.-R. Wang, J.-P. Ma, Y.-B. Dong *RSC Adv.* **2016**, *6*, 108645-108653.
- [10] T. Wen, D.-X. Zhang, J. Zhang *Inorg. Chem.* **2013**, *52*, 12-14.
- [11] a) J. Bai, E. Leiner, M. Scheer *Angew. Chem. Int. Ed.* **2002**, *41*, 783-786; *Angew. Chem.* **2002**, *114*, 820; b) M. Scheer, L. J. Gregoriades, M. Zabel, J. Bai, I. Krossing, G. Bruncklaus, H. Eckert *Chem. Eur. J.* **2008**, *14*, 282-295.
- [12] M. Scheer, L. J. Gregoriades, M. Zabel, M. Sierka, L. Zhang, H. Eckert *Eur. J. Inorg. Chem.* **2007**, 2775-2782.
- [13] M. E. Moussa, P. A. Shelyganov, B. Wegley, M. Seidl, M. Scheer *Eur. J. Inorg. Chem.* **2019**, 4241-4248.
- [14] M. E. Moussa, M. Seidl, G. Balázs, M. Hautmann, M. Scheer *Angew. Chem.* **2019**, *131*, 13035-13039.
- [15] M. Fleischmann, S. Welsch, E. V. Peresykina, A. V. Virovets, M. Scheer, *Chem. Eur. J.* **2015**, *21*, 14332-14336.
- [16] M. E. Moussa, M. Piesch, M. Fleischmann, A. Schreiner, M. Seidl, M. Scheer *Dalton Trans.* **2018**, *47*, 16031-16035.
- [17] M. E. Moussa, B. Attenberger, M. Seidl, A. Schreiner, M. Scheer *Eur. J. Inorg. Chem.* **2017**, 5616-5620.
- [18] Bianca Attenberger, *Dissertation* **2014**, Universität Regensburg.
- [19] B. Attenberger, S. Welsch, M. Zabel, E. Peresykina, M. Scheer *Angew. Chem.* **2011**, *123*, 11718-11722; *Angew. Chem. Int. Ed.* **2011**, *50*, 11516-11519.
- [20] W. L. Leong, J. J. Vittal, *Chem. Rev.* **2011**, *111*, 688-764.
- [21] M. E. Moussa, B. Attenberger, E. V. Peresykina, M. Fleischmann, G. Balázs, M. Scheer *Chem. Commun.* **2016**, *52*, 10004-10007.
- [22] Stefan Welsch, *Dissertation* **2010**, Universität Regensburg.
- [23] N. Wiberg, A. F. Hollemann *Holleman, Wiberg – Lehrbuch der Anorganischen Chemie* **2007**, 102<sup>nd</sup> Edition: de Gruyter Berlin.
- [24] P. Pyykkö, M. Atsumi *Chem. Eur. J.* **2009**, *15*, 12770-12779.
- [25] O. J. Scherer, H. Sitzmann, G. Wolmershäuser *J. Organomet. Chem.* **1984**, *268*, C9-C12.
- [26] CrysAlisPro Software System, Rigaku Oxford Diffraction, (2018).
- [27] Clark, R. C. & Reid, J. S. *Acta Cryst.* **1995**, *A51*, 887-897.
- [28] O. V. Dolomanov, L. J. Bourhis, R. J. Gildea, J. A. K. Howard, H. Puschmann, Olex2: A complete structure solution, refinement and analysis program, *J. Appl. Cryst.* **2009**, *42*, 339-341.
- [29] Sheldrick, G.M., ShelXT-Integrated space-group and crystal-structure determination, *Acta Cryst.* **2015**, *A71*, 3-8.5.G.
- [30] M. Sheldrick, Crystal structure refinement with ShelXL, *Acta Cryst.* **2015**, *C27*, 3-8.





- 4 The weakly coordinating anion  $[\text{Al}\{\text{OC}(\text{CF}_3)_3\}_4]^-$  in the selective, crystallisation method dependent synthesis of 1D and 2D coordination polymers with the  $\text{P}_2$  ligand complex  $[\text{Cp}_2\text{Mo}_2(\text{CO})_4(\mu, \eta^{2:2}\text{-P}_2)]$  and organic linkers



#### Author contribution

- Andrea Schreiner: Preparation of the manuscript, synthesis, and characterisation of compounds **4-1-4-7**
- Michael Seidl: Refinement of the solid-state structures of compounds **4-1-4-5** and **4-7**, support of the X-ray diffraction measurements and revision of the manuscript
- Eugenia Peresykina: Measurement and refinement of the preliminary crystal structure of compound **4-6**
- Manfred Scheer: Supervision of the research and revision of the manuscript

#### 4.1 Abstract

The  $\text{P}_2$  complex  $[\text{Cp}_2\text{Mo}_2(\text{CO})_4(\mu, \eta^{2:2}\text{-P}_2)]$  (**A**) was used as a building block for supramolecular coordination chemistry. **A** was reacted with the Ag(I) salt  $\text{Ag}[\text{Al}\{\text{OC}(\text{CF}_3)_3\}_4]$  (**B**) and the pyridine-based organic linkers 1,3-di(4-pyridyl)propane ( $\text{L}_{\text{flex1}}$ ) and 1,3-di(4-pyridyl)ethane ( $\text{L}_{\text{flex2}}$ ), respectively. New 1D and 2D coordination polymers (CPs) were synthesised by either layering of the crude reaction mixture with *n*-pentane or crystallisation at  $-28^\circ\text{C}$ , respectively, and characterised by single crystal X-ray crystallography. The resulting products have the general formulas  $[\text{Ag}_2\{\text{Cp}_2\text{Mo}_2(\text{CO})_4(\eta^{2:2:1:1}\text{-P}_2)\}_2(\mu, \eta^{1:1}\text{-L})_2][\text{TEF}]_{2n}$  (2D;  $\text{L} = \text{L}_{\text{flex1}}, \text{L}_{\text{flex2}}$ ) and  $[\text{Ag}_2\{\text{Cp}_2\text{Mo}_2(\text{CO})_4(\mu, \eta^{2:2:1:1}\text{-P}_2)\}_2(\mu, \eta^{1:1}\text{-L}_{\text{flex1}})_2][\text{TEF}]_{2n}$  (1D). Additionally, the complex with the formula  $[\text{Ag}_2\{\text{Cp}_2\text{Mo}_2(\text{CO})_4(\eta^{2:2:2:1}\text{-P}_2)\}_2(\mu, \eta^{1:1}\text{-L}_{\text{flex1}})_2][\text{TEF}]_{2n}$  (1D), containing a short Ag-Ag-distance, which lies within the sum of the covalent radii of silver, was once observed as a by-product of the latter 1D CP. The reaction of **A** with the analogue Cu(I) salt

$[\text{Cu}(\text{CH}_3\text{CN})_4][\text{Al}\{\text{OC}(\text{CF}_3)_3\}_4]$  (**C**) with  $\text{L}_{\text{flex1}}$  and  $\text{L}_{\text{flex2}}$  yielded new 2D CPs with the general formula  $[\text{Cu}_2\{\text{Cp}_2\text{Mo}_2(\text{CO})_4(\mu, \eta^{2:2:1:1}\text{-P}_2)\}_2(\mu, \eta^{1:1}\text{-L})_2]_n[\text{TEF}]_{2n}$  ( $\text{L} = \text{L}_{\text{flex1}}, \text{L}_{\text{flex2}}$ ). Additionally, the linker 1,2-di-(4-pyridyl)ethylene (**dpe**) was reacted with **A** and **C**, for which a similar compound,  $[\text{Cu}_2\{\text{Cp}_2\text{Mo}_2(\text{CO})_4(\mu, \eta^{2:2:1:1}\text{-P}_2)\}_2(\mu, \eta^{1:1}\text{-dpe})_2]_n[\text{TEF}]_{2n}$  was obtained.

## 4.2 Introduction

Ag(I) coordination polymers exhibit different properties like luminescence<sup>[1]</sup> and electrolytic activity.<sup>[2]</sup> Also anticancer and cytotoxic activity<sup>[3]</sup> and the selective adsorption of a carcinogenic dye have been reported.<sup>[4]</sup> Recently, a porous Ag(I) CP has shown to selectively trap and sense perrhenate and pertechnetate.<sup>[5]</sup> Due to these intriguing properties, novel Ag(I) coordination polymers could have the potential for many future applications. Therefore, the field of Ag(I) coordination polymers using polyphosphorus ligand complexes was explored. Besides spherical supramolecules,<sup>[6]</sup> nano-sized capsules<sup>[7]</sup> and nano-bowls,<sup>[8]</sup> a major research area of our group is the design of organometallic-organic coordination polymers. Over the years, different coordination compound and polymers using polyphosphorus ligand complexes in combination with coinage metal salts and organic linkers were reported.<sup>[9]</sup> By reacting the  $\text{P}_2$  complex  $[\text{Cp}_2\text{Mo}_2(\text{CO})_4(\mu, \eta^{2:2}\text{-P}_2)]$  (**A**) with the Ag(I) salt  $\text{AgBF}_4$  and organic linkers, one-, two- and three-dimensional coordination polymers were obtained.<sup>[10]</sup> Depending on the stoichiometry and reaction time, the reaction of the  $\text{P}_2$  ligand complex  $[\text{Cp}_2\text{Mo}_2(\text{CO})_4(\mu, \eta^{2:2}\text{-P}_2)]$  (**A**) with the Ag(I) WCA salt  $\text{Ag}[\text{TEF}]$  ( $\text{TEF} = \text{Al}\{\text{OC}(\text{CF}_3)_3\}_4$ ) (**B**) can yield a zero-dimensional coordination complex<sup>[11]</sup> or a one-dimensional coordination polymer.<sup>[9b]</sup> By reacting **A** with **B** and the organic linker 1,2-di-(4-pyridyl)ethylene (**dpe**), it was possible to show the formation of a zero-dimensional coordination complex and additionally of one-, two- and three-dimensional CPs.<sup>[12]</sup> The selectivity in those syntheses is still a great challenge. Small changes in the nature of the linker, changing the metal cation or the counter anion as well as the reaction conditions and crystallisation methods can have a huge influence on the formation of the final product.<sup>[13]</sup> The same combination of building blocks can therefore lead to a variety of different coordination compounds as it is the case for the system of **A**, **B** and **dpe**. However, it was recently possible to control the reactions for the selective synthesise of a specific type of organometallic-organic CP. The reaction of **A** with the Cu(I) salt  $[\text{Cu}(\text{CH}_3\text{CN})_4][\text{BF}_4]$  and flexible organic pyridine-based linkers selectively yielded one-dimensional coordination polymers.<sup>[9a]</sup> By changing the nature of the linker from flexible to rigid, which leads to a loss of conformational freedom, two-dimensional coordination polymers could be obtained selectively.<sup>[14]</sup> Herein, we report on the results obtained from the reactions of the  $\text{P}_2$  ligand complex **A** with the Ag(I) WCA salt  $\text{Ag}[\text{TEF}]$  ( $\text{TEF} = \text{Al}\{\text{OC}(\text{CF}_3)_3\}_4$ ; **B**) and the flexible organic linker molecules 1,3-bis(4-pyridyl)propane ( $\text{L}_{\text{flex1}}$ ) and 1,2-bis(4-pyridyl)ethane  $\text{L}_{\text{flex2}}$ , respectively. Further, the influence of the metal(I) cation on the system was explored by performing similar reactions with the respective Cu(I) salt  $[\text{Cu}(\text{CH}_3\text{CN})_4][\text{TEF}]$  (**C**). **A** was therefore reacted with **C** and the linkers  $\text{L}_{\text{flex1}}$ ,  $\text{L}_{\text{flex2}}$  and **dpe** (**Figure 4-1**).

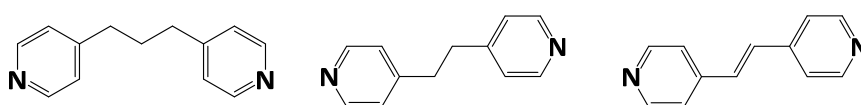
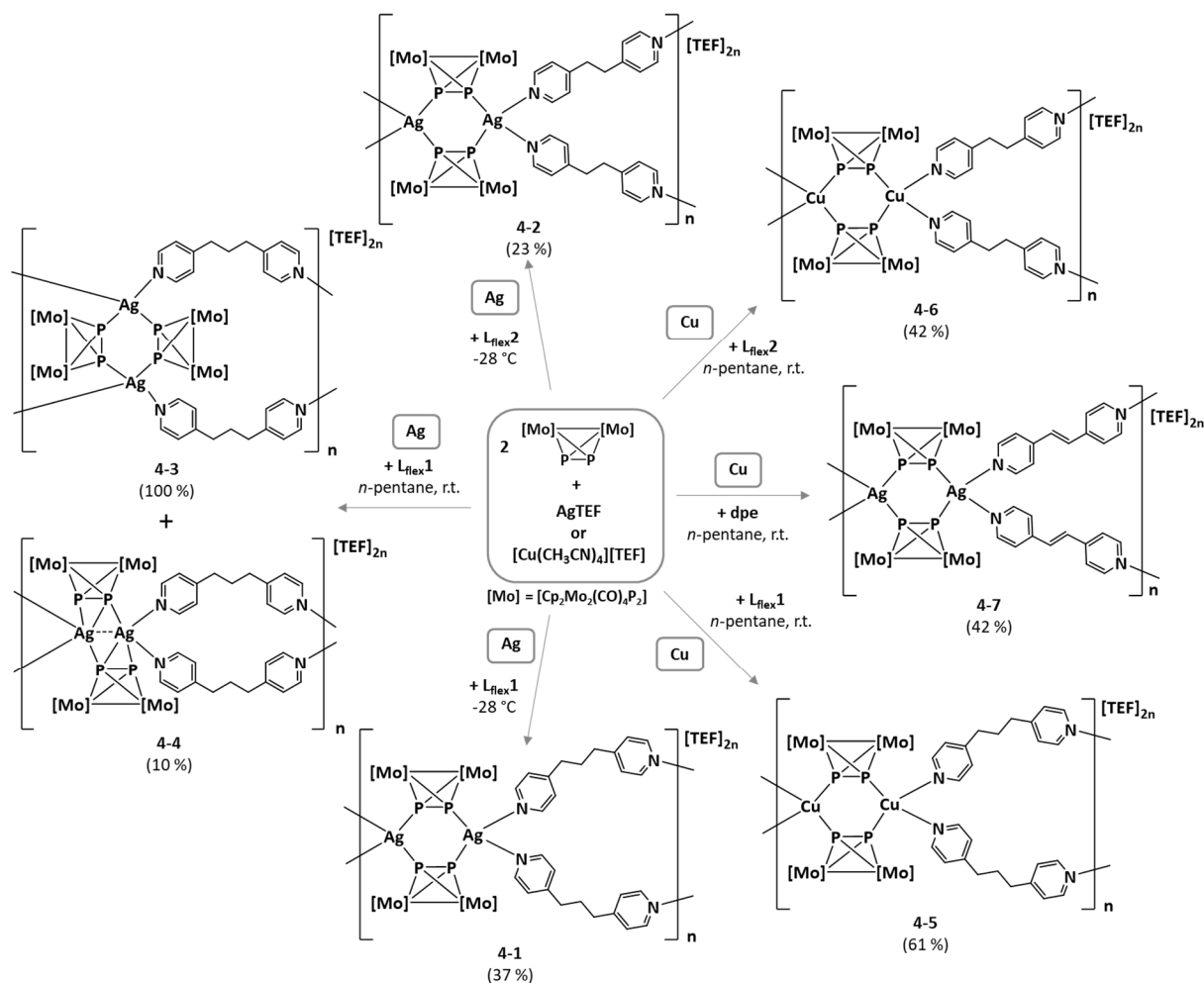


**Figure 4-1.** Organic pyridine-based linker molecules  $\text{L}_{\text{flex1}}$ ,  $\text{L}_{\text{flex2}}$  and **dpe**.

### 4.3 Results and Discussion

The P<sub>2</sub> ligand complex [Cp<sub>2</sub>Mo<sub>2</sub>(CO)<sub>4</sub>(μ,η<sup>2:2</sup>-P<sub>2</sub>)] (**A**) was reacted with either a Ag(I) or Cu(I) source with the weakly coordination TEF-anion as counter-anion and subsequently with one of the organic pyridine-based linker molecules **L<sub>flex1</sub>**, **L<sub>flex2</sub>** or **dpe**, respectively (**Scheme 4-1**).



**Scheme 4-1.** Summary of the reactions of the P<sub>2</sub> ligand complex **A** with the Ag(I) and Cu(I) salts **AgTEF** and **CuTEF** and the pyridine-based organic linker molecules 1,3-di(4-pyridyl)propane (**L<sub>flex1</sub>**), 1,3-di(4-pyridyl)ethane (**L<sub>flex2</sub>**) and 1,2-di(4-pyridyl)ethylene (**dpe**). Isolated yields of single crystals are given in parenthesis.

It is known that the two-component reaction of the P<sub>2</sub> ligand complex **A** with a metal salt (Cu or Ag) results in the dimeric compound [M<sub>2</sub>(Cp<sub>2</sub>Mo<sub>2</sub>(CO)<sub>4</sub>(μ,η<sup>2:2:1:1</sup>-P<sub>2</sub>)<sub>2</sub>(Cp<sub>2</sub>Mo<sub>2</sub>(CO)<sub>4</sub>(μ,η<sup>2:2:2</sup>-P<sub>2</sub>))<sub>2</sub>]<sup>2+</sup> (**D**, **Figure 4-2**).<sup>[11,15]</sup> Therefore all reactions were carried out by first preforming **D** by the reaction of the P<sub>2</sub> ligand complex **A** with the metal salt. Afterwards, the solution of the linker (**L<sub>flex1</sub>**, **L<sub>flex2</sub>** or **dpe**, respectively) was added to replace the η<sup>2</sup>-coordinated Mo<sub>2</sub>P<sub>2</sub> units at the metal(I) centre.<sup>[10]</sup> The crude reaction mixtures were either stored at -28 °C, which lead to the formation of compounds **4-1** and **4-2**, or layered with *n*-pentane or a 1:1-mixture of *n*-pentane and dichloromethane, which yielded the products **4-3** to **4-5** and **4-6** and **4-7**, respectively.

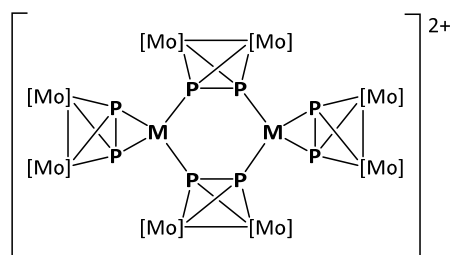


**Figure 4-2.** Dimeric cationic complex  $[M_2(Cp_2Mo_2(CO)_4(\mu,\eta^{2:2:1}-P_2)_2(Cp_2Mo_2(CO)_4(\mu,\eta^{2:2:2}-P_2)_2)]^{2+}$  (**D**).<sup>[11,15]</sup>

A first reaction was performed using the  $P_2$  ligand complex  $[Cp_2Mo_2(CO)_4(\mu,\eta^{2:2}-P_2)]$  (**A**),  $Ag[TEF]$  ( $TEF = Al\{OC(CF_3)_3\}_4$ , **B**) and the organic linker 1,3-di(4-pyridyl)propane (**L<sub>flex</sub>1**). Crystals of compound **4-1**, which crystallises in the triclinic space group  $P\bar{1}$ , were obtained after one week in the form of orange blocks. Single crystal X-ray analysis was performed to determine the structure of **4-1** and it was revealed that a 2D CP (**Figure 4-3**) containing the starting materials in a 1:1:1-ratio was obtained. A six-membered  $Ag_2P_4$ -ring serves as node and the  $Ag(I)$  centres are tetra-coordinated by two different units of the  $P_2$  ligand complex **A** and two molecules of linker. The four linker molecules attached to the same node are connecting to four different nodes, forming the two-dimensional network. Every second node is twisted by approximately  $68.887(3)^\circ$  in relation to the neighbouring nodes (*cf.* **Figure 4-3**). The cavities formed by the 2D network diameters up to approximately 1.88 nm, referring to the  $Ag-Ag$  distances,<sup>\*[16]</sup> and are filled with anions and solvent molecules. The bond lengths and angles within the CP are in accordance with the values found in complex **D**<sup>[11]</sup> and similar coordination compounds and polymers.<sup>[9b,10,11,12]</sup>

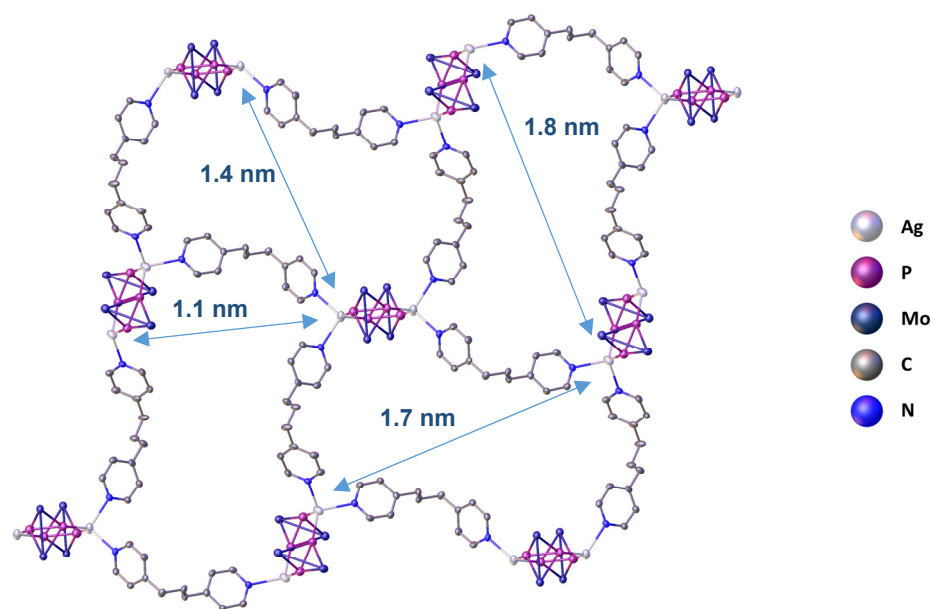


**Figure 4-3.** Section of the molecular structure of the two-dimensional cation of **4-1** in the solid-state. Hydrogen atoms, Cp- and CO-ligands, anions and solvent molecules are omitted for clarity. Thermal ellipsoids are shown at 50 % probability level. Selected bond lengths [Å] and angles [°]:  $Ag1-P1$  2.4971(8),  $Ag1-P2$  2.4542(8),  $Ag1-N1$  2.296(3),  $Ag1-N4$  2.329(3),  $Ag2-P3$  2.4572(9),  $Ag2-P4$  2.5115(8),  $Ag2-N2$  2.323(3),  $Ag2-N3$  2.287(3),  $P2-P1$

\* The cavity sizes of the CPs are calculated by taking the  $Cu-Cu$  distances obtained from the X-ray experiment and abstracting the sum of the *van-der-Waals*-radii of copper (1.7 Å).<sup>[16]</sup>

2.090(1), P4-P3 2.082(1), P2-Ag1-P1 118.77(3), P3-Ag2-P4 110.29(3), N1-Ag1-N4 102.0(1), N3-Ag2-N2 101.7(1).<sup>[16]</sup>

The reaction with the organic linker 1,3-di(4-pyridyl)ethane ( $L_{flex2}$ ) led to the formation of crystals in the colour and form of red plates. The crystals were analysed using single crystal X-ray crystallography. Unlike compounds **4-1**, **4-2** crystallises in the monoclinic space group  $P2_1/n$ . The ratio of the starting materials in the 2D CP (**Figure 4-4**) is also 1:1:1 and the structure is similar compared to the structure of **4-1**. A six-membered  $Ag_2P_4$ -ring with two tetra-coordinated Ag(I) centres serves as node. The coordination sphere of the Ag(I) centres is saturated by two molecules of linker  $L_{flex2}$ , which connect the nodes. As in **4-1**, all four linkers attached to one node are coordinated to four different nodes, resulting in the two-dimensionality of the network. The bond lengths and angles also have values in the expected range and the cavities formed by the CP, which are up to 1.82 nm in diameter,<sup>[16]</sup> are filled with anions and solvent molecules.

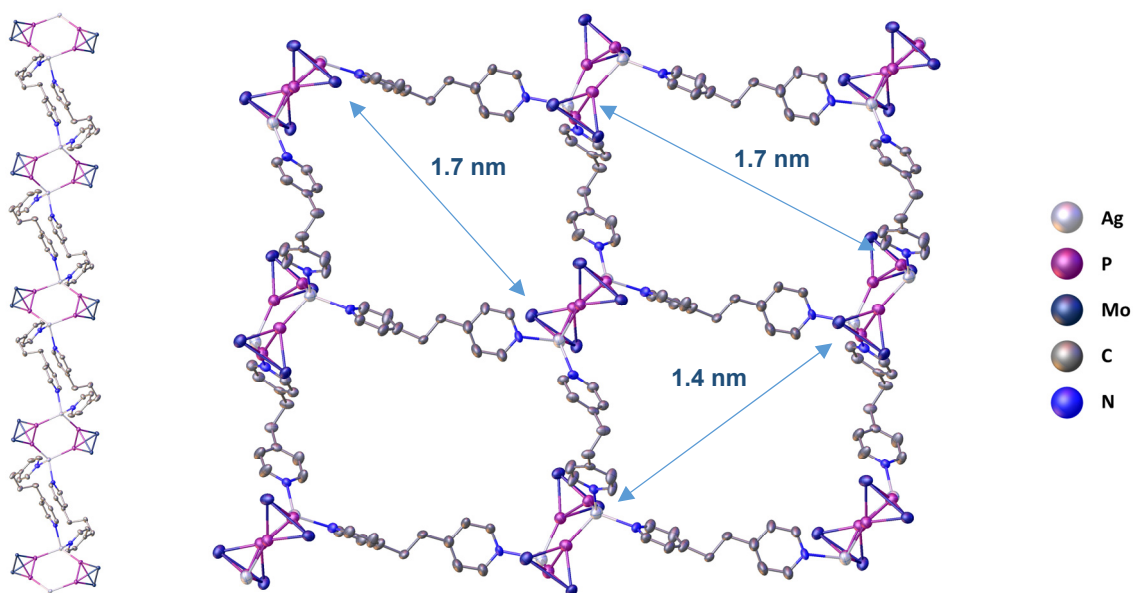


**Figure 4-4.** Section of the molecular structure of the two-dimensional cation of **4-2** in the solid-state (left: view along the *a*-axis). Hydrogen atoms, Cp- and CO-ligands, anions and solvent molecules are omitted for clarity. Thermal ellipsoids are shown at 50 % probability level. Selected bond lengths [Å] and angles [°]: Ag1-P1 2.457(2), Ag1-P4A 2.554(8), Ag1-N1 2.309(5), Ag1-N2 2.305(5), Ag2-P2 2.515(2), Ag2-P3 2.450(2), Ag2-N3 2.280(5), Ag2-N4A 2.37(2), P2-P1 2.086(2), P3-P4A 2.072(9), P1-Ag1-P4A 108.5(2), P3-Ag2-P2 111.97(5), N1-Ag1-P1 108.5(2), N2-Ag1-N1 101.9(2), N3-Ag2-N4A 102.6(3).<sup>[16]</sup>

The layering of the crude reaction mixture from the reaction of **A** with **B** and organic linker  $L_{flex1}$  leads to the formation of red, block-like crystals within one week. By performing single crystal X-ray analysis, the structure of the 1D CP of **4-3** (**Figure 4-5**), which crystallises in the monoclinic space group  $P2_1/c$ , was revealed. Like in the 2D CPs of **4-1** and **4-2**, the ratio of the educts in the network is 1:1:1 and a six-membered  $Ag_2P_4$ -ring serves as node. The Ag(I) centres are tetra-coordinated and their coordination spheres are completed by  $L_{flex1}$ . Thus, also four molecules of linker are attached to one node. Unlike to compounds **4-1** and **4-2**, a pair of linker molecules, each attached to a different Ag(I) centre of the same node, connect two nodes to form a one-dimensional coordination polymer. The cavities formed by this arrangement are 1.0-1.2 nm in diameter and are filled with  $BF_4^-$  anions and solvent

molecules.<sup>[16]</sup> The bond lengths and angles are comparable to complex **D**<sup>[11]</sup> and similar coordination polymers.<sup>[9b,10,11,12]</sup>

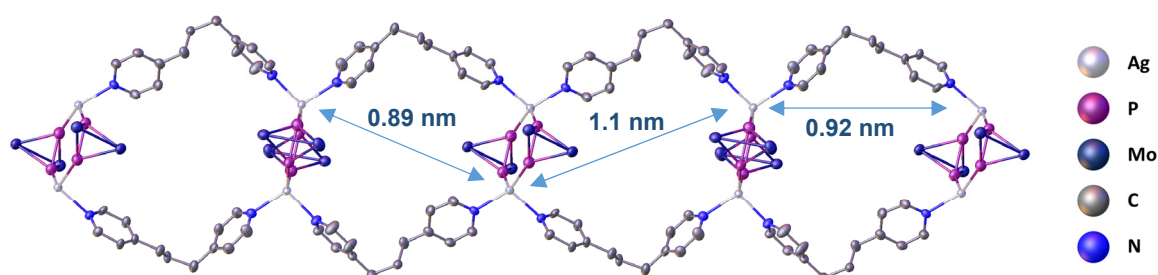


**Figure 4-5.** Section of the molecular structure of the one-dimensional cationic strand of **4-3** in the solid-state. Hydrogen atoms, Cp- and CO-ligands, anions and solvent molecules are omitted for clarity. Thermal ellipsoids are shown at 50 % probability level. Selected bond lengths [Å] and angles [°]: Ag1-P2A 2.597(2), Ag1-P1A 2.420(2), Ag1-N1 2.251(5), Ag1-N4 2.360(5), Ag2A-P3A 2.433(2), Ag2A-P4A3 2.548(4), Ag2A-N3 2.305(5), Ag2A-N2 2.322(5), P2A-P1A 2.086(3), P3A-P4A 2.085(3), P1A-Ag1-P2A 114.24(7), P3A-Ag2A-P4A 113.9(1), N1-Ag1-N3 97.50(11), N2-Ag2-N4 91.25(11).<sup>[16]</sup>

During the syntheses of **4-3**, the co-crystallisation of a second type of crystals could sometimes be observed. The orange blocks were analysed by single crystal X-ray analysis and the formation of a further one-dimensional polymer (triclinic space group  $P\bar{1}$ ) with the formula  $[Ag_2(CpMo_2(CO)_4(\mu, \eta^{2:2:1:1}-P_2))]_2(\mu, \eta^{1:1}-C_{13}H_{14}N_2)_2]_n[TEF]_{2n}$  (**4-4**, **Figure 4-6**) was revealed. The stoichiometry of the reactants in **4-4** is also 1:1:1. The solid-state structure of **4-4**, however, differs significantly from the previously described compounds **4-1-4-3**. There is also a six-membered  $Ag_2P_4$ -ring serving as node with tetra-coordinated Ag(I) centres. Like in **4-3**, the nodes are connected to each other via one pair of linker molecules per node, forming a one-dimensional CP. Unlike **4-3**, each of those pairs coordinate to the same Ag(I) centres of two different nodes. The major difference to the other compounds, however, is the coordination mode of the  $P_2$  ligand complex **A** within the node. The  $P_2$  units are coordinated to the Ag(I) centres in a  $\eta^{2:1}$ -coordination mode ( $\eta^{1:1}$  in complex **D**<sup>[11]</sup> and compounds **4-1-4-3** (cf. **Table 4-1**). As a result, the node is strongly distorted. The Ag-Ag distance, which is 4.7601(15) Å in **D**<sup>[11]</sup> is only 2.9100(4) Å in **4-4**. This value is still above the sum of the covalent radii of silver (128 pm).<sup>[17]</sup> However, compounds exhibiting larger Ag-Ag distances (> 3.0 Å) which are considered to have argentophilic interactions exist.<sup>[18]</sup> Further conclusions about the nature of the possible Ag-Ag-interaction in compound **4-4** would require additional investigations, e.g. DFT calculations.

**Table 4-1.** Comparison of the approximate cavity sizes [nm], the Ag-P, Ag-N and P-P bond lengths [Å] and P-Ag-P and N-Ag-N angles [°] of compounds **4-1-4-3**.

Compound	<b>4-1</b>	<b>4-2</b>	<b>4-3</b>
Linker	$L_{flex1}$	$L_{flex2}$	$L_{flex1}$
Cavity size <sup>[16]</sup>	1.1-1.8	1.4-1.7	0.89-1.1
Ag-P	2.4542(8)-2.5115(8)	2.450(2)- 2.554(8)	2.420(2)-2.597(2)
Ag-N	2.287(3)-2.329(3)	2.280(5)-2.37(2)	2.251(5)-2.360(5)
P-P	2.082(1), 2.090(1)	2.072(9), 2.086(2),	2.086(3), 2.085(3)
$\sphericalangle$ P-Ag-P	110.29(3), 118.77(3)	108.5(2), 111.97(5)	114.24(7), 113.9(1)
$\sphericalangle$ N-Ag-N	101.7(1), 102.0(1)	101.9(2), 102.6(3)	97.50(11), 91.25(11)

The Ag-P bond lengths in **4-4** (Ag1-P3 2.6371(9) Å, Ag2-P4 2.6575(9) Å, Ag1-P1 (2.6376(9) Å and Ag2-P2 2.5025(8) Å) are elongated compared to **D** (2.4740(9) to 2.4778(9) Å).<sup>[11]</sup> The distances between Ag1-P2 and Ag2-P3, 2.8245(9) and 2.8383(9) Å, respectively, are significantly smaller than in the dimeric complex **D**,<sup>[11,15]</sup> but not below the sum of the covalent radii of P and Ag (2.39 Å).<sup>[15]</sup> The angles between the Ag(I) centre and the phosphorus atoms of the P<sub>2</sub> units are 45.93(3) ° for P1-Ag1-P2 and 45.35(3) ° for P3-Ag2-P4. The other P-Ag-N angles have very different values that range from 101.76(3) ° for P3-Ag1-P2 to 141.42(3) for P3-Ag1-P1. The fold angle of the plane within the node is 136.96(3) ° regarding the planes Ag1-Ag2-P2/P3. As a further result of the node's distortion, the P-P bonds, 2.125(1) Å and 2.138(1) Å, are elongated by 0.03-0.05 Å compared to **D**.<sup>[11]</sup> The Ag-N bond lengths (2.280(5)-2.366(19) Å) are in the range the Ag-N bond length of compounds **4-1-4-3**, as are the N-Ag-N angles of 98.8(7)-102.6(3) ° (*cf.* Table 4-1).

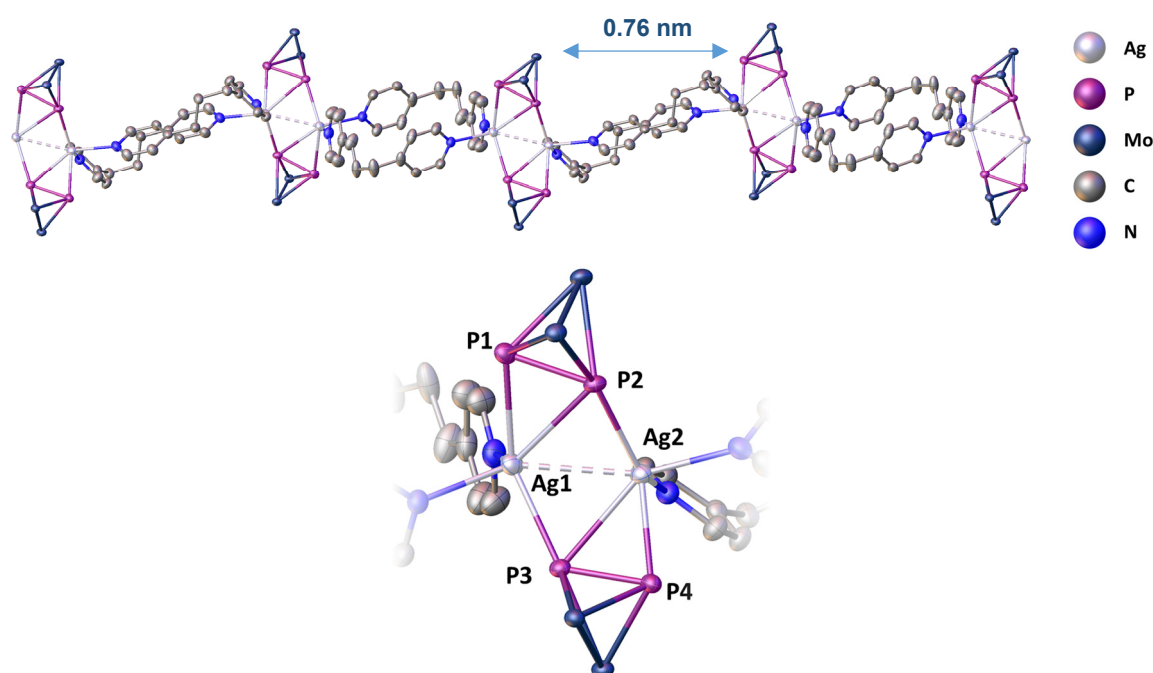


**Figure 4-6.** Sections of the molecular structure of the one-dimensional cationic strand of **4-4** in the solid-state. Hydrogen atoms, Cp- and CO-ligands, anions and solvent molecules are omitted for clarity. Thermal ellipsoids are shown at 50 % probability level. Selected bond lengths [Å] and angles [°]: Ag1-Ag2 2.9100(4), Ag1-P1 2.6376(9), Ag1-P2 2.8245(9), Ag1-P3 2.6371(9), Ag2-P2 2.5025(8), Ag2-P3 2.8383(9), Ag2-P4 2.6575(9), Ag1-N1 2.309(5), Ag1-N2 2.305(5), Ag2-N3 2.280(5), Ag2-N4A2 2.366(19), Ag2-N4B2 2.31(5), P2-P1 2.138(1), P3-P4 2.125(1), P1-Ag1-Ag2 96.76(2), P2-Ag1-Ag2 51.72(2), P3-Ag1-Ag2 61.32(2), P1-Ag1-P2 45.93(3), P3-Ag1-P1 141.42(3), P3-Ag1-P2 101.76(3), P2-Ag2-Ag1 62.38(2), P3-Ag2-Ag1 54.60(2), P4-Ag2-Ag1 99.38(2), P2-Ag2-P3 104.89(3), P2-Ag2-P4 128.90(3), P4-Ag2-P3 45.35(3), N2-Ag1-N1 101.85(19), N3-Ag2-N4A2 102.6(3), N3-Ag2-N4B2 98.8(7).<sup>[16]</sup>

To explore the influence of the metal on this system, the reactions of the P<sub>2</sub> ligand complex **A** with the organic linkers **L<sub>flex1</sub>** and **L<sub>flex2</sub>**, respectively, were performed using the Cu(I) salt [Cu(CH<sub>3</sub>CN)<sub>4</sub>][Al{OC(CF<sub>3</sub>)<sub>3</sub>}<sub>4</sub>] (**C**). The reaction with **L<sub>flex1</sub>** yielded clear orange block-like crystals within one week, which were characterised by single crystal X-ray analysis. **4-5** crystallises in the orthorhombic space group *Pbca* and features a 2D CP (**Figure 4-7**). The solid-state structure is analogous to compound **4-1** with minor differences in the bond lengths and angles (*cf.* Table 4-2). The cavities made-up by the networks have values up to 1.8 nm.<sup>[16]</sup> Compound **4-6** was obtained by using the organic linker **L<sub>flex2</sub>**, which is one CH<sub>2</sub>-group shorter than **L<sub>flex1</sub>**, in the reaction of **A** with the Cu(I)

source **C**. Crystals suitable for single crystal X-ray analysis were obtained within the following day as orange prisms. The solid-state structure of **4-6** (**Figure 4-8**), which crystallises in the monoclinic space group  $P2_1/n$ , is very similar to compound **4-2**, with the only main difference in the metal(I) moieties. A six-membered  $\text{Cu}_2\text{P}_4$ -ring with tetracoordinated Cu(I) centres serves as node and the nodes are connected to each other via four molecules of linker  $\text{L}_{\text{flex}}\mathbf{2}$  each. The cavities formed this way are also filled with anions and solvent molecules and are up to 1.8 nm in size.<sup>[16]</sup>

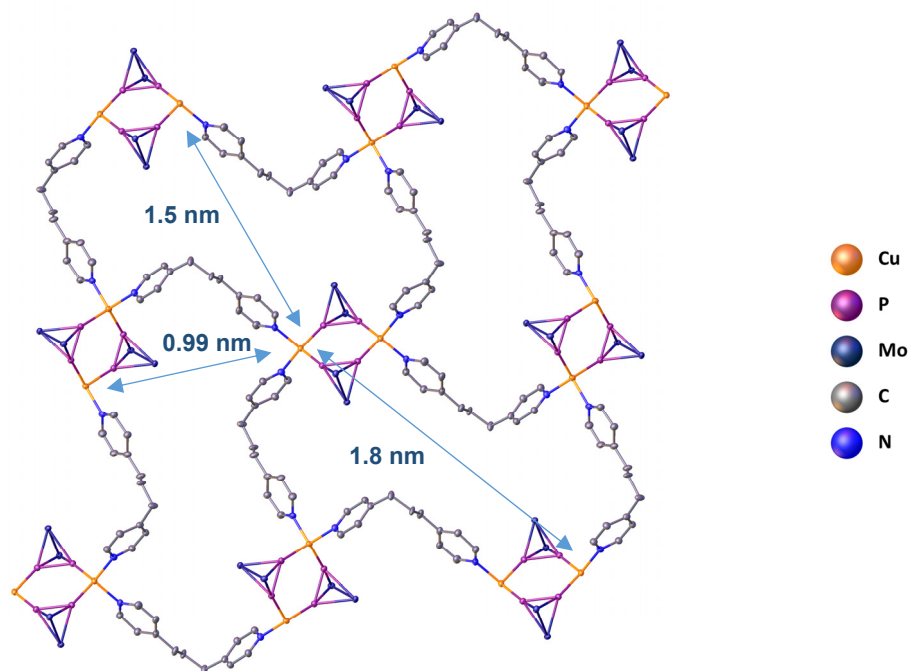


**Figure 4-7.** Molecular structure of the cation of **4-5** in the solid-state along the *a*-axis. Thermal ellipsoids are shown at 50 % probability level. Hydrogen atoms, Cp- and CO-ligands are omitted for clarity. Bond lengths and angles in [Å] and [°]: Cu1-P1 2.264(1), Cu1-P2 2.284(1), Cu1-N1A 2.02(3), Cu1-N2 2.047(3), P1-P2 2.083(1), P1-Cu1-P2 109.28(4), N1A-Cu1-N2 99.4(8).<sup>[16]</sup>



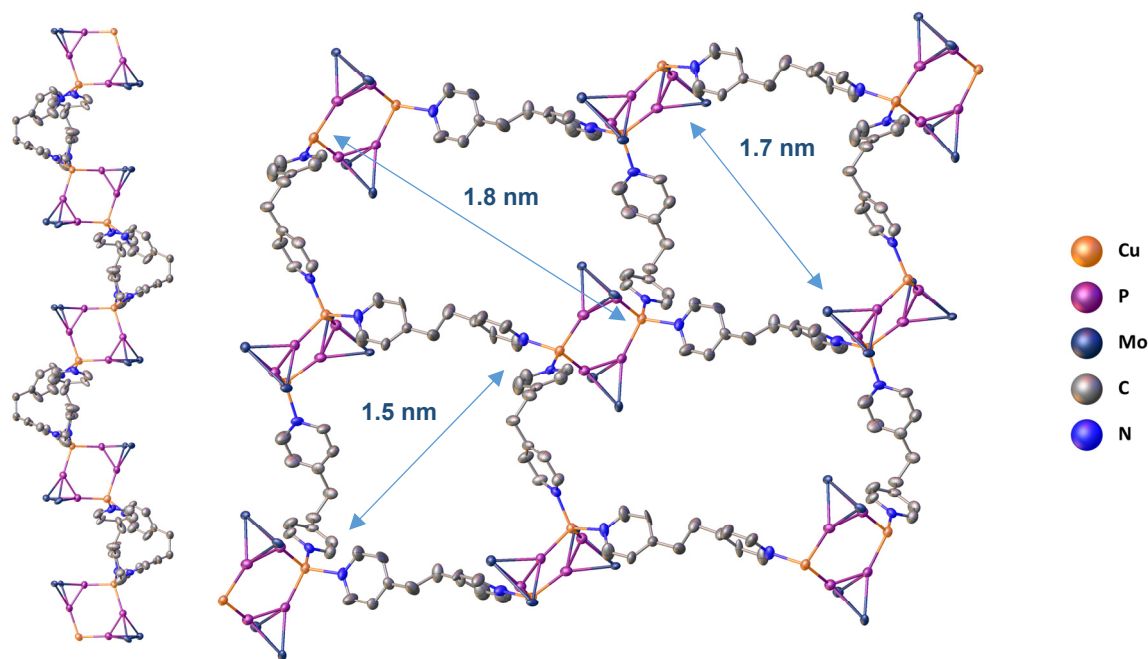


**Figure 4-8.** Preliminary molecular structure of the cation of **4-6** in the solid-state (left: view along the *a*-axis). Thermal ellipsoids are shown at 50 % probability level. Hydrogen atoms, Cp- and CO-ligands omitted for clarity. Bond lengths and angles in [Å] and [°]: Cu1-P12 2.285(2), Cu1-P21 2.276(2), Cu2-P11 , Cu2-P11 2.265(2), Cu2-P22 2.277(3), Cu1-N11 2.028(6), Cu1-N22 2.035(9), Cu2-N12 2.060(6), Cu2-N21 2.053(8), P11-P12 2.086(3), P22-P21 2.076(3), P21-Cu1-P12 106.44(9), P22-Cu2-P11 105.39(9), N11-Cu1-N22 106.2(3), N21-Cu2-N12 103.7(3).<sup>[16]</sup>

In former studies, the organic linker 1,2-di-(4-pyridyl)ethylene (**dpe**) was reacted with **A** and the Ag(I) salt **B**. By this combination, the synthesis of zero-dimensional coordination complexes and 1D, 2D and 3D CPs were realised.<sup>[12]</sup> To further explore the influence of the metal, the analogous reaction with the Cu(I) source **C** using a 1:1:1-ratio of the starting materials, was performed. Clear orange block-shaped crystals of **4-7** were obtained within one week. Compound **4-7** has the formula  $[\text{Cu}_2\{\text{CpMo}_2(\text{CO})_4(\mu, \eta^{2:2:1:1}\text{-P}_2)\}_2(\mu, \eta^{1:1}\text{-dpe})_2]_n[\text{TEF}]_{2n}$  and crystallises in the monoclinic space group  $P2_1/n$ . The solid-state structure of **4-7** (**Figure 4-9**) was also revealed by single crystal X-ray analysis and like in the previously discussed compounds **4-5** and **4-6**, a six-membered  $\text{Cu}_2\text{P}_4$ -ring serves as a node. The coordination sphere of the Cu(I) centres are completed by molecules of linker (**dpe**), which connect the nodes and lead to the two-dimensional extension of the network. The cavities formed by the network have sizes up to 2.0 nm and are filled anions and solvent molecules. The bond lengths and angles (**Table 4-2**) lie in the expected range.

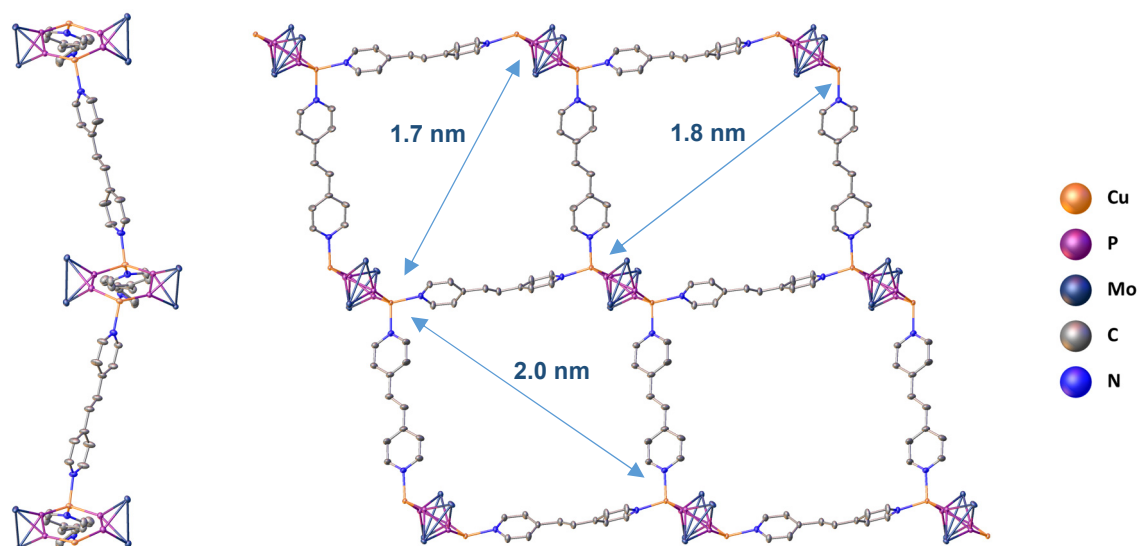


**Figure 4-9.** Molecular structure of the cation of **4-7** in the solid-state with view along the a-axis (left), showing the zig-zag formation of the 2D layer, and view along the b-axis, showing the cavities. Thermal ellipsoids are shown at 50 % probability level. Hydrogen atoms, Cp- and CO-ligands omitted for clarity. Bond lengths and angles in [Å] and [°]: Cu1-P1 2.2476(9), Cu1-P3 2.2760(9), Cu2-P2 2.2643(9), Cu2-P4 2.2828(9), Cu1-N1 2.019(3), Cu1-N2 2.046(3), Cu2-N3 2.037(3), Cu2-N4 2.028(3), P1-P2 2.0815(11), P3-P4 2.0848(11), P1-Cu1-P3 110.47(3), P2-Cu2-P4 111.78(3), N1-Cu1-N2 102.98(12), N4-Cu2-N3 105.25(12).<sup>[16]</sup>

**Table 4-2.** Comparison of the approximate cavity sizes [nm], the Cu-P, Cu-N and P-P bond lengths [Å] and P-Cu-P and N-Cu-N angles [°] of compounds **4-5-4-7**.

Compound	<b>4-5</b>	<b>4-6</b>	<b>4-7</b>
Linker	<b>L<sub>flex1</sub></b>	<b>L<sub>flex2</sub></b>	<b>dpe</b>
Cavity size <sup>[16]</sup>	0.99-1.8	1.5-1.8	1.7-2.0
Cu-P	2.264(1), 2.284(1),	2.265(2)-2.285(2)	2.2476(9)-2.2828(9)
Cu-N	2.02(3), 2.047(3)	2.028(6)-2.060(6)	2.019(3)-2.046(3)
P-P	2.083(1)	2.076(3), 2.086(3)	2.0848(11)
∠ P-Cu-P	109.28(4)	105.39(9), 106.44(9)	110.47(3), 111.78(3)
∠ N-Cu-N	99.4(8)	103.7(3), 106.2(3)	102.98(12), 105.25(12)

All compounds are well soluble in acetonitrile under dissociation and insoluble in other common solvents like dichloromethane, tetrahydrofurane, toluene, and *n*-pentane. The negative ion ESI-MS (CH<sub>3</sub>CN, r.t.) shows the peak for the TEF-anion. In the positive ion ESI-MS spectra (CH<sub>3</sub>CN, r.t.), only peaks referring to fragments of the compounds can be detected. The fragments contain different combinations of the metal, the P<sub>2</sub> ligand complex **A**, the respective organic linker and acetonitrile. In **4-5**, a peak for a fragment containing Cu, **A** and L<sub>flex1</sub> alike is observed. These results also support the assumption that the polymers are merely soluble under dissociation. The <sup>1</sup>H, <sup>13</sup>C{<sup>1</sup>H} and <sup>19</sup>F{<sup>1</sup>H}/<sup>19</sup>F{<sup>1</sup>H} NMR spectra (acetonitrile-*d*<sub>3</sub>, r.t.) for compounds **4-1** to **4-7** show the signals referring to the organic linker, the Cp- and CO ligands of the P<sub>2</sub> ligand complex **A** and the TEF-anion. The signals in the <sup>31</sup>P NMR spectra are shifted compared to the free P<sub>2</sub> ligand complex **A** (-42.9, C<sub>7</sub>D<sub>8</sub>)<sup>[19]</sup> and the respective Ag- and Cu dimers,<sup>[11,20,21]</sup> which have shifts of -82.0 and -83.1 ppm. The signals in the <sup>31</sup>P spectra observed for compounds **4-1**, **4-3** and **4-4** are singlets and have shifts of -78.4, -86.0 and -83.6 ppm. For compounds **4-2**, **4-5** and **4-6**, broad signals (-80.9 to -81.8 ppm, 54.8 and -44.1 ppm) are observed. This

suggests that the fragmentation of the compounds in solution is partial, as under a complete fragmentation, the signal for the free complex **A** should be detected.

#### 4.4 Conclusion

One goal of the study was to determine the influence of the crystallisation conditions on the three-component-system of the P<sub>2</sub> ligand complex [Cp<sub>2</sub>Mo<sub>2</sub>(CO)<sub>4</sub>(μ,η<sup>2:2</sup>-P<sub>2</sub>)] (**A**), the Ag(I) salt Ag[TEF] (**B**; TEF = Al{OC(CF<sub>3</sub>)<sub>3</sub>}<sub>4</sub>) and the flexible linkers 1,2-di(4-pyridyl)ethane (**L<sub>flex1</sub>**) and 1,3-di(4-pyridyl)propane (**L<sub>flex2</sub>**), respectively. The crude reaction mixtures were either stored at -28 °C or layered with *n*-pentane at room temperature. The crystallisation at -28 °C solely led to the formation of two-dimensional coordination polymers with the general formula [Ag<sub>2</sub>{Cp<sub>2</sub>Mo<sub>2</sub>(CO)<sub>4</sub>(μ,η<sup>2:2:1:1</sup>-P<sub>2</sub>)<sub>2</sub>(μ,η<sup>1:1</sup>-L)<sub>2</sub>]<sub>n</sub>[TEF]<sub>2n</sub> (**4-1**: L = **L<sub>flex1</sub>**; **4-2**: L = **L<sub>flex2</sub>**), whereas the layering led selectively to the formation of the one-dimensional CP [Ag<sub>2</sub>{Cp<sub>2</sub>Mo<sub>2</sub>(CO)<sub>4</sub>(η<sup>2:2:1:1</sup>-P<sub>2</sub>)<sub>2</sub>(μ,η<sup>1:1</sup>-**L<sub>flex1</sub>**)<sub>2</sub>]<sub>n</sub>[TEF]<sub>2n</sub> (**4-3**). The structures of **4-1** to **4-3** are very similar apart from the dimensionality of the CPs, which is due to the way the linkers connect the nodes. Additionally, compound **4-3** was sometimes accompanied by a second 1D CP (**4-4**), which features a very short Ag...Ag-distance of 2.9 Å, which is above the sum of the covalent radii of silver.<sup>[15]</sup> As Ag-Ag-interactions have been reported for values until 3 Å and larger, the existence of such interactions in **4-4** is likely.<sup>[16]</sup> To investigate the influence of the metal on this system, similar reactions using the Cu(I) salt [Cu(CH<sub>3</sub>CN)<sub>4</sub>][TEF] (**C**) and the flexible organic linkers **L<sub>flex1</sub>**, **L<sub>flex2</sub>** and **dpe** were performed. Layering of the crude reactions mixture at room temperature yielded three new 2D CPs with the general formula [Cu<sub>2</sub>{Cp<sub>2</sub>Mo<sub>2</sub>(CO)<sub>4</sub>(μ,η<sup>2:2:1:1</sup>-P<sub>2</sub>)<sub>2</sub>(μ,η<sup>1:1</sup>-L)<sub>2</sub>]<sub>n</sub>[TEF]<sub>2n</sub> (**4-5**: L = **L<sub>flex1</sub>**; **4-6**: L = **L<sub>flex2</sub>**; **4-7**: L = **dpe**) which are structurally very similar to compounds **4-1** and **4-2**.

## 4.5 Supporting Information

### General

All experiments were carried out in an inert atmosphere of nitrogen using standard Schlenk techniques. The nitrogen was dried and purified from traces of oxygen with a Cu/MgSO<sub>4</sub> catalyst, concentrated H<sub>2</sub>SO<sub>4</sub> and orange gel. Reactants were stored in a glovebox under argon atmosphere. All used solvents were taken from the solvent drying machine MB SPS-800 of the company MBRAUN.

### Chemicals

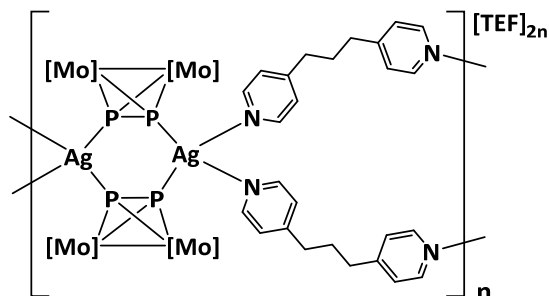
The precursor [Cp<sub>2</sub>Mo<sub>2</sub>(CO)<sub>4</sub>(μ,η<sup>2:2</sup>-P<sub>2</sub>)] (**A**) and the metal salts Ag[Al{OC(CF<sub>3</sub>)<sub>3</sub>}<sub>4</sub>] (**B**) and [Cu(CH<sub>3</sub>CN)<sub>4</sub>][Al{OC(CF<sub>3</sub>)<sub>3</sub>}<sub>4</sub>] (**C**) were prepared according to literature procedures.<sup>[17,22,19]</sup> The organic linker 1,3-di(4-pyridyl)propane (**L<sub>flex1</sub>**), 1,2-di(4-pyridyl)ethane (**L<sub>flex2</sub>**) and 1,2-di(4-pyridyl)ethylene (**dpe**) were purchased from TCI (**L<sub>flex1</sub>**) and Sigma Aldrich (**L<sub>flex2</sub>**, **dpe**) (now Merck) and used without further purification.

### Spectroscopic Methods

IR spectra were recorded as solids with an ATR-Ge disc on a varian FTS-800 spectrometer. Solution NMR spectra were recorded on a Bruker Avance III HD 400 spectrometer (<sup>1</sup>H: 400 MHz, <sup>31</sup>P: 161 MHz, <sup>13</sup>C: 100 MHz, <sup>19</sup>F: 376 MHz) with acetonitrile-d<sub>3</sub> as solvent at room temperature. The signals of tetramethylsilane (<sup>1</sup>H, <sup>13</sup>C), CFCl<sub>3</sub> (<sup>19</sup>F) and 85% H<sub>3</sub>PO<sub>4</sub> (<sup>31</sup>P) were used as reference for determining chemical shifts. The chemical shifts δ are presented in parts per million ppm and coupling constants *J* in Hz. The spectra were processed and analysed using the software Bruker TopSpin 3.0. Elemental analyses were performed on an Elementar vario MICRO cube apparatus. Mass spectra were recorded on an Agilent Q-TOF 6540 UHD mass spectrometer with acetonitrile as solvent.

### Experimental Procedures

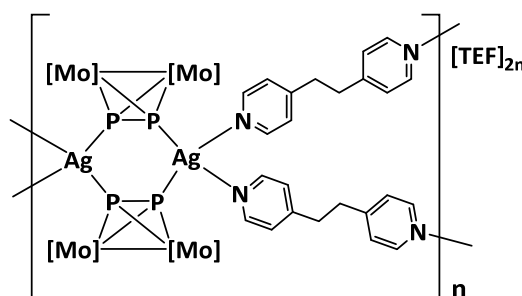
Synthesis of [Ag<sub>2</sub>{Cp<sub>2</sub>Mo<sub>2</sub>(CO)<sub>4</sub>(μ,η<sup>2:2:1:1</sup>-P<sub>2</sub>)}<sub>2</sub>(μ,η<sup>1:1</sup>-C<sub>13</sub>H<sub>14</sub>N<sub>2</sub>)<sub>2</sub>]<sub>n</sub>[TEF]<sub>2n</sub> (**4-1**):



Compounds **A** (2 eq., 50 mg, 0.1 mmol), **B** (1 eq., 53.7 mg, 0.05 mmol) and **L<sub>flex1</sub>** (1 eq., 9.9 mg, 0.05 mmol) were each dissolved in dichloromethane (5, 5 and 3 mL, respectively). The solution of **B** was slowly added to the solution of **A** and the mixture was stirred for 30 min. After this time, the solution of **L<sub>flex1</sub>** was added and the reaction mixture was further stirred for 3 h. The solution was filtered from brown precipitate and stored at -28 °C. After a few days, compound **4-1** was obtained as orange blocks. The supernatant was decanted off, the remaining crystals washed with *n*-pentane and dried in vacuo.

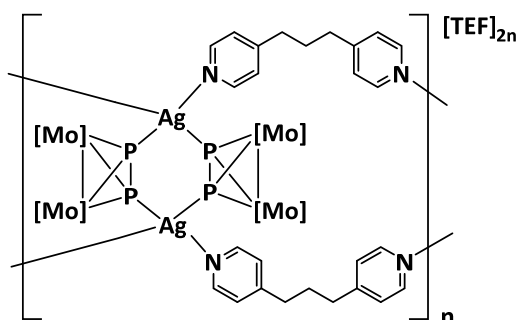
Crystalline Yield: 32.4 mg (37 %, related to **B** and **L<sub>flex</sub>1** equally). <sup>1</sup>H NMR δ[ppm] = 8.43 (d, 4H, CH<sub>pyr</sub>), 7.28 (d, 4H, CH<sub>pyr</sub>), 5.39 (s, 10 H, C<sub>5</sub>H<sub>5</sub>), 2.70 (t, J = 7.81 Hz, 6H, CH<sub>2</sub>). <sup>31</sup>P NMR δ[ppm] = -86.0 (s). <sup>13</sup>C{<sup>1</sup>H} NMR δ[ppm] = 224.1 (s, CO), 150.4 (s, CH<sub>pyr</sub>), 123.6 (s, CH<sub>pyr</sub>), 88.2 (s, C<sub>5</sub>H<sub>5</sub>), 35.1 (s, CH<sub>2</sub>), 31.2 (s, CH<sub>2</sub>). <sup>19</sup>F NMR δ[ppm] = -74.8 (s). Positive ion ESI-MS (CH<sub>3</sub>CN, r.t.): *m/z* (%) = 147.93 (100) [Ag(CH<sub>3</sub>CN)]<sup>+</sup>, 643.75 (90.5) [Ag(CH<sub>3</sub>CN){Cp<sub>2</sub>Mo<sub>2</sub>(CO)<sub>4</sub>P<sub>2</sub>}]<sup>+</sup>, 800.84 (55.5) [Ag{Cp<sub>2</sub>Mo<sub>2</sub>(CO)<sub>4</sub>P<sub>2</sub>}<sub>2</sub>-(C<sub>13</sub>H<sub>14</sub>N<sub>2</sub>)]<sup>+</sup>, 1100.54 (70.4) [Ag{Cp<sub>2</sub>Mo<sub>2</sub>(CO)<sub>4</sub>P<sub>2</sub>}<sub>2</sub>]<sup>+</sup>. Negative ion ESI-MS (CH<sub>3</sub>CN, r.t.): *m/z* (%) = 966.9 (100) [Al(OC(CF<sub>3</sub>)<sub>3</sub>)<sub>4</sub>]<sup>-</sup>. IR (solid, CO bands):  $\tilde{\nu}/\text{cm}^{-1}$ : 1986 (s), 1942 (s), 1919 (s). Elemental analysis calculated for C<sub>86</sub>H<sub>48</sub>Ag<sub>2</sub>Al<sub>2</sub>F<sub>72</sub>Mo<sub>4</sub>N<sub>4</sub>O<sub>16</sub>P<sub>4</sub> (3538.6 g·mol<sup>-1</sup>): 29.19 %C, 1.37 %H, 1.58 %N; Found: 29.07 %C, 1.48 %H, 1.53 %N.

Synthesis of [Ag<sub>2</sub>{CpMo<sub>2</sub>(CO)<sub>4</sub>(μ,η<sup>2:2:1:1</sup>-P<sub>2</sub>)}<sub>2</sub>(μ,η<sup>1:1</sup>-C<sub>12</sub>H<sub>12</sub>N<sub>2</sub>)<sub>2</sub>]<sub>n</sub>[TEF]<sub>2n</sub> (**4-2**):



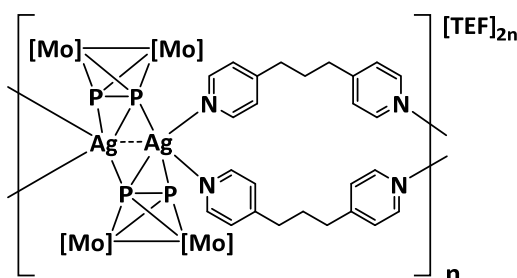
Compounds **A** (2 eq., 50 mg, 0.1 mmol), **B** (1 eq., 53.7 mg, 0.05 mmol) and **L<sub>flex</sub>2** (1 eq., 9.2 mg, 0.05 mmol) were each dissolved in dichloromethane (5, 5 and 3 mL, respectively). The solution of **B** was slowly added to the solution of **A** and the resulting mixture was stirred for 30 min. The solution of **L<sub>flex</sub>2** was added and the reaction solution was further stirred for 3 h. The solution was filtered from brown precipitate and stored at -28 °C. After a few days, compound **4-2** was obtained as red plates. The supernatant was decanted off, the remaining crystals washed with *n*-pentane and dried in vacuo. Crystalline Yield: 20.0 mg (23 %, related to **B** and **L<sub>flex</sub>2** equally). <sup>1</sup>H NMR δ[ppm] = 8.42 (dd, 4H, CH<sub>pyr</sub>), 7.24 (d, 4 H, CH<sub>pyr</sub>), 5.39 (s, 10 H, C<sub>5</sub>H<sub>5</sub>), 3.00 (s, 4H, CH<sub>2</sub>). <sup>31</sup>P NMR δ[ppm] = -84.6 (s). <sup>13</sup>C{<sup>1</sup>H} NMR δ[ppm] = 224.2 (s, CO), 150.5 (s, CH<sub>pyr</sub>), 123.59 (s, CH<sub>pyr</sub>), 88.1 (s, C<sub>5</sub>H<sub>5</sub>), 35.9 (s, CH<sub>2</sub>). <sup>19</sup>F NMR δ [ppm] = -74.8 (s). Positive ion ESI-MS (CH<sub>3</sub>CN, r.t.): *m/z* (%) = 106.9 (100) [Ag]<sup>+</sup>, 147.93 (100) [Ag(CH<sub>3</sub>CN)]<sup>+</sup>, 185.11 (100) [C<sub>12</sub>H<sub>13</sub>N<sub>2</sub>]<sup>+</sup>, 188.96 (100) [Ag(CH<sub>3</sub>CN)<sub>2</sub>]<sup>+</sup>, 291.0 (100) [Ag(C<sub>12</sub>H<sub>12</sub>N<sub>2</sub>)]<sup>+</sup>, 332.03 (100) [Ag(C<sub>12</sub>H<sub>12</sub>N<sub>2</sub>)(CH<sub>3</sub>CN)]<sup>+</sup>, 643.75 (90.5) [Ag(CH<sub>3</sub>CN){Cp<sub>2</sub>Mo<sub>2</sub>(CO)<sub>4</sub>P<sub>2</sub>}]<sup>+</sup>, 786.82 (79.1) [Ag{Cp<sub>2</sub>Mo<sub>2</sub>(CO)<sub>4</sub>P<sub>2</sub>}(C<sub>12</sub>H<sub>12</sub>N<sub>2</sub>)]<sup>+</sup>, 788.82 (100) [Ag{Cp<sub>2</sub>Mo<sub>2</sub>(CO)<sub>4</sub>P<sub>2</sub>}(C<sub>12</sub>H<sub>12</sub>N<sub>2</sub>)]<sup>+</sup>, 1099.54 (56.2) [Ag{Cp<sub>2</sub>Mo<sub>2</sub>(CO)<sub>4</sub>P<sub>2</sub>}<sub>2</sub>]<sup>+</sup>. Negative ion ESI-MS (CH<sub>3</sub>CN, r.t.): *m/z* (%) = 966.9 (100) [Al(OC(CF<sub>3</sub>)<sub>3</sub>)<sub>4</sub>]<sup>-</sup>. IR (solid, CO bands):  $\tilde{\nu}/\text{cm}^{-1}$ : 2022 (vs), 1990 (s), 1971 (vs), 1951 (s). Elemental analysis calculated for C<sub>84</sub>H<sub>44</sub>Ag<sub>2</sub>Al<sub>2</sub>F<sub>72</sub>Mo<sub>4</sub>N<sub>4</sub>O<sub>16</sub>P<sub>4</sub> · 3 CH<sub>2</sub>Cl<sub>2</sub> (3765.3 g·mol<sup>-1</sup>): 27.75 %C, 1.34 %H, 1.49 %N; Found: 27.75 %C, 1.19 %H, 0.97 %N.

Synthesis of  $[\text{Ag}_2\{\text{CpMo}_2(\text{CO})_4(\eta^{2:2:1:1}\text{-P}_2)\}_2(\mu, \eta^{1:1}\text{-C}_{13}\text{H}_{14}\text{N}_2)_2]_n[\text{TEF}]_{2n}$  (**4-3**):



Compounds **A** (2 eq., 35 mg, 0.07 mmol), **B** (1 eq., 38 mg, 0.035 mmol) and **L<sub>flex</sub>1** (1 eq., 6.9 mg, 0.035 mmol) were each dissolved in  $\text{CH}_2\text{Cl}_2$  (5 mL, 5 mL and 3 mL, respectively). The solution of **B** was slowly added to the solution of **A** and the mixture was stirred for 30 min. The solution of **L<sub>flex</sub>1** was added and the reaction solution was further stirred for 3 h. The solution was filtered from brown precipitate formed after addition of the linker and the clear red mixture was layered with *n*-pentane. After one day, compound **4-3** was obtained as orange blocks. The supernatant was decanted off, the remaining crystals washed with *n*-pentane and dried in vacuo. Crystalline Yield: 42.3 mg (100 %, related to **L<sub>flex</sub>1**).  $^1\text{H}$  NMR  $\delta$ [ppm] = 8.50 (dd, 4H,  $\text{CH}_{\text{pyr}}$ ), 7.56 (d, 4H,  $\text{CH}_{\text{pyr}}$ ), 5.34 (s, 10H,  $\text{C}_5\text{H}_5$ ), 2.84 (t, 6H,  $\text{CH}_2$ ).  $^{31}\text{P}$  NMR  $\delta$ [ppm] = -78.4 (s).  $^{13}\text{C}\{^1\text{H}\}$  NMR  $\delta$ [ppm] = 224.5 (s, **CO**), 145.9 (s,  $\text{CH}_{\text{pyr}}$ ), 123.6 (s,  $\text{CH}_{\text{pyr}}$ ), 88.1 (s,  $\text{C}_5\text{H}_5$ ), 35.4 (s,  $\text{CH}_2$ ), 30.7 (s,  $\text{CH}_2$ ).  $^{19}\text{F}$  NMR  $\delta$ [ppm] = -74.8 (s). Positive ion ESI-MS ( $\text{CH}_3\text{CN}$ , r.t.):  $m/z$  (%) = 147.93 (100)  $[\text{Ag}(\text{CH}_3\text{CN})]^+$ , 188.96 (100)  $[\text{Ag}(\text{CH}_3\text{CN})_2]^+$ , 199.12 (100)  $[\text{C}_{13}\text{H}_{15}\text{N}_2]^+$ , 305.02 (100)  $[\text{Ag}(\text{C}_{13}\text{H}_{14}\text{N}_2)]^+$ , 643.75 (90.5)  $[\text{Ag}(\text{CH}_3\text{CN})\{\text{Cp}_2\text{Mo}_2(\text{CO})_4\text{P}_2\}]^+$ , 802.84 (100)  $[\text{Ag}\{\text{Cp}_2\text{Mo}_2(\text{CO})_4\text{P}_2\}_2(\text{C}_{13}\text{H}_{14}\text{N}_2)]^+$ , 1100.54 (70.4)  $[\text{Ag}\{\text{Cp}_2\text{Mo}_2(\text{CO})_4\text{P}_2\}_2]^+$ . Negative ion ESI-MS ( $\text{CH}_3\text{CN}$ , r.t.):  $m/z$  (%) = 966.9 (100)  $[\text{Al}(\text{OC}(\text{CF}_3)_3)_4]^-$ . IR (solid, CO bands):  $\tilde{\nu}/\text{cm}^{-1}$ : 1990 (s), 1987 (s), 1966 (vs), 1923 (vs). Elemental analysis calculated for  $\text{C}_{86}\text{H}_{48}\text{Ag}_2\text{Al}_2\text{F}_{72}\text{Mo}_4\text{N}_4\text{O}_{16}\text{P}_4$  ( $3538,56 \text{ g}\cdot\text{mol}^{-1}$ ): 29.2 %C, 1.37 %H, 1.58 %N; Found: 29.5 %C, 1.20 %H, 1.58 %N.

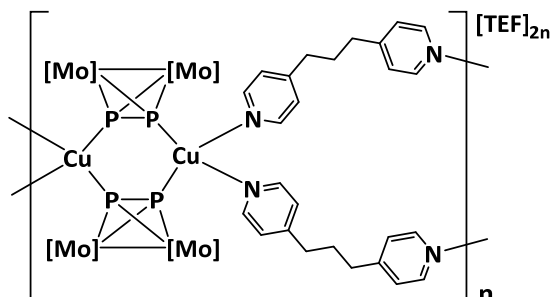
Synthesis of  $[\text{Ag}_2\{\text{CpMo}_2(\text{CO})_4(\eta^{2:2:1:1}\text{-P}_2)\}_2(\mu, \eta^{1:1}\text{-C}_{13}\text{H}_{14}\text{N}_2)_2]_n[\text{TEF}]_{2n}$  (**4-3**) +  $[\text{Ag}_2\{\text{CpMo}_2(\text{CO})_4(\mu, \eta^{2:2:2:1}\text{-P}_2)\}_2(\mu, \eta^{1:1}\text{-C}_{13}\text{H}_{14}\text{N}_2)_2]_n[\text{TEF}]_{2n}$  (**4-4**):



Compounds **A** (2 eq., 70 mg, 0.14 mmol), **B** (1 eq., 76 mg, 0.035 mmol) and **L<sub>flex</sub>1** (1 eq., 13.9 mg, 0.035 mmol) were each dissolved in  $\text{CH}_2\text{Cl}_2$  (5, 5 and 3 mL, respectively). The solution of **B** was slowly added to the solution of **A** and the resulting mixture was stirred for 30 min. The solution of **L<sub>flex</sub>1** was added and the reaction solution was further stirred for 3 h. The solution was filtered from brown precipitate and layered with *n*-pentane. After a few days, compounds **4-3** and **4-4** were obtained as orange (**4-3**) and red (**4-4**) blocks. The supernatant was decanted off, the remaining crystals separated manually and washed with *n*-pentane and dried in vacuo. Crystalline Yield (**4-4**): 12 mg (10 %, related to **B**).  $^1\text{H}$  NMR  $\delta$ [ppm] = 8.44 (dd, 4H,  $\text{CH}_{\text{pyr}}$ ), 7.29 (d, 4H,  $\text{CH}_{\text{pyr}}$ ), 5.38 (s, 10H,  $\text{C}_5\text{H}_5$ ), 3.03 (s, 6H,  $\text{CH}_2$ ).  $^{31}\text{P}$  NMR  $\delta$ [ppm] = -80.0 (bs), -81.8 (s).  $^{13}\text{C}\{^1\text{H}\}$  NMR  $\delta$ [ppm] = 224.4 (s, **CO**), 125.7 (s,  $\text{CH}_{\text{pyr}}$ ), 123.6 (s,  $\text{CH}_{\text{pyr}}$ ), 88.1

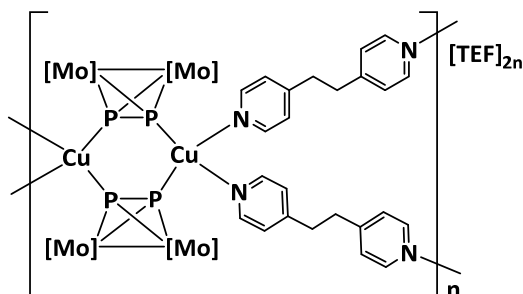
(s, C<sub>5</sub>H<sub>5</sub>), 35.9 (s, CH<sub>2</sub>). <sup>19</sup>F NMR δ[ppm] = -74.8 (s). IR (solid, CO bands):  $\tilde{\nu}/\text{cm}^{-1}$ : 1992 (ss), 1954 (ss). Elemental analysis calculated for C<sub>86</sub>H<sub>48</sub>Ag<sub>2</sub>Al<sub>2</sub>F<sub>72</sub>Mo<sub>4</sub>N<sub>4</sub>O<sub>16</sub>P<sub>4</sub> · CH<sub>2</sub>Cl<sub>2</sub> (3623,5 g·mol<sup>-1</sup>): 28.84 %C, 1.39 %H, 1.55 %N; Found: 28.60 %C, 1.28 %H, 1.54 %N.

Synthesis of compound [Cu<sub>2</sub>{CpMo<sub>2</sub>(CO)<sub>4</sub>(μ,η<sup>2:2:1:1</sup>-P<sub>2</sub>)<sub>2</sub>}(μ,η<sup>1:1</sup>-C<sub>13</sub>H<sub>14</sub>N<sub>2</sub>)<sub>2</sub>]<sub>n</sub>[TEF]<sub>2n</sub> (**4-5**):



Compound **A** (2 eq., 50 mg, 0.1 mmol), **C** (1 eq., 59 mg, 0.05 mmol) and **L<sub>flex1</sub>** (1 eq., 9.9 mg, 0.05 mmol) were each dissolved in dichloromethane (20, 10 and 10 mL, respectively). The solution of **C** was slowly added to the solution of **A** and the mixture was stirred for 1h. The solution of **L<sub>flex1</sub>** was slowly added, whereupon the reaction turned from a clear red to a turbid orange solution. Acetonitrile (2 mL) was added to clear the mixture and the reaction was stirred overnight. After filtration, the mixture was layered with *n*-pentane. After one day, compound **4-5** was obtained as clear orange blocks. The supernatant was decanted off, the remaining crystals washed with *n*-pentane and dried in vacuo. Crystalline Yield: 50 mg (62 %, related to **C**). <sup>1</sup>H-NMR δ[ppm] = 8.42 (dd, 4H, CH<sub>pyr</sub>), 7.22 (dd, 4H, CH<sub>arom</sub>), 5.31 (s, 10H, C<sub>5</sub>H<sub>5</sub>), 2.67 (m, 6H, CH<sub>2</sub>). <sup>31</sup>P-NMR δ[ppm] = -54.8 (bs). <sup>19</sup>F-NMR δ[ppm] = -74.8 (s). Positive ion ESI-MS (CH<sub>3</sub>CN, RT): *m/z* (%) = 103.96 (100) [Cu(CH<sub>3</sub>CN)]<sup>+</sup>, 144.98 (100) [Cu(CH<sub>3</sub>CN)<sub>2</sub>]<sup>+</sup>, 302.07 (100) [Cu(C<sub>13</sub>H<sub>14</sub>N<sub>2</sub>)]<sup>+</sup>, 459.16 (100) [Cu(C<sub>13</sub>H<sub>14</sub>N<sub>2</sub>)<sub>2</sub>]<sup>+</sup>, 599.77 (100) [Cu(CH<sub>3</sub>CN){Cp<sub>2</sub>Mo<sub>2</sub>(CO)<sub>4</sub>P<sub>2</sub>}]<sup>+</sup>, 1056.56 (60) [Cu{Cp<sub>2</sub>Mo<sub>2</sub>(CO)<sub>4</sub>P<sub>2</sub>}]<sup>+</sup>, 756.86 (55.5) [Cu(C<sub>13</sub>H<sub>14</sub>N<sub>2</sub>){Cp<sub>2</sub>Mo<sub>2</sub>(CO)<sub>4</sub>P<sub>2</sub>}]<sup>+</sup>. Negative ion ESI-MS (CH<sub>3</sub>CN, RT): *m/z* (%) = 966.9 (100) [Al(OC(CF<sub>3</sub>)<sub>3</sub>)<sub>4</sub>]<sup>-</sup>. IR (solid, CO bands):  $\tilde{\nu}/\text{cm}^{-1}$ : 2002 (s), 1982 (ws), 1946 (s), 1932 (s). Elemental analysis calculated for AlC<sub>43</sub>CuF<sub>36</sub>H<sub>24</sub>Mo<sub>2</sub>N<sub>2</sub>O<sub>8</sub>P<sub>2</sub> · CH<sub>3</sub>CN · 0.75 CH<sub>2</sub>Cl<sub>2</sub> (1831.76 g·mol<sup>-1</sup>): 29.97 %C, 1.57 %H, 2.29 %N; Found: 30.41 %C, 1.60 %H, 2.57 %N.

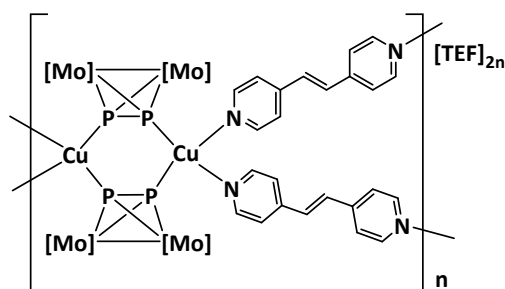
Synthesis of compound [Cu<sub>2</sub>{CpMo<sub>2</sub>(CO)<sub>4</sub>(μ,η<sup>2:2:1:1</sup>-P<sub>2</sub>)<sub>2</sub>}(μ,η<sup>1:1</sup>-C<sub>12</sub>H<sub>12</sub>N<sub>2</sub>)<sub>2</sub>]<sub>n</sub>[TEF]<sub>2n</sub> (**4-6**):



Compounds **A** (2 eq., 50 mg, 0.1 mmol), **C** (1 eq., 79.4 mg, 0.05 mmol) and **L<sub>flex2</sub>** (1 eq., 9.1 mg, 0.05 mmol) were dissolved in dichloromethane (10, 5 and 5 mL, respectively). The solution of **C** was slowly added to the solution of **A** and the reaction was stirred for 30 min. The solution of **L<sub>flex2</sub>** was added and the turbid reaction mixture was stirred overnight. Acetonitrile (2 mL) was added to dissolve the precipitate, which was formed after addition of the solution of **L<sub>flex2</sub>**. The mixture was filtrated and carefully layered with a 1:1-mixture of *n*-pentane and dichloromethane. Within the next days,

compound **4-6** was obtained as clear orange prisms. The supernatant was decanted off, the remaining crystals washed with *n*-pentane and dried in vacuo. Crystalline Yield: 68 mg (42.3 %, related to **C**).  $^1\text{H-NMR}$   $\delta$ [ppm] = 8.39 (dd,  $\text{CH}_{\text{pyr}}$ ), 7.13 (dd,  $\text{CH}_{\text{pyr}}$ ), 5.30 (s,  $\text{C}_5\text{H}_5$ ), 2.63 (t,  $\text{H}_{\text{sp}^3}$ ).  $^{31}\text{P-NMR}$   $\delta$ [ppm] = -44.1 (s).  $^{13}\text{C}\{^1\text{H}\}$ -NMR  $\delta$ [ppm] = 226.23 (s, **CO**), 150.46 (s,  $\text{CH}_{\text{pyr}}$ ), 125.51 (s,  $\text{CH}_{\text{pyr}}$ ), 87.50 (s,  $\text{C}_5\text{H}_5$ ), 35.81 (s,  $\text{CH}_2$ ).  $^{19}\text{F-NMR}$   $\delta$ [ppm] = -74.8 (s). Positive ion ESI-MS ( $\text{CH}_3\text{CN}$ , RT):  $m/z$  (%) = 103.96 (100)  $[\text{Cu}(\text{CH}_3\text{CN})]^+$ , 144.98 (100)  $[\text{Cu}(\text{CH}_3\text{CN})_2]^+$ , 288.06 (100)  $[\text{Cu}(\text{C}_{12}\text{H}_{12}\text{N}_2)(\text{CH}_3\text{CN})]^+$ , 599.77 (100)  $[\text{Cu}(\text{CH}_3\text{CN})\{\text{Cp}_2\text{Mo}_2(\text{CO})_4\text{P}_2\}]^+$ , 744.84 (100)  $[\text{Cu}(\text{C}_{12}\text{H}_{12}\text{N}_2)\{\text{Cp}_2\text{Mo}_2(\text{CO})_4\text{P}_2\}]^+$ , 1056.56 (60)  $[\text{Cu}\{\text{Cp}_2\text{Mo}_2(\text{CO})_4\text{P}_2\}]^+$ . Negative ion ESI-MS ( $\text{CH}_3\text{CN}$ , RT):  $m/z$  (%) = 966.9 (100)  $[\text{Al}(\text{OC}(\text{CF}_3)_3)_4]^-$ . IR (solid, CO bands):  $\tilde{\nu}/\text{cm}^{-1}$ : 2006 (s), 2000 (s), 1954 (s), 1924 (s). Elemental analysis calculated for  $\text{C}_{84}\text{H}_{44}\text{Cu}_2\text{Al}_2\text{F}_{72}\text{Mo}_4\text{N}_4\text{O}_{16}\text{P}_4$  (3427.50  $\text{g}\cdot\text{mol}^{-1}$ ): 29.41 %C, 1.29 %H, 1.63 %N; Found: 30.01 %C, 1.32 %H, 1.57 %N.

Synthesis of compound  $[\text{Cu}_2\{\text{CpMo}_2(\text{CO})_4(\mu, \eta^{2:2:1:1}\text{-P}_2)\}_2(\mu, \eta^{1:1}\text{-C}_{12}\text{H}_{10}\text{N}_2)_2]_n[\text{TEF}]_{2n}$  (**4-7**):



Compounds **A** (1 eq., 25 mg, 0.05 mmol), **C** (1eq., 79.4 mg, 0.05 mmol) and **dpe** (1 eq., 9.1 mg, 0.05 mmol) were dissolved in dichloromethane (10, 5 and 3 mL, respectively). The solution of **C** was slowly added to the solution of **A** and the reaction was stirred for 30 min. The solution of **dpe** was added and the turbid reaction mixture was stirred overnight. After filtration, the mixture was layered with a 1:1-mixture of *n*-pentane and dichloromethane. After a week, compound **4-7** was obtained as clear orange blocks. The supernatant was decanted off, the remaining crystals washed with *n*-pentane and dried in vacuo. Crystalline Yield: 71 mg (42 %, related to **A**, **C** and **dpe** equally). Positive ion ESI-MS ( $\text{CH}_3\text{CN}$ , RT):  $m/z$  (%) = 103.96 (100)  $[\text{Cu}(\text{CH}_3\text{CN})]^+$ , 144.98 (100)  $[\text{Cu}(\text{CH}_3\text{CN})_2]^+$ , 183.09 (100)  $[\text{C}_{12}\text{H}_{10}\text{N}_2]^+$ , 599.77 (100)  $[\text{Cu}(\text{CH}_3\text{CN})\{\text{Cp}_2\text{Mo}_2(\text{CO})_4\text{P}_2\}]^+$ , 1056.56 (60.5)  $[\text{Cu}\{\text{Cp}_2\text{Mo}_2(\text{CO})_4\text{P}_2\}]^+$ . Negative ion ESI-MS ( $\text{CH}_3\text{CN}$ , RT):  $m/z$  (%) = 966.92 (100)  $[\text{Al}(\text{OC}(\text{CF}_3)_3)_4]^-$ . IR (solid, CO bands):  $\tilde{\nu}/\text{cm}^{-1}$ : 1987 (ws), 1955 (ws), 1931 (ws).



## Crystallographic Data

**Crystal Structure Analysis:** The crystals were selected and measured on a Gemini Ultra diffractometer equipped with an AtlasS2 CCD detector (**4-1**, **4-2**, **4-4**, **4-7**), a GV50 diffractometer equipped with a TitanS2 CCD detector (**4-3**) and a SuperNova diffractometer equipped with an Atlas CCD detector (**4-5**), respectively. The crystals were kept at  $T = 123(1)$  K during data collection. Data collection and reduction were performed with **CrysAlisPro** [Version 171.38.46, 2015 (**4-1**, **4-2**, **4-3**, **4-4**), 171.39.37b, 2017 (**4-5**, **4-7**)].<sup>[23]</sup> For the compounds **4-2**, **4-3**, **4-4** and **4-7**, an analytical numeric absorption correction using a multifaceted crystal model based on expressions derived by R.C. Clark & J.S. Reid<sup>[24]</sup> and an empirical absorption correction using spherical harmonics as implemented in SCALE3 ABSPACK was applied. For compounds **4-1** and **4-5**, a numerical absorption correction based on gaussian integration over a multifaceted crystal model and an empirical absorption correction using spherical harmonics as implemented in SCALE3 ABSPACK was applied. Using **Olex2**,<sup>[25]</sup> the structures were solved with **ShelXT**<sup>[26]</sup> and a least-square refinement on  $F^2$  was carried out with **ShelXL**<sup>[27]</sup> for all structures. All non-hydrogen atoms were refined anisotropically. Hydrogen atoms at the carbon atoms were located in idealised positions and refined isotropically according to the riding model.

**Compound 4-1:** The asymmetric unit contains 5.5 CH<sub>2</sub>Cl<sub>2</sub> solvent molecules. Two of these CH<sub>2</sub>Cl<sub>2</sub> molecules are disordered over two positions (56:44;55:45) and another one is located near an inversion centre. The asymmetric unit further contains two [Al{OC(CF<sub>3</sub>)<sub>3</sub>}]<sub>4</sub> anions, two times half the complex [Ag<sub>2</sub>{Cp<sub>2</sub>Mo<sub>2</sub>(CO)<sub>4</sub>(μ<sub>4</sub>,η<sup>2:2:1:1</sup>-P<sub>2</sub>)}]<sub>2</sub> and two **L<sub>flex1</sub>** linker molecules. One of the four {O(CF<sub>3</sub>)<sub>3</sub>} substituents of each [Al{OC(CF<sub>3</sub>)<sub>3</sub>}]<sub>4</sub> anion is disordered over two positions (73:27;56:44). To describe these disorders the restraints DFIX, SADI and SIMU were applied.

**Compound 4-2:** The asymmetric unit contains 3 CH<sub>2</sub>Cl<sub>2</sub> solvent molecules. Two of these CH<sub>2</sub>Cl<sub>2</sub> solvent molecules are disordered over two positions (55:45; 61:39) and one is disordered over four positions (43:24:17:16). The asymmetric unit further contains two [Al{OC(CF<sub>3</sub>)<sub>3</sub>}]<sub>4</sub> anions, two times half the complex [Ag<sub>2</sub>{Cp<sub>2</sub>Mo<sub>2</sub>(CO)<sub>4</sub>(μ<sub>4</sub>,η<sup>2:2:1:1</sup>-P<sub>2</sub>)}]<sub>2</sub> and two **L<sub>flex2</sub>** linker molecules. One linker molecule is disordered over two positions (70:30). Additionally one half fragment of the complex [Ag<sub>2</sub>{Cp<sub>2</sub>Mo<sub>2</sub>(CO)<sub>4</sub>(μ<sub>4</sub>,η<sup>2:2:1:1</sup>-P<sub>2</sub>)}]<sub>2</sub> is disordered over two positions (65:35). Further, all four {O(CF<sub>3</sub>)<sub>3</sub>} substituents of both [Al{OC(CF<sub>3</sub>)<sub>3</sub>}]<sub>4</sub> anions are heavily disordered, at least over two positions. To describe these disorders the restraints DFIX, SADI, FLAT, SIMU and RIGU were applied.

**Compound 4-3:** The asymmetric unit contains 1.23 CH<sub>2</sub>Cl<sub>2</sub> and 0.77 pentane solvent molecules. One CH<sub>2</sub>Cl<sub>2</sub> molecule is disordered over two positions (80:20) and another CH<sub>2</sub>Cl<sub>2</sub> molecule shares the same position with a pentane molecule (23:77). Additionally the asymmetric unit contains two times half the complex [Ag<sub>2</sub>{Cp<sub>2</sub>Mo<sub>2</sub>(CO)<sub>4</sub>(μ<sub>4</sub>,η<sup>2:2:1:1</sup>-P<sub>2</sub>)}]<sub>2</sub>, two [Al{OC(CF<sub>3</sub>)<sub>3</sub>}]<sub>4</sub> anions and two **L<sub>flex1</sub>** linker molecules. Three {O(CF<sub>3</sub>)<sub>3</sub>} substituents at the two [Al{OC(CF<sub>3</sub>)<sub>3</sub>}]<sub>4</sub> anions are disordered over two positions (56:44;80:20;79:21). Further one **L<sub>flex1</sub>** linker is disordered over two positions (80:20). Additionally the two half fragments of the complexes [Ag<sub>2</sub>{Cp<sub>2</sub>Mo<sub>2</sub>(CO)<sub>4</sub>(μ<sub>4</sub>,η<sup>2:2:1:1</sup>-P<sub>2</sub>)}]<sub>2</sub> are also disordered over two positions (92:8;87:13). To describe these disorders the restraints DFIX, SADI, FLAT, SIMU and RIGU were applied.

**Compound 4-4:** The asymmetric unit contains 1 CH<sub>2</sub>Cl<sub>2</sub> solvent molecules, which is disordered over three positions (50:27:23). It further contains two [Al{OC(CF<sub>3</sub>)<sub>3</sub>}]<sub>4</sub> anions, the complex [Ag<sub>2</sub>{Cp<sub>2</sub>Mo<sub>2</sub>(CO)<sub>4</sub>(μ<sub>4</sub>,η<sup>2:2:2:1</sup>-P<sub>2</sub>)}]<sub>2</sub> and two **L<sub>flex1</sub>** linker molecules. All four {O(CF<sub>3</sub>)<sub>3</sub>}]<sub>4</sub> substituents of one [Al{OC(CF<sub>3</sub>)<sub>3</sub>}]<sub>4</sub> anion are heavily disordered over two or, respectively, three positions. The second [Al{OC(CF<sub>3</sub>)<sub>3</sub>}]<sub>4</sub> anion shows a disorder of two of the four {O(CF<sub>3</sub>)<sub>3</sub>} substituents over two positions

(77:23; 83:17). Additionally one Cp ligand is disordered over two positions (71:29). To describe these disorders the restraints DFIX, SADI, ISOR, SIMU and RIGU were applied.

Compound **4-5**: The asymmetric unit contains 0.75 CH<sub>2</sub>Cl<sub>2</sub> and one CH<sub>3</sub>CN solvent molecules. The CH<sub>2</sub>Cl<sub>2</sub> molecule was heavily disordered. Therefore, a solvent mask was calculated and 240 electrons were found in a volume of 760 Å<sup>3</sup> in one void per unit cell. This is consistent with the presence of 0.75 CH<sub>2</sub>Cl<sub>2</sub> molecules per asymmetric unit, which account for 252 electrons per unit cell. The CH<sub>3</sub>CN solvent molecule shows a disorder of the CH<sub>3</sub> group over two positions (59:41). The asymmetric unit further contains half the complex [Cu<sub>2</sub>{Cp<sub>2</sub>Mo<sub>2</sub>(CO)<sub>4</sub>(μ<sub>4</sub>,η<sup>2:2:1:1</sup>-P<sub>2</sub>)<sub>2</sub>], an [Al{OC(CF<sub>3</sub>)<sub>3</sub>}<sub>4</sub>] anion and one linker molecule (**L<sub>flex1</sub>**). The linker is disordered over two positions (69:31). Additionally all four {O(CF<sub>3</sub>)<sub>3</sub>} substituents of the [Al{OC(CF<sub>3</sub>)<sub>3</sub>}<sub>4</sub>] anion are heavily disordered, at least over two positions. To describe these disorders the restraints SADI, SIMU and ISOR were applied.

Compound **4-7**: The asymmetric unit contains 2 CH<sub>2</sub>Cl<sub>2</sub> solvent molecules, which are heavily disordered. Therefore, a solvent mask was calculated and 348.0 electrons were found in a volume of 1624.0 Å<sup>3</sup> in two voids. This is consistent with the presence of two CH<sub>2</sub>Cl<sub>2</sub> molecules per asymmetric unit, which account for 336.0 electrons. The asymmetric unit further contains the complex [Cu<sub>2</sub>{Cp<sub>2</sub>Mo<sub>2</sub>(CO)<sub>4</sub>(μ<sub>4</sub>,η<sup>2:2:1:1</sup>-P<sub>2</sub>)<sub>2</sub>], two [Al{OC(CF<sub>3</sub>)<sub>3</sub>}<sub>4</sub>] anions and two linker molecule (**dpe**). One Cp ligand of the complex is disordered over two positions (54:46). Further, the [Al{OC(CF<sub>3</sub>)<sub>3</sub>}<sub>4</sub>] anions are partly heavily disordered, at least over two positions. To describe these disorders the restraints SADI, SIMU and DFIX were applied.

**Table 4-3.** Crystallographic data and details of diffraction experiments for compounds **4-1-4-4**.

Compound	<b>4-1</b> · 5.5 CH <sub>2</sub> Cl <sub>2</sub>	<b>4-2</b> · 3 CH <sub>2</sub> Cl <sub>2</sub>	<b>4-3</b> · 1.23 CH <sub>2</sub> Cl <sub>2</sub> · 0.77 pentane	<b>4-4</b> · CH <sub>2</sub> Cl <sub>2</sub>
Data set (internal naming)	<b>abs214c</b>	<b>abs278</b>	<b>abs220a</b>	<b>abs214a</b>
Formula	C <sub>91.5</sub> H <sub>59</sub> Ag <sub>2</sub> Al <sub>2</sub> Cl <sub>11</sub> F <sub>7</sub> Mo <sub>4</sub> N <sub>4</sub> O <sub>16</sub> P <sub>4</sub>	C <sub>87</sub> H <sub>50</sub> Ag <sub>2</sub> Al <sub>2</sub> Cl <sub>6</sub> F <sub>72</sub> Mo <sub>4</sub> N <sub>4</sub> O <sub>16</sub> P <sub>4</sub>	C <sub>91.08</sub> H <sub>59.7</sub> Ag <sub>2</sub> Al <sub>2</sub> Cl <sub>2</sub> Mo <sub>4</sub> N <sub>4</sub> O <sub>16</sub> P <sub>4</sub>	C <sub>87</sub> H <sub>50</sub> Ag <sub>2</sub> Al <sub>2</sub> Cl <sub>2</sub> F <sub>72</sub> Mo <sub>4</sub> N <sub>4</sub> O <sub>16</sub> P <sub>4</sub>
<i>D</i> <sub>calc.</sub> / g · cm <sup>-3</sup>	1.990	1.973	1.994	2.009
$\mu$ /mm <sup>-1</sup>	1.091	8.883	8.433	1.012
Formula Weight	4005.71	3765.35	3698.63	3623.55
Colour	orange	red	red	orange
Shape	block	plate	block	block
Size/mm <sup>3</sup>	0.42×0.25×0.10	0.41×0.16×0.08	0.17×0.13×0.10	0.39×0.29×0.20
<i>T</i> /K	123(1)	123(1)	123.00(10)	123(1)
Crystal System	triclinic	monoclinic	monoclinic	triclinic
Space Group	<i>P</i> $\bar{1}$	<i>P</i> <sub>2</sub> <sub>1</sub> / <i>n</i>	<i>P</i> <sub>2</sub> <sub>1</sub> / <i>c</i>	<i>P</i> $\bar{1}$
<i>a</i> /Å	18.6279(6)	19.8410(2)	18.8487(3)	15.5020(4)
<i>b</i> /Å	19.0575(5)	30.9473(3)	33.2027(3)	16.2426(4)
<i>c</i> /Å	23.3232(7)	21.3714(3)	20.0570(3)	24.6188(6)
$\alpha$ /°	69.041(3)	90	90	86.920(2)
$\beta$ /°	67.494(3)	105.0090(10)	101.0290(10)	81.197(2)
$\gamma$ /°	63.829(3)	90	90	77.939(2)
<i>V</i> /Å <sup>3</sup>	6684.5(4)	12674.9(3)	12320.4(3)	5989.1(3)
<i>Z</i>	2	4	4	2
<i>Z'</i>	1	1	1	1
Wavelength/Å	0.71073	1.54184	1.54184	0.71073
Radiation type	MoK $\alpha$	CuK $\alpha$	CuK $\alpha$	MoK $\alpha$
<i>Q</i> <sub>min</sub> /°	3.175	3.530	3.483	3.327
<i>Q</i> <sub>max</sub> /°	32.441	72.957	74.040	32.647
Measured Refl.	101966	55148	66650	53999
Independent Refl.	43238	24463	23934	37409
Reflections with <i>I</i> > 2( <i>I</i> )	28762	21087	19847	28134
<i>R</i> <sub>int</sub>	0.0437	0.0366	0.0843	0.0223
Parameters	2147	3170	2656	2689
Restraints	615	4325	3101	4387
Largest Peak	1.246	1.192	2.210	1.410
Deepest Hole	-1.000	-1.205	-1.529	-1.174
GooF	1.031	1.029	1.025	1.043
<i>wR</i> <sub>2</sub> (all data)	0.1126	0.1873	0.1918	0.1272
<i>wR</i> <sub>2</sub>	0.0966	0.1786	0.1798	0.1119
<i>R</i> <sub>1</sub> (all data)	0.0896	0.0744	0.0773	0.0740
<i>R</i> <sub>1</sub>	0.0467	0.0655	0.0671	0.0499

**Table 4-4.** Crystallographic data and details of diffraction experiments for compounds **4-5** and **4-7**.

<b>Compound</b>	<b>4-5 · CH<sub>3</sub>CN · 0.75 CH<sub>2</sub>Cl<sub>2</sub></b>	<b>4-7 · 2 CH<sub>2</sub>Cl<sub>2</sub></b>
Data set (internal naming)	<b>abs273_2D</b>	<b>abs409d</b>
Formula	AlC <sub>45.75</sub> Cl <sub>1.5</sub> CuF <sub>36</sub> H <sub>2</sub> 8.5Mo <sub>2</sub> N <sub>3</sub> O <sub>8</sub> P <sub>2</sub>	Al <sub>2</sub> C <sub>86</sub> Cl <sub>4</sub> Cu <sub>2</sub> F <sub>72</sub> H <sub>44</sub> Mo <sub>4</sub> N <sub>4</sub> O <sub>16</sub> P <sub>4</sub>
$D_{calc.} / \text{g} \cdot \text{cm}^{-3}$	1.925	1.892
$\mu / \text{mm}^{-1}$	6.274	1.032
Formula Weight	1829.73	3587.73
Colour	clear orange	clear orange
Shape	block	block
Size/mm <sup>3</sup>	0.36×0.27×0.23	0.44×0.26×0.19
T/K	123.00(10)	123(1)
Crystal System	orthorhombic	monoclinic
Space Group	<i>Pbca</i>	<i>P2<sub>1</sub>/n</i>
$a / \text{Å}$	18.0017(2)	17.1427(2)
$b / \text{Å}$	21.8676(2)	23.9571(3)
$c / \text{Å}$	32.0746(3)	31.5314(5)
$\alpha / ^\circ$	90	90
$\beta / ^\circ$	90	103.4600(10)
$\gamma / ^\circ$	90	90
$V / \text{Å}^3$	12626.3(2)	12593.9(3)
Z	4	4
Z'	1	1
Wavelength/Å	1.54184	0.71073
Radiation type	CuK $\alpha$	MoK $\alpha$
$Q_{min} / ^\circ$	3.466	3.251
$Q_{max} / ^\circ$	74.355	32.727
Measured Refl.	76165	106871
Independent Refl.	12689	41920
Reflections with $I > 2(I)$	12157	31677
$R_{int}$	0.0743	0.0306
Parameters	1508	2638
Restraints	1124	3959
Largest Peak	1.000	3.304
Deepest Hole	-0.702	-1.299
GooF	1.129	1.017
$wR_2$ (all data)	0.1243	0.1638
$wR_2$	0.1234	0.1512
$R_1$ (all data)	0.0537	0.0819
$R_1$	0.0521	0.0598

The structure of compound **4-6** (data set: **abs432**) with the general formula  $[\text{Cu}\{\text{Cp}_2\text{Mo}_2(\text{CO})_4\text{P}_2\}(\text{C}_{12}\text{H}_{12}\text{N}_2)][\text{TEF}] \cdot \sim 0.75 \text{ CH}_2\text{Cl}_2$  is reported as preliminary data because of the so far unresolved disorder of many structural fragments. Two crystallographically unique TEF anions are disordered via different orientations caused by different conformations of  $\{\text{O}(\text{CF}_3)_3\}_4$  and  $\text{CF}_3$  groups due to possibility of rotation about single C-C and C-F bonds. Moreover, the  $\{\text{Cp}_2\text{Mo}_2(\text{CO})_4\text{P}_2\}$  units in the 2D cationic complex are disordered over two or three positions, respectively, for two crystallographically unique units. In addition, the numerous positions of  $\text{CH}_2\text{Cl}_2$  solvent molecules are also disordered. An experimental attempt was made to freeze out the thermal contribution to the disorder of these anions. For this purpose, the crystals were measured at PETRA III synchrotron (P24 beamline) at extra-low temperatures (He,  $T = 20 \text{ K}$ ). However, the disorder proved to be positional, related to overlap of different orientations of both the TEF anions and the cationic part, and the ordering of neither of the structural units occurred. The refinement of the disorder detail is underway. Preliminary data on crystal structure (for in-house measurement) are presented in **Table 4-3**.

**Table 4-5.** Crystallographic data and details of diffraction experiments for compound **4-6**.

<b>Crystal data</b>	
Tentative structural formula	$[\text{Cu}\{\text{Cp}_2\text{Mo}_2(\text{CO})_4\text{P}_2\}(\text{C}_{12}\text{H}_{12}\text{N}_2)][\text{TEF}] \cdot \sim 0.75 \text{ CH}_2\text{Cl}_2$
Formula	$\text{C}_{40.75}\text{H}_{23.50}\text{AlCl}_{1.46}\text{CuF}_{36}\text{Mo}_2\text{N}_2\text{O}_8\text{P}_2$
$M_r$	> 1730.30
Crystal system	monoclinic
space group	$P2_1/n$
Temperature (K)	123
$a, b, c$ (Å)	19.5472(3), 30.6060(4), 21.3795(4)
$\alpha, \beta, \gamma$ (°)	90, 104.7079(15), 90
$V$ (Å <sup>3</sup> )	12371.4(3)
$Z$	8
$F(000)$	6735
$D_x$ (mg · m <sup>-3</sup> )	> 1.858
Radiation type	$\text{MoK}\alpha$
$\mu$ (mm <sup>-1</sup> )	> 1.022
Crystal shape	Prism
Colour	Orange
Crystal size (mm)	0.25 × 0.20 × 0.13
<b>Data collection</b>	
Diffractometer	Gemini, Atlas <sup>S2</sup>
Absorption correction	Gaussian
No. of measured independent and observed [ $I > 2s(I)$ ] reflections	41252, 17685, 12454
$R_{\text{int}}$	0.0204
Range of $h, k, l$	$h = -21 \rightarrow 16, k = -34 \rightarrow 25, l = -16 \rightarrow 23$
<b>Preliminary refinement</b>	
$R[F^2 > 2s(F^2)], wR(F^2), S$	0.0796, 0.2322, 1.014
No. of reflections	17685
No. of parameters	2034
No. of restraints	1
H-atom treatment	H-atom parameters constrained
$\Delta\rho_{\text{max}}, \Delta\rho_{\text{min}}$ (e · Å <sup>-3</sup> )	1.119, -0.694

## 4.6 References

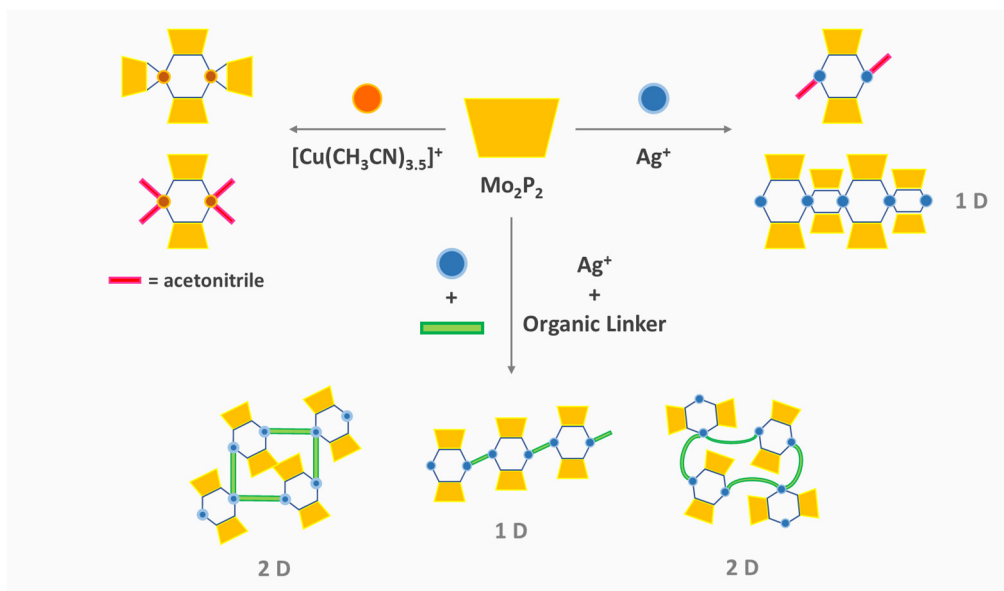
- [1] a) S.-C. Chen, X.-X. Cai, Z.-H. Zhang, Q. Yan, M.-Y. He, F. Tian, J. Gao, Q. Chen *Z. Anorg. Allg. Chem.* **2013**, *639*, 1726-1730; b) Lin Yu Jin, Meng Meng Li, Dong Bin Dang, Yan Bai, Yan Ning Zheng, *Z. Naturforsch.* **2013**, *68b*, 284-288; c) J. F. Lu, Y. H. Xu, P. A. Li, L. X. Jin, C. B. Zhao, X. H. Guoand, H. G. Ge *Crystallography Reports* **2017**, *62*, 1046-1050.
- [2] Y. Hu, S. Chen, Y. Han, H. Chen, Q. Wang, Z. Nie, Y. Huang, S. Yao, *Chem. Commun.* **2015**, *51*, 17611-17614.
- [3] R.-S. Wang, J. Feng, Y.-Z. Lei, D.-M. Chen, M.-L. Lian *Cryst. Res. Technol.* **2018**, *53*, 1800065.
- [4] C.-P. Li, H. Zhou, S. Wang, H.-H. Yuan, S.-Z. Zhang, M. Du *Chem. Commun.* **2017**, *53*, 4767-4770.
- [5] C.-P. Li, H. Zhou, J. Chen, J.-J. Wang, M. Du, W. Zhou *ACS Appl. Mater. Interfaces* **2020**, *12*, 15246-15254.
- [6] a) M. Scheer, J. Bai, B. P. Johnson, R. Merkle, A. V. Virovets, C. E. Anson, *Eur. J. Inorg. Chem.* **2005**, 4023-4026; b) M. Scheer, A. Schindler, R. Merkle, B. P. Johnson, M. Linseis, R. Winter, C. E. Anson, A. V. Virovets, *J. Am. Chem. Soc.* **2007**, *129*, 13386-13387; c) F. Dielmann, C. Heindl, F. Hastreiter, E. V. Peresyphkina, A. V. Virovets, R. M. Gschwind, M. Scheer *Angew. Chem. Int. Ed.* **2014**, *53*, 13605-13608; *Angew. Chem.* **2014**, *126*, 13823-13827; d) F. Dielmann, M. Fleischmann, C. Heindl, E. V. Peresyphkina, A. V. Virovets, R. M. Gschwind, Manfred Scheer *Chem. Eur. J.* **2015**, *21*, 6208-6214; e) C. Heindl, E. V. Peresyphkina, A. V. Virovets, W. Kremer, M. Scheer *J. Am. Chem. Soc.* **2015**, *137*, 10938-10941; f) F. Dielmann, E. V. Peresyphkina, B. Krämer, F. Hastreiter, B. P. Johnson, M. Zabel, C. Heindl, M. Scheer *Angew. Chem.* **2016**, *128*, 15053-15058; g) E. V. Peresyphkina, C. Heindl, A. V. Virovets, M. Scheer, *Struct. Bond.* **2016**, *174*, 321-374; h) Heindl, E. Peresyphkina, A. V. Virovets, I. S. Bushmarinov, M. G. Medvedev, B. Krämer, B. Dittrich, M. Scheer *Angew. Chem. Int. Ed.* **2017**, *56*, 13237-13243.
- [7] a) E. Peresyphkina, C. Heindl, A. Virovets, H. Brake, E. Mädler, M. Scheer *Chem. Eur. J.* **2018**, *24*, 2503-2508; b) S. Welsch, C. Gröger, M. Sierka, M. Scheer *Angew. Chem. Int. Ed.* **2011**, *50*, 1435-1438.
- [8] H. Brake, E. Peresyphkina, C. Heindl, A. V. Virovets, W. Kremer, Manfred Scheer *Chem. Sci.* **2019**, *10*, 2940-2944.
- [9] Selected publications: a) M. E. Moussa, B. Attenberger, E. V. Peresyphkina, M. Fleischmann, G. Balázs, M. Scheer *Chem. Commun.* **2016**, *52*, 10004-10007; b) M. E. Moussa, B. Attenberger, M. Seidl, A. Schreiner, M. Scheer *Eur. J. Inorg. Chem.* **2017**, 5616-5620; c) M. E. Moussa, S. Welsch, M. Lochner, E. V. Peresyphkina, A. V. Virovets, M. Scheer *Eur. J. Inorg. Chem.* **2018**, 2689-2694.
- [10] M. E. Moussa, B. Attenberger, M. Fleischmann, A. Schreiner, M. Scheer *Eur. J. Inorg. Chem.* **2016**, 4538-4541.
- [11] a) M. Scheer, L. J. Gregoriades, M. Zabel, J. Bai, I. Krossing, G. Brunklaus, H. Eckert *Chem. Eur. J.* **2008**, *14*, 282-295; b) M. Fleischmann, S. Welsch, E. V. Peresyphkina, A. V. Virovets, M. Scheer, *Chem. Eur. J.* **2015**, *21*, 14332-14336; c) M. E. Moussa, M. Piesch, M. Fleischmann, A. Schreiner, M. Seidl, M. Scheer *Dalton Trans.* **2018**, *47*, 16031-16035.
- [12] a) B. Attenberger, S. Welsch, M. Zabel, E. Peresyphkina, M. Scheer *Angew. Chem.* **2011**, *123*, 11718-11722; *Angew. Chem. Int. Ed.* **2011**, *50*, 11516-11519; b) B. Attenberger, E. V. Peresyphkina, M. Scheer *Inorg. Chem.* **2015**, *54*, 7021-7029.
- [13] W. L. Leong, J. J. Vittal *Chem. Rev.* **2011**, *111*, 688-764.
- [14] a) Stefan Welsch, Dissertation, **2010**, Universität Regensburg; b) B. Attenberger, S. Welsch, M. Zabel, E. Peresyphkina, M. Scheer *Angew. Chem.* **2011**, *123*, 11718-11722; *Angew. Chem. Int. Ed.* **2011**, *50*, 11516-11519.
- [15] a) M. Fleischmann, S. Welsch, E. V. Peresyphkina, A. V. Virovets, M. Scheer, *Chem. Eur. J.* **2015**, *21*, 14332-14336; b) M. E. Moussa, M. Piesch, M. Fleischmann, A. Schreiner, M. Seidl, M. Scheer *Dalton Trans.* **2018**, *47*, 16031-16035.
- [16] N. Wiberg, A. F. Hollemann *Hollemann, Wiberg – Lehrbuch der Anorganischen Chemie* **2007**, 102<sup>nd</sup> Edition: de Gruyter Berlin.
- [17] P. Pyykkö, M. Atsumi *Chem. Eur. J.* **2009**, *15*, 12770-12779; b) M. E. Moussa, M. Piesch, M. Fleischmann, A. Schreiner, M. Seidl, M. Scheer *Dalton Trans.* **2018**, *47*, 16031-16035.

- [18] H. Schmidbaur, A. Schier, *Angew. Chem. Int. Ed.* **2015**, *54*, 746-784; *Angew. Chem.* **2015**, *127*, 756-797.
- [19] O. J. Scherer, H. Sitzmann, G. Wolmershäuser, *J. Organomet. Chem.* **1984**, *268*, C9-C12.
- [20] M. Fleischmann, S. Welsch, E. V. Peresykina, A. V. Virovets, M. Scheer, *Chem. Eur. J.* **2015**, *21*, 14332-14336.
- [21] M. E. Moussa, M. Piesch, M. Fleischmann, A. Schreiner, M. Seidl, M. Scheer *Dalton Trans.* **2018**, *47*, 16031-16035.
- [22] I. Krossing, *Chem. Eur. J.* **2001**, *7*, 490-502.
- [23] CrysAlisPro Software System, Rigaku Oxford Diffraction, (2018).
- [24] Clark, R. C. & Reid, J. S. *Acta Cryst.* **1995**, *A51*, 887-897.
- [25] O. V. Dolomanov, L. J. Bourhis, R. J. Gildea, J. A. K. Howard, H. Puschmann, Olex2: A complete structure solution, refinement and analysis program, *J. Appl. Cryst.* **2009**, *42*, 339-341.
- [26] Sheldrick, G.M., ShelXT-Integrated space-group and crystal-structure determination, *Acta Cryst.* **2015**, *A71*, 3-8.5.G.
- [27] M. Sheldrick, Crystal structure refinement with ShelXL, *Acta Cryst.* **2015**, *C27*, 3-8.





5 The weakly coordinating anion  $[\text{FAl}\{\text{O}(\text{C}_6\text{F}_{10})(\text{C}_6\text{F}_5)\}_3]^-$  in the synthesis of novel phosphorus rich precursors for organometallic-organic coordination polymers



**Author contribution**

Andrea Schreiner: Preparation of the manuscript, synthesis, and characterisation of compounds **5-3-5-8** and X-ray measurement of compounds **5-1** and **5-2**

Mehdi Elsayed Moussa: Synthesis and characterisation of compounds **5-1** and **5-2**

Michael Seidl: Refinement of the solid-state structures, support of the X-ray diffraction measurements and revision of the manuscript

Manfred Scheer: Supervision of the research and revision of the manuscript

Compounds **5-1** and **5-2** have already been published:

Mehdi Elsayed Moussa, Martin Piesch, Martin Fleischmann, Andrea Schreiner, Michael Seidl and Manfred Scheer

*'Highly soluble Cu(I)-acetonitrile salts as building blocks for novel phosphorus-rich organometallic-inorganic compounds'*

*Dalton Trans.* **2018**, 47, 16031-16035

The experimental parts for compounds **5-1** and **5-2** were reproduced by permission of The Royal Society of Chemistry.

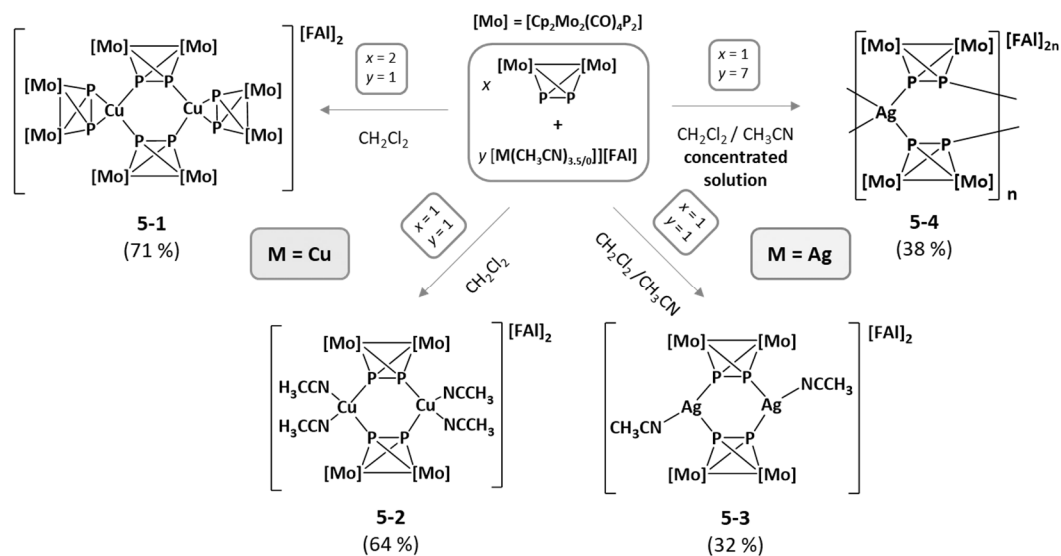
## 5.1 Abstract

The P<sub>2</sub> ligand complex [Cp<sub>2</sub>Mo<sub>2</sub>(CO)<sub>4</sub>(η<sup>2</sup>-P<sub>2</sub>)] (**A**) was reacted with the Cu(I) WCA salt [Cu(CH<sub>3</sub>CN)<sub>3.5</sub>][FAI] (**B**) ([FAI] = [FAI{O(C<sub>6</sub>F<sub>10</sub>)(C<sub>6</sub>F<sub>5</sub>)<sub>3</sub>}] to synthesise new potential starting materials for organometallic-organic hybrid compounds in coordination chemistry. Depending on the stoichiometry of **A**:**B**, one new (2:1) and one unprecedented (2:1) phosphorus rich dimer with the formulas [Cu<sub>2</sub>{Cp<sub>2</sub>Mo<sub>2</sub>(CO)<sub>4</sub>(μ,η<sup>2:2:1:1</sup>-P<sub>2</sub>)<sub>2</sub>{Cp<sub>2</sub>Mo<sub>2</sub>(CO)<sub>4</sub>(μ,η<sup>2:2:2</sup>-P<sub>2</sub>)<sub>2</sub>][FAI]<sub>2</sub> and [Cu<sub>2</sub>{Cp<sub>2</sub>Mo<sub>2</sub>(CO)<sub>4</sub>(μ,η<sup>2:2:1:1</sup>-P<sub>2</sub>)<sub>2</sub>(η<sup>1</sup>-CH<sub>3</sub>CN)<sub>4</sub>][FAI]<sub>2</sub>, respectively, were obtained. Similarly, the P<sub>2</sub> ligand complex **A** was reacted with the Ag(I) source Ag[FAI] (**C**) by using a 1:1-stoichiometry. The reaction yielded a potential new precursor for supramolecular coordination chemistry, [Ag<sub>2</sub>{Cp<sub>2</sub>Mo<sub>2</sub>(CO)<sub>4</sub>(μ,η<sup>2:2:1:1</sup>-P<sub>2</sub>)<sub>2</sub>(η<sup>1</sup>-CH<sub>3</sub>CN)<sub>2</sub>][FAI]<sub>2</sub>. The 1D coordination polymer (CP) [Cu<sub>2</sub>(Cp<sub>2</sub>Mo<sub>2</sub>(CO)<sub>4</sub>(μ,η<sup>2:2:1:1</sup>-P<sub>2</sub>)<sub>4</sub>]<sub>n</sub>[FAI]<sub>2n</sub> was obtained by an excess of the Ag(I) salt by performing the reaction in a concentrated solution. Furthermore, three-component reactions with **A**, **C** and organic pyridine-based linkers were performed. The combination with the linker 1,3-di(4-pyridyl)ethane (**L<sub>flex2</sub>**) yielded a novel 1D CP with the formula [Cu<sub>2</sub>{Cp<sub>2</sub>Mo<sub>2</sub>(CO)<sub>4</sub>(μ,η<sup>2:2:1:1</sup>-P<sub>2</sub>)<sub>2</sub>(μ,η<sup>1:1</sup>-**L<sub>flex2</sub>**)]<sub>n</sub>[FAI]<sub>2n</sub>. The reactions with linkers 1,3-di(4-pyridyl)propane (**L<sub>flex1</sub>**), 4,4'-bipyridyl (**bipy**) and trans-1,2-di(pyridine-4-yl)-ethene (**dpe**), respectively, yielded 2D CPs with the general formula [Cu<sub>2</sub>{Cp<sub>2</sub>Mo<sub>2</sub>(CO)<sub>4</sub>(μ,η<sup>2:2:1:1</sup>-P<sub>2</sub>)<sub>2</sub>(μ,η<sup>1:1</sup>-**L**)]<sub>n</sub>[FAI]<sub>2n</sub> (**L** = **L<sub>flex1</sub>**, **bipy**, **dpe**). All compounds were characterised by single crystal X-ray structure analysis and elemental analysis. Additionally, IR spectroscopy, NMR spectroscopy and mass spectrometry were used for further characterisation.

## 5.2 Introduction

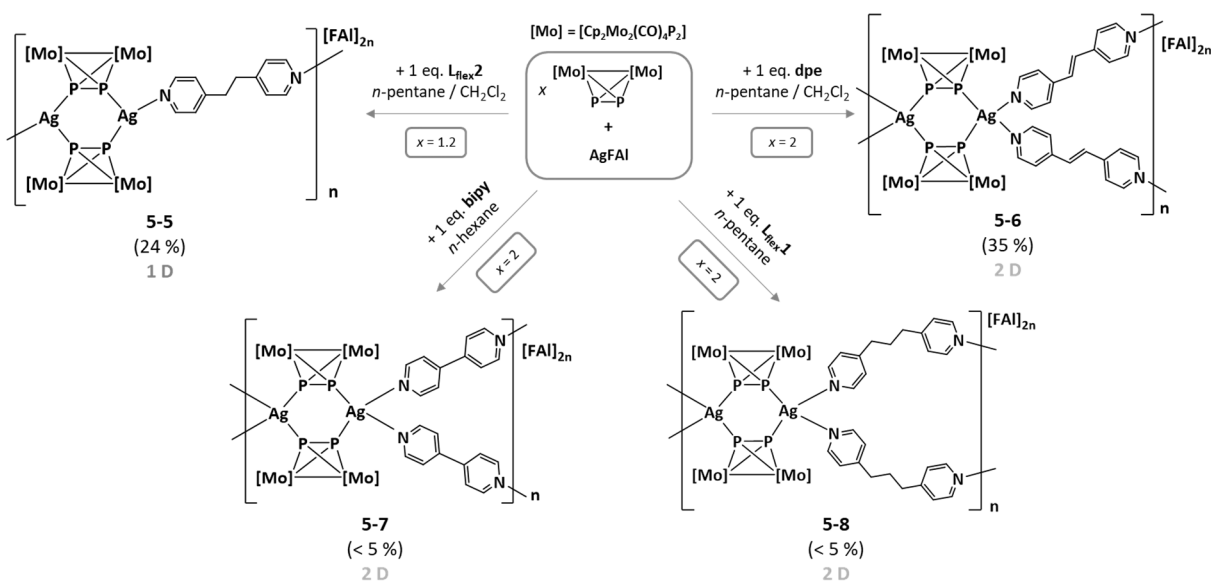
The need for suitable precursors for supramolecular coordination chemistry is highly in demand due to the rapid growth in the field of coordination polymers (CPs).<sup>[1]</sup> CPs exhibit a variety of interesting topologies<sup>[2]</sup> and properties including luminescence,<sup>[3]</sup> magnetic properties,<sup>[4]</sup> redox behaviour,<sup>[5]</sup> catalytic<sup>[6]</sup> and photocatalytic properties<sup>[7]</sup> and are therefore interesting in regard to future applications. One research topic is the design of suitable precursors for supramolecular coordination chemistry. Whereas CPs usually contain linker molecules bearing N, O and S donor atoms,<sup>[1b,6]</sup> the field of phosphorus rich ligands as linker is rather unexplored. One major research field in our group is the design of supramolecular coordination compounds from P<sub>n</sub> ligand complexes. Some P<sub>2</sub> and P<sub>3</sub> ligand complexes are known to react with Cu(I) halides to form one-dimensional CPs.<sup>[8]</sup> By reacting P<sub>2</sub> ligand complexes with coinage metal WCA (= weakly coordination anion) salts and organic linkers, discrete, zero-dimensional coordination compounds<sup>[9]</sup> and one- to three-dimensional CPs could be synthesised.<sup>[10]</sup> Using other P<sub>n</sub> ligand complexes, the synthesis of a huge variety of coordination polymers could be realised.<sup>[11]</sup> Also the formation of spherical supramolecules,<sup>[12]</sup> nano-sized capsules,<sup>[13]</sup> nano-bowls<sup>[14]</sup> and the connection of spherical supramolecules using organic dinitrile linker molecules was reported.<sup>[15]</sup> One further research topic is the design of suitable precursors for supramolecular coordination chemistry. The P<sub>2</sub> ligand complex [Cp<sub>2</sub>Mo<sub>2</sub>(CO)<sub>4</sub>(μ,η<sup>2:2</sup>-P<sub>2</sub>)] (**A**) has been reported to react with a variety of coinage metal WCA salts to discrete coordination complexes. The complexes have the general formula [M<sub>2</sub>{Cp<sub>2</sub>Mo<sub>2</sub>(CO)<sub>4</sub>(μ,η<sup>2:2:1:1</sup>-P<sub>2</sub>)<sub>2</sub>{Cp<sub>2</sub>Mo<sub>2</sub>(CO)<sub>4</sub>(μ,η<sup>2:2:2</sup>-P<sub>2</sub>)<sub>2</sub>}]<sup>2+</sup> (M = Cu, Ag) and exhibit a characteristic six-membered M<sub>2</sub>P<sub>4</sub>-ring<sup>[16]</sup> and are also suitable precursors for supramolecular coordination chemistry. Theoretical calculations suggest the presence of an unsaturated metal centre in solution due to dissociation, which enables the coordination of organic

linkers.<sup>[16a]</sup> DFT calculations have also shown that the substitution of the peripheral  $\eta^2$ -coordinated  $\text{Mo}_2\text{P}_2$ -units against pyridine is energetically favoured.<sup>[17]</sup> Herein, the reaction of the  $\text{P}_2$  ligand complex  $[\text{CpMo}_2(\text{CO})_4(\mu, \eta^{2:2}\text{-P}_2)]$  (**A**) with the Cu(I) source  $[\text{Cu}(\text{CH}_3\text{CN})_{3.5}][\text{FAI}]$  (**B**;  $\text{FAI} = \text{FAI}\{\text{O}(\text{C}_6\text{F}_{10})(\text{C}_6\text{F}_5)\}_3$ ) and the analogous Ag(I) source  $\text{Ag}[\text{FAI}]$  (**C**), respectively, are presented (**Scheme 5-1**).<sup>[18]</sup>



**Scheme 5-1.** Reactions of the  $\text{P}_2$  ligand complex  $[\text{Cp}_2\text{Mo}_2(\text{CO})_4(\mu, \eta^{2:2}\text{-P}_2)]$  (**A**) with  $[\text{Cu}(\text{CH}_3\text{CN})_{3.5}][\text{FAI}]$  ( $\text{FAI} = \text{FAI}\{\text{O}(\text{C}_6\text{F}_{10})(\text{C}_6\text{F}_5)\}_3$ , **B**) and  $\text{Ag}[\text{FAI}]$  (**C**). Isolated yields of single crystals are given in parenthesis.

The study focused on the synthesis of new phosphorus-based organometallic precursors for CPs and the investigation of the influence of stoichiometry and concentration of the reactions on reaction outcome. Subsequently, three-component reactions with **A**, the Ag(I) source **C** and the organic linkers  $\text{L}_{\text{flex1}}$ ,  $\text{L}_{\text{flex2}}$ , **bipy** and **dpe**, respectively, were performed (**Scheme 5-2**).



**Scheme 5-2.** Reactions of the  $\text{P}_2$  ligand complex **A** with the Ag(I) precursor **C** and the organic linkers 1,3-di(4-pyridyl)propane ( $\text{L}_{\text{flex1}}$ ), 1,3-di(4-pyridyl)ethane ( $\text{L}_{\text{flex2}}$ ), 4,4'-bipyridyl (**bipy**) and trans-1,2-di(pyridine-4-yl)ethene (**dpe**), respectively. Isolated yields of single crystals are given in parenthesis.

### 5.3 Results and Discussion

The reactions of the  $P_2$  ligand complex  $[Cp_2Mo_2(CO)_4(\mu,\eta^{2:2}-P_2)]$  (**A**) with the Cu(I) source  $[Cu(CH_3CN)_{3.5}][FAl]$  (**B**) were performed in dichloromethane. Depending on the used stoichiometry, the zero-dimensional coordination complexes  $[Cu_2\{Cp_2Mo_2(CO)_4(\mu,\eta^{2:2:1:1}-P_2)\}_2\{Cp_2Mo_2(CO)_4(\mu,\eta^{2:2:2}-P_2)\}_2][FAl]_2$  (**5-1**) and  $[Cu_2\{Cp_2Mo_2(CO)_4(\mu,\eta^{2:2:1:1}-P_2)\}_2(\eta^1-CH_3CN)_4][FAl]_2$  (**5-2**) were obtained selectively in 71 % and 64 % yield. Crystals of **5-1** (red blocks) and **5-2** (clear light orange blocks) were obtained by diffusion of *n*-pentane into the crude reaction mixture at room temperature. Both compounds were analysed by single crystal X-ray crystallography (**Figure 5-2**) and revealed the existence of two dinuclear Cu(I) complexes. Both compounds possess a six-membered  $Cu_2P_4$ -ring with two tetra-coordinated Cu(I) centres. In the case of compound **5-1**, two additional units of **A** are coordinated side-on in a  $\eta^2$ -coordination mode. This structural motif has already been reported from similar compounds obtained from the reaction of **A** with Cu(I), Ag(I), and Tl(I) salts.<sup>[16]</sup> In compound **5-2**, the coordination sphere of copper is saturated by acetonitrile ligands. **5-2** is therefore a potential suitable starting material for subsequent reactions with organic linkers in the synthesis of organometallic-organic CPs. Compared to the *side-on*-coordinated  $P_2$ -unit of complex **A**, the acetonitrile ligands can more easily be removed which facilitates the coordination of organic linker molecules. The bond lengths and angles in both **5-1** and **5-2** (*cf.* **Table 5-1**) are in the same range as reported for similar assemblies.<sup>10,11,16,17]</sup>

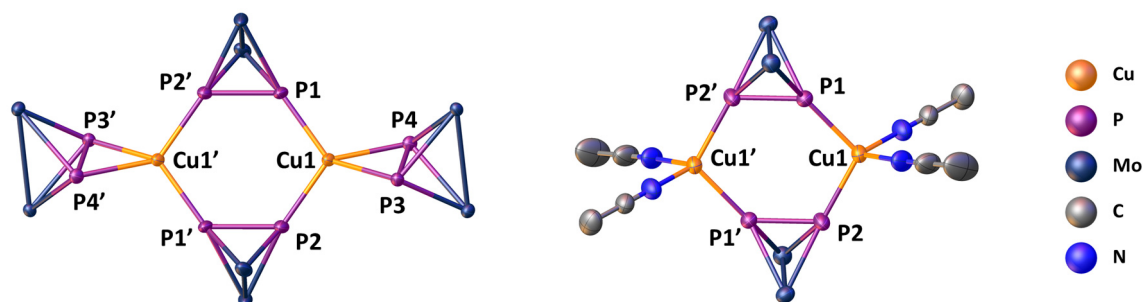


**Figure 5-2.** a) Molecular structure of the dication of **5-1** (left) and **5-2** (right) in the solid-state. Cp- and CO-ligands, hydrogen atoms, anions and solvent molecules are omitted for clarity. Thermal ellipsoids are shown at 50 % probability level. Average of selected bond lengths [ $\text{\AA}$ ] and angles [ $^\circ$ ] for **5-1**: Cu1-P1 2.2591(9), Cu1-P2 2.2571(9), Cu1-P3 2.3888(9), Cu1-P4 2.3335(9), P2-P1 2.0856(12), P3-P4 2.1509(11), P2-Cu1-P1 109.01(3), P1-Cu1-P3 132.21(3), P1-Cu1-P4 112.79(3), P4-Cu1-P3 54.17(3), P2-Cu1-P3 108.65(3), P2-Cu1-P4 133.07(3). Average of selected bond lengths [ $\text{\AA}$ ] and angles [ $^\circ$ ] for **5-2**: Cu1-P1 2.2665(8), Cu1-P2 2.2722(8), Cu1-N1 1.982(3), Cu1-N2 1.993(3), P2-P1 2.0760(10), P1-Cu1-P2 108.22(3), N1-Cu1-P1 115.00(9), N2-Cu1-P1 112.36(9), N1-Cu1-P2 110.72(9), N2-Cu1-P2 107.86(10), N1-Cu1-N2 102.42(14).

Further, reactions of the  $P_2$  ligand complex **A** with the analogous Ag(I) salt **C** were performed using a mixture of  $CH_2Cl_2$  and  $CH_3CN$  as solvent. This reaction afforded selectively the products  $[Ag_2\{Cp_2Mo_2(CO)_4(\mu,\eta^{2:2:1:1}-P_2)\}_2(\eta^1-CH_3CN)_2][FAl]_2$  (**5-3**) and  $[Ag_2\{Cp_2Mo_2(CO)_4(\mu,\eta^{2:2:1:1}-P_2)\}_4]_n[FAl]_{2n}$  (**5-4**) in 32 % and 38 % yield, respectively. The outcome of the reaction can be influenced by the ratio **A**:**C** used as well as by the concentration of the reaction solution. A 1:1-stoichiometry yielded the unprecedented phosphorus rich coordination complex **5-3**, whereas an excess of the Ag(I) source **C** in a concentrated solution led to the formation of the one-dimensional CP **5-4**, which was already synthesised using a 2:1-stoichiometry and a longer reaction time.<sup>[16c]</sup> Crystals of compounds **5-3** and **5-4** were obtained from diffusion of a 1:1-mixture of dichloromethane and *n*-pentane into the crude reaction mixtures. Both compounds crystallise in a monoclinic space group (**5-3**:  $P2_1/n$ ; **5-4**:  $I2/a$ ) as

clear light (**5-3**) or clear (**5-4**) orange blocks. The single crystal X-ray structure analysis of **5-3** revealed the formation of a dinuclear Ag(I) complex with a six-membered  $\text{Ag}_2\text{P}_4$ -ring and the  $\text{P}_2$  ligand complex **A** in  $\eta^{1:1}$ -coordination-mode (**Figure 5-3**). Unlike to **5-1**, **5-2** and other comparable compounds,<sup>[10,11,16,17]</sup> the Ag(I) centres are three-coordinated and are saturated by acetonitrile ligands. The values for the P-Ag-P angles (121.01(3) °) and P-Ag-N angles (107.45(10) ° and 117.97(10) °) are approximately between the angles of an ideal tetragonal (109.5 °) and ideal trigonal planar (120 °) coordination sphere. As a result to this distortion, the Ag(I) centres stick out of the P-P-N planes by 0.51 Å. The Ag-P, Ag-N and P-P bond lengths and angles in **5-3** (cf. **Table 5-1**) are comparable to similar coordination complexes.<sup>[16]</sup> The one-dimensional CP of compound **5-4** (**Figure 5-3**) also contains a six-membered  $\text{Ag}_2\text{P}_4$ -ring. The tetrahedral coordination sphere of the Ag(I) centres is occupied by phosphorus atoms from different units of **A**, exhibiting a  $\eta^{1:1}$ -coordination mode. The six-membered  $\text{Ag}_2\text{P}_4$ -rings are twisted by 94.11(3) ° or 95.00(3) ° to each other. The Ag-P and P-P bond lengths as well as the P-Ag-P angles are in the expected range (cf. **Table 5-1**).<sup>[10,11,16,17]</sup>

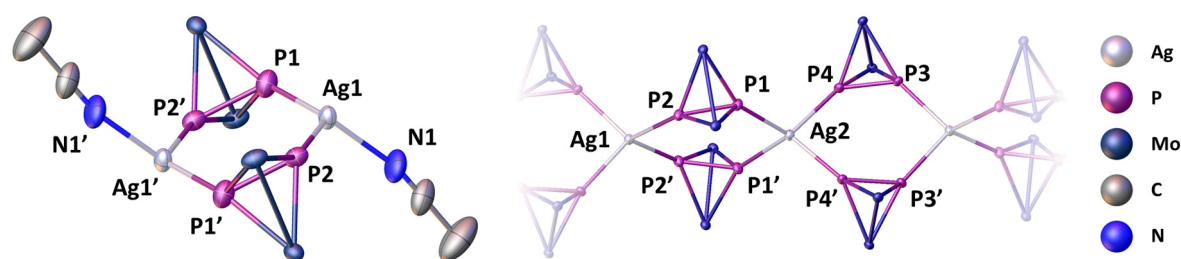


**Figure 5-3.** Molecular structure of the OD coordination compound of **5-3** (left) and the 1D CP of **5-4** in the solid-state. Cp- and CO-ligands, hydrogen atoms, anions and solvent molecules are omitted for clarity. Thermal ellipsoids are shown at 50 % probability level. Average of selected bond lengths [Å] and angles [°] for **5-3**: Ag1-P1 2.448(1), Ag1-P2 2.4648(8), Ag1-N1 2.278(3), P2-P1 2.099(1), P1-Ag1-P2 121.01(3), N1-Ag1-P1 118.0(1), N1-Ag1-P2 107.5(1). Average of selected bond lengths [Å] and angles [°] for **5-4**: Ag1-P2 2.5779(5), Ag1-P3 2.5923(5), Ag2-P1 2.6088(5), Ag2-P4 2.6043(5), P2-P1 2.0995(7) P3-P4 2.1010(7), P2-Ag1-P2 94.43(2), P3-Ag1-P3 94.74(2), P1-Ag2-P1 91.27(2), P4-Ag2-P4 92.50(2), P2-Ag1-P3 114.91(2), P2-Ag1-P3' 119.92(2), P4-Ag2-P1 116.01(2), P4-Ag2-P1' 121.91(2).

**Table 5-1.** Comparison of selected bond lengths [Å] and angles [°] of compounds **5-1-5-4**.

Compound	<b>5-1</b>	<b>5-2</b>	<b>5-3</b>	<b>5-4</b>
M	M = Cu	M = Cu	M = Ag	M = Ag
M-P	2.2571(9)-2.3888(9)	2.2665(8), 2.2722(8)	2.448(1), 2.4648(8)	2.5779(5)-2.6088(5)
M-N	-	1.982(3), 1.993(3)	2.278(3)	-
P-P	2.0856(12), 2.1509(11)	2.0760(10)	2.099(1)	2.0995(7), 2.1010(7)
∠ P-M-P	54.17(3), 108.65(3)-133.07(3)	108.22(3)	121.01(3)	91.27(2)-94.74(2), 114.91(2)-121.91(2)
∠ P-M-N	-	107.86(10)- 115.00(9)	107.5(1), 118.0(1)	-
∠ N-M-N	-	102.42(14)	-	-

In addition to the two-component-reactions, the P<sub>2</sub> ligand complex **A** was further used for the synthesis of organometallic-organic CPs in reactions with the Ag(I) source **C** and pyridine-based organic linkers. The reaction with the organic linker 1,3-di(4-pyridyl)ethane (**L<sub>flex2</sub>**) yielded a one-dimensional CP (**Figure 5-4**). Crystals of **5-5** were obtained as clear orange blocks in 24 % yield from layering of the crude reaction mixture with a 1:1-mixture of *n*-pentane and dichloromethane. Compound **5-5**, which has the formula [Ag<sub>2</sub>{Cp<sub>2</sub>Mo<sub>2</sub>(CO)<sub>4</sub>(μ,η<sup>2:2:1:1</sup>-P<sub>2</sub>)<sub>2</sub>(μ,η<sup>1:1</sup>-**L<sub>flex2</sub>**)]<sub>n</sub>[FAI]<sub>2n</sub>, is similar to the dinuclear complex **5-3**. In both compounds, a six-membered Ag<sub>2</sub>P<sub>4</sub>-ring with two three-coordinated Ag(I) centres is present. In **5-5**, however, the coordination sphere of the Ag(I) centres are completed by molecules of linker **L<sub>flex2</sub>** instead of acetonitrile ligands, which connect the nodes to form a one-dimensional CP. The stoichiometry of **A**:Cu:**L<sub>flex2</sub>** in the network is therefore 2:2:1. The Ag-P, Ag-N and P-P bond lengths (cf. **Table 5-2**) are in the expected range.<sup>[10,11,16,17]</sup> The P-Ag-P (122.76(3) °) and P-Ag-N (112.5(2) and 123.9(2) °) angles in **5-5** are comparable to the values found in the dinuclear complex **5-3** and are close to the angles of a trigonal planar coordination sphere (120°). The central Ag atoms slightly stick out of the P-P-N planes.

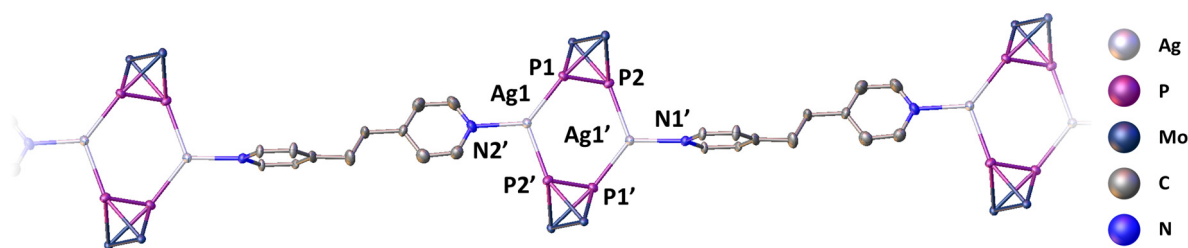


**Figure 5-4.** Molecular structure of the cation of **5-5** in the solid-state. Cp- and CO-ligands, hydrogen atoms, anions and solvent molecules are omitted for clarity. Thermal ellipsoids are shown at 50 % probability level. Average of selected bond lengths [Å] and angles [°]: Ag1-P1 2.4303(7), Ag1-P2' 2.4983(7), Ag1-N1 2.282(9), P1-P2 2.0843(7), P1-Ag1-P2' 122.76(3), N1-Ag1-P1 123.9(2), N1-Ag1-P2' 112.5(2).

By the reaction of **A** with **C** and linker 1,3-di(4-pyridyl)propane (**L<sub>flex1</sub>**), the two-dimensional CP [Ag<sub>2</sub>{Cp<sub>2</sub>Mo<sub>2</sub>(CO)<sub>4</sub>(μ,η<sup>2:2:1:1</sup>-P<sub>2</sub>)<sub>2</sub>(μ,η<sup>1:1</sup>-C<sub>13</sub>H<sub>14</sub>N<sub>2</sub>)<sub>2</sub>]<sub>n</sub>[FAI]<sub>2n</sub> (**5-6**, **Figure 5-7**) was obtained in 35 % yield. **5-6** crystallised within one week as clear red blocks in the monoclinic space group *P2<sub>1</sub>/c* after the crude reaction mixture was layered with a 1:1-mixture of *n*-pentane and dichloromethane. Like in compounds **5-4** and **5-5**, a six-membered Ag<sub>2</sub>P<sub>4</sub>-ring serves as node, the Ag(I) centres are tetra-coordinated and the P<sub>2</sub> ligand complexes **A** show a η<sup>1:1</sup>-coordination mode. Every node is connected to four different nodes by the linker molecules, forming the 2D network. The cavities formed by the network are up to 1.95 nm in size, referred to the Ag-Ag-distances,<sup>\*[19]</sup> and are filled with anions and solvent molecules. The bond lengths and angles (cf. **Table 5-2**) are comparable to similar CP.<sup>[10,11,16,17]</sup>

\* The cavity sizes of the CPs are calculated by taking the Cu-Cu distances obtained from the X-ray experiment and abstracting the sum of the *van-der-Waals*-radii of copper (1.7 Å).<sup>[19]</sup>

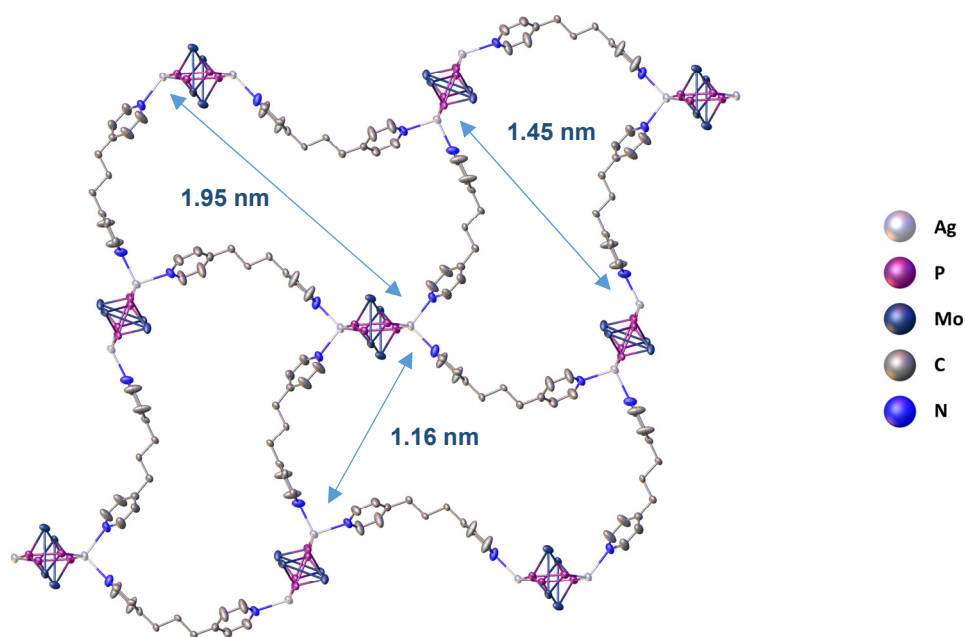


**Figure 5-5.** Molecular structure of the cationic 2D network of **5-6** in the solid-state. Cp- and CO-ligands, hydrogen atoms, anions and solvent molecules are omitted for clarity. Thermal ellipsoids are shown at 50 % probability level. Average of selected bond lengths [Å] and angles [°]: Ag1A-P1 2.394(2), Ag1A-P2 2.573(2), Ag1A-N1 2.281(5), Ag1A-N2 2.320(4), P2-P1 2.085(2), P1-Ag1A-P2 118.35(6), N1-Ag1A-P1 116.5(1), N2-Ag1A-P1 115.3(1), N1-Ag1A-P2 105.5(1), N2-Ag1A-P2 99.9(1), N1-Ag1A-N2 98.3(2).

The reactions of **A** with **C** and the linkers 4,4'-bipyridyl (**bipy**) and trans-1,2-di(pyridine-4-yl)-ethene (**dpe**), respectively, yielded two new 2D CPs (**Figure 5-6**) with the general formula  $[Ag_2(Cp_2Mo_2(CO)_4(\mu, \eta^{2:2:1:1}-P_2)_2(\mu, \eta^{1:1}-L)_2)_n[FAI]_{2n}]$  (**5-7**: L = **bipy**; **5-8**: L = **dpe**).

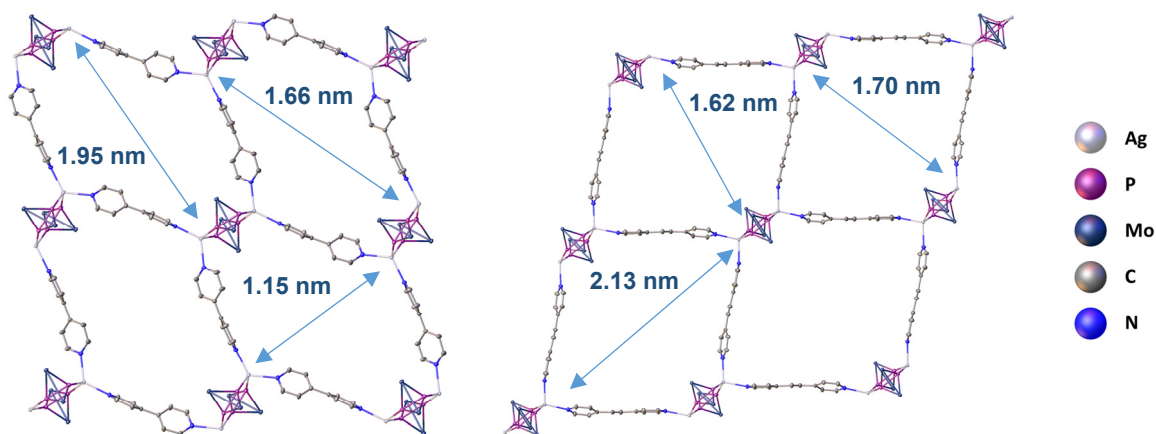


**Figure 5-6.** Molecular structure of the 2D CPs of **5-7** (left) and **5-8** (right) in the solid-state. Cp- and CO-ligands, hydrogen atoms, anions and solvent molecules are omitted for clarity. Thermal ellipsoids are shown at 50 % probability level. Average of selected bond lengths [Å] and angles [°]: **5-7**: P1-Ag1 2.5011(5), P2-Ag1 2.5291(5), Ag1-N1 2.2989(16), Ag1-N2 2.3795(17), P2-P1 2.0853(7), P1-Ag1-P2 113.44(2), N1-Ag1-P1 112.19(4), N2-Ag1-P1 99.51(4), N1-Ag1-P2 108.51(4), N2-Ag1-P2 100.96(5), N1-Ag1-N2 121.78(6). **5-8**: Ag1-P1 2.4690(5), Ag1-P2 2.4717(5), Ag1-N1 2.318(2), Ag1-N2 2.352(2), P1-P2 2.0843(7), P1-Ag1-P2 116.99(2), N1-Ag1-P1 113.15(5), N2-Ag1-P1 105.55(5), N1-Ag1-P2 111.24(4), N2-Ag1-P2 105.32(5), N1-Ag1-N2 103.09(6).

Crystals of **5-7** and **5-8** were obtained by diffusion of *n*-hexane into the crude reaction mixtures. Both compounds crystallise in a monoclinic space group (**5-7**:  $P2_1/c$ ; **5-8**:  $P2_1/n$ ) as orange (**5-7**) or clear orange (**5-8**) blocks and were analysed by crystal X-ray structure analysis. In both compounds, a six-membered  $\text{Ag}_2\text{P}_4$ -ring with tetra-coordinated Ag(I) centres serve as node. The  $\text{P}_2$  ligand complex **A** shows again a  $\eta^{1:1}$ -coordination mode. The coordination sphere of the Ag(I) centres are saturated by linker molecules (**5-7**: **bipy**, **5-8**: **dpe**). Every node is connected to four further nodes by one linker molecule each, thus forming the two-dimensional networks. The cavities formed by these networks have sizes of up to 2.03 nm (**5-7**) and 2.22 nm (**5-8**). The bond lengths and angles are in the expected range (cf. **Table 5-2**).<sup>[10,11,16,17]</sup>

**Table 5-2.** Comparison of approximate cavity sizes [nm] and selected bond lengths [Å] and angles [°] of compounds **5-5-5-8**.

Compound	<b>5-5</b>	<b>5-6</b>	<b>5-7</b>	<b>5-8</b>
Linker	<b>L<sub>flex2</sub></b>	<b>dpe</b>	<b>bipy</b>	<b>L<sub>flex1</sub></b>
Cavity sizes	-	1.62-2.13	1.15-1.95	1.45-1.95
Ag-P	2.4303(7), 2.4983(7)	2.394(2), 2.573(2)	2.5011(5), 2.5291(5)	2.4690(5), 2.4717(5)
Ag-N	2.282(9)	2.281(5), 2.320(4)	2.2989(16), 2.3795(17)	2.318(2), 2.352(2)
P-P	2.0843(7)	2.085(2)	2.0853(7)	2.0843(7)
$\sphericalangle$ P-Ag-P	122.76(3)	118.35(6)	113.44(2)	116.99(2)
$\sphericalangle$ P-Ag-N	123.9(2), 112.5(2)	99.9(1)-116.5(1)	99.51(4)-112.19(4)	105.32(5)-113.15(5)
$\sphericalangle$ N-Ag-N	-	98.3(2)	121.78(6)	103.09(6)

Compounds **5-1** to **5-3** are well soluble in  $\text{CH}_3\text{CN}$ , moderately soluble in dichloromethane and insoluble in less polar solvents like toluene, *n*-hexane, *n*-pentane, and tetrahydrofuran. Compounds **5-4** to **5-6** are soluble in  $\text{CH}_3\text{CN}$  under dissociation and insoluble in other common solvents. The positive ion ESI mass spectra ( $\text{CH}_3\text{CN}$ , r.t.) only show signals for fragments of the compounds, e.g.  $[\text{M}(\text{CH}_3\text{CN})]^+$ ,  $[\text{M}(\text{CH}_3\text{CN})_2]^+$ ,  $[\text{M}\{\text{Cp}_2\text{Mo}_2(\text{CO})_4\text{P}_2\}]^+$  and  $[\text{M}(\text{CH}_3\text{CN})\{\text{Cp}_2\text{Mo}_2(\text{CO})_4\text{P}_2\}]^+$  ( $\text{M} = \text{Ag}, \text{Cu}$ ) and fragments containing the respective linker. In the spectrum of **5-5**, a fragment containing the  $\text{P}_2$  ligand complex **A** and linker **L<sub>flex2</sub>** coordinated to Ag,  $[\text{Ag}\{\text{Cp}_2\text{Mo}_2(\text{CO})_4\text{P}_2\}(\text{C}_{12}\text{H}_{12}\text{N}_2)]^+$ , is detected as well. The room temperature  $^1\text{H}$ ,  $^{13}\text{C}\{^1\text{H}\}$ ,  $^{19}\text{F}$  and  $^{19}\text{F}\{^1\text{H}\}$  NMR spectra of compounds **5-1-5-6** show typical signals for the Cp- and CO-ligands of **A**, the  $\text{CH}_3\text{CN}$ -ligands, the FAI-anion and the organic linkers **L<sub>flex1</sub>** and **L<sub>flex2</sub>**. The room temperature  $^{31}\text{P}\{^1\text{H}\}$  NMR spectra of **5-1** and **5-2** ( $\text{CD}_2\text{Cl}_2$ ) and **5-3** to **5-6** ( $\text{CD}_3\text{CN}$ ) reveal signals at -84.7, -82.5, -75.9 (s), -86.1 (s), -72.8 (s) and -72.1 (s) ppm, respectively. Compared to the signal of the uncoordinated, free  $\text{P}_2$  ligand complex **A**, which has a chemical shift of -42.9 ppm in  $\text{C}_7\text{D}_8$ ,<sup>[20]</sup> the signals for compounds **5-1** to **5-6** are shifted about 29.2-43.3 ppm upfield. This hints that the dissociation of the compounds in solution is only partial and not complete. For compounds **5-7** and **5-8**, apart from the single crystal X-ray analysis, elemental analysis could be performed. Both compounds are soluble in acetonitrile under dissociation and insoluble in other common solvents. Additionally, mass spectrometry was performed for **5-8**. In the positive ion ESI mass spectra of **5-8**, the peaks for  $[\text{C}_{12}\text{H}_{13}\text{N}_2]^+$ ,  $[\text{Ag}(\text{CH}_3\text{CN})\{\text{Cp}_2\text{Mo}_2(\text{CO})_4\text{P}_2\}]^+$  and  $[\text{Ag}\{\text{Cp}_2\text{Mo}_2(\text{CO})_4\text{P}_2\}]^+$  were detected.



## 5.4 Conclusion

The synthesis of three new phosphorus rich dimers by the reaction of the  $P_2$  ligand complex **A** with the Cu(I) source  $[\text{Cu}(\text{CH}_3\text{CN})_{3.5}][\text{FAl}]$  (**B**) and the Ag(I) source  $\text{Ag}[\text{FAl}]$  (**C**), respectively, were presented (**Scheme 5-1**). The resulting new coordination complexes  $[\text{Cu}_2\{\text{Cp}_2\text{Mo}_2(\text{CO})_4(\mu, \eta^{2:2:1:1}\text{-P}_2)\}_2][\text{FAl}]_2$  (**5-1**),  $[\text{Cu}_2\{\text{Cp}_2\text{Mo}_2(\text{CO})_4(\mu, \eta^{2:2:1:1}\text{-P}_2)_2(\eta^1\text{-CH}_3\text{CN})_4][\text{FAl}]_2$  (**5-2**) and  $[\text{Ag}_2\{\text{Cp}_2\text{Mo}_2(\text{CO})_4(\mu, \eta^{2:2:1:1}\text{-P}_2)_2(\eta^1\text{-CH}_3\text{CN})_2][\text{FAl}]_2$  (**5-3**) are potential precursors for supramolecular coordination chemistry. **5-2** and **5-3** are especially interesting as the acetonitrile ligands attached to the metal(I) centres can easily be substituted towards pyridine-based linkers than the  $\eta^2$ -*end-on*-coordinated units of **A** in **5-1**. The reactions were directed by using different ratios of the starting materials (2:1 and 1:1). By changing the concentration of the reaction solution, the one-dimensional CP  $[\text{Cu}_2\{\text{Cp}_2\text{Mo}_2(\text{CO})_4(\mu, \eta^{2:2:1:1}\text{-P}_2)_4]_n[\text{FAl}]_{2n}$  (**5-4**) was obtained. The Ag(I) source  $\text{Ag}[\text{FAl}]$  (**C**) was subsequently used for the synthesis of organometallic-organic CPs. By reacting the  $P_2$  ligand complex **A** with **C** and organic pyridine-based linker in a ratio of 2:1:1, three similar two-dimensional CPs with the general formula  $[\text{Cu}_2\{\text{Cp}_2\text{Mo}_2(\text{CO})_4(\mu, \eta^{2:2:1:1}\text{-P}_2)_2(\mu, \eta^{1:1}\text{-L})_2]_n[\text{FAl}]_{2n}$  (**5-6: L = dpe; 5-7: L = bipy; 5-8: L = L<sub>flex</sub>1**) containing the starting materials in a ratio of 1:1:1 were obtained. In all three compounds, a six-membered  $\text{Ag}_2\text{P}_4$ -ring with tetra-coordinated Ag(I) centres serves as a node. The coordination sphere of the Ag(I) centres are completed by linker molecules and connect to four different nodes, forming the 2D network. The reaction of **A** with **C** and linker 1,3-di(4-pyridyl)ethane (**L<sub>flex</sub>2**), in which only 1.2 equivalents of **A** were used, yielded a one-dimensional CP with the formula  $[\text{Cu}_2\{\text{Cp}_2\text{Mo}_2(\text{CO})_4(\mu, \eta^{2:2:1:1}\text{-P}_2)_2(\mu, \eta^{1:1}\text{-L}_{\text{flex}2})]_n[\text{FAl}]_{2n}$  (**5-5**). **5-5** contains the starting materials in a ratio 2:2:1, as the Ag(I) centres within the six-membered  $\text{Ag}_2\text{P}_4$ -ring serving as node are three-coordinated like in the dimeric Ag(I) complex **5-3**, which therefore leads to the one-dimensional extension of the polymer.

## 5.5 Supporting Information

### General

All experiments were carried out in an inert atmosphere of nitrogen using standard Schlenk techniques. The nitrogen was dried and purified from traces of oxygen with a Cu/MgSO<sub>4</sub> catalyst, concentrated H<sub>2</sub>SO<sub>4</sub> and orange gel. Reactants were stored in a glovebox under argon atmosphere. All used solvents were taken from the solvent drying machine MB SPS-800 of the company MBRAUN.

### Chemicals

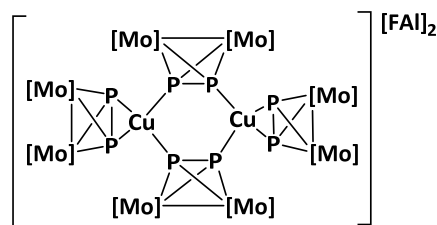
The precursor [Cp<sub>2</sub>Mo<sub>2</sub>(CO)<sub>4</sub>(μ,η<sup>2:2</sup>-P<sub>2</sub>)] (**A**) and the metal salts [Cu(CH<sub>3</sub>CN)<sub>3.5</sub>[FAI{O(C<sub>6</sub>F<sub>10</sub>)(C<sub>6</sub>F<sub>5</sub>)<sub>3</sub>}] (**B**) Ag[FAI{O(C<sub>6</sub>F<sub>10</sub>)(C<sub>6</sub>F<sub>5</sub>)<sub>3</sub>}] (**C**) were prepared according to literature procedures.<sup>[20,21,18]</sup> The organic linker 1,3-di(4-pyridyl)propane (**L<sub>flex1</sub>**) and 1,2-di(4-pyridyl)ethane (**L<sub>flex2</sub>**) were purchased from TCI (**L<sub>flex1</sub>**) and Sigma Aldrich (**L<sub>flex2</sub>**) (now Merck) and used without further purification.

### Spectroscopic Methods

IR spectra were recorded as solids with an ATR-Ge disc on a varian FTS-800 spectrometer. Solution NMR spectra were recorded on a Bruker Avance III HD 400 spectrometer (<sup>1</sup>H: 400 MHz, <sup>31</sup>P: 161 MHz, <sup>13</sup>C: 100 MHz, <sup>19</sup>F: 376 MHz) with acetonitrile-d<sub>3</sub> as solvent at room temperature. The signals of tetramethylsilane (<sup>1</sup>H, <sup>13</sup>C), CCl<sub>4</sub> (<sup>19</sup>F) and 85% H<sub>3</sub>PO<sub>4</sub> (<sup>31</sup>P) were used as reference for determining chemical shifts. The chemical shifts δ are presented in parts per million ppm and coupling constants *J* in Hz. The spectra were processed and analysed using the software Bruker TopSpin 3.0. Elemental analyses were performed on an Elementar vario MICRO cube apparatus. Mass spectra were recorded on an Agilent Q-TOF 6540 UHD or on a ThermoQuest Finnigan TSQ 7000 mass spectrometer with acetonitrile as solvent.

### Experimental Procedures

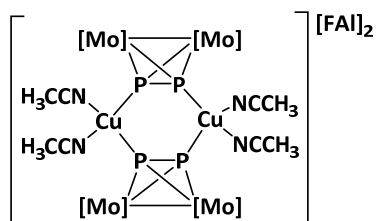
Synthesis of [Cu<sub>2</sub>{Cp<sub>2</sub>Mo<sub>2</sub>(CO)<sub>4</sub>(μ,η<sup>2:2:1:1</sup>-P<sub>2</sub>)}<sub>2</sub>{Cp<sub>2</sub>Mo<sub>2</sub>(CO)<sub>4</sub>(μ,η<sup>2:2:1</sup>-P<sub>2</sub>)}<sub>2</sub>][FAI]<sub>2</sub> (**5-1**):



[CpMo<sub>2</sub>(CO)<sub>4</sub>(η<sup>2</sup>-P<sub>2</sub>)] (**A**, 50 mg, 0.10 mmol) and [Cu(CH<sub>3</sub>CN)<sub>3.5</sub>][FAI] (**B**, 81 mg, 0.05 mmol) were dissolved in 25 mL of CH<sub>2</sub>Cl<sub>2</sub> and stirred for 1 hour at room temperature. The red solution is then filtrated and carefully layered with twofold amount of *n*-pentane and stored at room temperature. After several days red-orange crystals were formed. The crystals were washed with *n*-pentane and dried in vacuum. Yield: 88 mg (71 %). <sup>1</sup>H NMR (CD<sub>2</sub>Cl<sub>2</sub>) δ[ppm] = 5.38 (s, Cp). <sup>13</sup>C{<sup>1</sup>H} NMR (75.47 MHz, CD<sub>2</sub>Cl<sub>2</sub>) δ[ppm] = 222.9 (s, CO), 118.80 (s, CN),<sup>[22]</sup> 86.4 (s, C<sub>5</sub>H<sub>5</sub>), 2.63 (s, CH<sub>3</sub>). <sup>31</sup>P{<sup>1</sup>H} NMR (121.49 MHz, CD<sub>2</sub>Cl<sub>2</sub>) δ[ppm] = -84.7. <sup>19</sup>F{<sup>1</sup>H} NMR (282.40 MHz, CD<sub>2</sub>Cl<sub>2</sub>) δ[ppm] = -112.6 (d, *J*<sub>F-F</sub> = 280 Hz, CF<sub>2</sub>), -117.1 (d, *J*<sub>F-F</sub> = 279 Hz, CF<sub>2</sub>), -121.5 (d, *J*<sub>F-F</sub> = 277 Hz, CF<sub>2</sub>), -127.7 (s, CF<sub>2</sub>), -130.4 (d, *J*<sub>F-F</sub> = 275 Hz, CF<sub>2</sub>), -136.8 (d,

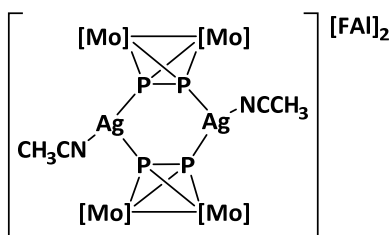
$J_{F-F} = 276$  Hz,  $CF_2$ ),  $-140.7$  (d,  $J_{F-F} = 277$ ,  $CF$ ),  $-154.2$  (t,  $J_{F-F} = 22$  Hz,  $CF$ ),  $-164.6$  (t,  $J_{F-F} = 18$  Hz,  $CF$ ),  $-170.0$  (s,  $AlF$ ). Positive ion ESI-MS ( $CH_2Cl_2$ , r.t.):  $m/z$  (%) = 1051.6 (68)  $[Cu\{Cp_2Mo_2(CO)_4P_2\}_2]^+$ . Negative ion ESI-MS ( $CH_2Cl_2$ , r.t.):  $m/z$  (%) = 1381.1 (100)  $[FAl\{O(C_6F_{10})(C_6F_5)\}_3]^-$ . IR (KBr):  $\tilde{\nu}/cm^{-1}$ : 3126 (w), 2951 (vw), 2047 (s), 2001 (vs), 1987 (s), 1650 (w), 1538 (m), 1437 (s), 1422 (w). Elemental analysis calculated for  $[Cu_2\{Cp_2Mo_2(CO)_4P_2\}_4][FAl]_2$ : C 31.46 %, H 1.21 %; found: C 30.97 %, H 1.24 %.

Synthesis of  $[Cu_2\{Cp_2Mo_2(CO)_4(\mu,\eta^{2:2:1:1}-P_2)\}_2(\mu,\eta^{1:1}-CH_3CN)_4][FAl]_2$  (**5-2**):



$[CpMo_2(CO)_4(\eta^2-P_2)]$  (**A**, 50 mg, 0.10 mmol) and  $[Cu(CH_3CN)_{3.5}][FAl]$  (**B**, 162 mg, 0.10 mmol) were dissolved in 25 mL of  $CH_2Cl_2$  and stirred for 1 hour at room temperature. The red solution is then filtrated and carefully layered with twofold amount of *n*-pentane and stored at room temperature. After several days red crystals were formed. The crystals were washed with *n*-pentane and dried in vacuum. Yield 132 mg (64 %).  $^1H$  NMR ( $CD_2Cl_2$ )  $\delta$ [ppm] = 5.33 (s, Cp), 2.21 (s,  $CH_3$ ).  $^{13}C\{^1H\}$  NMR (75.47 MHz,  $CD_2Cl_2$ )  $\delta$ [ppm] = 222.1 (s, CO), 118.80 (s, CN),  $^{22}$  86.0 (s,  $C_5H_5$ ), 2.63 (s,  $CH_3$ ).  $^{31}P\{^1H\}$  NMR (121.49 MHz,  $CD_2Cl_2$ )  $\delta$ [ppm] =  $-82.5$ .  $^{19}F\{^1H\}$  NMR (282.40 MHz,  $CD_2Cl_2$ )  $\delta$ [ppm] =  $-112.6$  (d,  $J_{F-F} = 275$  Hz,  $CF_2$ ),  $-117.1$  (d,  $J_{F-F} = 279$  Hz,  $CF_2$ ),  $-121.5$  (d,  $J_{F-F} = 277$  Hz,  $CF_2$ ),  $-127.7$  (s, 2F),  $-130.4$  (d,  $J_{F-F} = 275$  Hz,  $CF_2$ ),  $-136.8$  (d,  $J_{F-F} = 276$  Hz,  $CF_2$ ),  $-140.7$  (d,  $J_{F-F} = 277$ ,  $CF$ ),  $-154.2$  (t,  $J_{F-F} = 22$  Hz,  $CF$ ),  $-164.6$  (t,  $J_{F-F} = 18$  Hz,  $CF$ ),  $-170.2$  (s,  $AlF$ ). Positive ion ESI-MS ( $CH_2Cl_2$ , r.t.):  $m/z$  (%) = 1051.0 (42)  $[Cu\{Cp_2Mo_2(CO)_4P_2\}_2]^+$ , 1098.7(90)  $[Cu(CH_3CN)\{Cp_2Mo_2(CO)_4P_2\}_2]^+$ . Negative ion ESI-MS ( $CH_2Cl_2$ , r.t.):  $m/z$  (%) = 1381.0 (100)  $[FAl\{O(C_6F_{10})(C_6F_5)\}_3]^-$ . IR (KBr):  $\tilde{\nu}/cm^{-1}$ : 3103 (w), 2924 (vw), 2051 (s), 2121 (s), 1994 (s), 1978 (s), 1648 (w), 1530 (m), 1430 (s), 1419 (w). Elemental analysis calculated for  $[Cu_2\{Cp_2Mo_2(CO)_4P_2\}_2(CH_3CN)_4][FAl]_2$ : C 33.17 %, H 0.78 %; found: C 33.02 %, H 0.94 %.

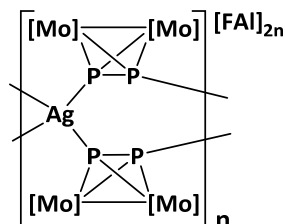
Synthesis of  $[Ag_2\{Cp_2Mo_2(CO)_4(\mu,\eta^{2:2:1:1}-P_2)\}_2(\eta^1-CH_3CN)_2][FAl]_2$  (**5-3**):



Compounds **A** (1 eq., 25 mg, 0.05 mmol) and **C** (1 eq. 74.4 mg, 0.05 mmol) were each dissolved in dichloromethane (5 mL and 20 mL, respectively). The solution of **C** was added to the solution of **A** and the resulting turbid orange mixture was stirred for 30 min. After this time 2 mL of acetonitrile were added to clear the solution and the mixture was layered with *n*-pentane after filtration. After one day, compound **5-3** was obtained as clear light orange blocks. The supernatant was decanted off, the remaining crystals washed with *n*-pentane and dried in vacuo. Crystalline Yield: 32 mg (32 %, related to **A** and **C** equally).  $^1H$  NMR ( $CD_3CN$ )  $\delta$ [ppm] = 5.39 (s,  $C_5H_5$ ).  $^{31}P$  NMR  $\delta$ [ppm] =  $-75.9$  (s).  $^{13}C\{^1H\}$  NMR  $\delta$ [ppm] = 224.7 (s, CO), 88.1 (s,  $C_5H_5$ ), 55.3 (s, CN).  $^{19}F$  NMR  $\delta$ [ppm] =  $-111.6$  (d,  $J_{F-F} = 275$  Hz,  $CF_2$ ), -

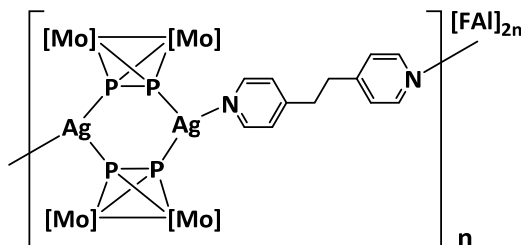
116.1 (d,  $J_{F-F} = 279$  Hz,  $CF_2$ ), -121.1 (d,  $J_{F-F} = 277$  Hz,  $CF_2$ ), -127.9 (s,  $2F$ ), -130.0 (d,  $J_{F-F} = 275$  Hz,  $CF_2$ ), -136.5 (d,  $J_{F-F} = 276$  Hz,  $CF_2$ ), -140.8 (d,  $J_{F-F} = 277$ ,  $CF$ ), -154.0 (t,  $J_{F-F} = 22$  Hz,  $CF$ ), -160.6 (t,  $J_{F-F} = 18$  Hz,  $CF$ ), -170.7 (s,  $AlF$ ). Positive ion ESI-MS ( $CH_3CN$ , r.t.):  $m/z$  (%) = 643.75 (90.5)  $[Ag(CH_3CN)\{Cp_2Mo_2(CO)_4P_2\}]^+$ , 1100.54 (70.4)  $[Ag\{Cp_2Mo_2(CO)_4P_2\}]^+$ . Negative ion ESI-MS ( $CH_3CN$ , r.t.):  $m/z$  (%) = 1380.91 (100)  $[FAl\{O(C_6F_{10})(C_6F_5)\}_3]^-$ . Elemental analysis calculated for  $AgAlC_{52}F_{46}H_{13}Mo_2NO_7P_2$  ( $2112.59$  g·mol<sup>-1</sup>): C 30.8 %, H 0.85 %, N 0.69 %; found: C 30.58 %, H 0.91 %, N traces.

Synthesis of  $[Ag_2\{Cp_2Mo_2(CO)_4(\mu,\eta^{2:2:1:1}-P_2)\}_2]_n[FAl]_{2n}$  (**5-4**):



Compounds **A** (1 eq., 12.5 mg, 0.025 mmol) and **C** (7 eq. 160 mg, 0.175 mmol) were each dissolved in dichloromethane (5 mL and 3 mL, respectively). The solution of **C** was added to the solution of **A**, whereupon the before clear red mixture turned to a turbid orange. After stirring for 30 min, acetonitrile (1 mL) and  $CH_2Cl_2$  (2 mL) were added and the reaction mixture filtered and layered with *n*-pentane. After one day, compound **5-4** was obtained as clear orange blocks. The supernatant was decanted off and the remaining crystals washed with *n*-pentane and dried in vacuo. Crystalline Yield: 11.9 mg (38 %, related to **A**). <sup>1</sup>H NMR ( $CD_3CN$ )  $\delta$ [ppm] = 5.38 (s,  $C_5H_5$ ), 2.13 (s, 3H,  $CH_3CN$ ). <sup>31</sup>P NMR  $\delta$ [ppm] = -86.11 (s). <sup>13</sup>C {<sup>1</sup>H} NMR  $\delta$ [ppm] = 224.9 (s,  $CO$ ), 88.0 (s,  $C_5H_5$ ). <sup>19</sup>F NMR  $\delta$ [ppm] = -111.7 (d,  $J_{F-F} = 275$  Hz,  $CF_2$ ), -116.1 (d,  $J_{F-F} = 279$  Hz,  $CF_2$ ), -121.1 (d,  $J_{F-F} = 277$  Hz,  $CF_2$ ), -127.8 (s,  $2F$ ), -129.5 (d,  $J_{F-F} = 275$  Hz,  $CF_2$ ), -136.4 (d,  $J_{F-F} = 276$  Hz,  $CF_2$ ), -140.7 (d,  $J_{F-F} = 277$ ,  $CF$ ), -154.0 (t,  $J_{F-F} = 22$  Hz,  $CF$ ), -165.7 (t,  $J_{F-F} = 18$  Hz,  $CF$ ), -170.6 (s,  $AlF$ ). Positive ion ESI-MS ( $CH_3CN$ , r.t.):  $m/z$  (%) = 643.75 (90.5)  $[Ag(CH_3CN)\{Cp_2Mo_2(CO)_4P_2\}]^+$ , 1100.54 (70.4)  $[Ag\{Cp_2Mo_2(CO)_4P_2\}]^+$ . Negative ion ESI-MS ( $CH_3CN$ , r.t.):  $m/z$  (%) = 1380.91 (100)  $[FAl\{O(C_6F_{10})(C_6F_5)\}_3]^-$ . IR (solid, CO bands):  $\tilde{\nu}/cm^{-1}$ : 2005 (s), 1979 (s), 1939 (s). Elemental analysis calculated for  $C_{64}H_{20}AgAlF_{46}Mo_4O_{11}P_4$  ( $2487.43$  g·mol<sup>-1</sup>): 30.88 %C, 0.81 %H; Found: 30.58 %C, 0.91 %H.

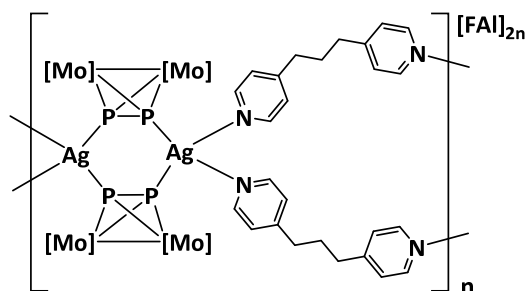
Synthesis of  $[Ag_2\{Cp_2Mo_2(CO)_4(\mu,\eta^{2:2:1:1}-P_2)\}_2(\mu,\eta^{1:1}-C_{12}H_{12}N_2)]_n[FAl]_{2n}$  (**5-5**):



Compounds **A** (1.2 eq., 30 mg, 0.06 mmol), **C** (1 eq. 74.4 mg, 0.05 mmol) and **L<sub>flex</sub>2** (1 eq., 9.2 mg, 0.05 mmol) were each dissolved in dichloromethane (5 mL, 3 mL and 2 mL, respectively). The solution of **C** was then added to the solution of **A** and the red mixture was stirred for one hour. After this time the solution of **L<sub>flex</sub>2** was added, whereupon the former dark red mixture turned to a turbid orange. Acetonitrile (1 mL) was added to dissolve the brown precipitate and the reaction was stirred overnight.

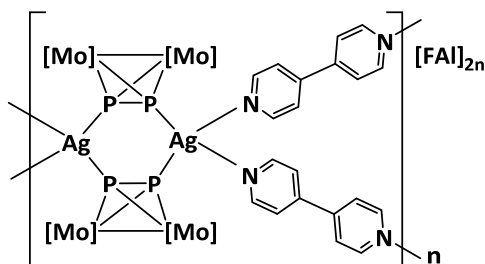
After filtration, the solution was layered with a 1:1-mixture of *n*-pentane and dichloromethane. After one day, compound **5-5** was obtained as clear orange blocks. The supernatant was decanted off and the remaining crystals washed with *n*-pentane and dried in vacuo. Crystalline Yield: 20 mg (24 %, related to **C**).  $^1\text{H}$  NMR ( $\text{CD}_3\text{CN}$ )  $\delta$ [ppm] = 8.42 (dd, 4 H,  $\text{CH}_{\text{pyr}}$ ), 7.20 (dd, 4 H,  $\text{CH}_{\text{pyr}}$ ), 5.38 (s, 10H,  $\text{C}_5\text{H}_5$ ), 2.98 (s, 4H,  $\text{CH}_2$ ).  $^{31}\text{P}$  NMR  $\delta$ [ppm] = -72.8 (s).  $^{13}\text{C}$   $\{^1\text{H}\}$  NMR  $\delta$ [ppm] = 224.9 (s,  $\text{CO}$ ), 150.3 (s,  $\text{CH}_{\text{pyr}}$ ), 124.8 (s,  $\text{CH}_{\text{pyr}}$ ), 88.0 (s,  $\text{C}_5\text{H}_5$ ), 35.5 (s,  $\text{CH}_2$ ).  $^{19}\text{F}$  NMR  $\delta$ [ppm] = -111.6 (d,  $J_{\text{F-F}} = 275$  Hz,  $\text{CF}_2$ ), -116.1 (d,  $J_{\text{F-F}} = 279$  Hz,  $\text{CF}_2$ ), -121.1 (d,  $J_{\text{F-F}} = 277$  Hz,  $\text{CF}_2$ ), -127.8 (s,  $\text{CF}_2$ ), -129.8 (d,  $J_{\text{F-F}} = 275$  Hz,  $\text{CF}_2$ ), -136.5 (d,  $J_{\text{F-F}} = 276$  Hz,  $\text{CF}_2$ ), -140.8 (d,  $J_{\text{F-F}} = 277$ ,  $\text{CF}$ ), -153.9 (t,  $J_{\text{F-F}} = 22$  Hz,  $\text{CF}$ ), -164.7 (t,  $J_{\text{F-F}} = 18$  Hz,  $\text{CF}$ ), -170.7 (s,  $\text{AlF}$ ). Positive ion ESI-MS ( $\text{CH}_3\text{CN}$ , r.t.):  $m/z$  (%) = 147.93 (100)  $[\text{Ag}(\text{CH}_3\text{CN})]^+$ , 188.96 (100)  $[\text{Ag}(\text{CH}_3\text{CN})_2]^+$ , 332.03 (100)  $[\text{Ag}(\text{C}_{12}\text{H}_{12}\text{N}_2)(\text{CH}_3\text{CN})]^+$ , 643.75 (90.5)  $[\text{Ag}(\text{CH}_3\text{CN})\{\text{Cp}_2\text{Mo}_2(\text{CO})_4\text{P}_2\}]^+$ , 786.82 (79.1)  $[\text{Ag}\{\text{Cp}_2\text{Mo}_2(\text{CO})_4\text{P}_2\}(\text{C}_{12}\text{H}_{12}\text{N}_2)]^+$ , 1100.54 (70.4)  $[\text{Ag}\{\text{Cp}_2\text{Mo}_2(\text{CO})_4\text{P}_2\}_2]^+$ . Negative ion ESI-MS ( $\text{CH}_3\text{CN}$ , r.t.):  $m/z$  (%) = 1380.90 (100)  $[\text{FAI}\{\text{O}(\text{C}_6\text{F}_{10})(\text{C}_6\text{F}_5)\}_3]^-$ . IR (solid, CO bands):  $\tilde{\nu}/\text{cm}^{-1}$ : 2009 (vs), 1994 (vs), 1952 (vs), 1942 (vs). Elemental analysis calculated for  $\text{C}_{56}\text{H}_{16}\text{AgAlF}_{46}\text{Mo}_2\text{NO}_7\text{P}_2$  (2077.33  $\text{g}\cdot\text{mol}^{-1}$ ): 32.4 %C, 0.78 %H, 0.67 %N; Found: 32.6 %C, 0.69 %H, 0.66 %.

Synthesis of  $[\text{Ag}_2\{\text{Cp}_2\text{Mo}_2(\text{CO})_4(\mu, \eta^{2:2:1:1}\text{-P}_2)\}_2(\mu, \eta^{1:1}\text{-C}_{13}\text{H}_{14}\text{N}_2)_2]_n[\text{FAI}]_{2n}$  (**5-6**):



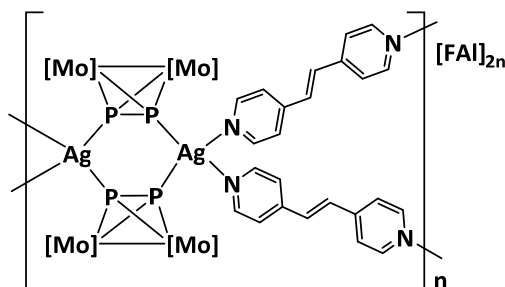
Compounds **A** (2 eq., 50 mg, 0.1 mmol), **C** (1 eq. 74.4 mg, 0.05 mmol) and **L<sub>flex</sub>1** (1 eq., 9.9 mg, 0.05 mmol) were each dissolved in dichloromethane (5 mL, 5 mL and 1 mL, respectively). The solution of **C** was added to the solution of **A** and the mixture was stirred for one hour. Afterwards, the solution of **L<sub>flex</sub>1** was added, whereupon the former dark red mixture turned to a turbid orange. Acetonitrile (1 mL) was added to dissolve the brown precipitate and the reaction was stirred overnight. After filtration, the solution was layered with a 1:1-mixture of *n*-pentane and dichloromethane and additionally with pure hexane. After one day, compound **1** was obtained as clear red blocks. The supernatant was decanted off and the remaining crystals washed with *n*-pentane and dried in vacuo. Crystalline Yield: 37.8 mg (35 %, related to **C** and **L<sub>flex</sub>2** equally).  $^1\text{H}$  NMR ( $\text{CD}_3\text{CN}$ )  $\delta$ [ppm] = 8.43 (dd, 4H,  $\text{CH}_{\text{pyr}}$ ), 7.21 (d, 4H,  $\text{CH}_{\text{pyr}}$ ), 5.37 (s, 10H,  $\text{C}_5\text{H}_5$ ), 2.66 (t, 6H,  $\text{CH}_2$ ).  $^{31}\text{P}$  NMR  $\delta$ [ppm] = -72.1 (s).  $^{13}\text{C}$   $\{^1\text{H}\}$  NMR  $\delta$ [ppm] = 150.7 (s,  $\text{CH}_{\text{pyr}}$ ), 87.9 (s,  $\text{C}_5\text{H}_5$ ), 35.0 (s,  $\text{CH}_2$ ).  $^{19}\text{F}$  NMR  $\delta$ [ppm] = -111.8 (d,  $J_{\text{F-F}} = 275$  Hz,  $\text{CF}_2$ ), -116.2 (d,  $J_{\text{F-F}} = 279$  Hz,  $\text{CF}_2$ ), -121.1 (d,  $J_{\text{F-F}} = 277$  Hz,  $\text{CF}_2$ ), -127.9 (s,  $\text{CF}_2$ ), -129.7 (d,  $J_{\text{F-F}} = 275$  Hz,  $\text{CF}_2$ ), -136.4 (d,  $J_{\text{F-F}} = 276$  Hz,  $\text{CF}_2$ ), -140.7 (d,  $J_{\text{F-F}} = 277$ ,  $\text{CF}$ ), -154.0 (t,  $J_{\text{F-F}} = 22$  Hz,  $\text{CF}$ ), -164.7 (t,  $J_{\text{F-F}} = 18$  Hz,  $\text{CF}$ ), -170.6 (s,  $\text{AlF}$ ). Positive ion ESI-MS ( $\text{CH}_3\text{CN}$ , r.t.):  $m/z$  (%) = 199.12 (100)  $[\text{C}_{13}\text{H}_{15}\text{N}_2]^+$ , 643.75 (90.5)  $[\text{Ag}(\text{CH}_3\text{CN})\{\text{Cp}_2\text{Mo}_2(\text{CO})_4\text{P}_2\}]^+$ , 1100.54 (70.4)  $[\text{Ag}\{\text{Cp}_2\text{Mo}_2(\text{CO})_4\text{P}_2\}_2]^+$ . Negative ion ESI-MS ( $\text{CH}_3\text{CN}$ , r.t.):  $m/z$  (%) = 1380.90 (100)  $[\text{FAI}\{\text{O}(\text{C}_6\text{F}_{10})(\text{C}_6\text{F}_5)\}_3]^-$ . IR (solid, CO bands):  $\tilde{\nu}/\text{cm}^{-1}$ : 2010 (ws), 1989 (s), 1955 (s), 1940 (s).

Synthesis of compound  $[\text{Ag}_2(\text{Cp}_2\text{Mo}_2(\text{CO})_4(\mu, \eta^{2:2:1:1}\text{-P}_2)_2(\mu, \eta^{1:1}\text{-C}_{10}\text{H}_8\text{N}_2)_2)_n[\text{FAI}]_{2n}$  (**5-7**):



The  $\text{P}_2$  ligand complex **A** (2 eq., 50 mg, 0.1 mmol), the  $\text{Ag(I)}$  salt **C** (1 eq., 74.4 mg, 0.05 mmol) and the organic linker **bipy** (1 eq., 7.8 mg, 0.05 mmol) were each dissolved in dichloromethane (5/5/1 mL). The solution of **C** was slowly added to the solution of **A** and the reaction mixture stirred for 1h. The solution of **bipy** was slowly added, whereupon the mixture turned from a clear dark red to turbid orange. Acetonitrile (1 mL) was added to clear the reaction mixture. After stirring overnight and filtration, the mixture was layered with *n*-hexane. After one day, compound **5-7** was obtained as orange blocks. The supernatant was decanted off, the remaining crystals washed with *n*-pentane and dried in vacuo. Crystalline Yield: a few crystals (<5 %). Elemental analysis calculated for  $\text{C}_{60}\text{H}_{18}\text{AgAlF}_{46}\text{Mo}_2\text{N}_2\text{O}_7\text{P}_2$  ( $2143,68 \text{ g}\cdot\text{mol}^{-1}$ ): C 33.59 %, H 0.85 %, N 1.30 %; found: C 33.31 %, H 0.87 %, N 1.05 %.

Synthesis of compound  $[\text{Ag}_2(\text{Cp}_2\text{Mo}_2(\text{CO})_4(\mu, \eta^{2:2:1:1}\text{-P}_2)_2(\mu, \eta^{1:1}\text{-C}_{12}\text{H}_{10}\text{N}_2)_2)_n[\text{FAI}]_{2n}$  (**5-8**):



The  $\text{P}_2$  ligand complex **A** (2 eq., 50 mg, 0.1 mmol), the  $\text{Ag(I)}$  salt **C** (1 eq., 74.4 mg, 0.05 mmol) and the organic linker **dpe** (1 eq., 9.1 mg, 0.05 mmol) were each dissolved in dichloromethane (5 mL, 10 mL and 5 mL, respectively). The solution of **C** was slowly added to the solution of **A** and the mixture stirred for 1h. The solution of **dpe** was slowly added and the reaction stirred overnight. After filtration, the mixture was layered with *n*-pentane. After one day, compound **5-8** was obtained as clear orange blocks. The supernatant was decanted off, the remaining crystals washed with *n*-pentane and dried in vacuo. Crystalline Yield: a few crystals (<5 %). Positive ion ESI-MS ( $\text{CH}_3\text{CN}$ , RT):  $m/z$  (%) = 183.09 (100)  $[\text{C}_{12}\text{H}_{13}\text{N}_2]^+$ , 643.75 (90.5)  $[\text{Ag}(\text{CH}_3\text{CN})\{\text{Cp}_2\text{Mo}_2(\text{CO})_4\text{P}_2\}]^+$ , 1100.54 (70.4)  $[\text{Ag}\{\text{Cp}_2\text{Mo}_2(\text{CO})_4\text{P}_2\}]^+$ . Negative ion ESI-MS ( $\text{CH}_3\text{CN}$ , RT):  $m/z$  (%) = 1380.89 (100)  $[\text{FAI}\{\text{O}(\text{C}_6\text{F}_{10})(\text{C}_6\text{F}_5)\}_3]^-$ . Elemental analysis calculated for  $\text{AgAlC}_{62}\text{F}_{46}\text{H}_{20}\text{Mo}_2\text{N}_2\text{O}_7\text{P}_2$  ( $2167.44 \text{ g}\cdot\text{mol}^{-1}$ ): C 34.36 %, H 0.93 %, N 1.29 %; found: C 34.07 %, H 0.96 %, N 1.26 %.

## Crystallographic Details

**Crystal Structure Analysis:** The crystals were selected and mounted on a suitable support on a Gemini Ultra diffractometer equipped with an AtlasS2 CCD detector (**5-1** and **5-3** to **5-8**) and a GV50 diffractometer equipped with a TitanS2 CCD detector (**5-2**), respectively. The crystals were kept at  $T = 123(1)$  K during data collection. Data collection and reduction were performed with **CrysAlisPro** [Version 171.39.37b, 2017 (**5-1** and **5-4** to **5-7**), 171.40.14a, 2018 (**5-3**, **5-8**), 171.38.43, 2015 (**5-2**)].<sup>[23]</sup> For compounds **5-1**, **5-3**, **5-4**, **5-5** and **5-7**, an analytical numeric absorption correction using a multifaceted crystal model based on expressions derived by R.C. Clark & J.S. Reid<sup>[24]</sup> and an empirical absorption correction using spherical harmonics as implemented in SCALE3 ABSPACK was applied. For compounds **5-2** and **5-8**, a numerical absorption correction based on gaussian integration over a multifaceted crystal model and an empirical absorption correction using spherical harmonics as implemented in SCALE3 ABSPACK was applied. For compound **5-6**, a multi-scan absorption correction was performed using spherical harmonics as implemented in SCALE3 ABSPACK. Using **Olex2**,<sup>[25]</sup> the structures were solved with **ShelXT**<sup>[26]</sup> and a least-square refinement on  $F^2$  was carried out with **ShelXL**<sup>[27]</sup> for all structures. All non-hydrogen atoms were refined anisotropically. Hydrogen atoms at the carbon atoms were located in idealised positions and refined isotropically according to the riding model.

**Compound 5-1:** The asymmetric unit contains 2 CH<sub>2</sub>Cl<sub>2</sub> solvent molecules, which were heavily disordered. Therefore, a solvent mask was calculated and 184.0 electrons were found in a volume of 697.0 Å<sup>3</sup> in 3 voids. This is consistent with the presence of 2 CH<sub>2</sub>Cl<sub>2</sub> molecules per asymmetric unit, which account for 168.0 electrons. The asymmetric unit further contains a Cu(I) atom, a [FAl{O(C<sub>6</sub>F<sub>10</sub>)(C<sub>6</sub>F<sub>5</sub>)}<sub>3</sub>] anion and two [Cp<sub>2</sub>Mo<sub>2</sub>(CO)<sub>4</sub>(η<sup>2</sup>-P<sub>2</sub>)] complexes. One of these complexes shows a disorder of a Cp and a CO ligand over two positions (51:49). To describe this disorder the SIMU restraint was applied.

**Compound 5-2:** The asymmetric unit contains 0.5 CH<sub>2</sub>Cl<sub>2</sub> solvent molecules and two CH<sub>3</sub>CN molecules coordinated to a Cu(I) atom. Further it contains a [FAl{O(C<sub>6</sub>F<sub>10</sub>)(C<sub>6</sub>F<sub>5</sub>)}<sub>3</sub>] anion and a [Cp<sub>2</sub>Mo<sub>2</sub>(CO)<sub>4</sub>(η<sup>2</sup>-P<sub>2</sub>)] complex. The Cp and CO ligands of this complex are each disordered over two positions with a ratio of 92:8 and 83:17, respectively. To describe these disorders the DFIX, SADI, SIMU and RIGU restraints were applied.

**Compound 5-3:** The asymmetric unit contains 2.5 CH<sub>2</sub>Cl<sub>2</sub> solvent molecules and one CH<sub>3</sub>CN molecule coordinated to a Cu(I) atom. Further it contains a [FAl{O(C<sub>6</sub>F<sub>10</sub>)(C<sub>6</sub>F<sub>5</sub>)}<sub>3</sub>] anion and a [Cp<sub>2</sub>Mo<sub>2</sub>(CO)<sub>4</sub>(η<sup>2</sup>-P<sub>2</sub>)] complex. The CH<sub>2</sub>Cl<sub>2</sub> molecules were heavily disordered. Therefore, a solvent mask was calculated and 436 electrons were found in a volume of 1284 Å<sup>3</sup> in one void per unit cell. This is consistent with the presence of 2.5 CH<sub>2</sub>Cl<sub>2</sub> molecules per asymmetric unit, which account for 420 electrons per unit cell.

**Compound 5-4:** The asymmetric unit contains 0.84 CH<sub>2</sub>Cl<sub>2</sub> solvent molecules. Further it contains a [FAl{O(C<sub>6</sub>F<sub>10</sub>)(C<sub>6</sub>F<sub>5</sub>)}<sub>3</sub>] anion and two [Cp<sub>2</sub>Mo<sub>2</sub>(CO)<sub>4</sub>(η<sup>2</sup>-P<sub>2</sub>)] complexes coordinated to a Ag(I) cation. The CH<sub>2</sub>Cl<sub>2</sub> molecule is disordered over two positions (62:22). To describe this disorder the DFIX, SADI and SIMU restraints were applied.

**Compound 5-5:** The asymmetric unit contains 0.7 CH<sub>2</sub>Cl<sub>2</sub> solvent molecules. Further it contains a [FAl{O(C<sub>6</sub>F<sub>10</sub>)(C<sub>6</sub>F<sub>5</sub>)}<sub>3</sub>] anion, a [Cp<sub>2</sub>Mo<sub>2</sub>(CO)<sub>4</sub>(η<sup>2</sup>-P<sub>2</sub>)] complex and a linker (C<sub>12</sub>H<sub>12</sub>N<sub>2</sub>), which are coordinated to a Ag(I) cation. The CH<sub>2</sub>Cl<sub>2</sub> molecule is disordered over two positions (40:30), as well as one C<sub>6</sub>F<sub>5</sub> unit of the anion (62:38). The linker molecule is also disordered over two positions and further

located at an inversion centre. To describe these disorders the SADI, SIMU, RIGU and ISOR restraints were applied.

Compound **5-6**: The asymmetric unit contains 2 CH<sub>2</sub>Cl<sub>2</sub> solvent molecules. Further it contains a [FAl{O(C<sub>6</sub>F<sub>10</sub>)(C<sub>6</sub>F<sub>5</sub>)<sub>3</sub>}] anion, a [Cp<sub>2</sub>Mo<sub>2</sub>(CO)<sub>4</sub>(η<sup>2</sup>-P<sub>2</sub>)] complex and a linker (C<sub>13</sub>H<sub>14</sub>N<sub>2</sub>), which are coordinated to a Ag(I) cation. One CH<sub>2</sub>Cl<sub>2</sub> solvent molecule is disordered over two positions (56:44) and the second CH<sub>2</sub>Cl<sub>2</sub> solvent molecule is so heavily disordered that it was not possible to get a satisfactorily model. Therefore, a solvent mask was calculated and 152 electrons were found in a volume of 444 Å<sup>3</sup> in 1 void per unit cell. This is consistent with the presence of 1 CH<sub>2</sub>Cl<sub>2</sub> molecule per asymmetric unit, which account for 168 electrons per unit cell. Further a CpMoCo fragment is disordered over two positions (51:49), as well as the Ag atom (89:11) and the linker molecule (75:25). To describe these disorders the SADI, SIMU and RIGU restraints were applied.

Compound **5-7**: The asymmetric unit contains 1 CH<sub>2</sub>Cl<sub>2</sub> solvent molecule, one [FAl{O(C<sub>6</sub>F<sub>10</sub>)(C<sub>6</sub>F<sub>5</sub>)<sub>3</sub>}] anion and an Ag atom coordinated by one **bipy** linker and the complex **A**.

Compound **5-8**: The asymmetric unit contains 3.71 CH<sub>2</sub>Cl<sub>2</sub> solvent molecules. Two of these CH<sub>2</sub>Cl<sub>2</sub> molecules were heavily disordered. Therefore, a solvent mask was calculated and 358 electrons were found in a volume of 1706 Å<sup>3</sup> in one void per unit cell. This is consistent with the presence of two CH<sub>2</sub>Cl<sub>2</sub> solvent molecules per asymmetric unit, which account for 336 electrons per unit cell.



**Table 5-3.** Crystallographic data and details of diffraction experiments for compounds 5-1-5-4.

Compound	5-1 · CH <sub>2</sub> Cl <sub>2</sub>	5-2 · CH <sub>2</sub> Cl <sub>2</sub>	5-3 · 2.5 CH <sub>2</sub> Cl <sub>2</sub>	5-4 · 0.84 CH <sub>2</sub> Cl <sub>2</sub>
Data Set (internal naming)	abs249	abs282	abs427Xa	abs427b
Deposition Number	1866458	1866459	-	-
Database Identifier	LIHYUZ	LIHZAG	-	-
Formula	C <sub>65</sub> H <sub>22</sub> Cl <sub>2</sub> AlCuF <sub>46</sub> Mo <sub>4</sub> O <sub>11</sub> P <sub>4</sub>	C <sub>109</sub> H <sub>34</sub> Al <sub>2</sub> Cl <sub>2</sub> Cu <sub>2</sub> F <sub>92</sub> Mo <sub>4</sub> N <sub>4</sub> O <sub>14</sub> P <sub>4</sub>	AgAlCl <sub>54.5</sub> Cl <sub>5</sub> F <sub>46</sub> H <sub>18</sub> Mo <sub>2</sub> NO <sub>7</sub> P <sub>2</sub>	C <sub>64.84</sub> H <sub>21.68</sub> AgAlCl <sub>1.68</sub> F <sub>46</sub> Mo <sub>4</sub> O <sub>11</sub> P <sub>4</sub>
<i>D</i> <sub>calc.</sub> / g · cm <sup>-3</sup>	1.982	2.036	2.073	2.184
<i>μ</i> /mm <sup>-1</sup>	1.131	6.005	1.029	1.198
Formula Weight	2521.88	4130.98	2238.62	2552.63
Colour	red	clear light orange	clear light orange	clear orange
Shape	block	block	block	block
Size/mm <sup>3</sup>	0.26×0.20×0.10	0.32×0.27×0.18	0.27×0.11×0.09	0.40×0.23×0.16
<i>T</i> /K	123.0(10)	122.9(2)	123(1)	123(1)
Crystal System	triclinic	monoclinic	monoclinic	monoclinic
Space Group	P $\bar{1}$	C2/c	P21/n	I2/a
<i>a</i> /Å	11.2011(3)	28.2675(2)	11.6008(3)	39.8160(5)
<i>b</i> /Å	18.7490(4)	18.77190(10)	19.7884(5)	11.27120(10)
<i>c</i> /Å	21.9934(5)	25.8322(2)	31.2556(8)	38.9201(5)
<i>α</i> /°	111.288(2)	90	90	90
<i>β</i> /°	95.767(2)	100.4620(10)	91.513(2)	117.243(2)
<i>γ</i> /°	96.550(2)	90	90	90
<i>V</i> /Å <sup>3</sup>	4225.04(18)	13479.58(16)	7172.6(3)	15528.8(4)
<i>Z</i>	2	4	4	8
<i>Z'</i>	1	0.5	1	1
Wavelength/Å	0.71073	1.54184	0.71073	0.71073
Radiation type	MoK <sub>α</sub>	CuK <sub>α</sub>	MoK <sub>α</sub>	MoK <sub>α</sub>
<i>Q</i> <sub>min</sub> /°	3.498	3.479	3.272	3.398
<i>Q</i> <sub>max</sub> /°	30.033	67.079	32.432	32.877
Measured Refl.	39177	35932	52185	75515
Independent Refl.	24509	11993	23317	25942
Reflections with <i>I</i> > 2( <i>I</i> )	17575	11733	14594	21651
<i>R</i> <sub>int</sub>	0.0383	0.0267	0.0451	0.0233
Parameters	1244	1198	1010	1235
Restraints	42	230	0	73
Largest Peak	1.501	1.187	1.420	0.931
Deepest Hole	-1.977	-0.796	-1.685	-0.450
GooF	0.980	1.031	1.011	1.072
<i>wR</i> <sub>2</sub> (all data)	0.1110	0.0974	0.0993	0.0640
<i>wR</i> <sub>2</sub>	0.1002	0.0968	0.0865	0.0600
<i>R</i> <sub>1</sub> (all data)	0.0714	0.0370	0.1008	0.0402
<i>R</i> <sub>1</sub>	0.0465	0.0364	0.0564	0.0289

**Table 5-4.** Crystallographic data and details of diffraction experiments for compounds **5-5-5-8**.

Compound	5-5 · 0.7 CH <sub>2</sub> Cl <sub>2</sub>	5-6 · 2 CH <sub>2</sub> Cl <sub>2</sub>	5-7 · CH <sub>2</sub> Cl <sub>2</sub>	5-8 · 3.71 CH <sub>2</sub> Cl <sub>2</sub>
Data Set (internal naming)	abs426b	abs443c	abs433d	abs426c
Formula	C <sub>56.7</sub> H <sub>17.4</sub> AgAlCl <sub>1.4</sub> F <sub>46</sub> Mo <sub>2</sub> NO <sub>7</sub> P <sub>2</sub>	AgAlC <sub>65</sub> Cl <sub>4</sub> F <sub>46</sub> H <sub>28</sub> Mo <sub>2</sub> N <sub>2</sub> O <sub>7</sub> P <sub>2</sub>	C <sub>61</sub> H <sub>20</sub> AgAlCl <sub>2</sub> F <sub>46</sub> Mo <sub>2</sub> N <sub>2</sub> O <sub>7</sub> P <sub>2</sub>	AgAlC <sub>65.71</sub> Cl <sub>7.43</sub> F <sub>46</sub> H <sub>27.43</sub> Mo <sub>2</sub> N <sub>2</sub> O <sub>7</sub> P <sub>2</sub>
<i>D</i> <sub>calc.</sub> / g · cm <sup>-3</sup>	2.174	1.981	2.084	1.872
<i>μ</i> /mm <sup>-1</sup>	0.983	0.909	0.931	0.919
Formula Weight	2136.81	2353.36	2226.36	2482.91
Colour	clear orange	clear red	orange	clear orange
Shape	block	block	block	block
Size/mm <sup>3</sup>	0.27×0.18×0.17	0.51×0.44×0.34	0.26×0.20×0.17	0.39×0.37×0.22
<i>T</i> /K	123(1)	123(1)	123(1)	123(1)
Crystal System	triclinic	monoclinic	monoclinic	monoclinic
Space Group	<i>P</i> $\bar{1}$	<i>P</i> <sub>2</sub> <sub>1</sub> / <i>c</i>	<i>P</i> <sub>2</sub> <sub>1</sub> / <i>c</i>	<i>P</i> <sub>2</sub> <sub>1</sub> / <i>n</i>
<i>a</i> /Å	11.3109(5)	15.3453(6)	18.4602(4)	18.9442(5)
<i>b</i> /Å	17.7348(6)	20.0345(7)	19.4517(3)	19.4265(4)
<i>c</i> /Å	18.1478(7)	25.9699(8)	20.9565(4)	24.0209(6)
<i>α</i> /°	102.301(3)	90	90	90
<i>β</i> /°	100.487(3)	98.799(4)	109.406(2)	94.619(2)
<i>γ</i> /°	107.828(3)	90	90	90
<i>V</i> /Å <sup>3</sup>	3264.2(2)	7890.1(5)	7097.6(2)	8811.4(4)
<i>Z</i>	2	4	4	4
<i>Z'</i>	1	1	1	1
Wavelength/Å	0.71073	0.71073	0.71073	0.71073
Radiation type	Mo K <sub>α</sub>	Mo K <sub>α</sub>	Mo K <sub>α</sub>	Mo K <sub>α</sub>
<i>Q</i> <sub>min</sub> /°	3.372	3.334	3.407	3.370
<i>Q</i> <sub>max</sub> /°	32.342	32.444	32.299	32.692
Measured Refl.	47217	65904	65815	71232
Independent Refl.	20752	25437	22839	29157
Reflections with <i>I</i> > 2( <i>I</i> )	15130	17841	18975	23306
<i>R</i> <sub>int</sub>	0.0385	0.0513	0.0254	0.0248
Parameters	1253	1324	1117	1163
Restraints	140	263	0	0
Largest Peak	0.774	2.309	0.864	1.032
Deepest Hole	-0.727	-2.182	-1.210	-1.364
Goof	1.029	1.066	1.049	1.032
<i>wR</i> <sub>2</sub> (all data)	0.0836	0.1623	0.0743	0.0876
<i>wR</i> <sub>2</sub>	0.0740	0.1466	0.0699	0.0821
<i>R</i> <sub>1</sub> (all data)	0.0759	0.1031	0.0467	0.0489
<i>R</i> <sub>1</sub>	0.0444	0.0746	0.0340	0.0353

## 5.6 References

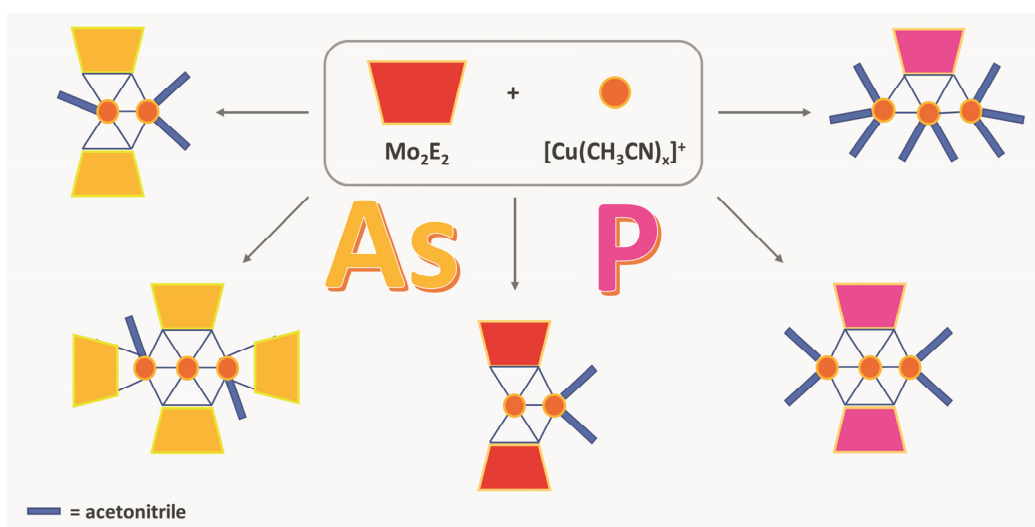
- [1] a) T. R. Cook, P. J. Stang *Chem. Rev.* **2015**, *115*, 7001-7045; b) T. R. Cook, Y.-R. Zheng, P. J. Stang *Chem. Rev.* **2013**, *113*, 734-777; c) W. L. Leong, J. J. Vittal *Chem. Rev.* **2011**, *111*, 688-764; d) R. Chakrabarty, P. S. Mukherjee, P. J. Stang *Chem. Rev.* **2011**, *111*, 6810-6918; e) A. J. Olson, Y. H. E. Hu, E. Keinan, *Proc. Natl. Acad. Sci. U.S.A.* **2007**, *104*, 20731-20736; f) Y.-R. Zheng, P. J. Stang, *J. Am. Chem. Soc.* **2009**, *131*, 3487-3489; g) S. Park, S. Y. Lee, K.-M. Park, S. S. Lee *Acc. Chem. Res.* **2012**, *45*, 391-403.
- [2] a) L. Carlucci, G. Ciani, D. M. Proserpio, T. G. Mitina, V. A. Blatov, *Chem. Rev.* **2014**, *114*, 7557-7580; b) R. Haldar, T. K. Maji, *Z. Anorg. Allg. Chem.* **2014**, *640*, 1102-1108.
- [3] a) S. Miao, Z. Li, C. Xu, D. Deng, B. Ji, *Crystals* **2019**, *9*, 592; b) J. Guo, D. Sun, L. Zhang, Q. Yang, X. Zhao, D. Sun, *Cryst. Growth Des.* **2012**, *12*, 5649-5654; c) W.-Q. Kan, J. Yang, Y.-Y. Liu, J.-F. Ma, *CrystEngComm*, **2012**, *14*, 6271-6281; d) J. Guo, D. Sun, L. Zhang, Q. Yang, X. Zhao, D. Sun, *Cryst. Growth Des.* **2012**, *12*, 5649-5654; e) T. Yoneda, C. Kasai, Yo Manabe, M. Tsurui, Y. Kitagawa, Y. Hasegawa, P. Sarkar, Y. Inokuma *Chem Asian J.* **2020**, *15*, 601- 605.
- [4] X.-Y. Dong, C.-D. Si, Y. Fan, D.-C. Hu, X.-Q. Yao, Y.-X. Yang, J.-C. Liu *Cryst. Growth Des.* **2016**, *16*, 2062-2073.
- [5] K. Banerjee, S. Roy, M. Kotal, K. Biradha *Cryst. Growth Des.* **2015**, *15*, 5604-5613.
- [6] N.-X. Zhu, C.-W. Zhao, J. Yang, X.-R. Wang, J.-P. Ma, Y.-B. Dong *RSC Adv.* **2016**, *6*, 108645-108653.
- [7] T. Wen, D.-X. Zhang, J. Zhang *Inorg. Chem.* **2013**, *52*, 12-14.
- [8] a) J. Bai, E. Leiner, M. Scheer *Angew. Chem.* **2002**, *114*, 820-823; *Angew. Chem. Int. Ed.* **2002**, *41*, 783-786; b) M. Scheer, L. Gregoriades, J. Bai, M. Sierka, G. Brunklaus, H. Eckert *Chem. Eur. J.* **2005**, *11*, 2163-2169; c) M. Scheer, L. J. Gregoriades, M. Zabel, M. Sierka, L. Zhang, H. Eckert *Eur. J. Inorg. Chem.* **2007**, 2775-2782; d) M. E. Moussa, P. A. Shelyganov, B. Wegley, M. Seidl, M. Scheer *Eur. J. Inorg. Chem.* **2019**, 4241-4248; e) M. E. Moussa, M. Seidl, G. Balázs, M. Hautmann, M. Scheer *Angew. Chem.* **2019**, *131*, 13035-13039.
- [9] M. E. Moussa, B. Attenberger, M. Seidl, A. Schreiner, M. Scheer *Eur. J. Inorg. Chem.* **2017**, 5616-5620.
- [10] a) B. Attenberger, S. Welsch, M. Zabel, E. Peresyphkina, M. Scheer *Angew. Chem.* **2011**, *123*, 11718-11722; *Angew. Chem. Int. Ed.* **2011**, *50*, 11516-11519; b) M. E. Moussa, B. Attenberger, M. Fleischmann, A. Schreiner, M. Scheer *Eur. J. Inorg. Chem.* **2016**, 4538-4541; c) B. Attenberger, E. V. Peresyphkina, M. Scheer *Inorg. Chem.* **2015**, *54*, 7021-7029.
- [11] a) M. E. Moussa, S. Welsch, M. Lochner, E. V. Peresyphkina, A. V. Virovets, M. Scheer *Eur. J. Inorg. Chem.* **2018**, 2689-2694; b) C. Heindl, E. V. Peresyphkina, A. V. Virovets, V. Yu. Komarov, M. Scheer *Dalton Trans.* **2015**, *44*, 10245-10252; c) A. V. Virovets, E. V. Peresyphkina, G. Brunklaus, H. Eckert, M. Scheer, *Chem. Eur. J.* **2012**, *18*, 1168-1179; d) C. Heindl, S. Reisinger, C. Schwarzmaier, L. Rummel, A. V. Virovets, E. V. Peresyphkina, M. Scheer *Eur. J. Inorg. Chem.* **2016**, 743-753; e) M. E. Moussa, S. Welsch, L. Dütsch, M. Piesch, S. Reichl, M. Seidl, M. Scheer *Molecules* **2019**, *24*, 325.
- [12] a) M. Scheer, J. Bai, B. P. Johnson, R. Merkle, A. V. Virovets, C. E. Anson, *Eur. J. Inorg. Chem.* **2005**, 4023-4026; b) M. Scheer, A. Schindler, R. Merkle, B. P. Johnson, M. Linseis, R. Winter, C. E. Anson, A. V. Virovets, *J. Am. Chem. Soc.* **2007**, *129*, 13386-13387; c) F. Dielmann, C. Heindl, F. Hastreiter, E. V. Peresyphkina, A. V. Virovets, R. M. Gschwind, M. Scheer *Angew. Chem. Int. Ed.* **2014**, *53*, 13605-13608; *Angew. Chem.* **2014**, *126*, 13823-13827; d) F. Dielmann, M. Fleischmann, C. Heindl, E. V. Peresyphkina, A. V. Virovets, R. M. Gschwind, Manfred Scheer *Chem. Eur. J.* **2015**, *21*, 6208-6214; e) C. Heindl, E. V. Peresyphkina, A. V. Virovets, W. Kremer, M. Scheer *J. Am. Chem. Soc.* **2015**, *137*, 10938-10941; f) F. Dielmann, E. V. Peresyphkina, B. Krämer, F. Hastreiter, B. P. Johnson, M. Zabel, C. Heindl, M. Scheer *Angew. Chem.* **2016**, *128*, 15053-15058; g) E. V. Peresyphkina, C. Heindl, A. V. Virovets, M. Scheer, *Struct. Bond.* **2016**, *174*, 321-374; h) Heindl, E. Peresyphkina, A. V. Virovets, I. S. Bushmarinov, M. G. Medvedev, B. Krämer, B. Dittrich, M. Scheer *Angew. Chem. Int. Ed.* **2017**, *56*, 13237-13243.
- [13] a) E. Peresyphkina, C. Heindl, A. Virovets, H. Brake, E. Mädler, M. Scheer *Chem. Eur. J.* **2018**, *24*, 2503-2508; b) S. Welsch, C. Gröger, M. Sierka, M. Scheer *Angew. Chem. Int. Ed.* **2011**, *50*, 1435-1438.
- [14] H. Brake, E. Peresyphkina, C. Heindl, A. V. Virovets, W. Kremer, Manfred Scheer *Chem. Sci.* **2019**, *10*, 2940-2944.

- [15] Barbara Hiltl (geb. Krämer), *Dissertation* **2018**, Universität Regensburg.
- [16] a) M. Scheer, L. J. Gregoriades, M. Zabel, J. Bai, I. Krossing, G. Brunklaus, H. Eckert, *Chem. Eur. J.* **2008**, *14*, 282; b) M. Fleischmann, S. Welsch, E. V. Peresykina, A. V. Virovets, M. Scheer *Chem. Eur. J.* **2015**, *21*, 14332-14336; c) M. E. Moussa, M. Fleischmann, E. V. Peresykina, L. Dütsch, M. Seidl, G. Balázs, M. Scheer *Eur. J. Inorg. Chem.* **2017**, 3222-3226; d) M. Fleischmann, S. Welsch, L. J. Gregoriades, C. Gröger, M. Scheer *Z. Naturforsch.* **2014**, *69b*, 1348-1356.
- [17] a) M. E. Moussa, B. Attenberger, E. V. Peresykina, M. Fleischmann, G. Balázs, M. Scheer *Chem. Commun.* **2016**, *52*, 10004-10007; b) M. E. Moussa, M. Seidl, G. Balázs, M. Zabel, A. V. Virovets, B. Attenberger, A. Schreiner, M. Scheer *Chem. Eur. J.* **2017**, *23*, 16199-16203.
- [18] M. E. Moussa, M. Piesch, M. Fleischmann, A. Schreiner, M. Seidl, M. Scheer *Dalton Trans.* **2018**, *47*, 16031-16035.
- [19] N. Wiberg, A. F. Hollemann *Hollemann, Wiberg – Lehrbuch der Anorganischen Chemie* **2007**, 102<sup>nd</sup> Edition: de Gruyter Berlin.
- [20] O. J. Scherer, H. Sitzmann, G. Wolmershäuser, *J. Organomet. Chem.* **1984**, *268*, C9-C12.
- [21] T. Köchner, N. Trapp, T. A. Engesser, A. J. Lehner, C. Röhr, S. Riedel, C. Knapp, H. Scherer, I. Krossing, *Angew. Chem. Int. Ed.* **2011**, *50*, 11253-11256; *Angew. Chem.* **2011**, *123*, 11449-11452.
- [22] Signal for remaining impurities of CH<sub>3</sub>CN.
- [23] CrysAlisPro Software System, Rigaku Oxford Diffraction, (2018).
- [24] Clark, R. C. & Reid, J. S. *Acta Cryst.* **1995**, *A51*, 887-897.
- [25] O.V. Dolomanov, L. J. Bourhis, R.J. Gildea, J.A.K. Howard, H. Puschmann, Olex2: A complete structure solution, refinement and analysis program *J. Appl. Cryst.* **2009**, *42*, 339-341.
- [26] Sheldrick, G.M., ShelXT-Integrated space-group and crystal-structure determination *Acta Cryst.* **2015**, *A71*, 3-8.5.G.
- [27] M. Sheldrick, Crystal structure refinement with ShelXL, *Acta Cryst.* **2015**, *C27*, 3-8.

## 6 Linking of Cu(I) units by tetrahedral Mo<sub>2</sub>E<sub>2</sub> complexes (E = P, As)

Jana Schiller,<sup>‡</sup> Andrea Schreiner,<sup>‡</sup> Michael Seidl, Gábor Balázs and Manfred Scheer

<sup>‡</sup> equally contributing authors



### Author contribution

Andrea Schreiner and Jana Schiller contributed equally to this work. The manuscript was written by Andrea Schreiner and Jana Schiller. The synthesis, characterisation and X-ray measurement of all phosphorus containing compounds (compounds **6-1-6-3**, **6-8**, **6-9**) and the X-ray measurement of compound **6-7** were performed by Andrea Schreiner. The synthesis, characterisation and X-ray measurement of all arsenic containing compounds (compounds **6-4-6-7** and **6-10**) were performed by Jana Schiller, apart from the X-ray measurement of compound **6-7**. Michael Seidl performed the refinement of the solid-state structures and also wrote the experimental part of the X-ray measurement. Michael Seidl also contributed by supporting the X-ray measurements and revision of the manuscript. Gábor Balázs performed the DFT calculations, including the manuscript regarding the DFT calculations. Manfred Scheer contributed by supervising the research and revision of the manuscript.

## 6.1 Abstract

The reaction of  $[\text{Cp}_2\text{Mo}_2(\text{CO})_4(\mu, \eta^{2:2}\text{-E}_2)]$  (**A**: E = P, **B**: E = As, Cp = C<sub>5</sub>H<sub>5</sub>) with the WCA-containing Cu(I) salts  $[\text{Cu}(\text{CH}_3\text{CN})_4][\text{Al}\{\text{OC}(\text{CF}_3)_3\}_4]$  (**CuTEF**, **C**),  $[\text{Cu}(\text{CH}_3\text{CN})_4][\text{BF}_4]$  (**D**) and  $[\text{Cu}(\text{CH}_3\text{CN})_{3.5}][\text{FAl}\{\text{OC}_6\text{F}_{12}(\text{C}_6\text{F}_5)\}_3]$  (**CuFAl**, **E**) affords seven unprecedented coordination compounds (**Scheme 6-1**). Depending on the E<sub>2</sub> ligand complex, the counter anion of the copper salt and the stoichiometry, four dinuclear copper dimers and three trinuclear copper compounds are accessible. The latter complexes reveal first linear Cu<sub>3</sub> arrays linked by E<sub>2</sub> units (E = P, As) coordinated in an  $\eta^{2,1,1}$  coordination mode. All compounds were characterised by X-ray crystallography, NMR and IR spectroscopy, mass spectrometry and elemental analysis. To define the nature of the Cu...Cu...Cu interactions, DFT calculations were performed.

## 6.2 Introduction

During the last two decades, the number of organometallic aggregates bearing Cu(I) units has rapidly increased, owing to their wide range of applications and their versatile coordination chemistry.<sup>[1]</sup> Cu(I) compounds have proven to be useful in mimicking enzyme interactions,<sup>[1a]</sup> as anticancer drugs,<sup>[1b]</sup> and in other materials.<sup>[1c]</sup> Furthermore, Cu(I) derivatives turned out to be smart and novel solid-state emitters because of their accessibility and low costs.<sup>[2]</sup> Therefore, the development of *inter alia* extended linear Cu(I) arrays for potential applications in molecular electronics and luminescent materials has become more and more important. Some linear trinuclear cationic Cu(I) complexes bridged by P/N hybrid ligands, such as 7-diphenylphosphino-2,4-dimethyl-1,8-naphthyridine,<sup>[3]</sup> *N,N,N',N'',N''*-pentamethyl-diethylentriamine,<sup>[4]</sup> diphosphine/*N*-heterocyclic-carbene hybrid ligands<sup>[5]</sup> or the synthesis of halide-bridged trinuclear Cu(I) complexes connected by (diphenylphosphinomethyl)phenyl-phosphine<sup>[6]</sup> with Cu...Cu distances below the sum of the van der Waals radii were reported. However, Cu...Cu interactions were not confirmed by calculations. A variety of compounds containing different Cu(I) and organometallic polyphosphorus ligand complexes were previously reported by our group.<sup>[7]</sup> We were able to show the formation of 1D, 2D and even 3D coordination polymers,<sup>[8]</sup> metal-organic nanosized capsules<sup>[9]</sup> and inorganic spherical supramolecules.<sup>[10]</sup> In addition to polyphosphorus complexes, organometallic polyarsenic ligand complexes have been known for many years.<sup>[11]</sup> However, their coordination chemistry has been a rather unexplored area so far.<sup>[12]</sup> To bring metals in close proximity to allow for metallophilic interactions, special building blocks are needed. One of such potential materials is the tetrahedral Mo<sub>2</sub>E<sub>2</sub> moiety in the compounds  $[\text{Cp}_2\text{Mo}_2(\text{CO})_4(\mu, \eta^{2:2}\text{-E}_2)]$ , (E = P (**A**), As (**B**)).<sup>[13]</sup> Until now, basically three coordination modes have been observed for these E<sub>2</sub> ligand complexes (Figure 1).<sup>[7c,e]</sup>

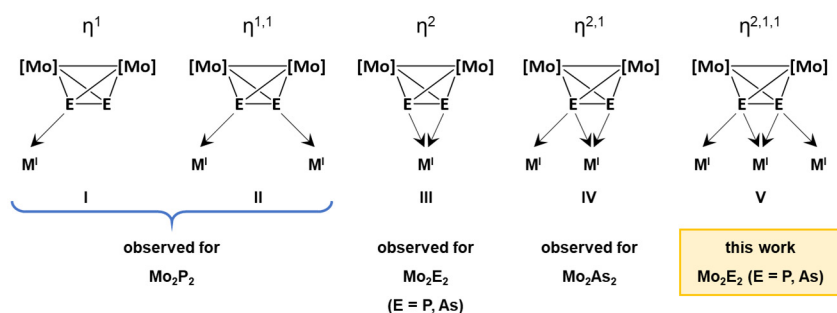


**Figure 6-1.** Reported and new coordination modes of  $\text{Mo}_2\text{E}_2$  complexes.  $\text{M}' = \text{Ag}(\text{I}), \text{Cu}(\text{I}), \text{Au}(\text{I})$ .  $[\text{Mo}] = [\text{CpMo}_2(\text{CO})_2]$ .<sup>[7c,e]</sup>

The lone pairs of one or two E atoms can either coordinate towards one or two metal centers via  $\sigma$ -coordination of the lone pairs (type I and II), or the E-E  $\sigma$ -orbital binds in a  $\pi$ -coordination to the metal center (type III).<sup>[7c,e]</sup> However, to bring metal cations in close proximity, the coordination modes IV and V are needed, which are unknown for homoelement  $\text{Mo}_2\text{E}_2$  compounds. Note that the coordination mode IV has so far only been observed for mixed  $\text{EE}'$  derivatives ( $\text{E} = \text{P}, \text{E}' = \text{As}, \text{Sb}$ ).<sup>[7b]</sup>

### 6.3 Results and Discussion

Herein, we report the reactions of the polypnictogen ligand complexes  $[\text{Cp}_2\text{Mo}_2(\text{CO})_4(\mu, \eta^{2:2}\text{-E}_2)]$  (**A**:  $\text{E} = \text{P}$ , **B**:  $\text{E} = \text{As}$ ,  $\text{Cp} = \text{C}_5\text{H}_5$ ) with the  $\text{Cu}(\text{I})$  salts  $[\text{Cu}(\text{CH}_3\text{CN})_4][\text{BF}_4]$ ,  $[\text{Cu}(\text{CH}_3\text{CN})_{3.5}][\text{FAI}\{\text{OC}_6\text{F}_{12}(\text{C}_6\text{F}_5)_3\}_3]$  ( $\text{CuFAI}$ ) and  $[\text{Cu}(\text{CH}_3\text{CN})_4]\text{-}[\text{Al}\{\text{OC}(\text{CF}_3)_3\}_4]$  ( $\text{CuTEF}$ ) which lead, by variation of the stoichiometry of the used reactants, to seven unprecedented coordination compounds (**6-1** to **6-7**, **Scheme 6-1**), showing a novel  $\eta^{2:1:1}$ -(**V**) and  $\eta^{2:1}$ -(**IV**) coordination behavior, respectively, of the  $\text{E}_2$  ligand complexes ( $\text{E} = \text{P}$ ). Moreover, compounds **6-1**, **6-2** and **6-6** reveal  $\text{Cu}\cdots\text{Cu}\cdots\text{Cu}$  interactions which were analysed by DFT calculations. For the first time, an  $\eta^{2,1,1}$ -coordination mode **V** was detected for the two complexes **A** and **B** to which both P/As atoms contribute via  $\sigma$ -bonding and  $\pi$ -coordination. That way, linear  $\text{Cu}_3$  chains stabilized only by polypnictogen ligand complexes are accessible.

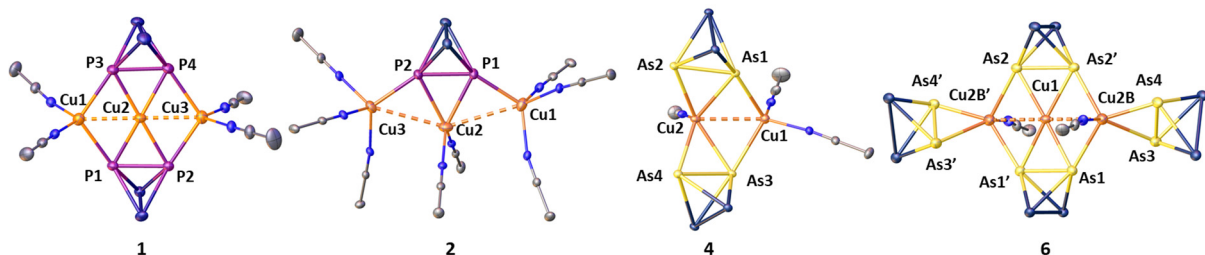


**Figure 6-2.** Molecular structures of the cationic parts of compounds **6-1**, **6-2**, **6-4** and **6-6** in the solid state. Cp- and CO-ligands and hydrogen atoms are omitted for clarity. Thermal ellipsoids are shown at 50% probability level. Only the major part of compound **6** is depicted (for further information see SI).

The reaction of  $[\text{Cu}(\text{o-DFB})][\text{TEF}]$  with **A** to give the dimeric compound  $[\text{Cu}_2(\text{Cp}_2\text{Mo}_2(\text{CO})_4(\mu_4, \eta^{2:2:1:1}\text{-P}_2)_2)(\text{Cp}_2\text{Mo}_2(\text{CO})_4(\mu_3, \eta^{2:2:1}\text{-P}_2)_2)][\text{TEF}]$  (**F**), containing a  $\text{P}_4\text{Cu}_2$  6-membered ring, was reported a time ago (**Figure 6-3**).<sup>[8c]</sup>

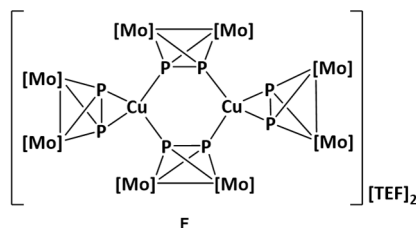
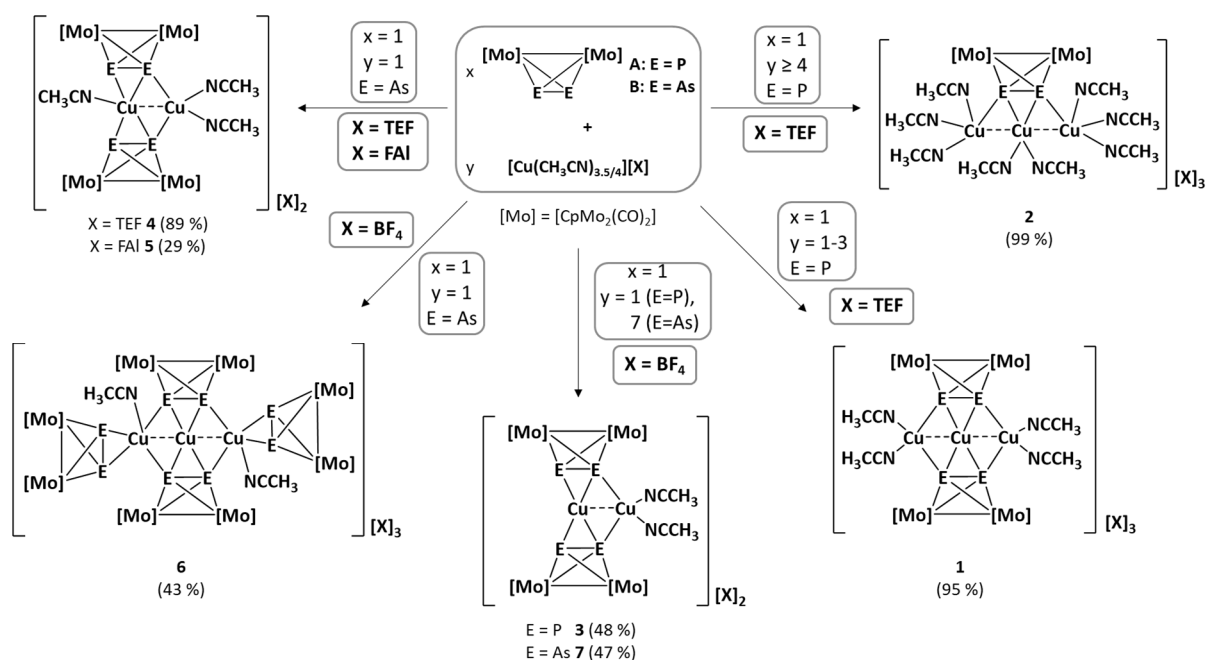


**Figure 6-3.** Structure of the dimeric compound **F**.<sup>[8c]</sup>

By using the different Cu(I) source  $[\text{Cu}(\text{CH}_3\text{CN})_4][\text{TEF}]$  (**C**)<sup>[73a]</sup> in the reaction with **A** we have been surprised to receive the new coordination compound  $[\text{Cu}\{\text{Cu}(\text{CH}_3\text{CN})_2\}_2\{\text{Cp}_2\text{Mo}_2(\text{CO})_4(\mu_5, \eta^{2:2:2:1:1}\text{-P}_2)\}_2][\text{TEF}]_3$  (**6-1**, **Figure 6-2**). Crystals of **6-1** as orange blocks in the trigonal space group  $P3_2$  were obtained by diffusion of *n*-pentane or toluene into the crude reaction mixture. When *n*-pentane was used, **6-1** crystallises as red plates in the monoclinic space group  $P2_1/c$ . In compound **6-1**, two  $\text{P}_2$  ligand complexes **A** are coordinated to a molecular chain of three copper atoms ( $\text{Cu}\cdots\text{Cu}$  2.4344(10)-2.4537(19) Å) in a  $\eta^{2:2:2:1:1}$ -coordination mode. The peripheral copper atoms  $\text{Cu}_{\text{per}}$  are coordinated by two acetonitrile ligands each. Unlike other known structures, which feature a characteristic six-membered  $\text{Cu}_2\text{P}_4$ -ring with **A** being coordinated in a  $\eta^{2:2:1:1}$ -coordination mode,<sup>[7c,8c]</sup> in **6-1**, a third additional copper atom is located in the center of this six-membered ring with an unprecedented type **V** like coordination (**Figure 6-1**). Therefore, the P-P bonds in **6-1** (2.4344(10)-2.4537(19) Å) are elongated compared to the free **A** (2.0798(3) Å).<sup>[13a]</sup> The bonds between the peripheral copper atoms and the respective phosphorus atoms have values from 2.3830(19) to 2.460(3) Å, which are significantly longer than in the dimer **F** (2.240(3)-2.277(2) Å). The Cu-Cu-Cu angles in **6-1** are between 177.95(9)° and 180°, depending on the space group of the product, and the angles around the central copper atom are between 57.70(6)-62.39(9)°. Compound **6-1** presents the first trinuclear Cu(I) complex with such short  $\text{Cu}\cdots\text{Cu}$  distances, stabilised by the  $\eta^{2:1:1}$  coordination of a polypnictogen unit.

By using an excess of the Cu(I) salt **C** in the reaction with **A** ( $\text{CH}_2\text{Cl}_2$ , room temperature), the compound  $[\{\text{Cu}(\text{CH}_3\text{CN})_2\}\text{-}\{\text{Cu}(\text{CH}_3\text{CN})_3\}_2\{\text{Cp}_2\text{Mo}_2(\text{CO})_4(\mu_5, \eta^{2:2:2:1:1}\text{-P}_2)\}][\text{TEF}]_3$  (**6-2**, **Figure 6-2**) was obtained. Compound **6-2** crystallizes as yellow blocks and consists of only one complex **A** coordinated to three copper atoms in the coordination mode type **V**. The peripheral copper atoms are further saturated with three acetonitrile ligands each; the central copper atom has two acetonitrile ligands attached. The  $\text{Cu}\cdots\text{Cu}$  distances in **6-2** (3.0013(6) Å and 3.0593(6) Å) are significantly elongated compared to **6-1**. The distance between the two peripheral copper atoms is also significantly larger in **6-2** (5.8238(8) Å; **6-1**: 4.869(2)-4.904(2) Å). The Cu-P bonds are slightly longer for  $\text{Cu}_{\text{cen}}\text{-P}$  (2.3706(8) and 2.3909(8) Å), but shorter for  $\text{Cu}_{\text{per}}\text{-P}$  (2.2446(8) and 2.2520(8) Å) as compared to **6-1**. Also, the Cu-Cu-Cu angle is with 147.861(19)° significantly more bent. The angles around the central copper atom possess values between 47.55(2) and 53.56(3)°.





**Scheme 6-1.** Products of the reaction of **A** with  $[Cu(CH_3CN)_4][Al\{OC(CF_3)_3\}_4]$  (**6-1/6-2**, depending on the stoichiometry) and with  $[Cu(CH_3CN)_4][BF_4]$  (**6-3**), and of the reaction of **B** with the Cu(I) salts  $[Cu(CH_3CN)_4][Al\{OC(CF_3)_3\}_4]$  (**6-4**),  $[Cu(CH_3CN)_{3.5}][FAI\{OC_6F_{12}(C_6F_5)_3\}]$  (**6-5**) and  $[Cu(CH_3CN)_4][BF_4]$  (**6-6/6-7**, depending on the stoichiometry). Yields are given in parentheses.

Furthermore, we were interested in the reactivity of the  $As_2$  ligand complex  $[Cp_2Mo_2(CO)_4(\mu, \eta^2-As_2)]$  (**B**) towards  $[Cu(CH_3CN)_4][TEF]$  (**C**). In a straightforward synthetic approach, mixing **B** with an equimolar amount of **C** in  $CH_2Cl_2$  at room temperature, the new compound  $[\{CpMo(CO)_2\}_2(\mu_5, \eta^{2:2:1-As_2})_2\{Cu(CH_3CN)_2\} Cu(CH_3CN)][TEF]_2$  (**6-4**) was obtained. Layering with *n*-pentane afforded **6-4** in a moderate yield as red needles suitable for X-ray structure analysis (Figure 2).<sup>[14]</sup> The solid state structure of **6-4** reveals a Cu dimer stabilized by two  $As_2$  ligands **B**. Additionally, the copper atom Cu1 is coordinated by two acetonitrile ligands and the copper atom Cu2 by one such ligand. Cu1 is  $\eta^1$ -coordinated by one As atom from both  $As_2$  ligand complexes **B**, Cu2 is  $\eta^2$ -coordinated by two complexes **B** in an novel  $\eta^{2:1}$ -coordination mode **IV**. The Cu...Cu distance (2.6925(7) Å) is elongated compared to **6-1**. The As-As bonds (2.3905(5)-2.3901(5) Å) are slightly elongated compared to the uncoordinated complex **B** (2.311(3) Å).<sup>[15]</sup> Additionally, the distances of the coordinating As atoms to Cu2 ( $\eta^2$ -coordination) are slightly longer (2.4849(6)-2.5312(6) Å) than the As-Cu1 distances ( $\eta^1$ -coordination, 2.4582(6)-2.4850(6) Å). A compound **6-5**, isostructural to **6-4**, containing a different counterion, was formed by the reaction of **B** with the Cu(I) salt  $[Cu(CH_3CN)_{3.5}][FAI]$  (**E**) (cf. Supporting Information).

Moreover, the trinuclear complex **6-6** was obtained by reacting **B** with  $[Cu(CH_3CN)_4][BF_4]$  in  $CH_2Cl_2$  at room temperature using equimolar amounts. By diffusion of *n*-pentane into the crude reaction mixture, **6-6** crystallizes as dark red blocks. X-ray crystallography of **6-6** revealed that the central Cu atom has an occupancy of 0.8. Therefore, a complex with only the peripheral copper atoms is present with an occupancy of only 0.2 (**F**-like). Furthermore, the acetonitrile molecules coordinated to the outer Cu atoms have an occupancy of 0.59 (for further details see SI). The major part (**Figure 6-2**) consists of a  $Cu_3$  ( $d(Cu-Cu) = 2.587(4)$  Å) chain coordinated by four  $As_2$  ligand complexes **B**, with the peripheral copper atoms (Cu2B and Cu2B') additionally coordinated by one acetonitrile ligand each. While Cu2B and Cu2B' are  $\eta^2$ -side-on-coordinated by one molecule of **B** and  $\eta^1$ -end-on-coordinated by

two other  $[\text{Cp}_2\text{Mo}_2(\text{CO})_4(\mu, \eta^{2:2}\text{-As}_2)]$  moieties, Cu1 shows only  $\eta^2$ -*side-on*-coordination by two molecules of **B**. The As-As bonds of the *side-on*-coordinated molecules **B** are tilted by an angle of  $133^\circ$  in relation to the plane As1-Cu1-As2'-Cu2B and accordingly tilted to an angle of  $47^\circ$  to the symmetry-generated plane.

By using a 1:1 stoichiometry of **B** and **D**, product **6-6** was obtained containing a 4:3 composition of **B** and **D**. It was expected that a higher ratio of **D** would lead to a product that is similar to complex **6-1**. Quite contrary to expectations, when using an excess of **D**, compound **6-7** was formed. The structure of **6-7** is comparable to the structures of compounds **6-4** and **6-5**, respectively, with the difference that the Cu2 atom is not coordinated by a  $\text{CH}_3\text{CN}$  molecule. However, the synthesis of the  $\text{Mo}_2\text{P}_2$ -containing compound  $[\text{Cu}(\text{CH}_3\text{CN})_2\{\text{Cu}\{\text{Cp}_2\text{Mo}_2(\text{CO})_4(\mu_4, \eta^{2:2:2:1}\text{-P}_2)\}_2][\text{BF}_4]_2$  (**6-3**) (**Figure 6-2**), which is isostructural with **6-7**, was achieved by reacting equimolar amounts of **A** with **D**. The use of two equivalents of **A** leads to a compound containing a  $\text{P}_4\text{Cu}_2$  6-membered ring similar to compound **F** (**Figure 3**).<sup>[8c]</sup> Compounds **6-3** (orange plates) and **7** (red plates) crystallize both in the monoclinic space group  $I2/m$ . For detailed information on their structures, see the Supporting Information.

The products **6-1** to **6-7** are well soluble in donor solvents such as  $\text{CH}_3\text{CN}$  and slightly soluble in  $\text{CH}_2\text{Cl}_2$ , but insoluble in other common organic solvents such as THF, toluene and *n*-pentane. The NMR spectra of all compounds were recorded in acetonitrile- $d_3$  at room temperature. The  $^1\text{H}$  and  $^{13}\text{C}\{^1\text{H}\}$  NMR spectra of compounds **6-1** to **6-7** indicate decomplexation by showing signals corresponding to the proton and carbon nuclei of the Cp and CO ligands of **A** or **B**, respectively. The  $^{31}\text{P}$  NMR spectra of the compounds **6-1** to **6-3** show broad signals that are upfield shifted compared to the free  $\text{P}_2$  ligand complex **A** ( $\delta = -43.2$  ppm).<sup>[13a]</sup> The broad signals in combination with former *variable-temperature* NMR studies on the Ag-dimer  $[\text{Ag}_2\{\text{Cp}_2\text{Mo}_2(\text{CO})_4(\mu, \eta^{2:2:1:1}\text{-P}_2)\}_2\{\text{Cp}_2\text{Mo}_2(\text{CO})_4(\mu, \eta^{2:2:1}\text{-P}_2)\}_2][\text{TEF}]$ <sup>[7c]</sup> indicate a dynamic behavior in solution between **6-1** to **6-3** and monomeric fragments of them. Therefore, with acetonitrile being a coordinating solvent, it is most likely decomplexation that is observed in solution. In the ESI mass spectra of **6-1** to **6-3**, peaks for the cationic fragments ( $[\{\text{Cu}\{\text{Cp}_2\text{Mo}_2(\text{CO})_2\text{P}_2\}_2]^+$ ,  $[\text{Cu}(\text{CH}_3\text{CN})\text{-}\{\text{Cp}_2\text{Mo}_2(\text{CO})_2\text{P}_2\}]^+$  and  $[\text{Cu}(\text{CH}_3\text{CN})_2]^+$ ) were detected. While the ESI mass spectra of **6-4** and **6-5** show peaks for the cationic fragments  $[\{\text{Cp}_2(\text{CO})_4\text{Mo}_2\text{As}_2\}_2\text{Cu}]^+$  and  $[\{\text{Cp}_2(\text{CO})_4\text{Mo}_2\text{As}_2\}\text{Cu}(\text{CH}_3\text{CN})]^+$ , compounds **6-6** and **6-7** reveal an additional peak for  $[\text{Cp}_2(\text{CO})_4\text{Mo}_2\text{As}_2]^+$ . All compounds are air- and light-stable in the solid state for several days but decompose within hours in solution when exposed to air.

The Cu...Cu distances in **6-1** and **6-6** are below the sum of the van-der-Waals radii<sup>[16]</sup> suggesting intramolecular metallophilic interactions. In order to elucidate the bonding situation in  $[\{\{\text{CpMo}(\text{CO})_2\}_2(\mu_5, \eta^{2:2:2:1:1}\text{-P}_2)\}_2\{\text{Cu}(\text{CH}_3\text{CN})_2\}_2\text{Cu}]^{3+}$  (**6-1**) and  $[\{\{\text{CpMo}(\text{CO})_2\}_2(\mu_5, \eta^{2:2:2:1:1}\text{-P}_2)\}_2\{\text{Cu}(\text{CH}_3\text{CN})_3\}_2\text{Cu}(\text{CH}_3\text{CN})_2]^{3+}$  (**6-2**), DFT calculations at the B3LYP/def2-TZVP level of theory were performed. The Cu...Cu distances in **6-1** in the gas phase (2.559 Å) are similar to the distances in the solid state (2.4344(10) - 2.4537(19) Å). For **6-2**, the Cu...Cu distances are even longer in the gas phase (3.380 and 3.384 Å) compared to the solid state (3.0013(6) and 3.0593(6) Å). When dispersion effects are included in the calculations, the Cu...Cu distance in **6-1** decreases to 2.483 Å, indicating that dispersion plays an important role in the geometry of **6-1**. The calculations also show that the bonding of the peripheral Cu ions to the  $\text{P}_2$  ligands in **6-1** takes place via the coordination of the phosphorus lone pairs, while the central Cu ion binds to the P-P  $\sigma$ -orbital of the  $\text{P}_2$  unit. This is clearly revealed by the Localized Molecular Orbitals (LMOs) (**Figure 6-4**).

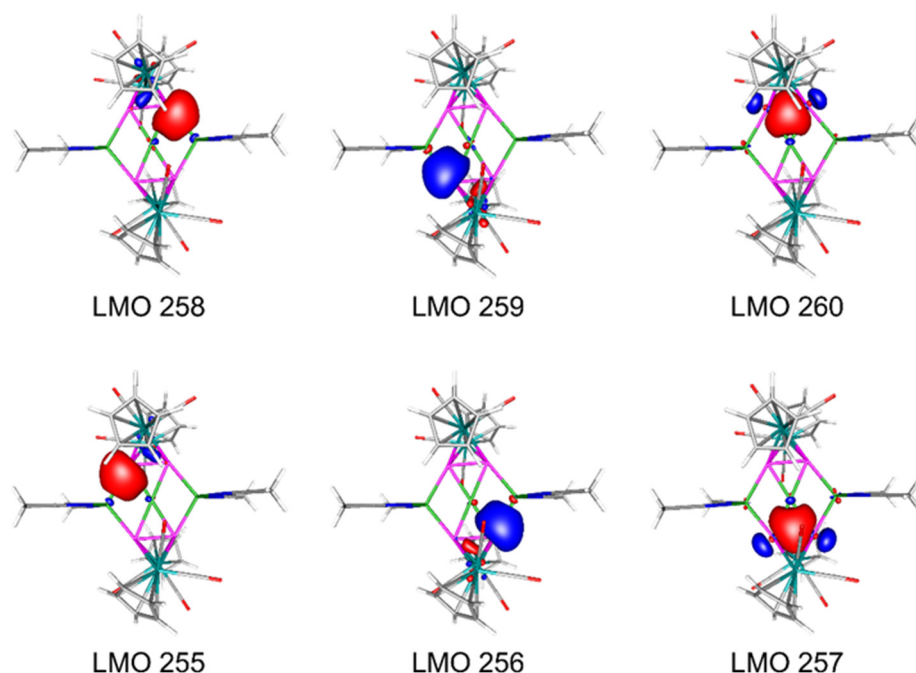


**Figure 6-4.** Selected Localized Molecular Orbitals (LMOs) representing the Cu-P bonding in  $[\{\{\text{CpMo}(\text{CO})_2\}_2(\mu_5, \eta^{2:2:2:1:1}\text{-P}_2)\}_2\{\text{Cu}(\text{CH}_3\text{CN})_2\}_2\text{Cu}]^{3+}$ , calculated at the B3LYP/def2-TZVP level of theory.

A small orbital contribution of the central Cu ion to the LMOs of the P-Cu<sub>per</sub> bond of roughly 7% was detected for **6-1**. A comparison of the LMOs of **6-1** with that of  $[\{\{\text{CpMo}(\text{CO})_2\}_2(\mu_4, \eta^{2:2:1:1}\text{-P}_2)\}_2\{\text{Cu}(\text{CH}_3\text{CN})_2\}_2]^{2+}$  (**G**)<sup>[7a]</sup> shows that the bonding of the P<sub>2</sub> ligand **A** to the peripheral Cu ions is very similar (Figure S3). The Wiberg Bond Indexes (WBIs) of the P-P bond in **G** are close to unity (1.06), while in **1** and **2** the WBIs of the P-P bonds are lower (0.78 in **6-1**; 0.72 in **6-2**), indicating a weaker P-P bond. This is not unexpected if considering the coordination of the P-P σ-bond additionally to the central Cu ion, which leads to the depletion of the electron density in this bonding orbital. The WBIs of the peripheral Cu-P bonds in **6-1**, *i.e.* 0.40-0.44, are slightly lower than in **G** (0.53-0.55) and **6-2** (0.55), respectively. The WBIs of the Cu<sub>cen</sub>-P bonds in **6-1** are 0.29 (Cu9-P6, Cu9-P8) and 0.40 (Cu9-P5, Cu9-P7), pointing to a slightly asymmetric bonding and a preference for a linear coordination geometry of the central Cu ion. This is an explanation for the elongation of the P-P bond in **6-1** (WBI (Wiberg Bond Index) 0.78) compared to **G** (1.06). The calculations indicate that between the three Cu ions an interaction is present since a WBI of 0.11 was found. In order to obtain deeper insight into the nature of the Cu-Cu interaction, we investigated the topology of the electron density of **6-2** by means of the Atoms In Molecules (AIM) method and were able to locate bond critical points (BCPs) between the Cu atoms. The electron density at these BCPs is rather low and the Laplacian of the electron density is positive, which nevertheless indicates that interaction is present (for details see SI). The ratio of the potential energy density ( $|V|$ ) and the kinetic energy density ( $G$ ) at the bond critical point of 1.20 is characteristic of intermediate interactions between typical covalent and closed shells, for which the  $|V|/G$  ratio lies between 1 and 2. Interestingly, the ellipticity at the BCP is rather high ( $\epsilon = 2.13$ ) pointing to a kind of π-type interaction. The interaction between the Cu atoms is also supported by the Density Overlap Regions Indicator (DORI) analysis which clearly identifies regions of overlapping electron density (see SI).

## 6.4 Conclusion

In conclusion, we synthesized seven unprecedented coordination compounds (**6-1** to **6-7**), obtained by reacting the P<sub>2</sub> (**A**) and As<sub>2</sub> (**B**) ligand complexes with three different Cu(I) salts (**C**, **D** and **E**) containing a WCA as counterion. Thus, four dinuclear copper dimers (**6-3**, **6-4**, **6-5** and **6-7**) and three trinuclear copper complexes (**6-1**, **6-2** and **6-6**) were obtained. For the first time, tetrahedral Mo<sub>2</sub>E<sub>2</sub> ligand complexes are able to connect different metal atoms forming a chain of three Cu atoms. The formation of these complexes reveal the decisive influence of WCAs as counterion in the used Cu(I) salts with different coordinating solvents, as [Cu(CH<sub>3</sub>CN)<sub>4</sub>][TEF] forms a trinuclear Cu(I) chain coordinated by two **A** units and [Cu(o-DFB)][TEF] forms a Cu<sub>2</sub>P<sub>4</sub> ring.<sup>[8c]</sup> The Cu...Cu distances in the trinuclear copper complexes **6-1**, **6-2** and **6-6** (2.4344(10)-2.4537(19) Å; 3.0013(6)/3.0593(6) Å; 2.587(4) Å) are below the sum of the van-der-Waals radii and in the range of Cu(I)-Cu(I) single bonds, suggesting intramolecular metallophilic interactions. DFT calculations for **6-1** at the B3LYP/def2-TZVP level of theory reveal that the bonding of the peripheral Cu ions to the Mo<sub>2</sub>P<sub>2</sub> ligands in **6-1** takes place via the coordination of the phosphorus lone pairs, while the central Cu ion binds to the P-P σ-orbital of the Mo<sub>2</sub>P<sub>2</sub> unit in an unprecedented coordination mode. As WBIs of 0.11 were found between the central and peripheral Cu ions, an interaction can be concluded, which are supported by AIM analysis bond critical points between the Cu atoms could be located. Moreover, under the same reaction conditions, the As<sub>2</sub> ligand complex **B** reveals a higher tendency to coordinate in an η<sup>2</sup>-fashion and additionally in an η<sup>1</sup>:η<sup>1</sup>-mode in comparison to the P<sub>2</sub> complex **A**.

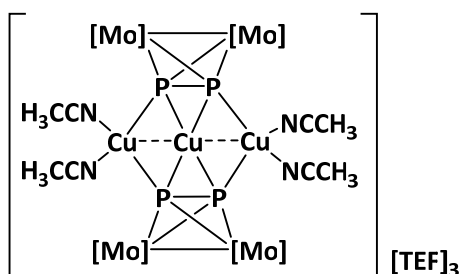
## 6.5 Supporting Information

### General

All experiments were carried out in an inert atmosphere of nitrogen or argon using standard Schlenk techniques. The nitrogen/argon was dried and purified from traces of oxygen with a Cu/MgSO<sub>4</sub> catalyst, concentrated H<sub>2</sub>SO<sub>4</sub> and orange gel. Reactants were stored in a glovebox under argon atmosphere. All used solvents were taken from the solvent drying machine MB SPS-800 of the company MBRAUN. The precursors [Cp<sub>2</sub>Mo<sub>2</sub>(CO)<sub>4</sub>(μ,η<sup>2:2</sup>-P<sub>2</sub>)]<sup>[17]</sup> (**A**), [Cp<sub>2</sub>Mo<sub>2</sub>(CO)<sub>4</sub>(μ,η<sup>2:2</sup>-As<sub>2</sub>)]<sup>[18]</sup> (**B**), [Cu(CH<sub>3</sub>CN)<sub>4</sub>][Al{OC(CF<sub>3</sub>)<sub>3</sub>}]<sup>[19]</sup> (**CuTEF**, **C**)<sup>[19]</sup> and [Cu(CH<sub>3</sub>CN)<sub>3.5</sub>][FAl{O(C<sub>6</sub>F<sub>10</sub>)(C<sub>6</sub>F<sub>5</sub>)<sub>3</sub>}] (**CuFAI**, **E**)<sup>[19]</sup> were prepared according to literature procedures. [Cu(CH<sub>3</sub>CN)<sub>4</sub>][BF<sub>4</sub>] (**D**) was purchased from the company TCI and used without further purification. IR spectra were recorded as solids with an ATR-Ge disc on a Thermo Fisher Nicolet iS5 spectrometer. Solution NMR spectra were recorded on a Bruker Avance III HD 400 spectrometer (<sup>1</sup>H: 400 MHz, <sup>31</sup>P: 161 MHz, <sup>13</sup>C: 100 MHz, <sup>19</sup>F: 376 MHz, <sup>11</sup>B: 128 MHz) with acetonitrile-d<sub>3</sub> as solvent at room temperature. The signals of tetramethylsilane (<sup>1</sup>H, <sup>13</sup>C), CFCl<sub>3</sub> (<sup>19</sup>F), Et<sub>2</sub>O x BF<sub>3</sub> (<sup>11</sup>B) and 85% H<sub>3</sub>PO<sub>4</sub> (<sup>31</sup>P) were used as reference for determining chemical shifts. The chemical shifts δ are presented in parts per million ppm and coupling constants *J* in Hz. The spectra were processed and analysed using the software Bruker TopSpin 3.0. Elemental analyses were performed on an Elementar vario MICRO cube apparatus. Mass spectra were recorded on an Agilent Q-TOF 6540 UHD mass spectrometer with acetonitrile as solvent.

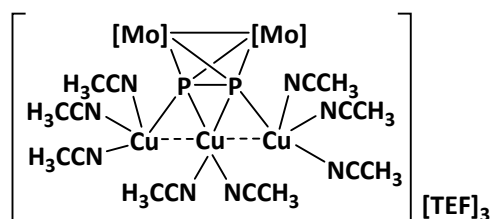
### Synthetic procedures

Synthesis of [{{CpMo(CO)<sub>2</sub>}}<sub>2</sub>(μ<sub>5</sub>,η<sup>2:2:2:1:1</sup>-P<sub>2</sub>)}<sub>2</sub>{Cu(CH<sub>3</sub>CN)<sub>2</sub>Cu}[TEF]<sub>3</sub> (**6-1**):



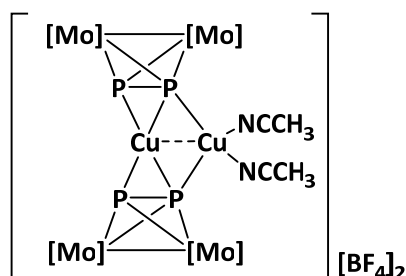
Compounds **A** (1 eq., 5 mg, 0.01 mmol) and **CuTEF** (3 eq., 79.4 mg, 0.05 mmol) were dissolved in CH<sub>2</sub>Cl<sub>2</sub> (5 mL each). Subsequently, the solution of **C** was added dropwise to the solution of **A**. The clear reaction mixture was stirred for 3h, filtered and stored at -30 °C. After one day, compound **1** was obtained as clear orange blocks (**1a**) or red plates (**1b**). The supernatant was decanted off, the remaining crystals washed with *n*-pentane and dried *in vacuo*. Crystalline Yield: 39 mg (95 %, related to **A**). <sup>1</sup>H NMR (CD<sub>3</sub>CN): δ = 5.32 (s, 10H, C<sub>5</sub>H<sub>5</sub>). <sup>31</sup>P NMR (CD<sub>3</sub>CN): δ = -54.0 - -59.5 (bs).<sup>[20]</sup> <sup>13</sup>C NMR (CD<sub>3</sub>CN) : δ = 226.1 (CO), 87.6 (C<sub>5</sub>H<sub>5</sub>). <sup>19</sup>F NMR (CD<sub>3</sub>CN): δ = -74.8 (s). Positive ion ESI-MS (CH<sub>3</sub>CN, RT): *m/z* (%) = 1056.56 (60) [Cu{Cp<sub>2</sub>Mo<sub>2</sub>(CO)<sub>2</sub>P<sub>2</sub>}<sub>2</sub>]<sup>+</sup>, 599.77 (100) [Cu(CH<sub>3</sub>CN){Cp<sub>2</sub>Mo<sub>2</sub>(CO)<sub>2</sub>P<sub>2</sub>}]<sup>+</sup>. IR (solid, CO bands):  $\tilde{\nu}/\text{cm}^{-1}$ : 2037 (w), 2013 (w), 1983 (w). Elemental analysis, calc. for C<sub>84</sub>H<sub>32</sub>Al<sub>3</sub>Cu<sub>3</sub>F<sub>108</sub>Mo<sub>4</sub>N<sub>4</sub>O<sub>20</sub>P<sub>4</sub> (4253.24 g/mol) (%): C, 23.75; H, 0.76; N 1.31; found: C, 23.89; H, 0.83; N, 1.29.

Synthesis of  $[\{\{\text{CpMo}(\text{CO})_2\}_2(\mu_5, \eta^{2:2:2:1:1}\text{-P}_2)\}\{\text{Cu}(\text{CH}_3\text{CN})_3\}_2\text{Cu}(\text{CH}_3\text{CN})_2][\text{TEF}]_3$  (**6-2**):



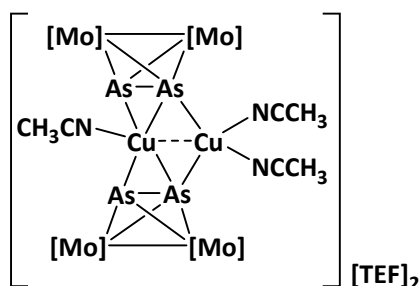
Compounds **A** (1 eq., 5 mg, 0.01 mmol) and **CuTEF** (4 eq., 64 mg, 0.04 mmol) were dissolved in  $\text{CH}_2\text{Cl}_2$  (5 mL each). Subsequently, the solution of **C** was added dropwise to the solution of **A**. The clear reaction mixture was stirred for 3h, filtered and stored at  $-30\text{ }^\circ\text{C}$ . After one day, compound **2** was obtained as yellow blocks. The supernatant was decanted off, the remaining crystals washed with *n*-pentane and dried *in vacuo*. Crystalline Yield: 38.7 mg (99 %, revered to **A**).  $^1\text{H}$  NMR ( $\text{CD}_3\text{CN}$ ):  $\delta = 5.32$  (s, 10H,  $\text{C}_5\text{H}_5$ ).  $^{31}\text{P}$  NMR ( $\text{CD}_3\text{CN}$ ):  $\delta = -57.8 - -64.3$  (bs).  $^{13}\text{C}$  NMR ( $\text{CD}_3\text{CN}$ ):  $\delta = 226.2$  (s, **CO**), 87.5 ( $\text{C}_5\text{H}_5$ ).  $^{19}\text{F}$  NMR ( $\text{CD}_3\text{CN}$ ):  $\delta = -74.8$  (s). Positive ion ESI-MS ( $\text{CH}_3\text{CN}$ , RT):  $m/z$  (%) = 1056.56 (60)  $[\text{Cu}\{\text{Cp}_2\text{Mo}_2(\text{CO})_2\text{P}_2\}_2]^+$ , 599.77 (100)  $[\text{Cu}(\text{CH}_3\text{CN})\{\text{Cp}_2\text{Mo}_2(\text{CO})_2\text{P}_2\}]^+$ . IR (solid, CO bands):  $\tilde{\nu}/\text{cm}^{-1}$ : 2009 (w), 1972 (w). Elemental analysis, calc. for  $\text{C}_{78}\text{H}_{34}\text{Al}_3\text{Cu}_3\text{F}_{108}\text{Mo}_2\text{N}_8\text{O}_{16}\text{P}_2$  (3917,53 g/mol) (%): C, 23.89; H, 0.87; N 2.86; found: C, 24.22; H, 0.70; N, 2.82.

Synthesis of  $[\{\{\text{CpMo}(\text{CO})_2\}_2(\mu_5, \eta^{2:2:1}\text{-P}_2)\}\{\text{Cu}(\text{CH}_3\text{CN})_2\}_2\text{Cu}][\text{BF}_4]_2$  (**6-3**):



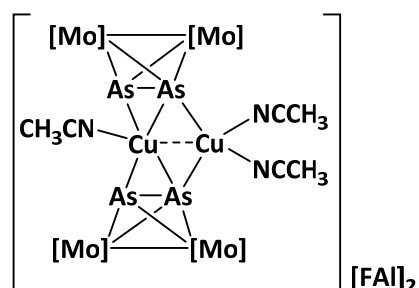
Compounds **A** (1.9 eq., 88 mg, 0.28 mmol) and  $[\text{Cu}(\text{CH}_3\text{CN})_4][\text{BF}_4]$  (1 eq., 351.7 mg, 0.15 mmol) were dissolved in  $\text{CH}_2\text{Cl}_2$  (5 mL each) and the solution of **D** was added dropwise to the solution of **A**. The clear reaction mixture was stirred for 3h, filtered and stored at  $-30\text{ }^\circ\text{C}$ . After one day, compound **3** was obtained as clear intense red blocks. The supernatant was decanted, the remaining crystals were washed with *n*-pentane and dried *in vacuo*. Crystalline yield: 46 mg (48 %, related to **A**).  $^1\text{H}$  NMR ( $\text{CD}_3\text{CN}$ ):  $\delta = 5.33$  (s, 10H,  $\text{C}_5\text{H}_5$ ).  $^{31}\text{P}$  NMR ( $\text{CD}_3\text{CN}$ ):  $\delta = -69.5\text{-}59.8$  (bs).  $^{13}\text{C}$  NMR ( $\text{CD}_3\text{CN}$ ):  $\delta = 225.4$  (**CO**), 87.7 ( $\text{C}_5\text{H}_5$ ).  $^{19}\text{F}$  NMR ( $\text{CD}_3\text{CN}$ ):  $\delta = -150.6$  (bs).  $^{11}\text{B}$  NMR ( $\text{CD}_3\text{CN}$ ):  $\delta = -0.56$  (s). Positive ion ESI-MS ( $\text{CH}_3\text{CN}$ , RT):  $m/z$  (%) = 1056.56 (60)  $[\text{Cu}\{\text{Cp}_2\text{Mo}_2(\text{CO})_2\text{P}_2\}_2]^+$ , 599.77 (100)  $[\text{Cu}(\text{CH}_3\text{CN})\{\text{Cp}_2\text{Mo}_2(\text{CO})_2\text{P}_2\}]^+$ , 144.98 (100)  $[\text{Cu}(\text{CH}_3\text{CN})_2]^+$ . IR (solid, CO bands):  $\tilde{\nu}/\text{cm}^{-1}$ : 1971 (s), 1932 (w), 1911(s). Elemental analysis, calc. for  $\text{C}_{32}\text{H}_{26}\text{B}_2\text{Cu}_2\text{F}_8\text{Mo}_4\text{N}_2\text{O}_8\text{P}_4$  (1381,55 g/mol) (%): C, 27.79; H, 1.90; N 2.03; found: C, 27.97; H, 1.89; N, 2.03.

Synthesis of  $[\{\{\text{CpMo}(\text{CO})_2\}_2(\mu_5, \eta^{2:2:2:1}\text{-As}_2)\}\{\text{Cu}(\text{CH}_3\text{CN})_2\}\text{Cu}(\text{CH}_3\text{CN})][\text{TEF}]_2$  (**6-4**):



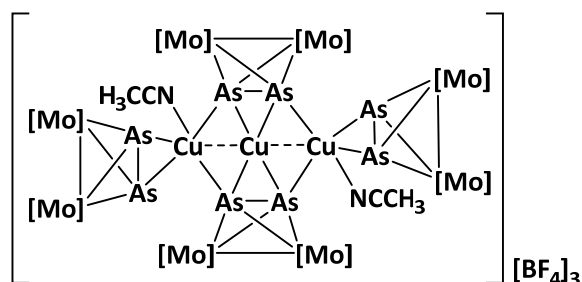
$[\text{Cu}(\text{CH}_3\text{CN})_4][\text{Al}\{\text{OC}(\text{CF}_3)_3\}_4]$  (1 eq., 60 mg, 0.05 mmol) was dissolved in  $\text{CH}_2\text{Cl}_2$  (5 mL) and was added to a solution of  $\text{Cp}_2\text{Mo}_2(\text{CO})_4(\eta^2\text{-As}_2)$  (**B**) (1 eq., 29 mg, 0.05 mmol) in  $\text{CH}_2\text{Cl}_2$  (5 mL) and stirred for 2h at room temperature. The red solution was carefully layered with threefold amount of *n*-pentane and stored at room temperature. After one day, red needles were formed. The crystals were washed with *n*-pentane and dried *in vacuo*. Crystalline Yield: 75 mg (89 %, referred to **B**).  $^1\text{H}$  NMR ( $\text{CD}_3\text{CN}$ ):  $\delta = 5.45$  (s, 10H,  $\text{C}_5\text{H}_5$ ) + 5.26  $\text{Mo}_2\text{As}_2$ .  $^{13}\text{C}$  NMR ( $\text{CD}_3\text{CN}$ ):  $\delta = 227.59$  (CO), 85.80 ( $\text{C}_5\text{H}_5$ ).  $^{19}\text{F}$  NMR ( $\text{CD}_3\text{CN}$ ):  $\delta = -74.78$ . Positive ion ESI-MS ( $\text{CH}_3\text{CN}$ , RT):  $m/z$  (%) = 1232.3 (60)  $[\{\text{Cp}_2\text{Mo}_2(\text{CO})_4\text{As}_2\}_2\text{Cu}]^+$ , 687.7 (100)  $[\{\text{Cp}_2\text{Mo}_2(\text{CO})_4\text{As}_2\}\text{Cu}(\text{CH}_3\text{CN})]^+$ , 583.7 (12)  $[\text{Cp}_2\text{Mo}_2(\text{CO})_4\text{As}_2]^+$ . IR (solid, CO bands):  $\tilde{\nu}/\text{cm}^{-1}$ : 1275 (s), 1298 (s), 1240 (vs), 1215 (vs). Elemental analysis, calc. for  $\text{C}_{66}\text{H}_{29}\text{Al}_2\text{As}_4\text{Cu}_2\text{F}_{72}\text{Mo}_4\text{N}_3\text{O}_{16}$  (3352.35  $\text{g}/\text{mol}$ ) (%): C, 23.92; H, 0.88; N 2.86; found: C, 24.22; H, 0.70; N, 2.82.

Synthesis of  $[\{\{\text{CpMo}(\text{CO})_2\}_2(\mu_5, \eta^{2:2:2:1}\text{-As}_2)\}\{\text{Cu}(\text{CH}_3\text{CN})_2\}\text{Cu}(\text{CH}_3\text{CN})][\text{FAI}]_2$  (**6-5**):



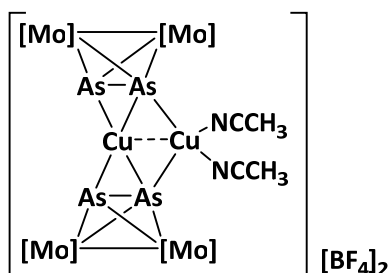
$[\text{Cu}(\text{CH}_3\text{CN})_{3.5}][\text{FAI}\{\text{O}(\text{C}_6\text{F}_{10})(\text{C}_6\text{F}_5)\}_3]$  (1 eq., 79 mg, 0.05 mmol) dissolved in  $\text{CH}_2\text{Cl}_2$  (5 mL), was added to a solution of  $\text{Cp}_2\text{Mo}_2(\text{CO})_4(\eta^2\text{-As}_2)$  (**B**) (1 eq., 29 mg, 0.05 mmol) in  $\text{CH}_2\text{Cl}_2$  (5 mL) and stirred for 2h at room temperature. The red solution was carefully layered with threefold amount of *n*-pentane and stored at room temperature. After one day, orange plates crystallised. The crystals were washed with *n*-pentane and dried *in vacuo*. Crystalline Yield: 60 mg (57 %, referred to **B**).  $^1\text{H}$  NMR ( $\text{CD}_3\text{CN}$ ):  $\delta = 5.45$  (s, 10H,  $\text{C}_5\text{H}_5$ ) + 5.26  $\text{Mo}_2\text{As}_2$ .  $^{13}\text{C}$  NMR ( $\text{CD}_3\text{CN}$ ):  $\delta = 227.75$  (CO), 85.85 ( $\text{C}_5\text{H}_5$ ).  $^{19}\text{F}$   $\{^1\text{H}\}$  NMR ( $\text{CD}_3\text{CN}$ ):  $\delta = -111.64$  (d,  $J_{\text{F,F}} = 283$  Hz, 2F),  $-116.14$  (d,  $J_{\text{F,F}} = 280$ Hz, 2F),  $-121.13$  (d,  $J_{\text{F,F}} = 280$ Hz, 2F),  $-127.84$  (s, 2F),  $-129.77$  (d,  $J_{\text{F,F}} = 280$ Hz, 2F),  $-136.46$  (d,  $J_{\text{F,F}} = 280$ Hz, 2F),  $-140.79$  (d,  $J_{\text{F,F}} = 280$ Hz 1F),  $-154.00$  (tt,  $^2J_{\text{F,F}} = 21$ Hz,  $^3J_{\text{F,F}} = 6$ Hz, 1F),  $164.70$  (td,  $^2J_{\text{F,F}} = 21$ Hz,  $^3J_{\text{F,F}} = 6$ Hz, 1F),  $-170.63$  (s, 1F). Positive ion ESI-MS ( $\text{CH}_3\text{CN}$ , RT):  $m/z$  (%) = 1232.3 (51)  $[\{\text{Cp}_2\text{Mo}_2(\text{CO})_4\text{As}_2\}_2\text{Cu}]^+$ , 687.7 (100)  $[\{\text{Cp}_2\text{Mo}_2(\text{CO})_4\text{As}_2\}\text{Cu}(\text{CH}_3\text{CN})]^+$ , 583.7 (37)  $[\text{Cp}_2\text{Mo}_2(\text{CO})_4\text{As}_2]^+$ . IR (solid, CO bands):  $\tilde{\nu}/\text{cm}^{-1}$ : 2005 (s), 1979 (s), 1950 (s), 1934 (s). Elemental analysis, calc. for  $\text{C}_{106}\text{H}_{29}\text{Al}_2\text{As}_4\text{Cu}_2\text{F}_{92}\text{Mo}_4\text{N}_3\text{O}_{14}$  (4180.73  $\text{g}/\text{mol}$ ) (%): C, 30.45; H, 0.70; N, 1.01; found: C, 30.38; H, 0.61; N, 0.61.

Synthesis of  $[\{\{\text{CpMo}(\text{CO})_2\}_2(\mu_5, \eta^{2:2:2:1:1}\text{-As}_2)\}_2\{\{\text{CpMo}(\text{CO})_2\}_2(\mu_5, \eta^{2:2:2}\text{-As}_2)\}_2\{\text{Cu}(\text{CH}_3\text{CN})\}_2\text{Cu}][\text{BF}_4]_3$  (**6-6**):



$[\text{Cu}(\text{CH}_3\text{CN})_4][\text{BF}_4]$  (1 eq., 16 mg, 0.05 mmol), dissolved in  $\text{CH}_2\text{Cl}_2$  (5 mL), was added to a solution of  $\text{Cp}_2\text{Mo}_2(\text{CO})_4(\eta^2\text{-As}_2)$  (**B**) (1 eq., 29 mg, 0.05 mmol) in  $\text{CH}_2\text{Cl}_2$  (5 mL) and stirred for 2h at room temperature. The red solution was filtered and carefully layered with threefold amount of *n*-pentane and stored at room temperature. After one day dark red block-shaped crystals were formed. The crystals were washed with *n*-pentane and dried *in vacuo*. Crystalline Yield: 15 mg (43%, referred to **B**).  $^1\text{H}$  NMR ( $\text{CD}_3\text{CN}$ ):  $\delta = 5.45$  (s, 10H, Cp) + 5.26  $\text{Mo}_2\text{As}_2$ .  $^{13}\text{C}$  NMR ( $\text{CD}_3\text{CN}$ ):  $\delta = 227.22$  (CO), 85.82 ( $\text{C}_5\text{H}_5$ ).  $^{19}\text{F}$  NMR ( $\text{CD}_3\text{CN}$ ):  $\delta = -150.66$  (d,  $^1J_{\text{B,F}} = 19.8$  Hz).  $^{11}\text{B}$  NMR ( $\text{CD}_3\text{CN}$ ):  $\delta = -0.57$  (s). Positive ion ESI-MS ( $\text{CH}_3\text{CN}$ , RT):  $m/z$  (%) = 1232.4 (100)  $[\{\{\text{Cp}_2\text{Mo}_2(\text{CO})_4\text{As}_2\}_2\text{Cu}\}]^+$ , 687.7 (99)  $[\{\{\text{Cp}_2\text{Mo}_2(\text{CO})_4\text{As}_2\}\text{Cu}(\text{CH}_3\text{CN})\}]^+$ . IR (solid, CO bands):  $\tilde{\nu}/\text{cm}^{-1}$ : 1953 (vs), 1917 (vs). Elemental analysis, calc. (%) for  $\text{C}_{56}\text{H}_{40}\text{As}_8\text{B}_3\text{Cu}_3\text{F}_{12}\text{Mo}_8\text{O}_{16}$  (2786.85  $\text{g}/\text{mol}$ ): C, 24.13; H, 1.45; found: C, 24.11; H, 1.57.

Synthesis of  $[\{\{\text{CpMo}(\text{CO})_2\}_2(\mu_5, \eta^{2:2:1}\text{-As}_2)\}_2\{\text{Cu}(\text{CH}_3\text{CN})_2\text{Cu}\}][\text{BF}_4]_2$  (**6-7**):



$[\text{Cu}(\text{CH}_3\text{CN})_4][\text{BF}_4]$  (7 eq., 110 mg, 0.35 mmol), dissolved in  $\text{CH}_2\text{Cl}_2$  (5 mL), was added to a solution of **B** (1 eq., 29 mg, 0.05 mmol) in  $\text{CH}_2\text{Cl}_2$  (8 mL) and stirred for 2h at room temperature. The light red solution was carefully layered with threefold amount of *n*-pentane and stored at room temperature. After one day dark red block-shaped crystals were formed. The crystals were washed with *n*-pentane and dried *in vacuo*. Crystalline yield: 21 mg (47%, referred to **B**).  $^1\text{H}$  NMR ( $\text{CD}_3\text{CN}$ ):  $\delta = 5.45$  (s,  $\text{C}_5\text{H}_5$ ) + 5.26  $\text{Mo}_2\text{As}_2$ .  $^{13}\text{C}$  NMR ( $\text{CD}_3\text{CN}$ ):  $\delta = 226.8$  (CO), 85.45 ( $\text{C}_5\text{H}_5$ ).  $^{19}\text{F}$  NMR ( $\text{CD}_3\text{CN}$ ):  $\delta = -150.65$  (d,  $^1J_{\text{B,F}} = 19.7$  Hz).  $^{11}\text{B}$  NMR ( $\text{CD}_3\text{CN}$ ):  $\delta = -0.56$  (s). Positive ion ESI-MS ( $\text{CH}_3\text{CN}$ , RT):  $m/z$  (%) = 1232.4 (100)  $[\{\{\text{Cp}_2\text{Mo}_2(\text{CO})_4\text{As}_2\}_2\text{Cu}\}]^+$ , 687.7 (48)  $[\{\{\text{Cp}_2\text{Mo}_2(\text{CO})_4\text{As}_2\}\text{Cu}(\text{CH}_3\text{CN})\}]^+$ . IR (solid, CO bands):  $\tilde{\nu}/\text{cm}^{-1}$ : 1992 (s), 1939 (s). Elemental analysis did not deliver matching values, because an excess of starting material is used which crystallises simultaneously with the product.  $[\text{Cu}(\text{CH}_3\text{CN})_4][\text{BF}_4]$  cannot be separated from the product, due to similar solubilities.



## Crystallographic Data

**Crystal Structure Analysis:** The crystals were selected and measured on a Gemini Ultra diffractometer equipped with an AtlasS2 CCD detector (**6-1** (2 CH<sub>2</sub>Cl<sub>2</sub>), **6-1** (toluene), **6-2**, **6-3**) and a GV50 diffractometer equipped with a TitanS2 detector (**6-7**), respectively. The crystals were kept at  $T = 123(1)$  K during data collection. Data collection and reduction were performed with **CrysAlisPro** [Version V1.171.38.46, 2015 (**1** (2 CH<sub>2</sub>Cl<sub>2</sub>)), V1.171.40.14a, 2018 (**6-1** (toluene), **6-2** to **6-7**)].<sup>[21]</sup> For the compounds **6-1** (toluene), **6-2**, **6-3** and **6-6** an analytical numeric absorption correction using a multifaceted crystal model based on expressions derived by R.C. Clark & J.S. Reid<sup>[22]</sup> and an empirical absorption correction using spherical harmonics as implemented in SCALE3 ABSPACK was applied. For the compounds **6-1** (2 CH<sub>2</sub>Cl<sub>2</sub>), **6-4**, **6-5** and **6-7** a numerical absorption correction based on gaussian integration over a multifaceted crystal model and an empirical absorption correction using spherical harmonics as implemented in SCALE3 ABSPACK was applied. Using **Olex2**,<sup>[23]</sup> the structures were solved with **ShelXT**<sup>[24]</sup> and a least-square refinement on  $F^2$  was carried out with **ShelXL**<sup>[25]</sup> for all structures. All non-hydrogen atoms were refined anisotropically. Hydrogen atoms at the carbon atoms were located in idealised positions and refined isotropically according to the riding model.

Compound **6-1** (2 CH<sub>2</sub>Cl<sub>2</sub>): The asymmetric unit contains two CH<sub>2</sub>Cl<sub>2</sub> solvent molecules, which are respectively disordered over two positions (79:21; 74:26). Further, the asymmetric unit contains two halves of the complex  $[\{\{\text{CpMo}(\text{CO})_2\}_2(\mu_5, \eta^{2:2:2:1:1}\text{-P}_2)\}_2\{\text{Cu}(\text{CH}_3\text{CN})_2\}_2\text{Cu}]$  and additionally three  $[\text{Al}\{\text{OC}(\text{CF}_3)_3\}_4]$  anions. Almost all the  $\{\text{O}(\text{CF}_3)_3\}$  units at the three  $[\text{Al}\{\text{OC}(\text{CF}_3)_3\}_4]$  anions are disordered over at least two positions. Further, one Cp ligand at one half of a  $[\{\{\text{CpMo}(\text{CO})_2\}_2(\mu_5, \eta^{2:2:2:1:1}\text{-P}_2)\}_2\{\text{Cu}(\text{CH}_3\text{CN})_2\}_2\text{Cu}]$  complex is disordered over two positions (53:47). To describe these disorders the FLAT, DFIX, SADI, SIMU, RIGU and ISOR restraints were applied.

Compound **6-1** (toluene): The asymmetric unit contains one toluene solvent molecule, the cationic complex  $[\{\{\text{CpMo}(\text{CO})_2\}_2(\mu_5, \eta^{2:2:2:1:1}\text{-P}_2)\}_2\{\text{Cu}(\text{CH}_3\text{CN})_2\}_2\text{Cu}]$  and three  $[\text{Al}\{\text{OC}(\text{CF}_3)_3\}_4]$  anions. One Cp and one CO ligand of the complex  $[\{\{\text{CpMo}(\text{CO})_2\}_2(\mu_5, \eta^{2:2:2:1:1}\text{-P}_2)\}_2\{\text{Cu}(\text{CH}_3\text{CN})_2\}_2\text{Cu}]$  are disordered over two positions (73:27). Further, almost all the  $\{\text{O}(\text{CF}_3)_3\}$  units at the three  $[\text{Al}\{\text{OC}(\text{CF}_3)_3\}_4]$  anions are disordered over at least two positions. To describe these disorders the SADI, SIMU and RIGU restraints were applied.

Compound **6-2**: The asymmetric unit contains one CH<sub>2</sub>Cl<sub>2</sub> solvent molecule, the cationic complex  $[\{\{\text{CpMo}(\text{CO})_2\}_2(\mu_5, \eta^{2:2:2:1:1}\text{-P}_2)\}_2\{\text{Cu}(\text{CH}_3\text{CN})_3\}_2\text{Cu}(\text{CH}_3\text{CN})_2]$  and three  $[\text{Al}\{\text{OC}(\text{CF}_3)_3\}_4]$  anions. The Cl atoms of CH<sub>2</sub>Cl<sub>2</sub> solvent molecule are disordered over two positions (69:31). Further, almost all the  $\{\text{O}(\text{CF}_3)_3\}$  units at the three  $[\text{Al}\{\text{OC}(\text{CF}_3)_3\}_4]$  anions are disordered over at least two positions. To describe these disorders the SADI, SIMU, RIGU and ISOR restraints were applied.

Compound **6-3**: The asymmetric unit contains half a BF<sub>4</sub> anion and one quarter of the complex  $[\{\{\text{CpMo}(\text{CO})_2\}_2(\mu_4, \eta^{2:2:2:1}\text{-P}_2)\}_2\{\text{Cu}(\text{CH}_3\text{CN})_2\}_2\text{Cu}]$  at which one CO group is disordered over two positions (50:50). To describe this disorder, the SIMU restraint was applied.

Compound **6-4**: The asymmetric unit contains one CH<sub>2</sub>Cl<sub>2</sub> solvent molecule, the cationic complex  $[\{\{\text{CpMo}(\text{CO})_2\}_2(\mu_4, \eta^{2:2:2:1}\text{-As}_2)\}_2\{\text{Cu}(\text{CH}_3\text{CN})_2\}_2\text{Cu}(\text{CH}_3\text{CN})_1]$  and three  $[\text{Al}\{\text{OC}(\text{CF}_3)_3\}_4]$  anions. At one  $[\text{Al}\{\text{OC}(\text{CF}_3)_3\}_4]$  anion two  $\{\text{O}(\text{CF}_3)_3\}$  units are disordered over two (60:40) and one  $\{\text{O}(\text{CF}_3)_3\}$  unit is disordered over three positions (37:37:26). To describe these disorders the SADI, SIMU and RIGU restraints were applied.

Compound **6-5**: The asymmetric unit contains 1.75 CH<sub>2</sub>Cl<sub>2</sub> solvent molecules, two  $[\text{FAl}\{\text{O}(\text{C}_6\text{F}_{10})(\text{C}_6\text{F}_5)\}_3]$  anions and the cationic complex  $[\{\{\text{Cp}_2\text{Mo}_2(\text{CO})_4(\mu_4, \eta^{2:2:2:1}\text{-As}_2)\}_2\{\text{Cu}(\text{CH}_3\text{CN})_2\}_2\{\text{Cu}(\text{CH}_3\text{CN})\}]$ . One and a

half of the CH<sub>2</sub>Cl<sub>2</sub> solvent molecules were heavily disordered. Therefore, a solvent mask was calculated and 252 electrons were found in a volume of 1252 Å<sup>3</sup> in two voids per unit cell. This is consistent with the presence of 1.5 CH<sub>2</sub>Cl<sub>2</sub> molecules per asymmetric unit, which account for 252 electrons per unit cell. Additionally 0.25 CH<sub>2</sub>Cl<sub>2</sub> molecules were disordered over two positions (15:10). Further, one Cp ligand (70:30) and a CH<sub>3</sub>CN molecule (53:47) of the complex [ $\{\text{Cp}_2\text{Mo}_2(\text{CO})_4(\mu_4, \eta^{2:2:2:1}\text{-As}_2)\}\{\text{Cu}(\text{CH}_3\text{CN})_2\}\{\text{Cu}(\text{CH}_3\text{CN})\}$ ] are disordered over two positions. Furthermore, two of the three  $\{\text{O}(\text{C}_6\text{F}_{10})(\text{C}_6\text{F}_5)\}$  substituents of one  $[\text{FAl}\{\text{O}(\text{C}_6\text{F}_{10})(\text{C}_6\text{F}_5)\}_3]$  anion are disordered over two positions (72:28; 61:39). To describe these disorders the SADI, SIMU and ISOR restraints were applied.

Compound **6-6**: The asymmetric unit contains 2.19 CH<sub>2</sub>Cl<sub>2</sub> solvent molecules and 1.4 BF<sub>4</sub> anions. It further contains four overlaying complexes [ $\{\text{Cp}_2\text{Mo}_2(\text{CO})_4(\mu_5, \eta^{2:2:2:1:1}\text{-As}_2)\}_2\{\text{Cp}_2\text{Mo}_2(\text{CO})_4(\mu_3, \eta^{2:2:2}\text{-As}_2)\}_2\{\text{Cu}(\text{NCMe})_2\text{Cu}\}$  (**6a**, 39 - 59% occupancy), [ $\{\text{Cp}_2\text{Mo}_2(\text{CO})_4(\mu_5, \eta^{2:2:2:1:1}\text{-As}_2)\}_2\{\text{Cp}_2\text{Mo}_2(\text{CO})_4(\mu_3, \eta^{2:2:2}\text{-As}_2)\}_2\text{Cu}_3]$  (**6b**, 21 - 41% occupancy), [ $\{\text{Cp}_2\text{Mo}_2(\text{CO})_4(\mu_4, \eta^{2:2:1:1}\text{-As}_2)\}_2\{\text{Cp}_2\text{Mo}_2(\text{CO})_4(\mu_3, \eta^{2:2:2}\text{-As}_2)\}_2\text{Cu}_2]$  (**6c**; 0 - 20% occupancy) and [ $\{\text{Cp}_2\text{Mo}_2(\text{CO})_4(\mu_5, \eta^{2:2:2:1:1}\text{-As}_2)\}_2\{\text{Cp}_2\text{Mo}_2(\text{CO})_4(\mu_3, \eta^{2:2:2}\text{-As}_2)\}_2\{\text{Cu}(\text{NCMe})_2\}$ ] (**6d**; 0 - 20% occupancy), which are located on a 2-fold rotation axis and therefore only half present in the asymmetric unit. The vague allocation of these complexes is a result of the unequal occupation of the central Cu atom (0.8% occupancy) and the NCMe ligands (0.59% occupancy). The SADI and SIMU restraints were applied to describe one BF<sub>4</sub> anion, which is located on a 2-fold rotation axis. Further, these restraints were also used to describe a CH<sub>2</sub>Cl<sub>2</sub> molecule, which shares the same position with an NCMe molecule coordinated to a Cu atom.

Compound **6-7**: The asymmetric unit contains one quarter of a BF<sub>4</sub> anion and one quarter of the complex [ $\{\text{Cp}_2\text{Mo}_2(\text{CO})_4(\mu_4, \eta^{2:2:2:1}\text{-As}_2)\}_2\{\text{Cu}(\text{NCCH}_3)_2\text{Cu}\}$ ]. Due to the special position of the Cu(NCCH<sub>3</sub>)<sub>2</sub> fragment on a mirror plane near an inversion center the SIMU restraint was applied to this fragment.

**Table S1.** Crystallographic data and details of diffraction experiments for compounds **6-1a-6-3**.

<b>Compound</b>	<b>6-1a · 2 CH<sub>2</sub>Cl<sub>2</sub></b>	<b>6-1b</b>	<b>6-2 · CH<sub>2</sub>Cl<sub>2</sub></b>	<b>6-3 · 4 CH<sub>3</sub>CN · 4 CH<sub>2</sub>Cl<sub>2</sub></b>
Data Set (internal naming)	<b>abs268</b>	<b>abs461a</b>	<b>abs437a</b>	<b>abs444b_2</b>
Formula	C <sub>86</sub> H <sub>36</sub> Al <sub>3</sub> Cl <sub>4</sub> Cu <sub>3</sub> F <sub>108</sub> Mo <sub>4</sub> N <sub>4</sub> O <sub>20</sub> P <sub>4</sub>	C <sub>91</sub> H <sub>40</sub> Al <sub>3</sub> Cu <sub>3</sub> F <sub>108</sub> Mo <sub>4</sub> N <sub>4</sub> O <sub>20</sub> P <sub>4</sub>	C <sub>79</sub> H <sub>36</sub> Al <sub>3</sub> Cl <sub>2</sub> Cu <sub>3</sub> F <sub>108</sub> Mo <sub>2</sub> N <sub>8</sub> O <sub>16</sub> P <sub>2</sub>	C <sub>32</sub> H <sub>26</sub> B <sub>2</sub> Cu <sub>2</sub> F <sub>8</sub> Mo <sub>4</sub> N <sub>2</sub> O <sub>8</sub> P <sub>4</sub>
<i>D</i> <sub>calc.</sub> / g · cm <sup>-3</sup>	2.117	2.059	2.008	2.077
<i>μ</i> /mm <sup>-1</sup>	6.645	5.879	0.954	2.284
Formula Weight	4418.19	4340.47	4001.44	1374.89
Colour	red	clear orange	yellow	clear orange
Shape	plate	block	block	plate
Size/mm <sup>3</sup>	0.46×0.28×0.06	0.25×0.16×0.08	0.41×0.31×0.28	0.44×0.22×0.07
<i>T</i> /K	123(1)	123(1)	123.15	123(1)
Crystal System	monoclinic	trigonal	monoclinic	monoclinic
Flack Parameter	-	-0.010(8)	-	-
Hooft Parameter	-	-0.007(4)	-	-
Space Group	<i>P</i> 2 <sub>1</sub> / <i>c</i>	<i>P</i> 3 <sub>2</sub>	<i>P</i> 2 <sub>1</sub> / <i>c</i>	<i>I</i> 2/ <i>m</i>
<i>a</i> /Å	28.5401(2)	17.35370(10)	27.3674(7)	8.3221(3)
<i>b</i> /Å	18.57590(14)	17.35370(10)	23.2498(6)	25.8028(9)
<i>c</i> /Å	26.6845(2)	40.2585(2)	20.7996(5)	10.2632(4)
<i>α</i> /°	90	90	90	90
<i>β</i> /°	101.5352(8)	90	90.654(2)	94.027(3)
<i>γ</i> /°	90	120	90	90
<i>V</i> /Å <sup>3</sup>	13861.24(19)	10499.58(13)	13233.6(6)	2198.41(14)
<i>Z</i>	4	3	4	2
<i>Z'</i>	1	1	1	0.25
Wavelength/Å	1.54184	1.54184	0.71073	0.71073
Radiation type	CuK <sub>α</sub>	CuK <sub>α</sub>	MoK <sub>α</sub>	MoK <sub>α</sub>
<i>Q</i> <sub>min</sub> /°	3.434	3.293	3.278	3.411
<i>Q</i> <sub>max</sub> /°	72.915	73.056	32.310	32.327
Measured Refl.	57598	39410	119824	16969
Independent Refl.	26486	23136	41829	3773
Reflections with <i>I</i> > 2( <i>I</i> )	20576	22123	31376	3435
<i>R</i> <sub>int</sub>	0.0551	0.0304	0.0296	0.0255
Parameters	3249	3327	3116	229
Restraints	4244	2605	3335	24
Largest Peak	3.618	0.958	1.232	0.454
Deepest Hole	-1.195	-0.541	-0.788	-0.651
GooF	1.049	1.016	1.073	1.179
<i>wR</i> <sub>2</sub> (all data)	0.2255	0.1421	0.1453	0.0535
<i>wR</i> <sub>2</sub>	0.2104	0.1395	0.1332	0.0520
<i>R</i> <sub>1</sub> (all data)	0.0971	0.0551	0.0802	0.0319
<i>R</i> <sub>1</sub>	0.0783	0.0530	0.0559	0.0267

**Table S2.** Crystallographic data and details of diffraction experiments for compounds **6-4-6-7**.

Compound	6-4	6-5 · 1.75 CH <sub>2</sub> Cl <sub>2</sub>	6-6 · 4.38 CH <sub>2</sub> Cl <sub>2</sub>	6-7
Data Set (internal naming)	<b>JS200</b>	<b>JS151</b>	<b>JS120_2</b>	<b>JS164_2</b>
Formula	C <sub>67</sub> H <sub>31</sub> Al <sub>2</sub> As <sub>4</sub> Cl <sub>2</sub> Cu <sub>2</sub> F <sub>72</sub> Mo <sub>4</sub> N <sub>3</sub> O <sub>16</sub>	Al <sub>2</sub> As <sub>4</sub> C <sub>107.75</sub> Cl <sub>3.5</sub> Cu <sub>2</sub> F <sub>92</sub> H <sub>32.5</sub> Mo <sub>4</sub> N <sub>3</sub> O <sub>14</sub>	C <sub>62.74</sub> H <sub>52.3</sub> As <sub>8</sub> B <sub>2.58</sub> Cl <sub>8.76</sub> Cu <sub>2.79</sub> F <sub>10.32</sub> Mo <sub>8</sub> N <sub>1.18</sub> O <sub>16</sub>	C <sub>16</sub> H <sub>13</sub> As <sub>2</sub> BCuF <sub>4</sub> Mo <sub>2</sub> NO <sub>4</sub>
<i>D</i> <sub>calc.</sub> / g · cm <sup>-3</sup>	2.213	2.080	2.309	2.316
<i>μ</i> /mm <sup>-1</sup>	8.170	4.958	11.674	10.433
Formula Weight	3437.33	4329.42	3157.42	775.34
Colour	orange	clear orange	orange	orange
Shape	block	plate	plate	plate
Size/mm <sup>3</sup>	0.20×0.15×0.12	0.22×0.12×0.04	0.26×0.15×0.05	0.12×0.06×0.05
<i>T</i> /K	122.97(11)	122.98(14)	123.00(12)	123.00(11)
Crystal System	triclinic	monoclinic	monoclinic	monoclinic
Space Group	<i>P</i> $\bar{1}$	<i>P</i> 2 <sub>1</sub> / <i>n</i>	<i>C</i> 2/ <i>c</i>	<i>I</i> 2/ <i>m</i>
<i>a</i> /Å	15.2567(3)	23.5326(6)	14.6204(4)	8.2869(2)
<i>b</i> /Å	15.8605(3)	18.9404(4)	26.8116(5)	26.2286(6)
<i>c</i> /Å	23.6139(5)	31.4016(8)	23.3084(5)	10.2500(2)
<i>α</i> /°	72.159(2)	90	90	90
<i>β</i> /°	75.865(2)	98.942(2)	96.168(2)	93.660(2)
<i>γ</i> /°	74.451(2)	90	90	90
<i>V</i> /Å <sup>3</sup>	5157.7(2)	13826.1(6)	9083.9(3)	2223.33(9)
<i>Z</i>	2	4	4	4
<i>Z'</i>	1	1	0.5	0.5
Wavelength/Å	1.54184	1.39222	1.39222	1.39222
Radiation type	CuK <sub>α</sub>	CuK <sub>α</sub>	CuK <sub>α</sub>	CuK <sub>α</sub>
<i>Q</i> <sub>min</sub> /°	3.342	1.978	3.123	3.043
<i>Q</i> <sub>max</sub> /°	74.188	61.639	57.000	60.027
Measured Refl.	58028	129209	29745	9499
Independent Refl.	20296	28445	8329	2274
Reflections with <i>I</i> > 2( <i>I</i> )	18284	22099	8089	2230
<i>R</i> <sub>int</sub>	0.0361	0.0505	0.0384	0.0498
Parameters	1939	2601	618	181
Restraints	471	1303	49	36
Largest Peak	1.444	0.706	2.503	1.389
Deepest Hole	-0.908	-0.711	-1.120	-1.052
GooF	1.011	1.029	1.185	1.243
<i>wR</i> <sub>2</sub> (all data)	0.0827	0.0996	0.1868	0.1280
<i>wR</i> <sub>2</sub>	0.0796	0.0899	0.1860	0.1275
<i>R</i> <sub>1</sub> (all data)	0.0384	0.0605	0.0697	0.0487
<i>R</i> <sub>1</sub>	0.0336	0.0420	0.0685	0.0481

**Table S3.** Selected bond lengths and atom-atom distances of 1-7 in Å. Only the major part of compound **6-6** is described.

	6-1 abs268 / abs461a E = P	6-2 abs437a E = P	6-3 abs444b E = P	6-4 JS200 E = As	6-5 JS151 E = As	6-6 JS120 E = As	6-7 JS164 E = As
Cu <sub>peripheral</sub> <sup>-</sup> Cu <sub>peripheral</sub>	2.4344(10)/ 2.4537(19)	3.0013(6)/ 3.0593(6)	2.5645(9)	2.6925(7)	2.6668(10)	2.587(4)	2.470(3)
Cu <sub>peripheral</sub> <sup>-</sup> Cu <sub>peripheral</sub>	4.869(2)- 4.904(2)	5.8238(8)	-	-	-	5.175(9)	-
Cu-E	2.2830(19)- 2.437(2)	2.2446(8)- 2.3909(8)	2.3545(6)/ 2.491(7)	2.4582(6)- 2.5312(6)	2.4465(8)- 2.5689(8)	2.382(4)- 2.714(4)	2.4197(7)/ 2.4488(18)
Cu <sub>central</sub> -E	2.2838(17)- 2.3132(16)	2.3706(8)/ 2.3909(8)	2.491(7)	2.4849(6)- 2.5312(6)	2.4647(8)- 2.5689(8)	2.410(3)/ 2.415(3)	2.4197(7)
Cu <sub>peripheral</sub> <sup>-</sup> E	2.3830(19)- 2.460(3)	2.2446(8)/ 2.2520(8)	2.3545(6)	2.4582(6)/ 2.4850(6)	2.4465(8)/ 2.3604(8)	2.382(4)- 2.714(4)	2.4488(18)
E-E	2.213(3)- 2.238(2)	2.1455(10)	2.1796(11)	2.3901(5)- 2.3905(5)	2.3816(6)/ 2.3849(6)	2.3860(16)- 2.4372(2)	2.4282(14)

### Disorder of compound 6-6

The solid-state molecular structure of **6-6** shows a superposition of four possible species (**6-6a-6-6d**) with different occupancies. For the central copper atom Cu1, an occupancy of 0.8 was determined, while the acetonitrile molecules have an occupancy of 0.59. Hence, the resulting occupancies are 0.39-0.59 for **6-6a**, 0.21-0.41 for **6-6b**, 0-0.20 for **6-6c** and **6-6d**, respectively. As **6-6a** appears to be the species with the highest occupancy, it is considered as the major product in this work.

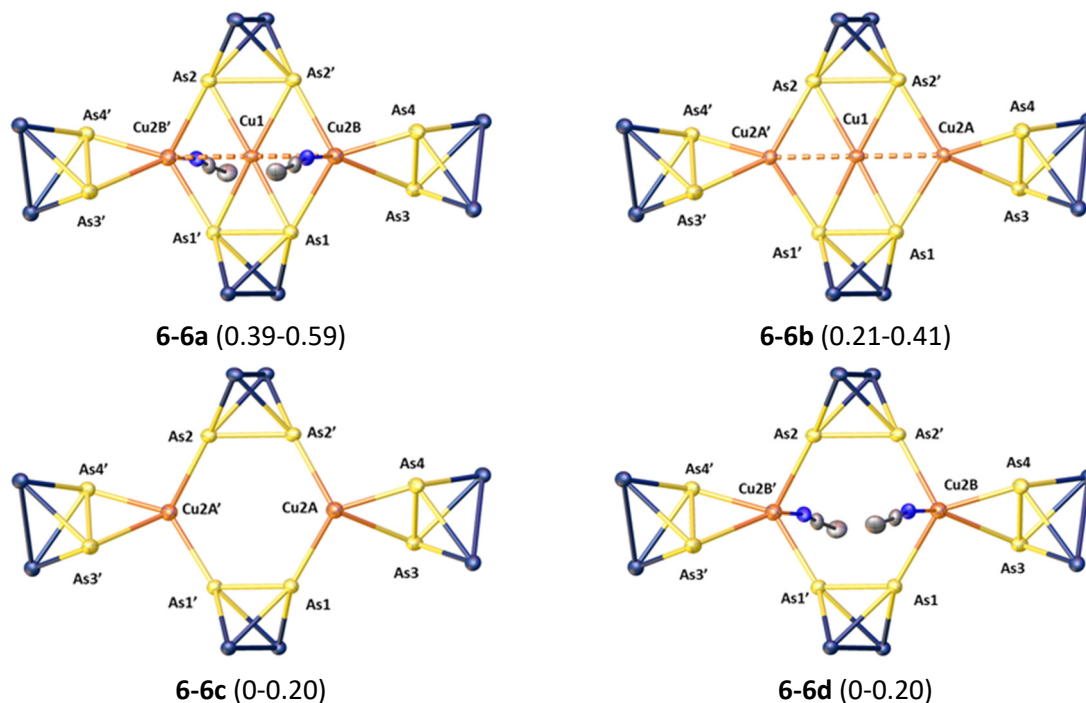


**Figure S1.** Possible occupancies of the compounds **6-6a-6-6d** in brackets. Only the cationic fragments are depicted. Cp-, CO-ligands and hydrogen atoms were omitted for clarity. Thermal ellipsoids are shown at 50 % probability level.

## DFT calculations

All calculations have been performed with the TURBOMOLE program package<sup>[26]</sup> at the RI<sup>[27]</sup>-B3LYP<sup>[28]</sup>/def2-TZVP<sup>[29]</sup> level of theory. The geometries were optimised in the gas phase using the Multipole Accelerated Resolution of Identity (MARI-J)<sup>[30]</sup> approximation during the geometry optimisation steps. The solvent effects were incorporated as single point calculations (without the RI approximation) on the gas phase optimised geometries via the Conductor-like Screening Model (COSMO)<sup>[31]</sup> using the dielectric constant of CH<sub>2</sub>Cl<sub>2</sub> ( $\epsilon = 8.930$ ). For the reaction energies the SCF energies, corrected for the “outlying charge” were used. The energy minimum structure of  $[\{\{\text{CpMo}(\text{CO})_2\}_2(\mu_5, \eta^{2:2:2:1:1}\text{-P}_2)\}_2\{\text{Cu}(\text{CH}_3\text{CN})_2\}_2\text{Cu}]^{3+}$  (**6-1**) have been proven by frequency calculations which shows no imaginary frequencies. The population analysis has been performed on the gas phase optimised geometries.

In order to elucidate the bonding situation in  $[\{\{\text{CpMo}(\text{CO})_2\}_2(\mu_5, \eta^{2:2:2:1:1}\text{-P}_2)\}_2\{\text{Cu}(\text{CH}_3\text{CN})_2\}_2\text{Cu}]^{3+}$  (**6-1**) and  $[\{\{\text{CpMo}(\text{CO})_2\}_2(\mu_5, \eta^{2:2:2:1:1}\text{-P}_2)\}_2\{\text{Cu}(\text{CH}_3\text{CN})_3\}_2\text{Cu}(\text{CH}_3\text{CN})_2]^{3+}$  (**6-2**) DFT calculations at the B3LYP/def2-TZVP level of theory have been performed. The optimised geometry of **6-1** in the gas phase is very similar to the experimental structure determined by single crystal X-ray diffraction, *i.e.* the Cu-Cu distances in the gas phase optimised geometry of 2.559 Å are similar to the experimental values of 2.4344(10) - 2.4537(19) Å. In the case of **3** the Cu-Cu distances are longer in the gas phase optimised geometry (Cu...Cu 3.380 and 3.384 Å) compared to that in the solid-state (Cu...Cu 3.0013(6) and 3.0593(6) Å). This indicates that the chelating effect of a second  $[\{\{\text{CpMo}(\text{CO})_2\}_2(\mu, \eta^{2:2}\text{-P}_2)]$  is responsible for the relatively short Cu-Cu distances in **6-1**. The energy minimum structure of **6-1** have been proven by frequency calculations which shows no imaginary frequencies.

The calculations also show that the bonding of the peripheral Cu ions to the Mo<sub>2</sub>P<sub>2</sub> ligand in **1** takes place via the coordination of the phosphorus lone pairs, while the central Cu ion binds to the P-P sigma orbital of the Mo<sub>2</sub>P<sub>2</sub> unit. This is nicely shown by the Localised Molecular Orbitals (LMOs) (**Figure S2**). A small orbital contribution of the central Cu ion to the LMOs of the P-Cu<sub>peripheral</sub> bonding of roughly 7% has been observed. This is not the case for **6-2**. A comparison of the LMOs of **6-1** with that of  $[\{\{\text{CpMo}(\text{CO})_2\}_2(\mu_4, \eta^{2:2:1:1}\text{-P}_2)\}_2\{\text{Cu}(\text{CH}_3\text{CN})_2\}_2]^{2+}$  (**G**) shows that the bonding of the Mo<sub>2</sub>P<sub>2</sub> Ligand to the peripheral Cu ions is very similar (**Figure S3**). The Wiberg Bond Indexes (WBIs) of the P-P bond in **G** is close to unity (1.06), while in **6-1** and **6-2** the WBIs of the P-P bonds are lower (0.78 in **6-1** and 0.72 in **6-2**) indicating a weaker P-P bond. This is not unexpected if consider that the coordination of the P-P sigma bond to the central Cu ion, which leads to depletion of the electron density in this bonding orbital. The WBIs of the peripheral Cu-P bonds in **6-1** are slightly lower than in **G** and **6-2**, *i.e.* 0.40 – 0.44 in **1** and 0.53 – 0.55 and 0.55 in **G** and **6-2**, respectively. The WBIs of the Cu<sub>central</sub>-P bonds are 0.29 (Cu9-P6, Cu9-P8) and 0.40 (Cu9-P5, Cu9-P7) indicating a slightly asymmetric bonding and a preference for a linear coordination geometry of the central Cu ion (for labeling see **Figure S4**). The calculations indicate that between the three Cu ions an interaction is presence since a WBI of 0.11 has been found.

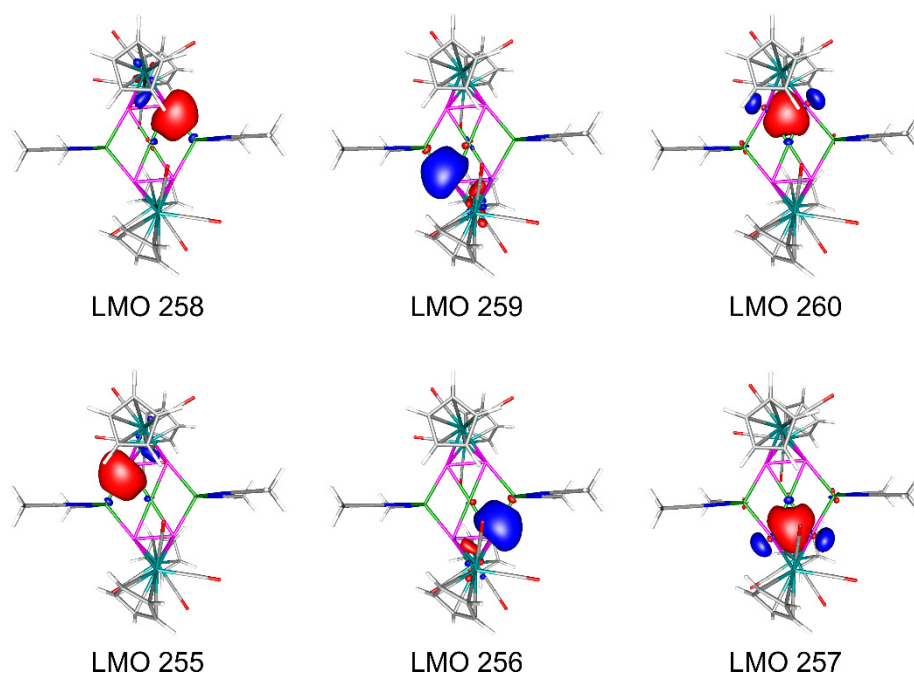


**Figure S2.** Selected Localised Molecular Orbitals (LMOs) representing the Cu-P bonding in  $[\{\{\text{CpMo}(\text{CO})_2\}_2(\mu_5, \eta^{2:2:2:1:1}\text{-P}_2)\}_2\{\text{Cu}(\text{MeCN})_2\}_2\text{Cu}]^{3+}$  (**6-1**). Calculated at the B3LYP/def2-TZVP level of theory.

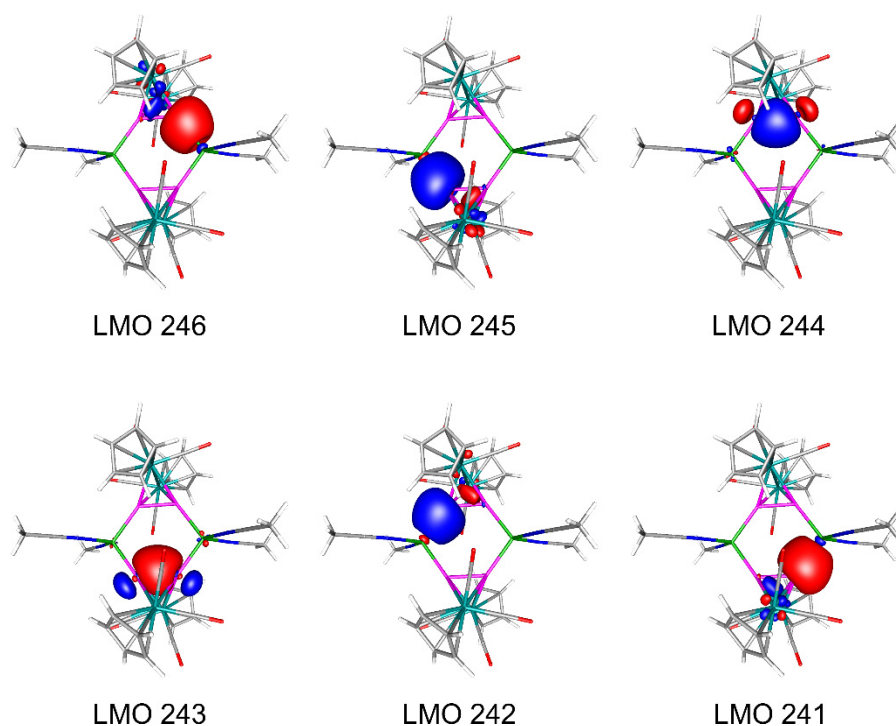


**Figure S3.** Selected Localised Molecular Orbitals (LMOs) representing the Cu-P bonding in  $[\{\{\text{CpMo}(\text{CO})_2\}_2(\mu_4, \eta^{2:2:1:1}\text{-P}_2)\}_2\{\text{Cu}(\text{MeCN})_2\}_2]^{2+}$  (**G**). Calculated at the B3LYP/def2-TZVP level of theory.

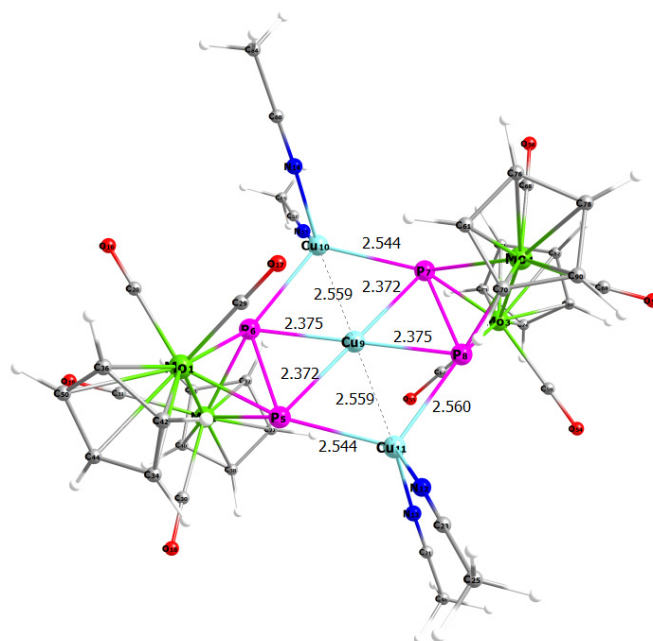


**Figure S4.** Optimised geometry and selected geometric parameters of  $[\{\{\text{CpMo}(\text{CO})_2\}_2(\mu_5, \eta^{2:2:2:1:1}\text{-P}_2)\}_2\{\text{Cu}(\text{MeCN})_2\}_2\text{Cu}]^{3+}$  (**6-1**) at the B3LYP/def2-TZVP level of theory.

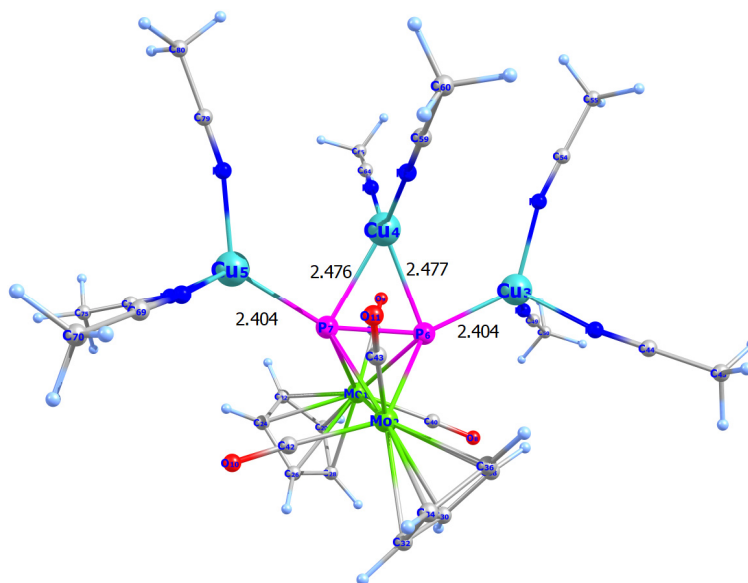
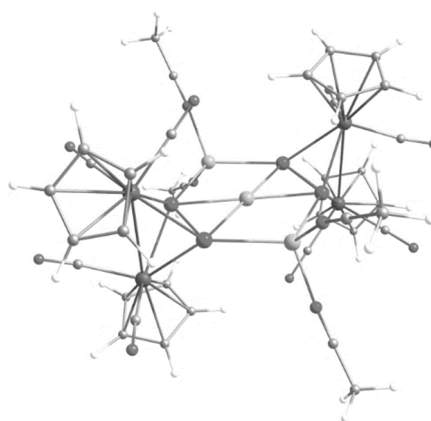


**Figure S5.** Optimised geometry and selected geometric parameters of  $[\{\{\text{CpMo}(\text{CO})_2\}_2(\mu_5, \eta^{2:2:2:1:1}\text{-P}_2)\}\{\text{Cu}(\text{MeCN})_3\}_2\{\text{Cu}(\text{MeCN})_2\}]^{3+}$  (**6-2**) at the B3LYP/def2-TZVP level of theory.



**Table S4.** Cartesian coordinates of the optimised geometry of  $\{[\text{CpMo}(\text{CO})_2]_2(\mu_5, \eta^{2:2:2:1:1}\text{-P}_2)\}_2\{\text{Cu}(\text{MeCN})_2\}_2\text{Cu}^{3+}$  (**6-1**).

Atom	x	y	z
Mo	1.6912025	3.2304868	-1.6450839
Mo	1.9990712	3.1753909	1.5251320
Mo	-1.6911198	-3.2304863	1.6449352
Mo	-1.9989085	-3.1753706	-1.5252966
P	2.0140406	1.2468919	-0.1183611
P	0.1175368	2.3689693	0.1213012
P	-2.0139739	-1.2468899	0.1182200
P	-0.1174381	-2.3689319	-0.1214054
Cu	0.0000291	0.0000106	0.0000022
Cu	-2.2025092	1.2893836	0.1929427
Cu	2.2024820	-1.2894585	-0.1929527
N	3.2031299	-1.9347044	-1.8448166
N	3.2971686	-1.9774515	1.3692341
N	-3.2974532	1.9775323	-1.3689751
N	-3.2030104	1.9346190	1.8449216
O	-0.6164617	5.3932285	-1.5928664
O	-0.1678400	1.4871114	-3.4694739
O	5.0917287	3.0572322	0.9267115
O	1.9237373	6.2091307	0.7100018
C	0.2100544	4.6114691	-1.5714240
C	4.0062542	-2.4590205	2.1333324
C	1.6129283	1.8423368	3.4760805
C	3.9208651	-2.3934233	-2.6156718
H	1.5649104	0.7659719	3.4545258
C	4.8322419	-2.9779966	-3.5815378
H	4.4869410	-2.7744672	-4.5961615
H	5.8295464	-2.5541238	-3.4535909
H	4.8854830	-4.0578123	-3.4336736
C	0.4890097	2.1223548	-2.7809440
C	3.9639736	3.1241706	1.0904378
C	1.9371295	5.0840674	0.9198213
C	0.5098626	2.7294313	3.3502430
H	-0.5205034	2.4413040	3.2235791
C	3.9870577	3.0506915	-2.3027542
H	4.6723524	2.3281781	-1.8916364
C	2.4509201	4.0846951	-3.6751102
H	1.7913214	4.2881416	-4.5031985
C	2.7804130	2.6217382	3.6721140
H	3.7740749	2.2419248	3.8485094
C	2.4038854	3.9968184	3.6635119
H	3.0560648	4.8354060	3.8477096
C	3.1550972	2.8625524	-3.4350418
H	3.1077270	1.9770220	-4.0476985
C	3.8116550	4.3845799	-1.8463924
H	4.3403307	4.8536518	-1.0339160
C	4.9057555	-3.0723545	3.0919656
H	4.5602870	-2.8772018	4.1081012
H	4.9400590	-4.1507364	2.9290735
H	5.9102525	-2.6634553	2.9723663
C	2.8620519	5.0184295	-2.6832318
H	2.5442250	6.0467130	-2.6084615
C	0.9922637	4.0572015	3.4624085
H	0.3943782	4.9543015	3.4506854
O	0.6166455	-5.3931238	1.5928270



O	0.1677627	-1.4869608	3.4693555
O	-5.0915979	-3.0573459	-0.9269733
C	-3.9207591	2.3933049	2.6157848
O	-1.9235447	-6.2091181	-0.7101974
C	-0.2099051	-4.6114004	1.5713445
C	-4.0068335	2.4591301	-2.1327821
C	-1.6128378	-1.8422793	-3.4762501
H	-1.5649676	-0.7659077	-3.4547167
C	-4.8321580	2.9778300	3.5816593
H	-4.4868439	2.7743092	4.5962801
H	-5.8294426	2.5539099	3.4537140
H	-4.8854516	4.0576445	3.4338051
C	-0.4890258	-2.1222695	2.7808258
C	-3.9638361	-3.1242285	-1.0906761
C	-1.9369473	-5.0840523	-0.9200035
C	-0.5096620	-2.7292219	-3.3503163
H	0.5206563	-2.4409565	-3.2235826
C	-3.9870032	-3.0507762	2.3025008
H	-4.6722945	-2.3282831	1.8913453
C	-2.4508998	-4.0847309	3.6749248
H	-1.7913327	-4.2881566	4.5030426
C	-2.7802040	-2.6218406	-3.6723419
H	-3.7739065	-2.2421652	-3.8488061
C	-2.4034951	-3.9968679	-3.6636908
H	-3.0555511	-4.8355437	-3.8479202
C	-3.1551107	-2.8626147	3.4348323
H	-3.1077981	-1.9770841	4.0474935
C	-3.8115290	-4.3846542	1.8461390
H	-4.3401422	-4.8537396	1.0336311
C	-4.9067171	3.0724886	-3.0910390
H	-4.5615856	2.8774753	-4.1073158
H	-4.9410618	4.1508503	-2.9280209
H	-5.9111347	2.6634838	-2.9711350
C	-2.8619446	-5.0184740	2.6830194
H	-2.5440685	-6.0467416	2.6082499
C	-0.9918782	-4.0570616	-3.4624872
H	-0.3938750	-4.9540815	-3.4507110

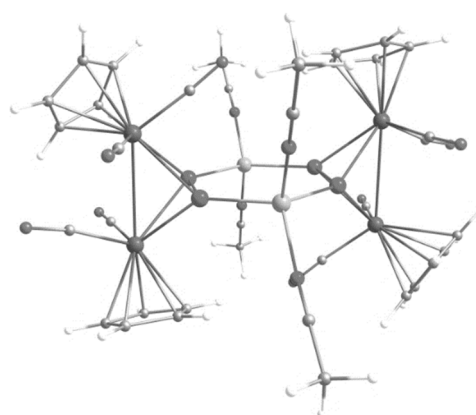
ENERGIES [a.u.]:

Total energy = -8771.0678177315

Total energy + OC corr. = -8771.068050097

**Table S5.** Cartesian coordinates of the optimised geometry of  $\{[\{\text{CpMo}(\text{CO})_2\}_2(\mu_4, \eta^{2:2:1:1}\text{-P}_2)]_2\{\text{Cu}(\text{MeCN})_2\}_2\}^{2+}$  (**G**).

Atom	x	y	z
Mo	1.5636762	3.1668807	-1.6165327
Mo	1.9579801	3.1052378	1.5232183
Mo	-1.5636666	-3.1668293	1.6164772
Mo	-1.9579561	-3.1052715	-1.5232450
P	1.9073930	1.1535960	-0.1299055
P	0.0958917	2.1401870	0.1823365
P	-1.9073760	-1.1535798	0.1298150
P	-0.0958676	-2.1401677	-0.1824039
Cu	-2.1083992	1.2226720	0.2534735
Cu	2.1084037	-1.2226449	-0.2535302
N	3.2021402	-1.8576163	-1.8971982
N	3.2498971	-1.9830596	1.2718297
N	-3.2499522	1.9831285	-1.2718143
N	-3.2020532	1.8575402	1.8972017
O	-0.7461471	5.2966273	-1.3229077
O	-0.4426161	1.5363698	-3.3821857
O	4.9841502	2.4773146	0.9716905
O	2.3288308	6.0567915	0.5634651
C	0.0855754	4.5165659	-1.3875733
C	3.9103554	-2.4517902	2.0846672
C	1.3130961	1.9587824	3.5293399
C	3.9380449	-2.2724902	-2.6750032
H	1.1485648	0.8938865	3.5562723
C	4.8717681	-2.8016244	-3.6526463
H	4.5358610	-2.5596224	-4.6617154
H	5.8603816	-2.3686699	-3.4940698
H	4.9399049	-3.8856517	-3.5517270
C	0.2689951	2.1169995	-2.6937695
C	3.8725375	2.7206188	1.1183011
C	2.1775047	4.9399401	0.8010644
C	0.3222224	2.9533387	3.2924922
H	-0.7243868	2.7687222	3.1181166
C	3.8174540	2.8551443	-2.4057941
H	4.4638392	2.0629474	-2.0672763
C	2.2879367	4.0685026	-3.6333689
H	1.5984820	4.3598306	-4.4086184
C	2.5475306	2.6181898	3.7475446
H	3.4841872	2.1452593	3.9948310
C	2.3270913	4.0211236	3.6346224
H	3.0605351	4.7943078	3.7960514
C	2.9144748	2.7909712	-3.4969968
H	2.7642132	1.9431218	-4.1452510
C	3.7550345	4.1647316	-1.8655296
H	4.3462599	4.5404761	-1.0479848
C	4.7450875	-3.0479269	3.1111154
H	4.3361281	-2.8269346	4.0977569
H	4.7824820	-4.1297320	2.9764332
H	5.7572488	-2.6464141	3.0473373
C	2.8062885	4.9103487	-2.6099315
H	2.5578143	5.9475570	-2.4519301
C	0.9411198	4.2222759	3.3565873
H	0.4502401	5.1760798	3.2506291
O	0.7461838	-5.2965665	1.3229681
O	0.4425859	-1.5362251	3.3820831



O	-4.9841062	-2.4773192	-0.9716678
C	-3.9379298	2.2723811	2.6750495
O	-2.3287831	-6.0568063	-0.5634162
C	-0.0855497	-4.5165111	1.3875810
C	-3.9104806	2.4518472	-2.0846020
C	-1.3131265	-1.9588469	-3.5294004
H	-1.1486218	-0.8939479	-3.5563648
C	-4.8716200	2.8014665	3.6527426
H	-4.5356620	2.5594394	4.6617874
H	-5.8602303	2.3684954	3.4941962
H	-4.9397811	3.8854954	3.5518592
C	-0.2690166	-2.1168923	2.6936901
C	-3.8724986	-2.7206360	-1.1183021
C	-2.1774591	-4.9399596	-0.8010407
C	-0.3222230	-2.9533705	-3.2925424
H	0.7243845	-2.7687227	-3.1181901
C	-3.8174433	-2.8550475	2.4057290
H	-4.4638171	-2.0628486	2.0671970
C	-2.2879497	-4.0684019	3.6333269
H	-1.5984997	-4.3597230	4.4085830
C	-2.5475426	-2.6182970	-3.7475766
H	-3.4842154	-2.1454029	-3.9948717
C	-2.3270669	-4.0212218	-3.6346163
H	-3.0604936	-4.7944305	-3.7960086
C	-2.9144676	-2.7908665	3.4969337
H	-2.7641982	-1.9430113	4.1451758
C	-3.7550429	-4.1646454	1.8654843
H	-4.3462762	-4.5403997	1.0479536
C	-4.7452972	3.0479573	-3.1109918
H	-4.3363972	2.8269731	-4.0976596
H	-4.7827109	4.1297620	-2.9763075
H	-5.7574413	2.6464135	-3.0471427
C	-2.8063057	-4.9102603	2.6099036
H	-2.5578362	-5.9474710	2.4519163
C	-0.9410868	-4.2223269	-3.3565996
H	-0.4501788	-5.1761140	-3.2506200

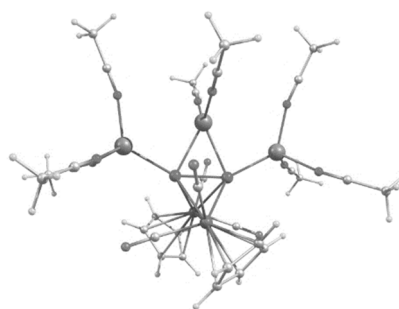
ENERGIES [a.u.]:

Total energy = -7130.7434091722

Total energy + OC corr. = -7130.7381750726

**Table S6.** Cartesian coordinates of the optimised geometry of  $[[\{\text{CpMo}(\text{CO})_2\}_2(\mu_5, \eta^{2:2:2:1:1}\text{-P}_2)]\{\text{Cu}(\text{MeCN})_3\}_2\text{Cu}(\text{MeCN})_2]^{3+}$  (**6-2**).

Atom	x	y	z
Mo	-1.4764508	-0.2411396	2.2242238
Mo	1.5859373	0.3398631	2.1283441
Cu	0.5357696	-3.1609302	-0.5573098
Cu	-0.0546305	-0.0354771	-1.7126697
Cu	-0.5675516	3.1373673	-0.6679758
P	0.2859753	-1.0313115	0.5297532
P	-0.2664491	1.0573640	0.4990335
O	-0.7712909	-3.1364112	3.2472733
O	-3.3745933	-1.5215576	0.0825565
O	0.9361374	3.2804819	3.0552226
O	3.3625655	1.5183828	-0.1703459
N	2.2573691	-4.1077019	0.1313365
N	-0.9673046	-4.4177119	0.0603291
N	0.6634930	-3.4792297	-2.5766409
N	1.5849703	0.2477298	-2.8167359
N	-1.7610229	-0.3698998	-2.6959545
N	0.9932545	4.3946439	-0.2190323
N	-2.2218444	4.1425348	0.0995445
N	-0.8424115	3.3628348	-2.6844520
C	-3.4003863	-0.1147126	3.5390969
H	-4.1517834	-0.8874330	3.5406526
C	-3.3798451	1.0416245	2.7013857
H	-4.1062132	1.2847179	1.9431153
C	-2.2755629	1.8423754	3.0871317
H	-2.0066602	2.7946501	2.6620126
C	-1.6167154	1.1963373	4.1682370
H	-0.7758360	1.5812099	4.7191988
C	-2.3047089	-0.0108630	4.4406324
H	-2.0725511	-0.7072175	5.2308782
C	1.8323513	-1.0097031	4.1240694
H	1.0232325	-1.3677336	4.7371305
C	2.5339941	0.2068563	4.3042501
H	2.3453035	0.9384394	5.0740274
C	3.5787146	0.2681147	3.3405343
H	4.3284669	1.0388822	3.2662879
C	3.5126854	-0.9244323	2.5577320
H	4.1962190	-1.2026163	1.7722751
C	2.4312727	-1.7047699	3.0384909
H	2.1403162	-2.6746529	2.6719053
C	-0.9929313	-2.0876538	2.8479119
C	-2.6431024	-1.0668105	0.8369939
C	1.1364659	2.2140814	2.6931802
C	2.6742313	1.0998295	0.6434183
C	3.1014519	-4.8430872	0.3891135
C	4.1630605	-5.7786260	0.7132724
H	4.0230217	-6.7048364	0.1538839
H	4.1482603	-6.0056496	1.7802235
H	5.1323703	-5.3512476	0.4531951



C	-1.6936642	-5.2433166	0.3897430
C	-2.6061500	-6.2910282	0.8082460
H	-3.3082971	-6.5179664	0.0049503
H	-3.1635979	-5.9702062	1.6891246
H	-2.0453483	-7.1938620	1.0544221
C	0.7555711	-3.9374140	-3.6253772
C	0.8730164	-4.5310175	-4.9448730
H	1.8699007	-4.9547490	-5.0747125
H	0.7051886	-3.7766828	-5.7144927
H	0.1352107	-5.3263219	-5.0608094
C	2.5636797	0.4551461	-3.3788906
C	3.8058004	0.7223676	-4.0782235
H	3.6040292	1.2363183	-5.0189633
H	4.3228553	-0.2142475	-4.2912159
H	4.4485672	1.3491813	-3.4584009
C	-2.7747529	-0.6045561	-3.1799138
C	-4.0607101	-0.9060665	-3.7787612
H	-3.9223923	-1.4761909	-4.6983574
H	-4.5893892	0.0189624	-4.0127896
H	-4.6617571	-1.4913578	-3.0813077
C	1.7565063	5.2179778	0.0202725
C	2.7162374	6.2624289	0.3259698
H	2.5455974	7.1246369	-0.3202861
H	3.7311783	5.8958400	0.1671210
H	2.6076961	6.5724308	1.3662829
C	-3.0343808	4.9040300	0.3817460
C	-4.0559785	5.8727694	0.7354490
H	-4.8241274	5.9039099	-0.0384878
H	-3.6089631	6.8633526	0.8317015
H	-4.5194586	5.6009521	1.6847895
C	-1.0086860	3.7706895	-3.7447588
C	-1.2193756	4.3008090	-5.0796070
H	-2.2174615	4.7349241	-5.1541237
H	-1.1215932	3.5068204	-5.8208900
H	-0.4819956	5.0765312	-5.2913130

ENERGIES [a.u.]:

Total energy = -7130.7434091722

Total energy + OC corr. = -7130.7381750726

## Additional Compounds

During the studies on this work, additional experiments were performed. The additional compounds obtained during these studies will be discussed in the following.

### $[\{\{\text{CpMo}(\text{CO})_2\}_2(\mu_4, \eta^{2:2:2:1}\text{-E}_2)\}_2\{\text{Cu}(\text{CH}_3\text{CN})_2\}\text{Cu}(\text{CH}_3\text{CN})][\text{TEF}]_2$ (E = 56% P, 44% As) (6-8)

The P<sub>2</sub> ligand complex **A** was reacted with [Cu(CH<sub>3</sub>CN)<sub>4</sub>][TEF] (**C**, TEF = Al{OC(CF<sub>3</sub>)<sub>3</sub>}<sub>4</sub>) and the As<sub>2</sub> ligand complex **B** in one reaction in order to synthesise a mixed coordination compound. Single crystal X-ray analysis revealed the formation of a Cu<sub>2</sub>E<sub>4</sub><sup>2+</sup> unit (**Figure S6**) with the formula  $[\{\{\text{CpMo}(\text{CO})_2\}_2(\mu_4, \eta^{2:2:2:1}\text{-E}^1_2)\}\{\{\text{CpMo}(\text{CO})_2\}_2(\mu_4, \eta^{2:2:2:1}\text{-E}^2_2)\}\{\text{Cu}(\text{CH}_3\text{CN})_2\}\text{Cu}(\text{CH}_3\text{CN})][\text{TEF}]_2$  (E<sup>1</sup> = 50 % P, 50 % As; E<sup>2</sup> = 62% As, 38 % P) (**6-8**).

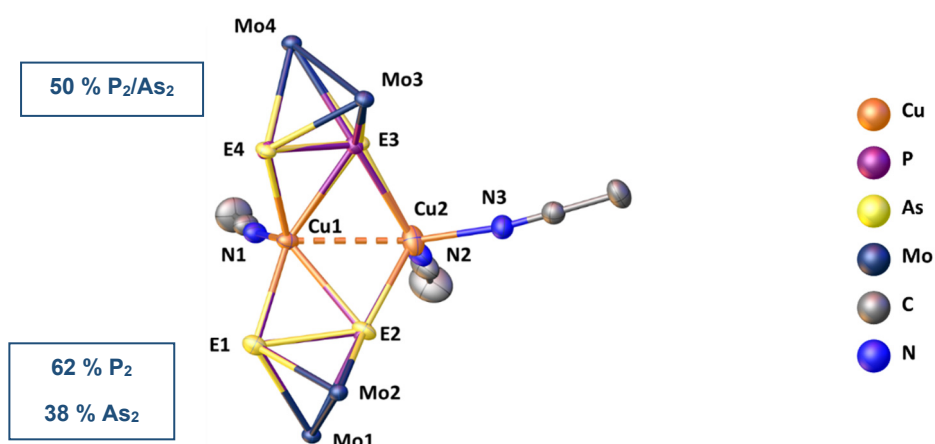


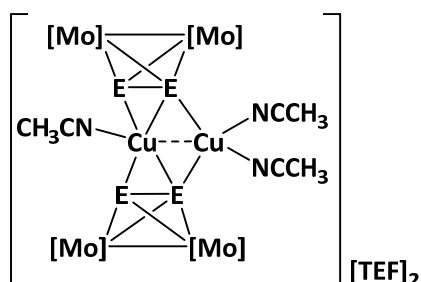
**Figure S6.** Molecular structure of the cationic fragment of **6-8** in the solid-state. Cp- and CO- ligands and hydrogen atoms are omitted for clarity. Thermal ellipsoids are shown at 50 % probability level. Average of selected bond lengths [Å] and angles [°]: Cu1 Cu2 2.6494(7), Cu1-N1 1.994(3), Cu2 N3 1.982(3), Cu2-N2 1.988(3), N1-Cu1-Cu2 97.79(9), N3-Cu2-Cu1 146.96(9), N2 Cu2 Cu1 105.77(9), N3 Cu2 N2 107.0(1).

Crystals of compound **6-8** were obtained as clear orange blocks in 97% yield (referred to **A**) by diffusion of *n*-pentane into the crude reaction mixture. **6-8** crystallised in the triclinic space group  $P\bar{1}$ . Single crystal X-ray analysis (**Figure S6**) showed that **6-8** is isostructural to compounds **6-4** and **6-5**. The E<sub>2</sub> position have an As<sub>2</sub>:P<sub>2</sub> ratio of 50:50 and 62:38, respectively. The stoichiometry of P<sub>2</sub>:As<sub>2</sub> in the compound therefore is approximately 1.12 : 0.88. Compound **6-8** could be also be characterised by NMR spectroscopy and mass spectrometry, IR spectroscopy and elemental analysis. In the <sup>1</sup>H NMR (400 MHz, CD<sub>3</sub>CN, r.t.) of **8**, the signals for the P<sub>2</sub> and As<sub>2</sub> ligand complexes can be observed. The signal in the <sup>31</sup>P NMR is observed at -47.5 ppm. In the <sup>13</sup>C{<sup>1</sup>H} NMR, signals for the CO and Cp ligand of P<sub>2</sub> and As<sub>2</sub> are observed. In the positive ESI mass spectrum, the signals for [Cu(CH<sub>3</sub>CN){Cp<sub>2</sub>Mo<sub>2</sub>(CO)<sub>4</sub>P<sub>2</sub>}]<sup>+</sup>, [Cu{Cp<sub>2</sub>Mo<sub>2</sub>(CO)<sub>4</sub>P<sub>2</sub>}]<sup>+</sup>, [Cu(CH<sub>3</sub>CN){Cp<sub>2</sub>Mo<sub>2</sub>(CO)<sub>4</sub>As<sub>2</sub>}]<sup>+</sup>, [Cu{Cp<sub>2</sub>Mo<sub>2</sub>(CO)<sub>4</sub>P<sub>2</sub>}]{Cp<sub>2</sub>Mo<sub>2</sub>(CO)<sub>4</sub>As<sub>2</sub>}]<sup>+</sup> and [Cu{Cp<sub>2</sub>Mo<sub>2</sub>(CO)<sub>4</sub>As<sub>2</sub>}]<sup>+</sup> are detected. Compound **6-8** is well soluble in acetonitrile, moderately soluble in dichloromethane and insoluble in other common solvents.

**Table S7.** Comparison of selected bond length [Å] and angles [°] of compound **6-8**.

	E = P	E = As
E1-E2	2.17(2), 2.258(8)	2.314(7), 2.38(1)
Cu1-E	2.402(6) - 2.489(5)	2.422(5) - 2.531(8)
Cu2-E2	2.373(7)	2.344(5)
Cu2-E3	2.469(19)	2.409(8)
E-Mo	2.474(6) - 2.608(10)	2.491(5) - 2.633(5)
E1-Cu1-Cu2, E4-Cu1-Cu2	109.7(1), 107.1(3)	110.2(1), 107.8(1)
E2-Cu1-Cu2, E3-Cu1-Cu2	54.9(2), 57.8(4)	54.2(1), 55.4(2)
E1-Cu1-E2, E3-Cu1-E4	55.0(2), 53.2(5)	56.2(2), 57.1(2)
E1-Cu1-E3	150.6(4)	152.0(2)
E1-Cu1-E4	118.4(3)	117.1(2)
E2-Cu1-E3	105.2(4)	103.3(2)
E2-Cu1-E4	128.0(2)	127.4(2)
N1-Cu1-E	101.9(4) - 115.5(2)	99.89(2) - 115.9(1)
Cu1-Cu2-E2, Cu1-Cu2-E3	59.1(1), 57.0(5)	59.4(1), 59.8(2)
E2-Cu2-E3	108.2(5)	111.9(2)
N-Cu2-E	103.5(4) - 117.0(4)	102.1(2) - 114.6(2)

Synthesis of  $[\{\{\text{CpMo}(\text{CO})_2\}_2(\mu_4, \eta^{2:2:2:1}\text{-E}^1_2)\}\{\{\text{CpMo}(\text{CO})_2\}_2(\mu_4, \eta^{2:2:2:1}\text{-E}^2_2)\}\{\text{Cu}(\text{CH}_3\text{CN})_2\}\text{Cu}(\text{CH}_3\text{CN})][\text{TEF}]_2$  ( $\text{E}^1 = 50\% \text{P}$ ,  $50\% \text{As}$ ;  $\text{E}^2 = 62\% \text{As}$ ,  $38\% \text{P}$ ) (**6-8**):



The P<sub>2</sub> ligand complex **A** (1 eq., 25 mg, 0.05 mmol), the As<sub>2</sub> ligand complex **C** (1.5 eq., 148.8 mg, 0.1 mmol) and the Cu<sup>I</sup> salt **B** (1 eq., 29.4 mg, 0.05 mmol) were each dissolved in dichloromethane (4 mL). The solution of **C** was slowly added to the solution of **A** and the mixture stirred for half an hour. The solution of **C** was slowly added and the reaction stirred for 3 h. The crude reaction mixture was filtered and layered with *n*-pentane. After one day, crystals of compound **8** were obtained as clear orange blocks. The supernatant was decanted off, the remaining crystals washed with *n*-pentane and dried in vacuo. Crystalline Yield: 72 mg (97%, related to **A**). <sup>1</sup>H NMR δ[ppm] = 5.32 (s, C<sub>5</sub>H<sub>5</sub>, P<sub>2</sub>), 5.26 (s, C<sub>5</sub>H<sub>5</sub>,

**As<sub>2</sub>**). <sup>31</sup>P-NMR δ[ppm] = -47.5 (s). <sup>13</sup>C{<sup>1</sup>H} NMR δ[ppm] = 226.6 (s, CO), 87.5 (s, C<sub>5</sub>H<sub>5</sub>, P<sub>2</sub>), 85.9 (s, C<sub>5</sub>H<sub>5</sub>, **As<sub>2</sub>**). <sup>19</sup>F-NMR δ[ppm] = -74.8 (s). Positive ion ESI-MS (CH<sub>3</sub>CN, RT): *m/z* (%) = 599.77 (100) [Cu(CH<sub>3</sub>CN){Cp<sub>2</sub>Mo<sub>2</sub>(CO)<sub>4</sub>P<sub>2</sub>}<sup>+</sup>, 1056.56 (60) [Cu{Cp<sub>2</sub>Mo<sub>2</sub>(CO)<sub>4</sub>P<sub>2</sub>}<sub>2</sub>]<sup>+</sup>, 689.67 (100) [Cu(CH<sub>3</sub>CN){Cp<sub>2</sub>Mo<sub>2</sub>(CO)<sub>4</sub>As<sub>2</sub>}]<sup>+</sup>, 1144.46 (64) [Cu{Cp<sub>2</sub>Mo<sub>2</sub>(CO)<sub>4</sub>P<sub>2</sub>}{Cp<sub>2</sub>Mo<sub>2</sub>(CO)<sub>4</sub>As<sub>2</sub>}]<sup>+</sup>, 1231.35 (58) [Cu{Cp<sub>2</sub>Mo<sub>2</sub>(CO)<sub>4</sub>As<sub>2</sub>}]<sup>+</sup>. Negative ion ESI-MS (CH<sub>3</sub>CN, RT): *m/z* (%) = 966.9 (100) [Al(OC(CF<sub>3</sub>)<sub>3</sub>)<sub>4</sub>]<sup>-</sup>. IR (solid, CO bands):  $\tilde{\nu}$ /cm<sup>-1</sup>: 2015 (vs), 1991 (s), 1980 (s), 1967 (vs), 1954 (vs), 1941 (s), 1933 (s), 1918 (vs). Elemental analysis calculated for C<sub>66</sub>H<sub>29</sub>Al<sub>2</sub>As<sub>1.8</sub>Cu<sub>2</sub>F<sub>72</sub>Mo<sub>4</sub>N<sub>3</sub>O<sub>16</sub>P<sub>2.2</sub> (3255,6 g·mol<sup>-1</sup>): 24.3 %C, 0.90 %H, 1.29 %N; Found: 24.53 %C, 0.79 %H, 1.26 %N.

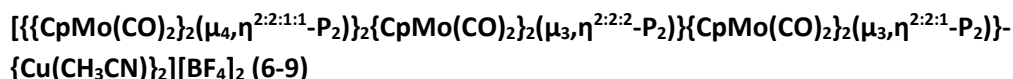
## Crystallographic Details

**Crystal Structure Analysis:** The crystal was selected and measured on a Gemini Ultra diffractometer equipped with an AtlasS2 CCD detector. The crystal was kept at *T* = 123(1) K during data collection. Data collection and reduction was performed with **CrysAlisPro** [Version 171.40.14a, 2018].<sup>[21]</sup> An analytical numeric absorption correction using a multifaceted crystal model based on expressions derived by R.C. Clark & J.S. Reid<sup>[22]</sup> and an empirical absorption correction using spherical harmonics as implemented in SCALE3 ABSPACK was applied. Using **Olex2**,<sup>[23]</sup> the structure was solved with **ShelXT**<sup>[24]</sup> and a least-square refinement on *F*<sup>2</sup> was carried out with **ShelXL**.<sup>[25]</sup> All non-hydrogen atoms were refined anisotropically. Hydrogen atoms at the carbon atoms were located in idealised positions and refined isotropically according to the riding model.

Compound **6-8**: The asymmetric unit contains a CH<sub>2</sub>Cl<sub>2</sub> solvent molecule, two [Al{OC(CF<sub>3</sub>)<sub>3</sub>}<sub>4</sub>]<sup>-</sup> anions and the cationic complex [{CpMo(CO)<sub>2</sub>}<sub>2</sub>(μ<sub>4</sub>,η<sup>2:2:2:1</sup>-E<sub>2</sub>)<sub>2</sub>{Cu(CH<sub>3</sub>CN)<sub>2</sub>}<sub>2</sub>Cu(CH<sub>3</sub>CN)] (E = P, As). In this cationic complex, the complex fragments **A** and **B** superpose each other in a ratio of 50:50 and 62:38, respectively. Further, one of the two [Al{OC(CF<sub>3</sub>)<sub>3</sub>}<sub>4</sub>]<sup>-</sup> anions shows a disorder of two OC(CF<sub>3</sub>)<sub>3</sub> groups in the ratio 86:14. The second [Al{OC(CF<sub>3</sub>)<sub>3</sub>}<sub>4</sub>]<sup>-</sup> anion shows a disorder of three of the four OC(CF<sub>3</sub>)<sub>3</sub> groups over two (56:44; 64:36) and three (40:30:30) positions respectively. To describe these disorders the restrains SADI, ISOR, SIMU and RIGU were applied.

**Table S8.** Crystallographic data and details of diffraction experiments for compound **6-8**.

Compound	6-8 · CH <sub>2</sub> Cl <sub>2</sub>
Data set (internal naming)	abs445
Formula	C <sub>67</sub> H <sub>31</sub> Al <sub>2</sub> As <sub>1.76</sub> Cl <sub>2</sub> Cu <sub>2</sub> F <sub>72</sub> Mo <sub>4</sub> N <sub>3</sub> O <sub>16</sub> P <sub>2.24</sub>
<i>D</i> <sub>calc.</sub> / g · cm <sup>-3</sup>	2.152
μ/mm <sup>-1</sup>	7.707
Formula Weight	3338.88
Colour	clear orange
Shape	block
Size/mm <sup>3</sup>	0.39×0.31×0.22
<i>T</i> /K	123(1)
Crystal System	triclinic
Space Group	<i>P</i> $\bar{1}$
<i>a</i> /Å	15.1935(3)
<i>b</i> /Å	15.8577(3)
<i>c</i> /Å	23.6045(5)
α/°	72.586(2)
β/°	76.091(2)
γ/°	74.721(2)
<i>V</i> /Å <sup>3</sup>	5153.4(2)
<i>Z</i>	2
<i>Z</i> '	1
Wavelength/Å	1.54184
Radiation type	CuK <sub>α</sub>
<i>Q</i> <sub>min</sub> /°	3.653
<i>Q</i> <sub>max</sub> /°	73.264
Measured Refl.	57168
Independent Refl.	20098
Reflections with <i>I</i> > 2( <i>I</i> )	19381
<i>R</i> <sub>int</sub>	0.0293
Parameters	2299
Restraints	1599
Largest Peak	0.923
Deepest Hole	-0.753
GooF	1.056
<i>wR</i> <sub>2</sub> (all data)	0.0854
<i>wR</i> <sub>2</sub>	0.0844
<i>R</i> <sub>1</sub> (all data)	0.0354
<i>R</i> <sub>1</sub>	0.0341



Compound **6-9** was obtained by the reaction of **A** with the Cu<sup>I</sup> salt [Cu(CH<sub>3</sub>CN)<sub>4</sub>][BF<sub>4</sub>] (**D**) and characterised by single crystal X-ray crystallography (**Figure S7**). The reaction was performed in CH<sub>2</sub>Cl<sub>2</sub> using a 1:1 stoichiometry. The storage of the reaction mixture at -30°C resulted in crystals of **6-9**, which crystallise as clear intense red blocks in the triclinic space group  $P\bar{1}$ . Single crystal X-ray analysis revealed the presence of two units of **A**, which are coordinated in a  $\eta^{2:2:1:1}$ -coordination mode to two Cu atoms, resulting in a Cu<sub>2</sub>P<sub>4</sub> dimer. Two additional complexes **A** coordinated to the Cu<sup>I</sup> centers in a  $\eta^{2:2:1}$  and  $\eta^{2:2:1}$  coordination mode, respectively. Additionally, each Cu<sup>I</sup> center is coordinated by one acetonitrile ligand.

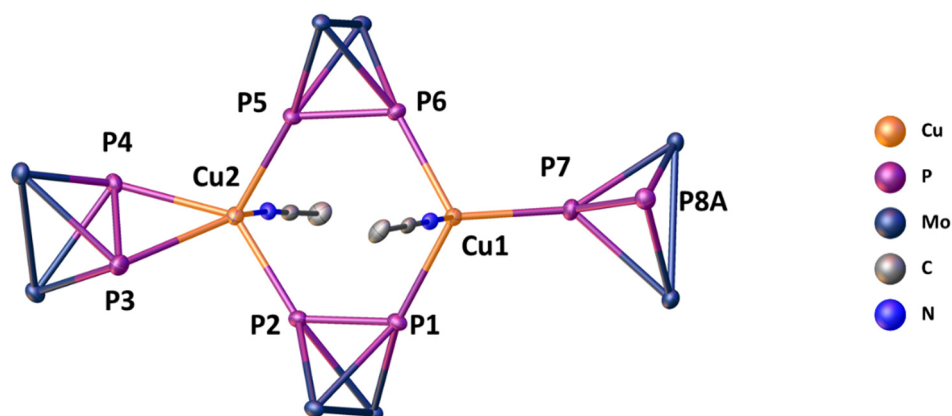
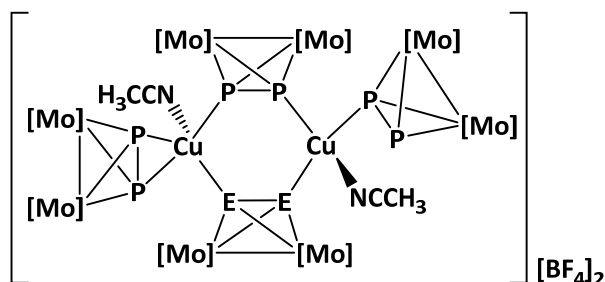


**Figure S7.** Molecular structure of the cation of compound **6-9** in the solid-state. Cp- and CO-ligands, the hydrogen atoms and the minor parts of the disorder are omitted for clarity. Thermal ellipsoids are shown at 50 % probability level. Average of selected bond lengths [Å] and angles [°]: Cu1-P1 2.3339(5), Cu1-P6 2.3267(5), Cu1-P7 2.2844(5), Cu1-N2 2.017(2), Cu2-P2 2.3357(6), Cu2-P3 2.6306(7), Cu2-P4 2.4184(8), Cu2-P5 2.3214(6), Cu2-N1 2.080(2), P6-Cu1-P1 114.76(2), P7-Cu1-P1 116.61(2), P7-Cu1-P6 110.99(2), N2-Cu1-P1 98.33(5), N2-Cu1-P6 100.97(5), N2-Cu1-P7 113.44(5), P2-Cu2-P3 92.49(2), P2-Cu2-P4 137.19(2), P4-Cu2-P3 49.55(2), P5-Cu2-P2 109.32(2), P5-Cu2-P3 121.59(3), P5-Cu2-P4 108.06(2), N1-Cu2-P2 96.32(5), N1-Cu2-P3 131.54(5), N1-Cu2-P4 97.07(5), N1-Cu2-P5 99.97(5).

The <sup>1</sup>H NMR spectra (400 MHz, CD<sub>3</sub>CN, r.t.) of **6-9** reveals signals for the Cp ligand and free acetonitrile. In the <sup>31</sup>P NMR spectra, a chemical shift of -49.1 ppm (s) was observed. In the <sup>13</sup>C{<sup>1</sup>H} NMR, the signals referring to the CO- and Cp-ligands are observed. In the positive ion ESI mass spectrum, signals for [Cu(CH<sub>3</sub>CN)<sub>2</sub>]<sup>+</sup>, [Cu(CH<sub>3</sub>CN){Cp<sub>2</sub>Mo<sub>2</sub>(CO)<sub>4</sub>P<sub>2</sub>}]<sup>+</sup> and [Cu{Cp<sub>2</sub>Mo<sub>2</sub>(CO)<sub>4</sub>P<sub>2</sub>}]<sup>+</sup> were detected.



Synthesis of  $[\{\{\text{CpMo}(\text{CO})_2\}_2(\mu_4, \eta^{2:2:1:1}\text{-P}_2)\}_2\{\text{CpMo}(\text{CO})_2\}_2(\mu_3, \eta^{2:2:2}\text{-P}_2)\}\{\text{CpMo}(\text{CO})_2\}_2(\mu_3, \eta^{2:2:1}\text{-P}_2)\}\text{-}\{\text{Cu}(\text{CH}_3\text{CN})\}_2][\text{BF}_4]_2$  (**6-9**):



A solution of **A** (35 mg, 0.07 mmol) in  $\text{CH}_2\text{Cl}_2$  (5 mL) was added dropwise to a solution of **D** (22 mg, 0.07 mmol) in  $\text{CH}_2\text{Cl}_2$  (5 mL). The clear reaction mixture was stirred for 3h, filtered and stored at  $-30\text{ }^\circ\text{C}$ . After one day, compound **9** was obtained as clear orange plates. The supernatant was decanted off, the remaining crystals washed with *n*-pentane and dried in vacuo. Crystalline Yield: 23 mg (28 %, related to **P**<sub>2</sub>). <sup>1</sup>H NMR (400 MHz,  $\text{CD}_3\text{CN}$ ):  $\delta$  = 5.30 (s, 10H,  $\text{C}_5\text{H}_5$ ), 2.11 (s,  $\text{CH}_3\text{CN}$ ). <sup>31</sup>P NMR (400 MHz,  $\text{CD}_3\text{CN}$ ):  $\delta$  = -49.10 (s). <sup>13</sup>C NMR (400 MHz,  $\text{CD}_3\text{CN}$ ):  $\delta$  = 226.5 (s, CO), 87.5 (s,  $\text{C}_5\text{H}_5$ ). <sup>19</sup>F NMR (400 MHz,  $\text{CD}_3\text{CN}$ ):  $\delta$  = -150.7 (s). <sup>11</sup>B NMR (400 MHz,  $\text{CD}_3\text{CN}$ ):  $\delta$  = 0.57 (s). Positive ion ESI-MS ( $\text{CH}_3\text{CN}$ , RT):  $m/z$  (%) = 144.98 (100)  $[\text{Cu}(\text{CH}_3\text{CN})_2]^+$ , 599.77 (100)  $[\text{Cu}(\text{CH}_3\text{CN})\{\text{Cp}_2\text{Mo}_2(\text{CO})_4\text{P}_2\}]^+$ , 1056.56 (60)  $[\text{Cu}\{\text{Cp}_2\text{Mo}_2(\text{CO})_4\text{P}_2\}_2]^+$ . Negative ion ESI-MS ( $\text{CH}_3\text{CN}$ , RT):  $m/z$  (%) = 87.00 (100)  $[\text{BF}_4]^-$ . IR (solid, CO bands):  $\tilde{\nu}/\text{cm}^{-1}$ : 1972 (s), 1932 (s), 1912 (s). Elemental analysis, calc. for  $\text{B}_2\text{C}_{62}\text{Cl}_4\text{Cu}_2\text{F}_8\text{H}_{50}\text{Mo}_8\text{N}_2\text{O}_{16}\text{P}_8$  (= **6-9** · 2  $\text{CH}_2\text{Cl}_2$ ) (2549,09 g/mol) (%): C, 29.35; H, 1.99; N 1.10; found: C, 29.13; H, 1.98; N, 1.04.

### Crystallographic Details

**Crystal Structure Analysis:** The crystal was selected and measured on a Gemini Ultra diffractometer equipped with an AtlasS2 CCD detector. The crystal was kept at  $T = 123(1)$  K during data collection. Data collection and reduction were performed with **CrysAlisPro** [Version 171.39.37b, 2017].<sup>[21]</sup> An analytical numeric absorption correction using a multifaceted crystal model based on expressions derived by R.C. Clark & J.S. Reid<sup>[22]</sup> and an empirical absorption correction using spherical harmonics as implemented in SCALE3 ABSPACK was applied. Using **Olex2**,<sup>[23]</sup> the structure was solved with **ShelXT**<sup>[24]</sup> and a least-square refinement on  $F^2$  was carried out with **ShelXL**<sup>[25]</sup>. All non-hydrogen atoms were refined anisotropically. Hydrogen atoms at the carbon atoms were located in idealised positions and refined isotropically according to the riding model.

Compound **6-9**: The asymmetric unit contains two  $\text{CH}_2\text{Cl}_2$  and two  $\text{CH}_3\text{CN}$  solvent molecules, which are heavily disordered. Therefore, a solvent mask was calculated and 268 electrons were found in a volume of  $774\text{ \AA}^3$  in two voids per unit cell. This is consistent with the presence of two  $\text{CH}_2\text{Cl}_2$  and two  $\text{CH}_3\text{CN}$  solvent molecules per asymmetric unit, which account for 256 electrons per unit cell. The asymmetric unit further contains the cationic complex  $[\{\{\text{CpMo}(\text{CO})_2\}_2(\mu_4, \eta^{2:2:1:1}\text{-P}_2)\}_2\{\text{CpMo}(\text{CO})_2\}_2(\mu_3, \eta^{2:2:2}\text{-P}_2)\}\{\text{CpMo}(\text{CO})_2\}_2(\mu_3, \eta^{2:2:1}\text{-P}_2)\}\text{-}\{\text{Cu}(\text{CH}_3\text{CN})\}_2]^{2+}$  and two  $\text{BF}_4$  anions. One of the two  $\text{BF}_4$  anions is disordered over three positions (39:36:25), a Cu atom is disordered over two positions (96:4) and further both of the terminal complexes **A** are disordered over two positions (96:4; 93:7). To model this disorders the restraints DFIX, SADI, FLAT, ISOR, SIMU and RIGU were applied.

**Table S9.** Crystallographic data and details of diffraction experiments for compound **6-9**.

<b>Compound</b>	<b>6-9 · 2 CH<sub>2</sub>Cl<sub>2</sub> · 2 CH<sub>3</sub>CN</b>
Data set (internal naming)	abs444b_2
Formula	B <sub>2</sub> C <sub>66</sub> Cl <sub>4</sub> Cu <sub>2</sub> F <sub>8</sub> H <sub>56</sub> Mo <sub>8</sub> N <sub>4</sub> O <sub>16</sub> P <sub>8</sub>
<i>D</i> <sub>calc.</sub> / g · cm <sup>-3</sup>	2.247
μ/mm <sup>-1</sup>	2.066
Formula Weight	2952.99
Colour	clear intense red
Shape	block
Size/mm <sup>3</sup>	0.38×0.31×0.28
<i>T</i> /K	123.15
Crystal System	triclinic
Space Group	<i>P</i> $\bar{1}$
<i>a</i> /Å	14.5777(3)
<i>b</i> /Å	14.8078(3)
<i>c</i> /Å	23.6001(4)
α/°	100.584(2)
β/°	93.8500(10)
γ/°	117.715(2)
<i>V</i> /Å <sup>3</sup>	4364.53(16)
<i>Z</i>	2
<i>Z</i> '	1
Wavelength/Å	0.71073
Radiation type	MoK <sub>α</sub>
<i>Q</i> <sub>min</sub> /°	3.348
<i>Q</i> <sub>max</sub> /°	32.546
Measured Refl.	78860
Independent Refl.	28165
Reflections with <i>I</i> > 2( <i>I</i> )	23497
<i>R</i> <sub>int</sub>	0.0267
Parameters	1265
Restraints	497
Largest Peak	1.222
Deepest Hole	-0.975
Goof	1.030
<i>wR</i> <sub>2</sub> (all data)	0.0587
<i>wR</i> <sub>2</sub>	0.0557
<i>R</i> <sub>1</sub> (all data)	0.0378
<i>R</i> <sub>1</sub>	0.0281

### **[{Cp<sub>2</sub>Mo<sub>2</sub>(CO)<sub>4</sub>(μ<sub>3</sub>,η<sup>2:2:2</sup>-As<sub>2</sub>)<sub>2</sub>(η<sup>1</sup>-CH<sub>3</sub>CN)Cu][TEF] (6-10)**

As mentioned before, the E<sub>2</sub>/Cu<sup>I</sup> systems are highly dynamic in solution. Due to this, the compound [{Cp<sub>2</sub>Mo<sub>2</sub>(CO)<sub>4</sub>(μ<sub>3</sub>,η<sup>2:2:2</sup>-As<sub>2</sub>)<sub>2</sub>-(CH<sub>3</sub>CN)Cu][TEF] (**6-10**), once co-crystallised with compound **6-4**. Except of preliminary X-ray measurements (**Figure S8**), no further characterisation was performed for **6-10**. The measurement revealed a Cu<sup>I</sup> monomer with the Cu<sup>I</sup> center η<sup>2:2:1</sup>-coordinated by two molecules of As<sub>2</sub> and saturated with one acetonitrile ligand.



**Figure S8.** Molecular structure of the cationic fragment of **compound 6-10**. Cp-, Co-ligands and hydrogen atoms are omitted for clarity. Thermal ellipsoids are shown at 50 % probability level.

**Crystal Structure Analysis:** The crystal was selected and measured on a GV50 diffractometer equipped with a TitanS2 CCD detector. The crystal was kept at  $T = 153(1)$  K during data collection. Data collection and reduction were performed with **CrysAlisPro** [Version V1.171.41.21a, 2019].<sup>[21]</sup> A numerical absorption correction based on gaussian integration over a multifaceted crystal model and an empirical absorption correction using spherical harmonics as implemented in SCALE3 ABSPACK was applied. Using **Olex2**,<sup>[23]</sup> the structure was solved with **ShelXT**<sup>[24]</sup> and a least-square refinement on  $F^2$  was carried out with **ShelXL**.<sup>[25]</sup> All non-hydrogen atoms were refined anisotropically. Hydrogen atoms at the carbon atoms were located in idealised positions and refined isotropically according to the riding model.

**Compound 6-10:** The asymmetric unit contains two CH<sub>2</sub>Cl<sub>2</sub> solvent molecule, two independent units of the cationic complex [{Cp<sub>2</sub>Mo<sub>2</sub>(CO)<sub>4</sub>(μ<sub>3</sub>,η<sup>2:2:2</sup>-As<sub>2</sub>)<sub>2</sub>(η<sup>1</sup>-CH<sub>3</sub>CN)Cu]<sup>+</sup> and two [Al{OC(CF<sub>3</sub>)<sub>3</sub>}<sub>4</sub>]<sup>-</sup> anions. For one of the complexes [{Cp<sub>2</sub>Mo<sub>2</sub>(CO)<sub>4</sub>(μ<sub>3</sub>,η<sup>2:2:2</sup>-As<sub>2</sub>)<sub>2</sub>(η<sup>1</sup>-CH<sub>3</sub>CN)Cu]<sup>+</sup> a [Cp<sub>2</sub>Mo<sub>2</sub>(CO)<sub>4</sub>(As<sub>2</sub>)] unit and a CH<sub>3</sub>CN molecule are disordered over two positions (78:22; 68:32). Further, one of the CH<sub>2</sub>Cl<sub>2</sub> molecules is disordered (72:28). One of the two [Al{OC(CF<sub>3</sub>)<sub>3</sub>}<sub>4</sub>]<sup>-</sup> anions shows a disorder of one OC(CF<sub>3</sub>)<sub>3</sub> group over two positions (73:27). For the second [Al{OC(CF<sub>3</sub>)<sub>3</sub>}<sub>4</sub>]<sup>-</sup> anion all four OC(CF<sub>3</sub>)<sub>3</sub> groups are disordered over two positions (60:40; 54:46; 55:45; 54:46). To describe this disorder the restraints DFIX, SADI and SIMU were applied.

**Table S10.** Crystallographic data and details of diffraction experiments for compound **6-10**.

Compound	6-10 · 2 CH <sub>2</sub> Cl <sub>2</sub>
Data set (internal naming)	JS200_3
Formula	C <sub>47</sub> H <sub>25</sub> AlAs <sub>4</sub> Cl <sub>2</sub> Cu F <sub>36</sub> Mo <sub>4</sub> NO <sub>12</sub>
<i>D</i> <sub>calc.</sub> / g · cm <sup>-3</sup>	2.223
μ/mm <sup>-1</sup>	10.465
Formula Weight	2324.54
Colour	clear orange
Shape	needle
Size/mm <sup>3</sup>	0.50×0.09×0.06
<i>T</i> /K	152.96(13)
Crystal System	triclinic
Space Group	<i>P</i> $\bar{1}$
<i>a</i> /Å	11.9908(2)
<i>b</i> /Å	19.2373(3)
<i>c</i> /Å	31.4734(3)
α/°	87.8510(10)
β/°	88.7130(10)
γ/°	73.2230(10)
<i>V</i> /Å <sup>3</sup>	6945.57(18)
<i>Z</i>	4
<i>Z</i> '	2
Wavelength/Å	1.54184
Radiation type	CuK <sub>α</sub>
<i>Q</i> <sub>min</sub> /°	3.637
<i>Q</i> <sub>max</sub> /°	74.218
Measured Refl.	79129
Independent Refl.	27517
Reflections with <i>I</i> > 2( <i>I</i> )	25208
<i>R</i> <sub>int</sub>	0.0738
Parameters	2614
Restraints	1833
Largest Peak	1.468
Deepest Hole	-1.351
Goof	1.101
<i>wR</i> <sub>2</sub> (all data)	0.1825
<i>wR</i> <sub>2</sub>	0.1803
<i>R</i> <sub>1</sub> (all data)	0.0784
<i>R</i> <sub>1</sub>	0.746

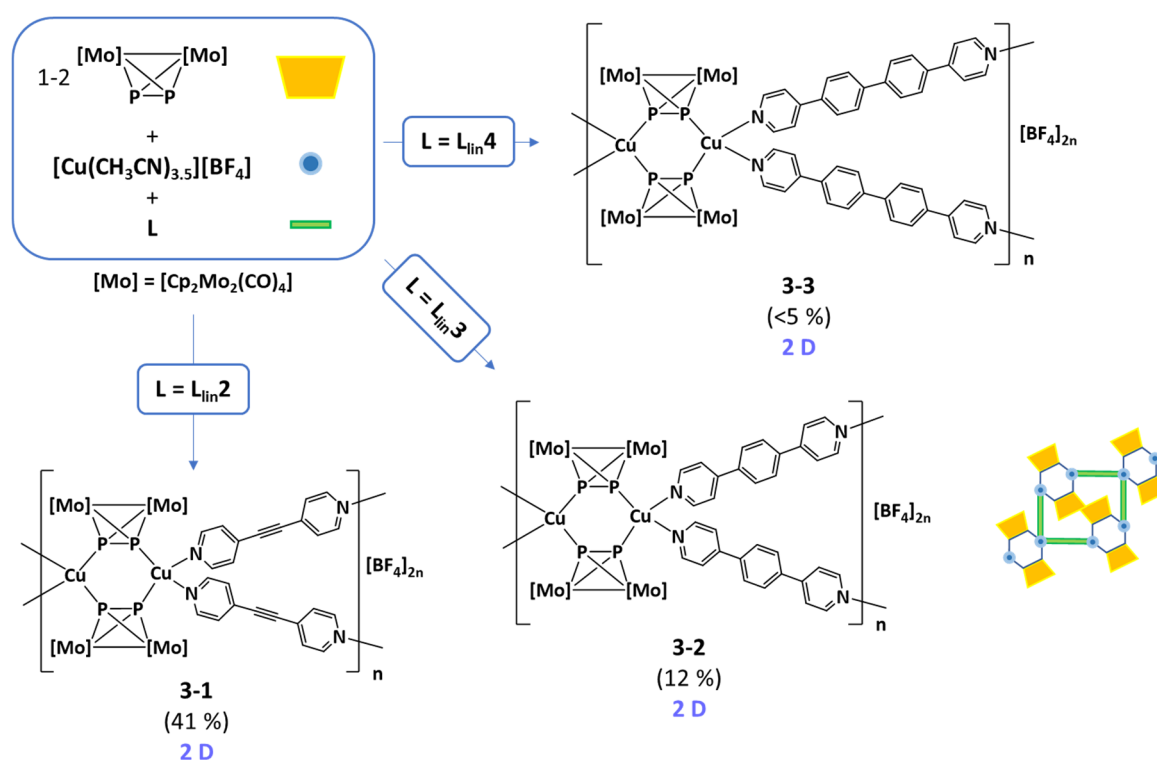
## 6.6 References

- [1] a) S. T. Li, B. B. Cula, S. Hoof, C. Limberg, *Dalton Trans.* **2018**, 47, 544-560; b) C. Marzano, V. Gandin, M. Pellei, D. Colavito, G. Papini, G. G. Lobbia, E. D. Giudice, M. Porchia, F. Tisato, C. Santini, *J. Med. Chem.* **2008**, 51, 798; c) O. A. Filippov, A. A. Titov, E. A. Guseva, D. A. Loginov, A. F. Smol'yakov, F. M. Dolgushin, N. V. Belkova, L. M. Epstein, E. S. Shubina, *Chem. Eur. J.* **2015**, 21, 13176-13180.
- [2] a) B. Hupp, C. Schiller, C. Lenczyk, M. Stanoppi, K. Edkins, A. Lorbach A. Steffen, *Inorg. Chem.* **2017**, 56, 8996-9008; b) M. E. Moussa, S. Evariste, H.-L. Wong, L. Le Bras, C. Roiland, L. Le Polles, B. Le Guennic, K. Costuas, V. W.-W. Yam, C. Lescop, *Chem. Commun.* **2016**, 52, 11370-11373; c) F. Böppler, M. Zimmer, F. Dietrich, M. Gruppe, M. Wallesch, D. Volz, S. Bräse, M. gerhards, R. Diller, *Phys. Chem. Chem. Phys.* **2017**, 19, 29438-29448; d) T. Hofbeck, U. Monkowius, H. Yersin, *J. Am. Chem. Soc.* **2015**, 137, 399-404.
- [3] W.-H. Chan, S.-M. Peng, C.-M. Che, *J. Chem. Soc. Dalton Trans.* **1998**, 2867-2871.
- [4] X. He, K. Ruhlandt-Senge, P. P. Power, S. H. Bertz, *J. Am. Chem. Soc.* **1994**, 116, 6963-6964.
- [5] P. Ai, A. A. Danopoulos, P. Braunstein. K. Y. Monakhov, *Chem. Commun.* **2014**, 50, 103-105.
- [6] M. Fleischmann, L. Dütsch, M. E. Moussa, G. Balázs, W. Kremer, C. Lescop, M. Scheer, *Inorg. Chem.* **2016**, 55, 2840-2854.
- [7] a) M. E. Moussa, M. Piesch, M. Fleischmann, A. Schreiner, M. Seidl, M. Scheer, *Dalton Trans.* **2018**, 47, 16031-16035; b) M. E. Moussa, M. Seidl, G. Balázs, M. Hautmann, M. Scheer, *Angew. Chem. Int. Ed.* **2019**, 58, 12903-12907; c) M. Scheer, L. J. Gregoriades, M. Zabel, J. Bai, I. Krossing, G. Brunklaus, H. Eckert, *Chem. Eur. J.* **2008**, 14, 282-295; d) M. E. Moussa, B. Attenberger, E. V. Peresykina, M. Fleischmann, G. Balázs, M. Scheer, *Chem. Commun.* **2016**, 52, 10004-10007; e) J. J. Bai, E. Leiner, M. Scheer *Angew. Chem.* **2002**, 114, 820-823; *Angew. Chem. Int. Ed.* **2002**, 41, 783-786; f) M. Scheer, L. Gregoriades, J. Bai, M. Sierka, G. Brunklaus, H. Eckert, *Chem. Eur. J.* **2005**, 11, 2163-2169; g) M. E. Moussa, P. A. Shelyganov, B. Wegley, M. Seidl, M. Scheer, *Eur. J. Inorg. Chem.* **2019**, 4241-4248.
- [8] a) C. Heindl, A. Kuntz, E. V. Peresykina, A. V. Virovets, M. Zabel, D. Ludeker, G. Brunklaus, M. Scheer, *Dalton Trans.* **2015**, 44, 6502-6509; b) C. Heindl, E. V. Peresykina, A. V. Virovets, V. Y. Komarov, M. Scheer, *Dalton Trans.* **2015**, 44, 10245-10252; c) M. Fleischmann, S. Welsch, E. V. Peresykina, A. V. Virovets, M. Scheer, *Chem. Eur. J.* **2015**, 21, 14332-14336; d) E.-M. Rummel, M. Eckhardt, M. Bodensteiner, E. V. Peresykina, W. Kremer, C. Groger, M. Scheer, *Eur. J. Inorg. Chem.* **2014**, 1625-1637; e) M. E. Moussa, E. Peresykina, A. V. Virovets, D. Venus, G. Balázs, M. Scheer, *CrystEngComm* **2018**, 20, 7417-7422; f) M. E. Moussa, S. Welsch, M. Lochner, E. Peresykina, A. V. Virovets, M. Scheer, *Eur. J. Inorg. Chem.* **2018**, 2689-2694; g) M. E. Moussa, B. Attenberger, E. V. Peresykina, M. Scheer, *Dalton Trans.* **2018**, 47, 1014; h) M. E. Moussa, B. Attenberger, M. Seidl, A. Schreiner, M. Scheer, *Eur. J. Inorg. Chem.* **2017**, 5616-5620; i) C. Heindl, E. V. Peresykina, D. Ludeker, G. Brunklaus, A. V. Virovets, M. Scheer, *Chem. Eur. J.* **2016**, 22, 2599-2604.
- [9] S. Welsch, C. Groger, M. Sierka, M. Scheer, *Angew. Chem. Int. Ed.* **2011**, 50, 1435; *Angew. Chem.* **2011**, 123, 1471.
- [10] a) C. Heindl, E. Peresykina, A. V. Virovets, I. S. Bushmarinov, M. G. Medvedev, B. Krämer, B. Dittrich, M. Scheer, *Angew. Chem. Int. Ed.* **2017**, 56, 13237-13243; *Angew. Chem.* **2017**, 129, 13420; b) F. Dielmann, E. V. Peresykina, B. Krämer, F. Hastreiter, B. P. Johnson, M. Zabel, C. Heindl, M. Scheer, *Angew. Chem. Int. Ed.* **2016**, 55, 14833-14837; c) C. Heindl, E. V. Peresykina, A. V. Virovets, W. Kremer, M. Scheer, *J. Am. Chem. Soc.* **2015**, 137, 10938-10941; d) M. Scheer, A. Schindler, R. Merkle, B. P. Johnson, M. Linseis, R. Winter, C. E. Anson, A. V. Virovets, *J. Am. Chem. Soc.* **2007**, 129, 13386-13387; e) J. Bai, A. V. Virovets, M. Scheer, *Science* **2003**, 300, 781-783; f) F. Dielmann, C. Heindl, F. Hastreiter, E. V. Peresykina, A. V. Virovets, R. M. Gschwind, M. Scheer, *Angew. Chem. Int. Ed.* **2014**, 53, 13605-13608; *Angew. Chem.* **2014**, 126, 13823-13826.
- [11] a) P. J. Sullivan, A. L. Rheingold, *Organometallics* **1982**, 1, 1547-1549; b) O. J. Scherer, C. Blath, G. Wolmershäuser, *J. Organomet. Chem.* **1990**, 387, C21-C24.
- [12] a) H. Krauss, G. Balázs, M. Bodensteiner, M. Scheer, *Chem. Sci.* **2010**, 1, 337-342; C. Schwarzmaier, M. Sierka, M. Scheer, *Angew. Chem. Int. Ed.* **2013**, 52, 858-861; c) L. J. Gregoriades, H. Krauss, J. Wachter, A. V. Virovets,

- M. Sierka, M. Scheer, *Angew. Chem. Int. Ed.* **2006**, *45*, 4189-4192; d) M. Scheer, L. J. Gregoriades, A. V. Virovets, W. Kunz, R. Neueder, I. Krossing, *Angew. Chem. Int. Ed.* **2006**, *45*, 5689-5693.
- [13] a) O. J. Scherer, H. Sitzmann, G. Wolmershäuser, *J. Organomet. Chem.* **1984**, *268*, C9-C12; b) O. J. Scherer, H. Sitzmann, G. Wolmershäuser, *J. Organomet. Chem.*, **1986**, *309*, 77-86.
- [14] Once another compound could be isolated (cf. Supporting information).
- [15] M. L. Ziegler, K. Blechschmitt, B. Nuber, T. Zahn, *Chem. Ber.* **1988**, *121*, 159-171.
- [16] A. Bondi, *J. Phys. Chem.* **1964**, *68*, 441-451.
- [17] O. J. Scherer, H. Sitzmann, G. Wolmershäuser, *J. Organomet. Chem.* **1984**, *268*, C9-C12.
- [18] O. J. Scherer, H. Sitzmann, G. Wolmershäuser, *J. Organomet. Chem.* **1986**, *309*, 77-86.
- [19] M. E. Moussa, M. Piesch, M. Fleischmann, A. Schreiner, M. Seidl, M. Scheer, *Dalton Trans.* **2018**, *47*, 16031-16035.
- [20] In the  $^{31}\text{P}\{^1\text{H}\}$  spectra of compounds **1-3**, broad signals are detected. This is most likely due to an equilibrium in a highly dynamic solution. This has already been discussed in the main part of this paper.
- [21] CrysAlisPro Software System, Rigaku Oxford Diffraction, (2018).
- [22] Clark, R. C. & Reid, J. S. *Acta Cryst.* **1995**, *A51*, 887-897.
- [23] O.V. Dolomanov, L.J. Bourhis, R.J. Gildea, J.A.K. Howard, H. Puschmann, Olex2: A complete structure solution, refinement and analysis program, *J. Appl. Cryst.* **2009**, *42*, 339-341.
- [24] Sheldrick, G.M., ShelXT-Integrated space-group and crystal-structure determination, *Acta Cryst.* **2015**, *A71*, 3-8.5.G.
- [25] M. Sheldrick, Crystal structure refinement with ShelXL, *Acta Cryst.* **2015**, *C27*, 3-8.
- [26] a) F. Furche, R. Ahlrichs, C. Hättig, W. Klopper, M. Sierka, F. Weigend, *WIREs Comput. Mol. Sci.* **2014**, *4*, 91-100; b) R. Ahlrichs, M. Bär, M. Häser, H. Horn, C. Kölmel, *Chem. Phys. Lett.* **1989**, *162*, 165-169; c) O. Treutler, R. Ahlrichs, *J. Chem. Phys.* **1995**, *102*, 346-354; d) TURBOMOLE V6.4, <http://www.turbomole.com>.
- [27] a) K. Eichkorn, O. Treutler, H. Oehm, M. Häser, R. Ahlrichs, *Chem. Phys. Lett.* **1995**, *242*, 652-660; b) K. Eichkorn, F. Weigend, O. Treutler, R. Ahlrichs, *Theor. Chem. Acc.* **1997**, *97*, 119.
- [28] a) P. A. M. Dirac, *Proc. Royal Soc. A.* **1929**, *123*, 714; b) J. C. Slater, *Phys. Rev.* **1951**, *81*, 385; c) S. H. Vosko, L. Wilk, M. Nusair, *Can. J. Phys.* **1980**, *58*, 1200; d) A. D. Becke, *Phys. Rev. A*, **1988**, *38*, 3098; e) C. Lee, W. Yang, R. G. Parr, *Phys. Rev. B.* **1988**, *37*, 785. f) A. D. Becke, *J. Chem. Phys.* **1993**, *98*, 5648.
- [29] a) A. Schäfer, C. Huber, R. Ahlrichs, *J. Chem. Phys.* **1994**, *100*, 5829; b) K. Eichkorn, F. Weigend, O. Treutler, R. Ahlrichs, *Theor. Chem. Acc.* **1997**, *97*, 119.
- [30] M. Sierka, A. Hogekamp, R. Ahlrichs, *J. Chem. Phys.* **2003**, *118*, 9136.
- [31] A. Klamt, G. Schüürmann, *J. Chem. Soc. Perkin Trans.* **1993**, *2*, 799-805; A. Schäfer, A. Klamt, D. Sattel, J. C. W. Lohrenz, F. Eckert, *Phys. Chem. Chem. Phys.*, **2000**, *2*, 2187-2193.

## 7 Conclusion

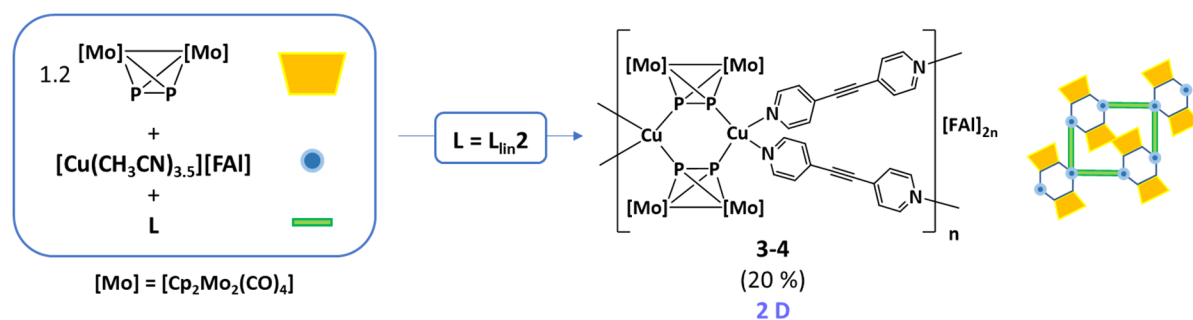
The chemistry of coordination compounds and organometallic-organic coordination polymers (CPs) with the  $P_2$  ligand complex  $[Cp_2Mo_2(CO)_4(\mu, \eta^{2:2}-P_2)]$  (**A**) as central building block was explored. **A** was reacted in two-component-reactions with different Cu(I) and Ag(I) WCA salts or in three-component reactions with the addition of organic pyridine-based linkers. By changing the nature of the linker, the WCA and the metal, respectively, the influence of those factors on the reaction outcome should be investigated. In addition, the crystallisation method turned out to be a crucial parameter for the product formation. Concerning the two-component reactions of **A** with metal salts, also the stoichiometry of the reactants can be a powerful tool for tuning the reaction outcome. Very first experiments were about the influence of the nature of the linker. A recent study had shown that the reaction of the  $P_2$  ligand complex **A** with the Cu(I) source  $[Cu(CH_3CN)_4][BF_4]$  (**B**) and flexible organic linker selectively yielded one-dimensional CPs.<sup>[1]</sup> Instead of bendable linkers with flexible  $CH_2$  groups, linkers containing triple bonds and benzene rings were chosen to make the formation of analogous 1D CPs impossible due to their length and rigidity. By reacting **A** with **B** and linkers **L<sub>lin</sub>2**, **L<sub>lin</sub>3** and **L<sub>lin</sub>4**, respectively, three new analogous 2D CPs were obtained (**Scheme 7-1**).



**Scheme 7-1.** Reactions of the  $Mo_2P_2$  complex  $[Cp_2Mo_2(CO)_4(\mu, \eta^{2:2}-P_2)]$  with  $[Cu(CH_3CN)_4][BF_4]$  and the rigid organic linkers **L<sub>lin</sub>2**, **L<sub>lin</sub>3** and **L<sub>lin</sub>4**, respectively.

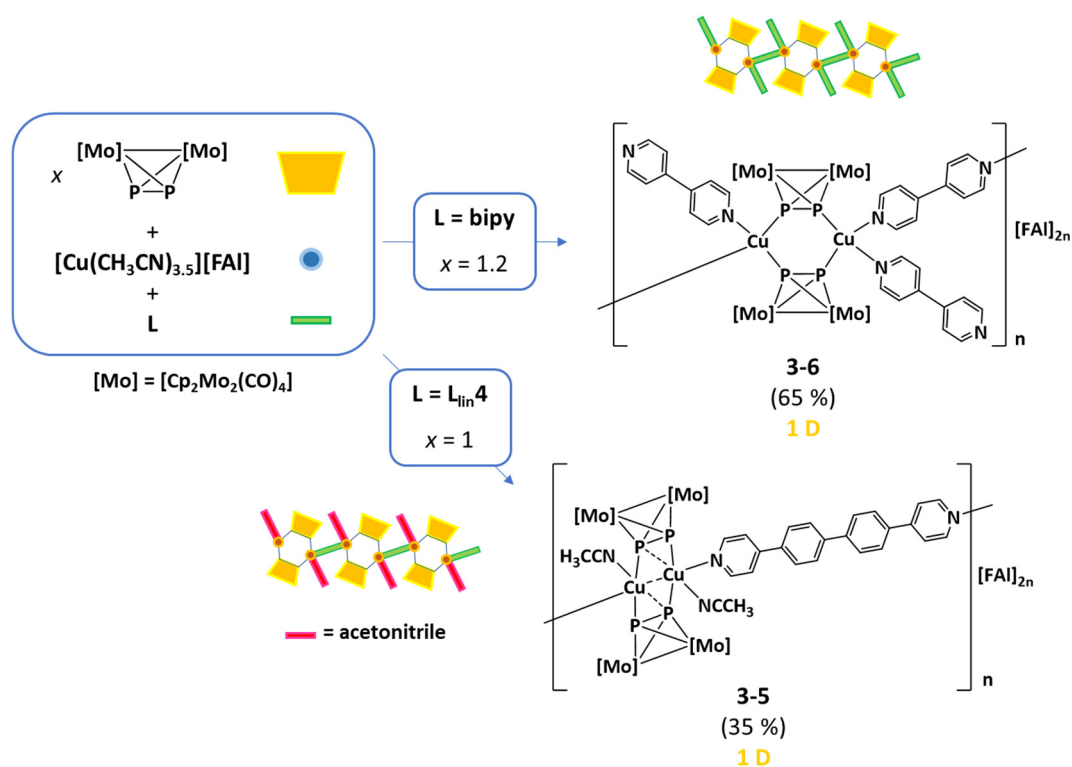
The products with the general formula  $[Cu_2\{Cp_2Mo_2(CO)_4(\mu_4, \eta^{2:2:1:1}-P_2)\}_2(\mu, \eta^{1:1}-L)_2]_n [BF_4]_{2n}$  (**3-1**: **L** = **L<sub>lin</sub>2**, **3-2**: **L** = **L<sub>lin</sub>3**, **3-3**: **L** = **L<sub>lin</sub>4**) all contain a six-membered  $Cu_2P_4$ -ring with two tetra-coordinated Cu(I) centres, which serves as node. The nodes are connected to each other by four molecules of linker each.

The networks have cavities formed by four nodes and four linker molecules each, which have sizes of up to 2.21 nm ( $L_{lin2}$ ), 2.26 nm ( $L_{lin3}$ ) and 3.19 nm ( $L_{lin4}$ ).<sup>[2]</sup> Then, a different WCA was used in the reaction of **A** with a Cu(I) source and rigid linkers. The WCA  $[FAI\{O(C_6F_{10})(C_6F_5)\}_3]^-$  ( $= [FAI]^-$ ) is significantly bigger than  $[BF_4]^-$ , so some differences were expected. However, in the case of linker  $L_{lin2}$ , the change of the WCA did not affect the reaction outcome. The reaction of the  $P_2$  ligand complex **A** with  $[Cu(CH_3CN)_{3.5}][FAI]$  (**C**) and  $L_{lin2}$  also yielded a 2D CP with a to compound **3-1** similar structure and analogous formula ( $[Cu_2\{Cp_2Mo_2(CO)_4(\mu_4, \eta^{2:2:1:1}-P_2)\}_2(\mu, \eta^{1:1}-L_{lin2})_2]_n[FAI]_{2n}$ , **Scheme 7-2**).



**Scheme 7-2.** Reaction of the  $P_2$  ligand complex  $[Cp_2Mo_2(CO)_4(\mu, \eta^{2:2}-P_2)]$  (**A**) with  $[Cu(CH_3CN)_{3.5}][FAI]$  (**C**) and  $L_{lin2}$ .

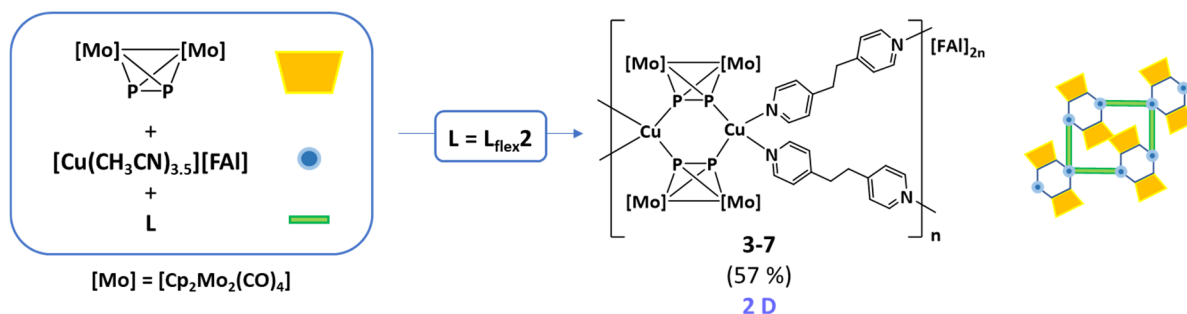
In the case of linkers **bipy** and  $L_{lin4}$ , the reaction outcome was not as straight forward. Two new 1D CPs with the formulas  $[Cu_2[Cp_2Mo_2(CO)_4(\mu_4, \eta^{2:2:2:1}-P_2)]_2(\mu, \eta^{1:1}-L_{lin4})(CH_3CN)_2]_n[FAI]_{2n}$  (**3-5**) and  $[Cu_2\{Cp_2Mo_2(CO)_4(\mu, \eta^{2:2:1:1}-P_2)\}_2(\mu, \eta^{1:1}-bipy)(bipy)_2]_n[BF_4]_{2n}$  (**3-6**) were obtained (**Scheme 7-3**).



**Scheme 7-3.** Reaction of the  $P_2$  ligand complex  $[Cp_2Mo_2(CO)_4(\mu, \eta^{2:2}-P_2)]$  (**A**) with  $[Cu(CH_3CN)_{3.5}][FAI]$  and the organic linkers **bipy** and  $L_{lin4}$ .

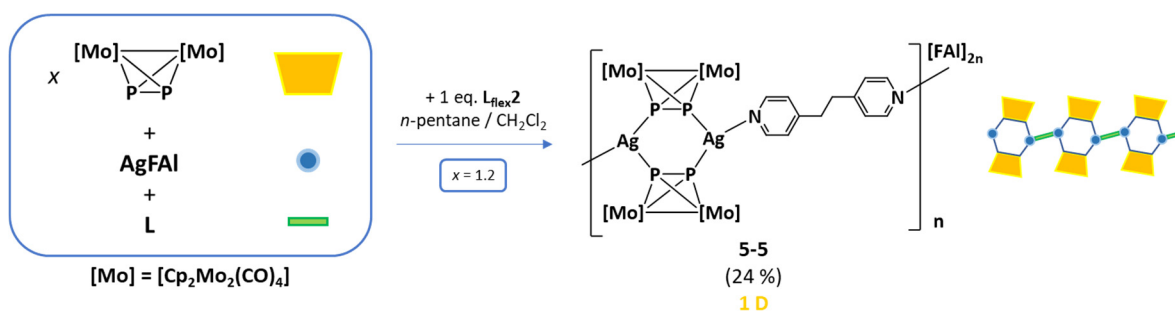


Both compounds contain a six-membered  $\text{Cu}_2\text{P}_4$ -ring serving as node. The Cu(I) centres are tetra-coordinated. The structural difference to compounds **3-1** to **3-4** is that there is only one  $\mu, \eta^{1:1}$ -connecting linker moiety per Cu(I) centre instead of two. The coordination spheres of the Cu(I) centres are saturated by acetonitrile ligands in the case of **3-5** and  $\eta^1$ -coordinated **bipy** molecules in the case of **3-6**. Compound **3-5** exhibits another feature. The  $\text{P}_2$  units are  $\eta^{2:1}$ -coordinated to the two Cu(I) centres, which have a Cu...Cu-distance of 2.5927(4) Å. This is still above the sum of the covalent radii<sup>[3]</sup> but results in a strong distortion of the six-membered  $\text{Cu}_2\text{P}_4$ -ring. As the WCA apparently has a huge influence on the system, the Cu(I) salt  $[\text{Cu}(\text{CH}_3\text{CN})_{3.5}][\text{FAI}]$  (**C**) was used in another reaction with **A** and the flexible linker **L<sub>flex2</sub>**. Sterically, both the formation of a one- and two-dimensional CP is possible. The reaction yielded a 2D CP with the formula  $[\text{Cu}_2\{\text{Cp}_2\text{Mo}_2(\text{CO})_4(\mu_4, \eta^{2:2:1:1}\text{-P}_2)\}_2(\mu, \eta^{1:1}\text{-L}_{\text{flex}2})_2]_n[\text{FAI}]_{2n}$  (**3-7**, **Scheme 7-4**). Its structure is analogous to compounds **3-1** to **3-4**. This leads to the conclusion that in the system of **A** with a Cu(I) source and flexible linkers, the anion seems to have a bigger influence in comparison to the linker.



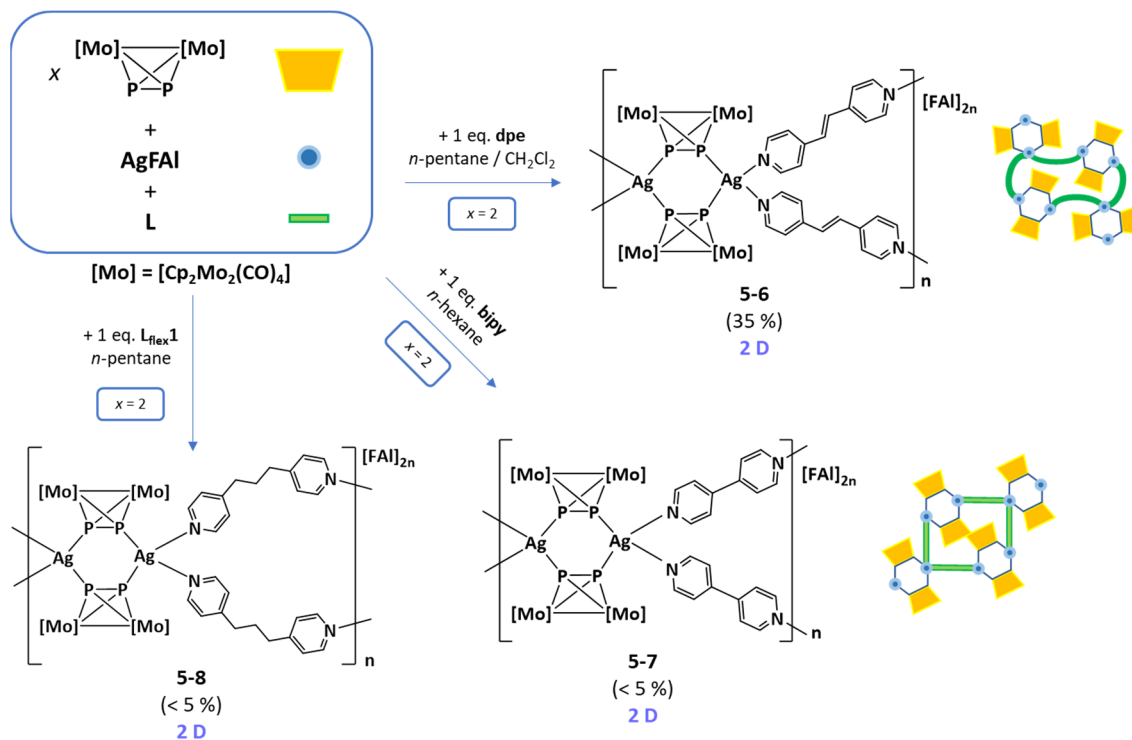
**Scheme 7-4.** Reaction of the  $\text{P}_2$  ligand complex  $[\text{Cp}_2\text{Mo}_2(\text{CO})_4(\mu_4, \eta^{2:2:1:1}\text{-P}_2)]$  (**A**) with  $[\text{Cu}(\text{CH}_3\text{CN})_{3.5}][\text{FAI}]$  and **L<sub>flex2</sub>**.

A reaction of linker **L<sub>flex2</sub>** with the  $\text{P}_2$  complex ligand **A** and the Ag(I) salt  $\text{Ag}[\text{FAI}]$  (**D**) was performed for further investigation of the influence of the metal on the formation of CPs. The reaction yielded a surprising product, which is not comparable to either compound **3-7** nor the 1D CP obtained from the reaction of **A**, **L<sub>flex2</sub>** and the Cu(I) source  $[\text{Cu}(\text{CH}_3\text{CN})_4][\text{BF}_4]$  (**B**) mentioned earlier. Compound **5-5** (**Scheme 7-5**) also possesses a six-membered  $\text{M}_2\text{P}_4$ -ring ( $\text{M} = \text{Ag}$ ) with the units of **A** coordinated in  $\eta^{1:1}$ -mode. The Ag(I) centres, however, are not four-fold but three-fold coordinated. Their coordination sphere is completed by one molecule of linker **L<sub>flex2</sub>** each and the polymer therefore only extends in one dimension.



**Scheme 7-5.** Reactions of the  $\text{P}_2$  ligand complex **A** with the Ag(I) precursor  $\text{Ag}[\text{FAI}]$  (**D**) and the organic linker 1,3-di(4-pyridyl)ethane (**L<sub>flex2</sub>**).

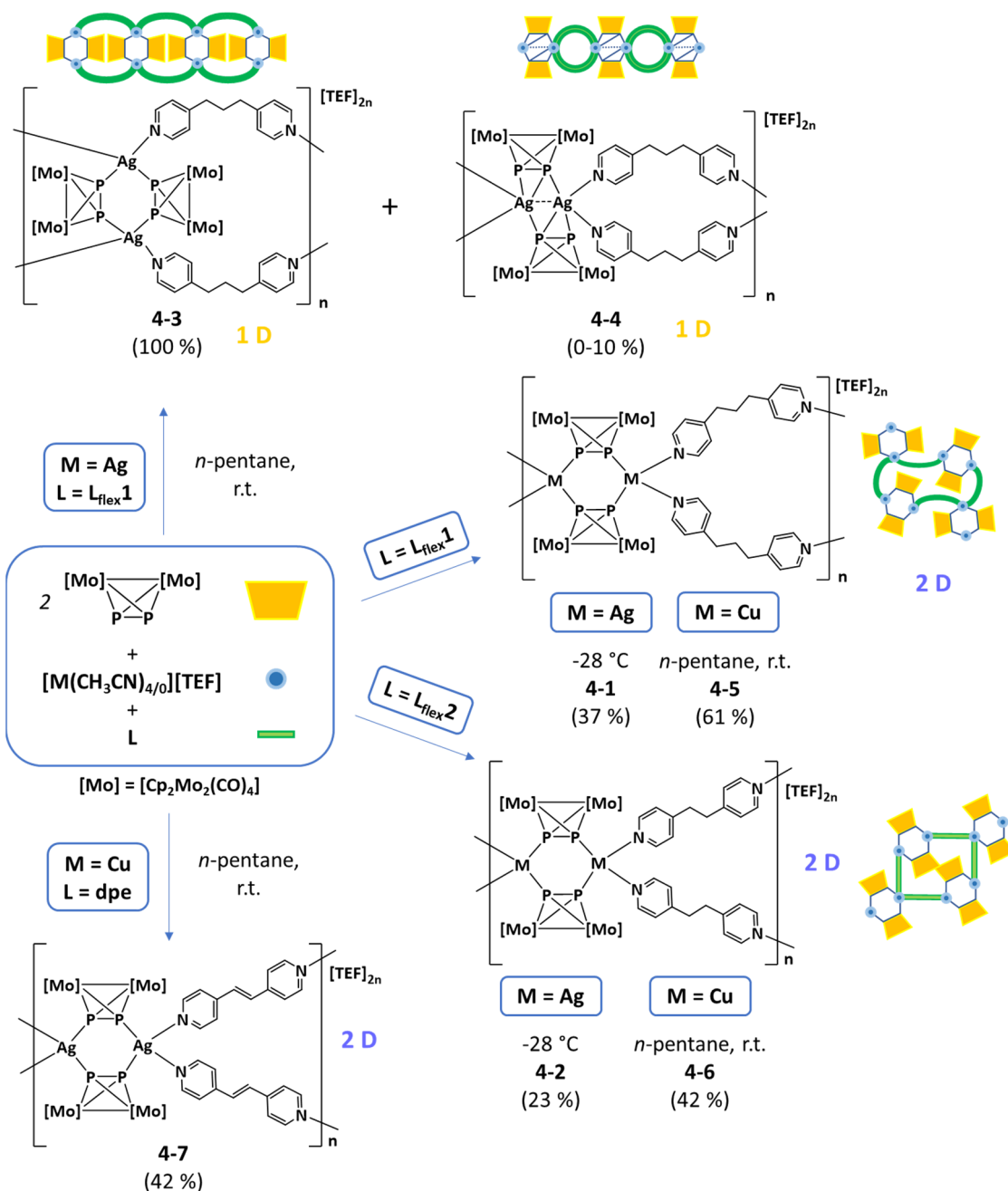
By performing the reactions with linkers **L<sub>flex</sub>1**, **bipy** and **dpe**, respectively, three similar two-dimensional CPs with the general formula  $[\text{Cu}_2\{\text{Cp}_2\text{Mo}_2(\text{CO})_4(\mu, \eta^{2:2:1:1}\text{-P}_2)\}_2(\mu, \eta^{1:1}\text{-L}_2)_n][\text{FAI}]_{2n}$  (**5-6**: **L** = **dpe**; **5-7**: **L** = **bipy**; **5-8**: **L** = **L<sub>flex</sub>1**) were obtained (**Scheme 7-6**). A six-membered  $\text{Ag}_2\text{P}_4$ -ring with tetra-coordinated  $\text{Ag}(\text{I})$  centres serves as a node in all three compounds. The nodes are linked to each other by four molecules of linker per node which connect to different nodes. The cavities formed by the networks have diameters of up to 2.22 nm and are filled with anions and solvent molecules.



**Scheme 7-6.** Reactions of the  $\text{P}_2$  ligand complex **A** with the  $\text{Ag}(\text{I})$  precursor  $\text{Ag}[\text{FAI}]$  (**D**) and the organic linkers 1,3-di(4-pyridyl)propane (**L<sub>flex</sub>1**), 4,4'-bipyridyl (**bipy**) and trans-1,2-di(pyridine-4-yl)-ethene (**dpe**), respectively.

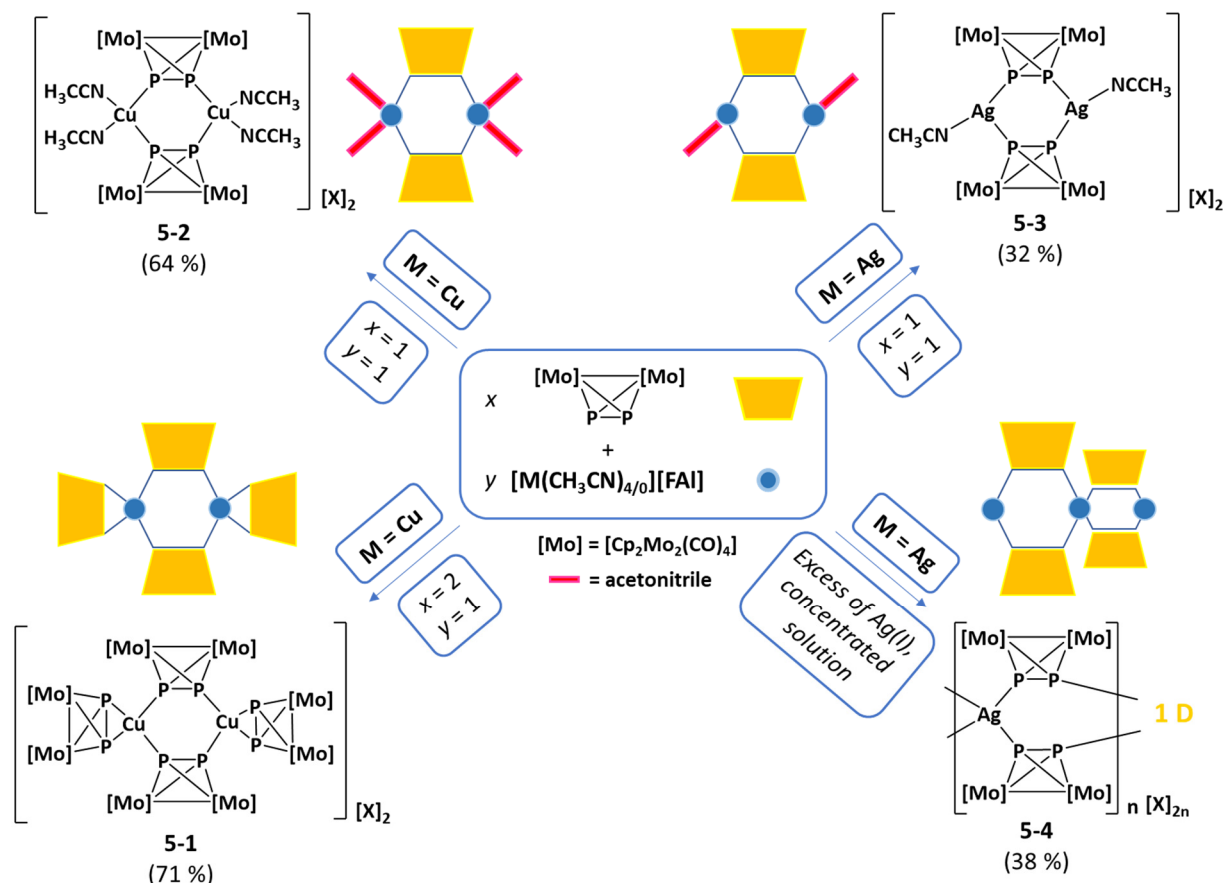
Another study focused on the differences between the  $\text{Ag}(\text{I})$  and  $\text{Cu}(\text{I})$  salts  $\text{Ag}[\text{TEF}]$  (**D**) and  $[\text{Cu}(\text{CH}_3\text{CN})_4][\text{TEF}]$  (**E**) in the synthesis of organometallic-organic CPs with the  $\text{P}_2$  ligand complex **A** and organic linkers (**Scheme 7-7**). First, the system of **A**, the  $\text{Ag}(\text{I})$  source **E** and linker **L<sub>flex</sub>1** was studied. Different crystallisation methods yielded different products. By diffusion of  $n$ -pentane into the crude reaction mixture, the 1D CP **4-3** with the formula  $[\text{Ag}_2\{\text{Cp}_2\text{Mo}_2(\text{CO})_4(\mu, \eta^{2:2:1:1}\text{-P}_2)\}_2(\mu, \eta^{1:1}\text{-L}_{\text{flex}1})_2]_n[\text{TEF}]_{2n}$  was obtained. Sometimes, a by-product to **4-3** with the formula  $[\text{Ag}_2\{\text{Cp}_2\text{Mo}_2(\text{CO})_4(\mu, \eta^{2:2:2:1}\text{-P}_2)\}_2(\mu, \eta^{1:1}\text{-L}_{\text{flex}1})_2]_n[\text{TEF}]_{2n}$  (**4-4**) could be obtained as well. Compound **4-3** features a six-membered  $\text{Ag}_2\text{P}_4$ -ring with tetra-coordinated  $\text{Ag}(\text{I})$  centres whose coordination sphere is saturated by linker molecules. Two linker molecules from one node but different  $\text{Ag}(\text{I})$  centres connect to the two  $\text{Ag}(\text{I})$  centres of the next node, leading to a one-dimensional strand. Compound **4-4** also has a six-membered  $\text{Ag}_2\text{P}_4$ -ring as node. One difference to **4-3** is that the nodes are connected to each other by a pair of linker molecules coordinating to two  $\text{Ag}(\text{I})$  centres of different nodes. The second difference is that the  $\text{P}_2$  units of **A** are coordinating in a  $\eta^{2:1}$ -mode. The  $\text{Ag}_2\text{P}_4$ -ring is therefore strongly distorted and features a short  $\text{Ag}$ - $\text{Ag}$ -distance of 2.9 Å. Even though this value is above the sum of the covalent radii of silver (1.28 Å),<sup>[3]</sup>  $\text{Ag}$ - $\text{Ag}$ -interactions cannot be ruled out.<sup>[4]</sup>

Storage of the crude reaction mixture of **A**, the Ag(I) source **D** and linker  $L_{flex1}$  or  $L_{flex2}$ , respectively, at a temperature of  $-28\text{ }^{\circ}\text{C}$  selectively yielded the 2D CPs **4-1** and **4-2** with the general formula  $[\text{Ag}_2\{\text{CpMo}_2(\text{CO})_4(\mu, \eta^{2:2:1:1}\text{-P}_2)\}_2(\mu, \eta^{1:1}\text{-L})_2]_n[\text{TEF}]_{2n}$  ( $L = L_{flex1}, L_{flex2}$ ). The two compounds are analogous to compound **4-3** with the difference that all four linker molecules attached to one node connect to four different nodes instead of two, leading to the two-dimensional extension of the network. Similar compounds (**4-5**, **4-6** and **4-7**) with the general formula  $[\text{Cu}_2\{\text{Cp}_2\text{Mo}_2(\text{CO})_4(\mu, \eta^{2:2:1:1}\text{-P}_2)\}_2(\mu, \eta^{1:1}\text{-L})_2]_n[\text{TEF}]_{2n}$  (**4-5**:  $L = L_{flex1}$ ; **4-6**:  $L = L_{flex2}$ ; **4-7**:  $L = \text{dpe}$ ) could be obtained by the reaction of **A** with the analogous Cu(I) salt **E** when the crude reaction mixture was layered with *n*-pentane at r.t.



**Scheme 7-7.** Reactions of the P<sub>2</sub> ligand complex **A** with M[TEF] (M = Ag, [Cu(CH<sub>3</sub>CN)] ) and the organic linkers  $L_{flex1}$ ,  $L_{flex2}$  and **dpe**, respectively.

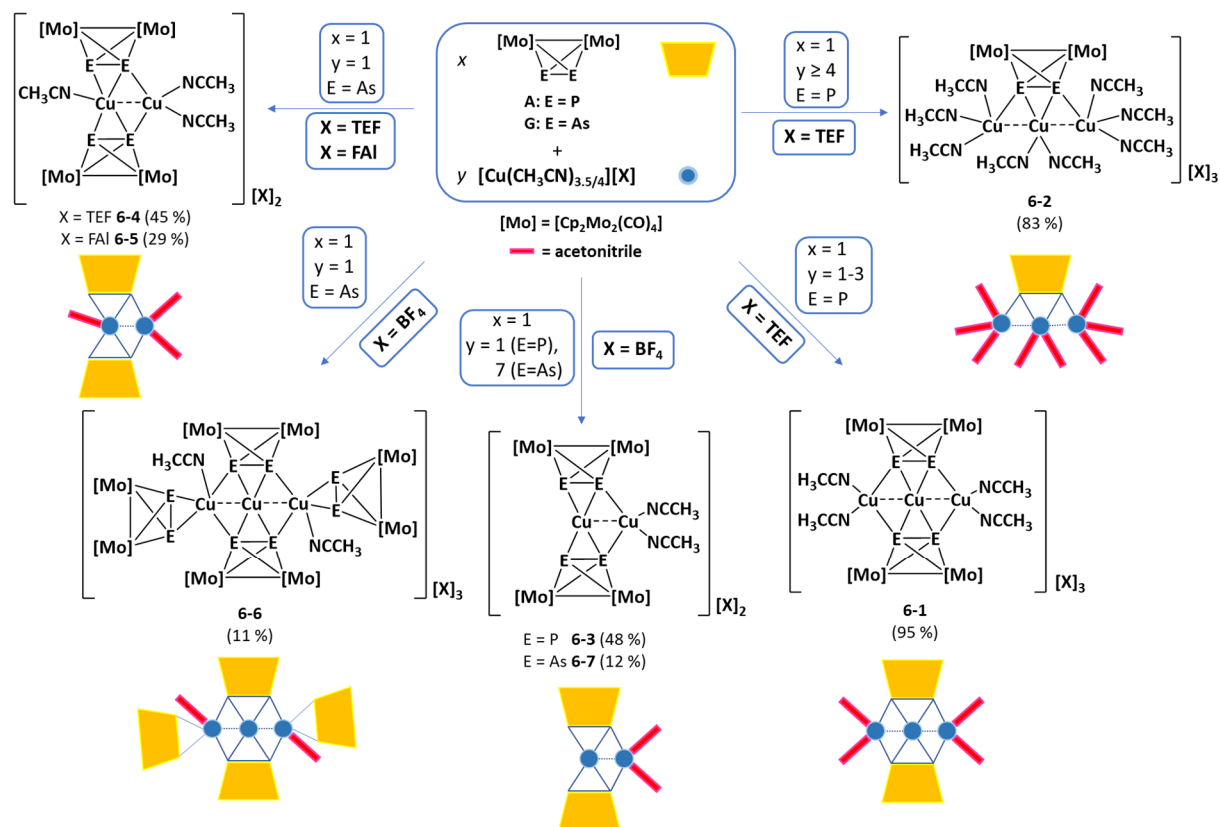
The second topic of this thesis was the synthesis of suitable precursors for supramolecular coordination chemistry. The P<sub>2</sub> ligand complex **A** was therefore reacted with different Cu(I) and Ag(I) sources with weakly coordinating anions. The reactions with the Cu(I) and Ag(I) salts [Cu(CH<sub>3</sub>CN)<sub>3.5</sub>][FAI] (**C**) and Ag[FAI] (**D**), respectively, yielded one new coordination complex [Cu<sub>2</sub>{Cp<sub>2</sub>Mo<sub>2</sub>(CO)<sub>4</sub>(μ,η<sup>2:2:1:1</sup>-P<sub>2</sub>)<sub>2</sub>{Cp<sub>2</sub>Mo<sub>2</sub>(CO)<sub>4</sub>(μ,η<sup>2:2:2</sup>-P<sub>2</sub>)<sub>2</sub>][FAI]<sub>2</sub> (**5-1**) and two unprecedented coordination complexes [Cu<sub>2</sub>{Cp<sub>2</sub>Mo<sub>2</sub>(CO)<sub>4</sub>(μ,η<sup>2:2:1:1</sup>-P<sub>2</sub>)<sub>2</sub>(η<sup>1</sup>-CH<sub>3</sub>CN)<sub>4</sub>][FAI]<sub>2</sub> (**5-2**), of which all three phosphorus-rich dimers are potential precursors for subsequent coordination chemistry. Additionally, one known 1D CP [Ag<sub>2</sub>{Cp<sub>2</sub>Mo<sub>2</sub>(CO)<sub>4</sub>(μ,η<sup>2:2:1:1</sup>-P<sub>2</sub>)<sub>2</sub>]<sub>n</sub>[FAI]<sub>2n</sub> (**5-4**) was obtained (**Scheme 7-8**).



**Scheme 7-8.** Reactions of the Mo<sub>2</sub>P<sub>2</sub> complex **A** with the Cu(I) source [Cu(CH<sub>3</sub>CN)<sub>4</sub>][FAI] (**C**) and the Ag(I) source Ag[FAI] (**D**), respectively.

**5-1** and **5-2** were obtained from similar reactions by using different stoichiometries of the starting materials. An **A**:**C**-ratio of 2:1 yielded compound **5-1**, whereas the reaction in 1:1-ratio yielded compound **5-2**. Both structures contain the same ratios of the starting materials as has been used in the reaction. The structure of the Cu-dimer **5-1** is analogous to Cu- and Ag-dimers obtained from the reaction of **A** with other coinage metal salts.<sup>[1,5]</sup> It contains a six-membered Cu<sub>2</sub>P<sub>4</sub>-ring with two Cu(I) centres and four units of **A** in η<sup>1:1</sup>- and η<sup>1</sup>-coordination mode. The dimer **5-2** also contains a six-membered Cu<sub>2</sub>P<sub>4</sub>-ring with two Cu(I) centres and two units of **A** in η<sup>1:1</sup>-coordination mode. The tetrahedral coordination sphere of the Cu(I) centres are, however, saturated by acetonitrile ligands. This ranks **5-2** an even more suitable precursor for supramolecular coordination chemistry, as the acetonitrile ligands can be removed easier than the P<sub>2</sub> ligand complex **A**.<sup>[1,6]</sup> The Ag-dimer **5-3** is similar

to **5-2** with the main difference that the Ag(I) centres of the six-membered Ag<sub>2</sub>P<sub>4</sub>-ring are three-coordinated. **5-3** was also obtained by using a 1:1-ratio of both starting materials. The one-dimensional CP [Cu<sub>2</sub>(Cp<sub>2</sub>Mo<sub>2</sub>(CO)<sub>4</sub>(μ,η<sup>2:2:1:1</sup>-P<sub>2</sub>)<sub>4</sub>)<sub>n</sub>[FAI]<sub>2n</sub> **5-4** was obtained by using an excess of the Ag(I) salt and performing the reaction in a very concentrated solution. **5-4** contains a six-membered Ag<sub>2</sub>P<sub>4</sub>-ring and P<sub>2</sub> ligand complexes **A** coordinated in η<sup>1:1</sup>-mode only. Further, the P<sub>2</sub> ligand complex **A** was reacted with the Cu(I) salts [Cu(CH<sub>3</sub>CN)<sub>4</sub>][BF<sub>4</sub>] (**B**) and [Cu(CH<sub>3</sub>CN)<sub>4</sub>][TEF] (**E**), respectively (**Scheme 7-9**).



**Scheme 7-9.** Reactions of the Mo<sub>2</sub>E<sub>2</sub> complexes **A** (E = P) and **G** (E = As) with the Cu(I) sources [Cu(CH<sub>3</sub>CN)<sub>4</sub>][BF<sub>4</sub>] (**B**), [Cu(CH<sub>3</sub>CN)<sub>3.5</sub>][FAI] (**C**) and [Cu(CH<sub>3</sub>CN)<sub>4</sub>][TEF] (**F**).

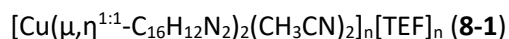
Similar reactions using the As<sub>2</sub> ligand complex [Cp<sub>2</sub>Mo<sub>2</sub>(CO)<sub>4</sub>(μ,η<sup>2:2</sup>-As<sub>2</sub>)] (**G**) and the Cu(I) salts **B**, [Cu(CH<sub>3</sub>CN)<sub>4</sub>][FAI] (**C**) and **E**, respectively, were performed as well. The reactions yielded seven unprecedented coordination compounds, amongst them four novel dinuclear and three novel trinuclear copper complexes. This is the first time that a tetrahedral Mo<sub>2</sub>E<sub>2</sub> (E = P, As) ligand complex was able to connect different metal atoms while also forming a chain of three Cu atoms. The Cu⋯Cu distances in the trinuclear copper complexes **6-1**, **6-2** and **6-6** are below the sum of the *van-der-Waals*-radii and in the range of Cu(I)-Cu(I) single bonds. DFT calculations for **6-1** at the B3LYP/def2-TZVP level of theory could also support the suggested intramolecular metallophilic interactions. They further revealed that the bonding of the peripheral Cu ions to the Mo<sub>2</sub>P<sub>2</sub> ligands in **6-1** takes place via the coordination of the phosphorus lone pairs, while the central Cu ion binds to the P-P σ-orbital of the Mo<sub>2</sub>P<sub>2</sub> unit. A Wiberg Bond Index (WBI) of 0.11 has been found between the central and peripheral Cu(I) ions, leading to the conclusion that a Cu-Cu interaction is present. It can further be concluded, that the As<sub>2</sub> ligand complex **G** has a higher tendency to coordinate in an η<sup>2</sup>-fashion and additionally in a η<sup>1:1</sup>-mode in comparison to the P<sub>2</sub> complex **A**.

## References:

- [1] M. E. Moussa, B. Attenberger, E. V. Peresykina, M. Fleischmann, G. Balázs, M. Scheer *Chem. Commun.* **2016**, *52*, 10004-10007.
- [2] The CPs' cavities are calculated by subtracting the sum of the *van-der-Waals*-radii from the distances obtained from the X-ray experiment. The *van-der-Waals*-radii are taken from: P. Pykkö, M. Atsumi, *Chem. Eur. J.* **2009**, *15*, 186-197.
- [3] P. Pykkö, M. Atsumi, *Chem. Eur. J.* **2009**, *15*, 186-197.
- [4] H. Schmidbaur, A. Schier, *Angew. Chem. Int. Ed.* **2015**, *54*, 746-784; *Angew. Chem.* **2015**, *127*, 756-797.
- [5] a) M. Scheer, L. J. Gregoriades, M. Zabel, J. Bai, I. Krossing, G. Bruncklaus, H. Eckert *Chem. Eur. J.* **2008**, *14*, 282-295; M. Fleischmann, S. Welsch, E. V. Peresykina, A. V. Virovets, M. Scheer, *Chem. Eur. J.* **2015**, *21*, 14332-14336.
- [6] M. E. Moussa, M. Seidl, G. Balázs, M. Zabel, A. V. Virovets, B. Attenberger, A. Schreiner, M. Scheer *Chem. Eur. J.* **2017**, *23*, 16199-16203.

## 8 Thesis Treasury

### 8.1 Discussion



Compound **8-1** was obtained in a reaction of the P<sub>2</sub> ligand complex [Cp<sub>2</sub>Mo<sub>2</sub>(CO)<sub>4</sub>(μ, η<sup>2:2</sup>-P<sub>2</sub>)] (**A**) with the Cu(I) salt [Cu(CH<sub>3</sub>CN)<sub>4</sub>][TEF] (TEF = Al{OC(CF<sub>3</sub>)<sub>3</sub>}<sub>4</sub>, **CuTEF**) and the organic linker 1,4-di(4-pyridyl)benzene (**L<sub>lin</sub>3**) and layering of the crude reaction mixture with *n*-pentane/dichloromethane (1:1). **8-1** crystallises as clear light-yellow blocks in the tetragonal space group *P4<sub>2</sub>bc* (**Table 8-1**, **Figure 8-1**). The Cu(I) centres are tetra-coordinated. Two molecules of linker **L<sub>lin</sub>3** are coordinated to every Cu(I) centre, whose coordination sphere is completed by two acetonitrile ligands. The Cu-N bond lengths lie in the range of 1.924(4)-2.067(4) Å and the N-Cu-N angles have values between 96.5(2) and 127.1(3) °.

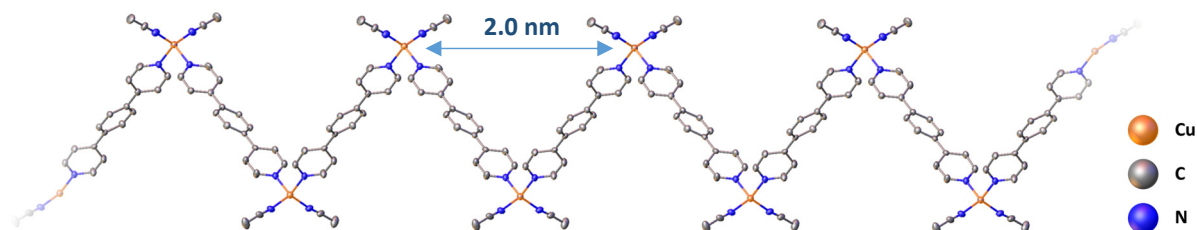
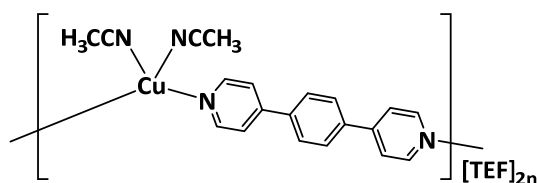
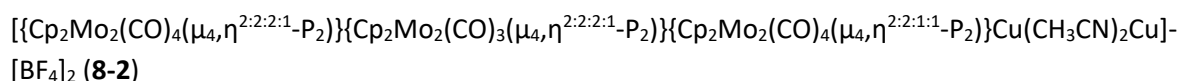


**Figure 8-1.** Molecular structure of the cationic chain of **8-1** in the solid-state. Cp- and CO-ligands and hydrogen atoms are omitted for clarity. Thermal ellipsoids are shown at 50 % probability level.<sup>[1]</sup>

Experimental Procedure:



The P<sub>2</sub> ligand complex **A** (1 eq., 50 mg, 0.1 mmol), **CuTEF** (1 eq., 186 mg, 0.1 mmol) and **L<sub>lin</sub>3** (1 eq., 23 mg, 0.1 mmol) were dissolved in a 1:1-mixture of acetonitrile/dichloromethane (5 mL) and stirred for 3 h. The reaction mixture was filtered and layered with *n*-pentane/dichloromethane (1:1-mixture). After one day, crystals of **8-1** were obtained as clear light-yellow blocks. The supernatant was decanted off, the remaining crystals washed with *n*-pentane and dried in vacuo. Crystalline Yield: 7 mg (5.3 %, related to **L<sub>lin</sub>3**).



Compound **8-2** was obtained during the reaction of the P<sub>2</sub> ligand complex [Cp<sub>2</sub>Mo<sub>2</sub>(CO)<sub>4</sub>(μ,η<sup>2:2</sup>-P<sub>2</sub>)] (**A**) with the Cu(I) salt [Cu(CH<sub>3</sub>CN)<sub>4</sub>BF<sub>4</sub>] (**CuBF<sub>4</sub>**) and layering of the crude reaction mixture with *n*-pentane/dichloromethane (1:1). **8-2** crystallises as metallic dark black blocks in the triclinic space group *P* $\bar{1}$  (**Table 8-1, Figure 8-2**); its structure was revealed by single crystals X-ray crystallography. The coordination complex **8-2** contains two Cu(I) centres with a Cu1...Cu2 distance of 2.5864(7) Å, which is still above the sum of the covalent radii of Cu (112 pm).<sup>[2]</sup> Two units of Mo<sub>2</sub>P<sub>2</sub> are coordinated to the Cu(I) centres in a η<sup>2:1</sup>-coordination mode; a third unit is coordinated to Cu1 and Mo3 in a η<sup>1:1</sup>-coordination mode. One CO-ligand of Mo3 has been removed and two acetonitrile ligands are coordinated to Cu2, completing the tetragonal coordination sphere of Cu2. The coordination sphere of Cu1 can either be described as distorted tetragonal pyramidal or a hexagonal pyramid with one position unoccupied, depending on the existence of an interaction between the two copper(I) centres. In both cases, Cu1 sticks out of the plane by 0.7049(6) Å and the P<sub>axial</sub>-Cu-P angles have, due to the distortion, values larger than 90° (99.79(3)-123.91(3)°). The angles with Cu1 as central atom have values close to 60° (52.25(3)-56.08(2)°) and 120° (P1-Cu1-P3 126.53(3)°), respectively, supporting the suggestion of a hexagonal pyramidal coordination sphere. Reason for the CO-abstraction at Mo3 could be the influence of UV light. A directed abstraction of CO- ligands of P<sub>n</sub> ligand complexes could lead to a whole new field of coordination compounds.

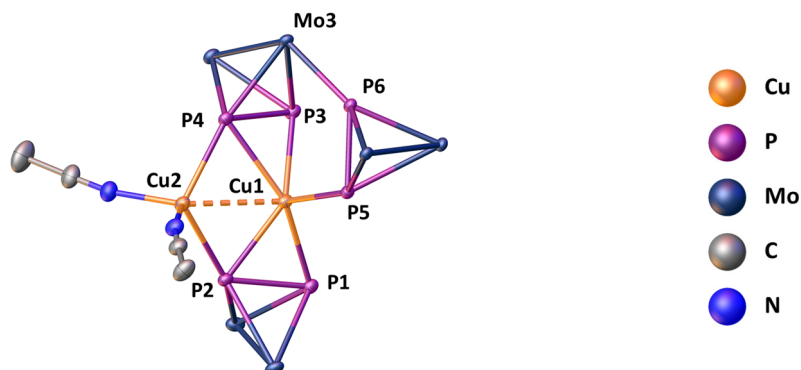
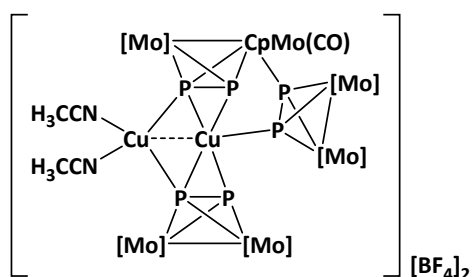


**Figure 8-2.** Molecular structure of the cation of **8-2** in the solid-state. Cp- and CO- ligands and hydrogen atoms are omitted for clarity. Thermal ellipsoids are shown at 50 % probability level. Average of selected bond lengths [Å] and angles [°]: Cu1-Cu2 2.5864(7), Cu1-P1 2.3654(9), Cu1-P2 2.4037(9), Cu1-P3 2.3957(9), Cu1-P4 2.4864(9), Cu1-P5 2.3711(9), Cu2-P2 2.3513(9), Cu2-P4 2.3398(9), P2-P1 2.1612(12), P4-P3 2.1511(11), P6-P5 2.1051(11), Mo3-P6 2.4398(8), P1-Cu1-Cu2 109.96(3), P2-Cu1-Cu2 56.08(2), P3-Cu1-Cu2 102.58(3), P4-Cu1-Cu2 54.89(2), P5-Cu1-Cu2 113.57(3), P5-Cu1-Cu2 113.57(3), P5-Cu1-P4 99.79(3), P5-Cu1-P3 100.85(3), P5-Cu1-P2 123.91(3), P3-Cu1-P4 52.25(3), P3-Cu1-P2 134.73(3), P2-Cu1-P4 108.09(3), P1-Cu1-P5 103.31(3), P1-Cu1-P4 156.36(3), P1-Cu1-P3 126.53(3), P1-Cu1-P2 53.89(3).



Experimental procedure:



The P<sub>2</sub> ligand complex **A** (25 mg, 0.05 mmol) was reacted with the Cu(I) salt **CuBF<sub>4</sub>** (110 mg, 0.35 mmol). Both **A** and **CuBF<sub>4</sub>** were dissolved in dichloromethane (4 mL and 2 mL, respectively) and the solution of **CuBF<sub>4</sub>** slowly added to the solution of **A**. Additional dichloromethane (5 mL) and acetonitrile (0.5 mL) were added. After stirring for 1 h, the reaction mixture was filtered and layered with a 1:1-mixture of *n*-pentane and dichloromethane. After one week, a few small metallic dark black crystals could be observed on the bottom of the schlenk. The crystals were analysed by single crystal X-ray analysis. The supernatant was decanted off, the remaining crystals washed with *n*-pentane and dried in vacuo. Crystalline Yield: A few crystals (< 5%).

$[\text{Cu}_2\{\text{Cp}_2\text{Mo}_2(\text{CO})_4(\mu, \eta^{2:2:1:1}\text{-P}_2)\}_2(\mu, \eta^{1:1}\text{-C}_{13}\text{H}_{14}\text{N}_2)_2]_n[\text{FAI}]_{2n}$  (**8-3**) and  $\{[\text{Cp}_2\text{Mo}_2(\text{CO})_4(\mu, \eta^{2:2:1:1}\text{-P}_2)\}_2(\mu, \eta^{1:1}\text{-C}_{13}\text{H}_{14}\text{N}_2)(\text{CH}_3\text{CN})_2\text{Cu}_2\}_n[\text{FAI}]_{2n}$  (**8-4**)

**8-3** was obtained by the reaction of  $\text{P}_2$  ligand complex  $[\text{Cp}_2\text{Mo}_2(\text{CO})_4(\mu, \eta^{2:2}\text{-P}_2)]$  (**A**) with the Cu(I) salt  $[\text{Cu}(\text{CH}_3\text{CN})_{3.5}][\text{FAI}]$  (**CuFAI**,  $\text{FAI} = \text{FAI}\{\text{O}(\text{C}_6\text{F}_{10})(\text{C}_6\text{F}_5)\}_3$ ) and the organic linker 1,3-bis(4-pyridyl)propane (**L<sub>flex</sub>1**) in a solution of dichloromethane and acetonitrile, layering of the crude reaction mixture with *n*-pentane/dichloromethane (1:1) and storage at -28 °C. **8-3** crystallises as clear orange blocks in the monoclinic space group  $P2_1/c$ . X-ray crystallography (**Table 8-1**) revealed the formation of a one-dimensional coordination polymer (**Figure 8-3**). The structure of **8-3** is analogous to the one of compound **4-1**, with exception of the metal ion. As in **4-1**, a six-membered  $\text{Cu}_2\text{P}_4$ -ring serves as node. The tetragonal coordination sphere of the Cu(I) centres are made-up of two phosphorus atoms from the  $\text{P}_2$  ligand complex **A** and two nitrogen atoms of linker **L<sub>flex</sub>1**. The nodes are connected to each other via two molecules of linker per node. Two linker molecules of the same node but different Cu(I) centres are attached to the next node, meaning that the six-membered  $\text{Cu}_2\text{P}_4$ -ring is not in alignment with the direction of the one-dimensional strand but turned by 90 °. Like in **4-3**, the cavities have sizes of approximately 1 nm<sup>[1]</sup> and are filled with solvent molecules and anions. The bond lengths and angles are comparable to **4-3**, the reported dimeric complexes  $[\text{Cu}_2(\text{Cp}_2\text{Mo}_2(\text{CO})_4(\mu, \eta^{2:2:1:1}\text{-P}_2)_2\text{-}(\text{Cp}_2\text{Mo}_2(\text{CO})_4(\mu, \eta^{2:2:2}\text{-P}_2)_2)]^{2+}$  (**D**)<sup>[3,4]</sup> and similar coordination polymers.<sup>[3,5]</sup>

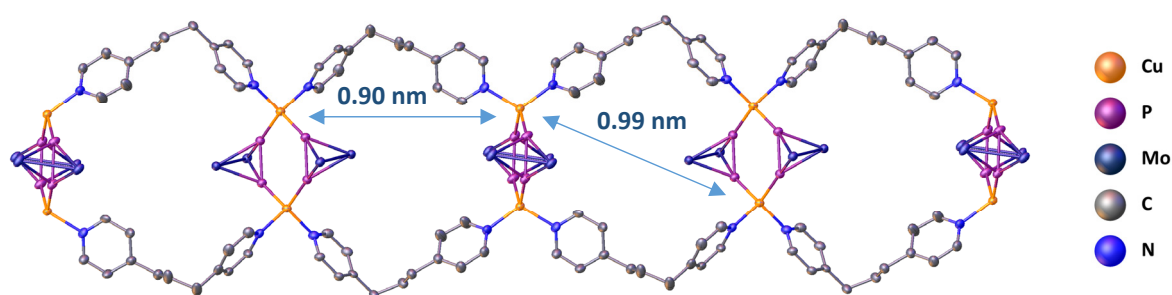


**Figure 8-3.** Molecular structure of the cation of **8-3** in the solid-state along the *a*-axis. Thermal ellipsoids are shown at 50 % probability level. Hydrogen atoms, Cp- and CO-ligands omitted for clarity. Selected bond lengths [Å] and angles [°]: Cu1-P2 2.2939(7), Cu1-P1 2.2673(6), Cu1-N1A 2.01(1), Cu1-N4A 2.01(2), Cu2A-P3A 2.304(6), Cu2A-P4A 2.235(5), Cu2A-N2A 2.024(5), Cu2A-N3A 2.067(8), P2-P1 2.0809(8), P3A-P4A 2.083(7), P1-Cu1-P2 107.03(2), N1A-Cu1-P1 110.0(4), N1A-Cu1-P2 121.0(3), N4A-Cu1-P1 117.3(4), N4A-Cu1-P2 103.1(4), N4A-Cu1-N1A 98.8(5), P4A-Cu2A-P3A 106.2(2), N3A-Cu2A-P3A 104.6(5), N2A-Cu2A-P3A 114.8(3), N2A-Cu2A-P4A 105.1(2), N3A-Cu2A-P4A 113.8(5), N2A-Cu2A-N3A 112.5(4).<sup>[1]</sup>

**8-4** was obtained as a side product to **8-3** when the crude reaction mixture was layered with *n*-pentane. The clear orange blocks were also analysed by single crystal X-ray analysis. **8-4** also crystallizes in a monoclinic space group ( $P2_1/c$ ) and consists of a one-dimensional CP (**Figure 8-4**). Like in **8-3**, a six-membered  $\text{Cu}_2\text{P}_4$ -ring serves as a node and the Cu(I) centres of the node are tetra-coordinated. The nodes are connected to each other via one molecule of linker per node. The coordination sphere of the Cu(I) centres are saturated by acetonitrile ligands. The bond lengths and angles in **8-4**, like **8-3**, are comparable to those of the reported  $\text{Cu}_2\text{A}_4$  complexes<sup>[3]</sup> and similar coordination polymers.<sup>[3b,5]</sup> The sizes of the cavities formed by this network are also approximately 1 nm in diameter.<sup>[1]</sup>

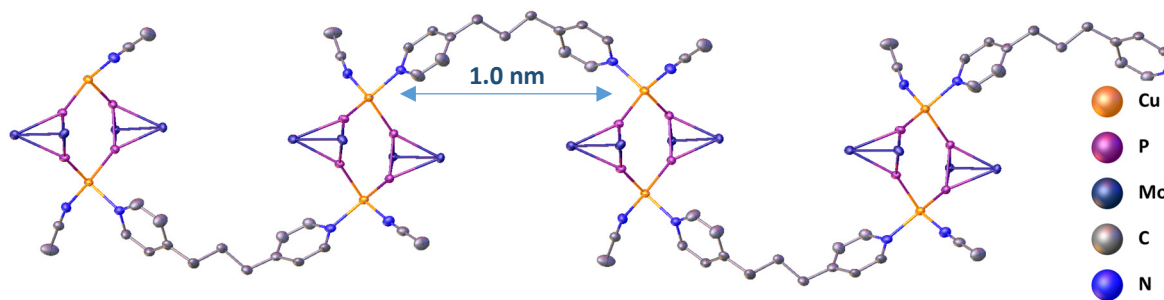
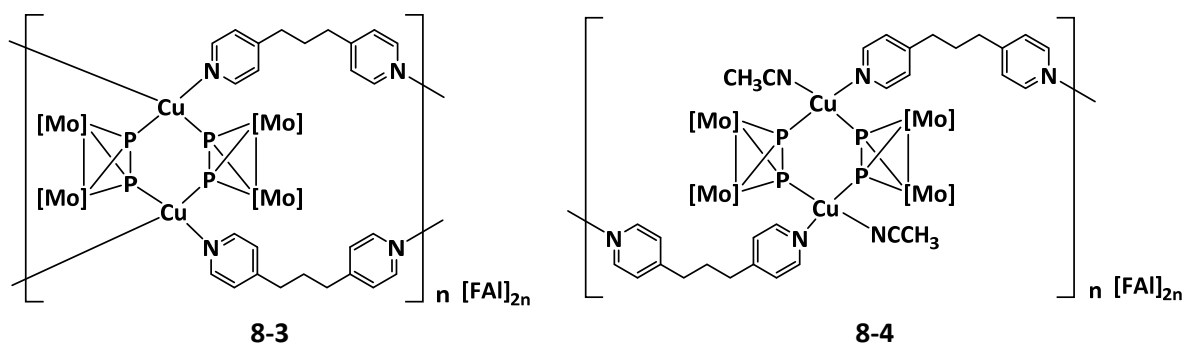


**Figure 8-4.** Molecular structure of the cation of **8-4** in the solid-state along the *a*-axis. Thermal ellipsoids are shown at 50 % probability level. Hydrogen atoms, Cp- and CO-ligands are omitted for clarity. Selected bond lengths [Å] and angles [°]: P2-P1 2.086(1), P4-P3 2.082(1), Cu2-P2 2.2853(8), Cu2-P3 2.2506(8), Cu2-N3 2.048(2), Cu2-N4 1.991(2), Cu1-P1 2.2523(8), Cu1-P4 2.3243(8), Cu1-N1 2.040(2), Cu1-N2 1.995(3), P1-Cu1-P4 107.81(3), N1-Cu1-P1 124.09(7), N1-Cu1-P4 100.07(7), N2-Cu1-P1 112.75(8), N2-Cu1-P4 107.22(8), N2-Cu1-N1 103.3(1), P3-Cu2-P2 107.44(3), N3-Cu2-P2 103.47(7), N4-Cu2-P2 109.70(8), N3-Cu2-P3 115.30(7), N4-Cu2-P3 118.59(8), N4-Cu2-N3 101.3(1).<sup>[1]</sup>

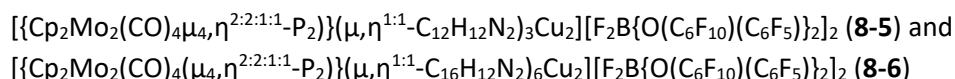
Experimental Procedures:



**8-3:** The P<sub>2</sub> ligand complex **A** (1 eq., 50 mg, 0.1 mmol), **CuFAI** (1 eq., 159 mg, 0.1 mmol) and **L<sub>flex</sub>1** (1 eq., 20mg, 0.1 mmol) were dissolved in a 1:1 mixture of dichloromethane and acetonitrile. The reaction was stirred for 3 h, filtered and layered with a 1:1 mixture of *n*-pentane and dichloromethane and pure *n*-pentane. As no crystals had formed after several days, the mixture was stored at -28 °C. After some days, few orange blocks of compound **8-3** could be obtained. The supernatant was decanted off, the remaining crystals washed with *n*-pentane and dried in vacuo. Crystalline Yield: A few crystals (< 5%).

**8-3 + 8-4:**

The P<sub>2</sub> ligand complex **A** (1 eq., 25 mg, 0.05 mmol), **CuFAI** (1.5 eq., 119 mg, 0.075 mmol) and **L<sub>flex</sub>1** (1 eq., 10 mg, 0.05 mmol) were dissolved in dichloromethane (15 mL) and acetonitrile (2 mL) and stirred overnight. Acetonitrile (1 mL) was added to clear the turbid solution and the reaction was stirred overnight, filtrated, and layered with *n*-pentane. After a few days, compounds **8-3** and **8-4** were obtained as orange blocks. The supernatant was decanted off, the remaining crystals washed with *n*-pentane and dried in vacuo. Crystalline Yield: A few crystals (< 5%).



**8-5** was obtained by the reaction of the  $\text{P}_2$  ligand complex  $[\text{Cp}_2\text{Mo}_2(\text{CO})_4(\mu, \eta^{2:2}\text{-P}_2)]$  (**A**) with the Cu(I) salt  $[\text{Cu}(\text{CH}_3\text{CN})_{3.5}][\text{FAI}]$  (**CuFAI**,  $\text{FAI} = \text{FAI}\{\text{O}(\text{C}_6\text{F}_{10})(\text{C}_6\text{F}_5)\}_3$ ) and the organic linker 1,2-bis(4-pyridyl)ethane (**L<sub>flex</sub>2**) in a concentrated mixture of dichloromethane (5 mL) and acetonitrile (2 mL) and diffusion of *n*-pentane into the crude reaction mixture. **8-5** crystallises as clear orange blocks in the triclinic space group  $P\bar{1}$  (**Table 8-2**). A six-membered  $\text{Cu}_2\text{P}_4$ -ring served as a node. The terminal units of **A** are substituted against **L<sub>flex</sub>2**, which connect the nodes leading to a two-dimensional network. The size of the cavities are up to 2.2 nm in diameter.<sup>[1]</sup> The bond lengths and angles are comparable to **4-6** and the reported Cu complexes **D**<sup>[3]</sup> and coordination polymers.<sup>[3,4]</sup>

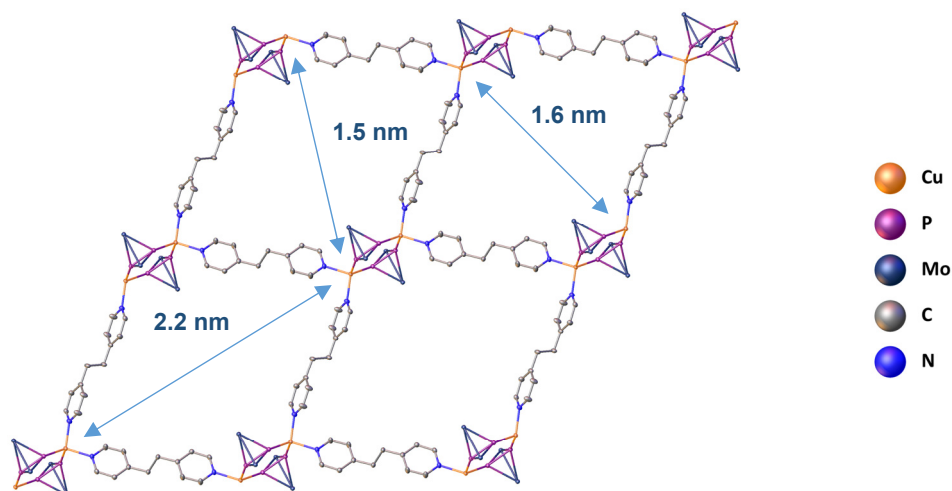


**Figure 8-5.** Molecular structure of the cationic network of **8-5** in the solid-state. Thermal ellipsoids are shown at 50 % probability level. Average of selected bond lengths [Å] and angles [°]: Cu1-P1 2.2611(5), Cu1-P2 2.2939(5), Cu1-N1 2.049(2), Cu1-N2 2.054(2), P1-P2 2.0839(6), P1-Cu1-P2 108.97(2), N1-Cu1-P1 112.19(5), N1-Cu1-P2 116.15(5), N1-Cu1-N2 99.63(7), N2-Cu1-P1 119.16(5), N2-Cu1-P2 100.38(5).<sup>[1]</sup>

**8-6** was obtained by the reaction of the  $\text{P}_2$  ligand complex  $[\text{Cp}_2\text{Mo}_2(\text{CO})_4(\mu, \eta^{2:2}\text{-P}_2)]$  (**A**) with the Cu(I) salt  $[\text{Cu}(\text{CH}_3\text{CN})_{3.5}][\text{FAI}]$  (**CuFAI**,  $\text{FAI} = \text{FAI}\{\text{O}(\text{C}_6\text{F}_{10})(\text{C}_6\text{F}_5)\}_3$ ) and the organic linker 1,4-di(4-pyridyl)benzene (**L<sub>lin</sub>3**) in a concentrated 1:1-mixture of dichloromethane and acetonitrile (5 mL) and diffusion of *n*-pentane into the crude reaction mixture. **8-6** crystallises as orange blocks in the triclinic space group  $P\bar{1}$ . The solid-state structure of **8-6** was determined by single crystal X-ray crystallography (**Table 8-2**). Unlike **8-5**, there is no six-membered  $\text{Cu}_2\text{P}_2$  ring serving as node. Instead, a unit of the  $\text{P}_2$  complex **A** between two Cu(I) centres is the smallest metal-organic building block in the network (**Figure 8-6**). This structural motif has not been observed in the compounds presented in the thesis. However, a two-dimensional organometallic-organic CP exhibiting a six-membered  $\text{Ag}_2\text{P}_2$  ring as node have been reported using the Ag(I) salt  $\text{AgAl}\{\text{OC}(\text{CF}_3)_3\}_4$  and the organic linker 1,2-di-(4-pyridyl)ethylene (**dpe**).<sup>[6]</sup>

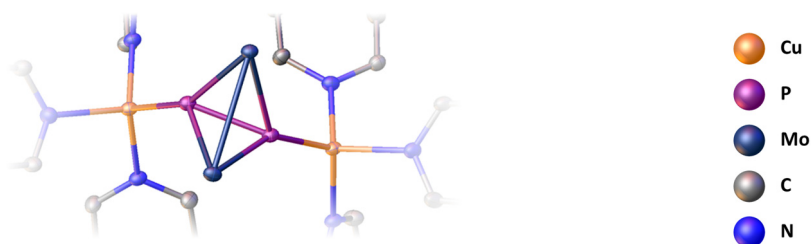


**Figure 8-6.** Section of solid-state structure of the cation of **8-6**, showing the  $\text{Cu}_2\text{P}_2$  building block. Thermal ellipsoids are shown at 50 % probability level. Average of selected bond lengths [ $\text{\AA}$ ] and angles [ $^\circ$ ]: Cu-P 2.2049(5)-2.2350(5), P1-P2 2.0915(7), Cu-N 2.026(2)-2.064(2), P-Cu-N 105.38(5)-121.48(5), N-Cu-N 102.19(7)-109.49(7).

The Cu atoms are tetracoordinated, meaning that three linker molecules connect to each Cu(I) centre. The  $\text{Cu}_2\text{P}_2$  building blocks are connected to each other by two linker molecules, forming a one-dimensional zig zag strand (**Figure 8-7**).

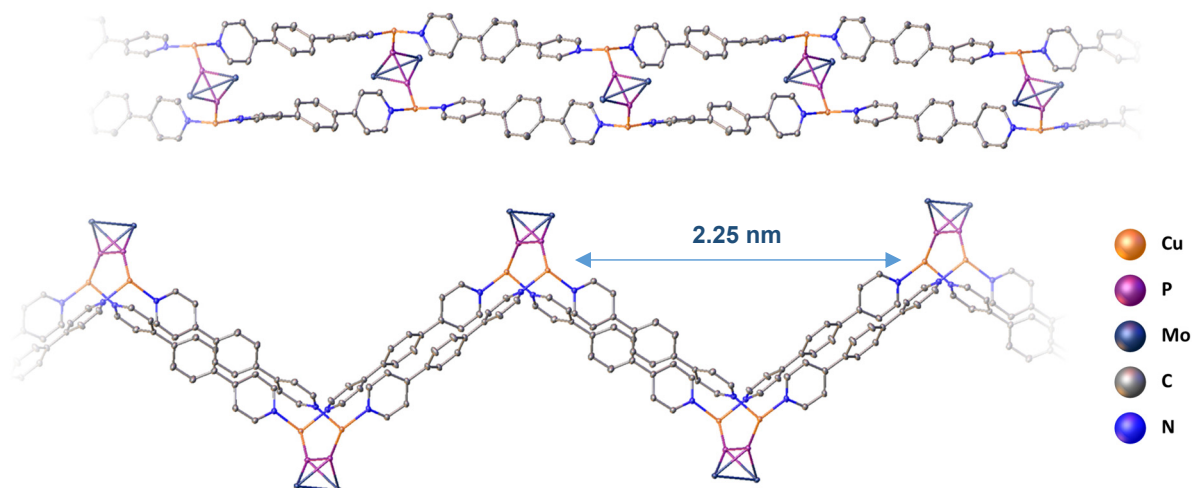


**Figure 8-7.** Two different views on sections of the one-dimensional strand within the solid-state structure of compound **8-6**. Thermal ellipsoids are shown at 50 % probability level.<sup>[1]</sup>

Furthermore, these one-dimensional strands are linked to each other by linker molecules (**Figure 8-8**, red rectangles). Every second of those one-dimensional strands is twisted by about  $180^\circ$ . By this connection, cavities made-up of  $[(\text{Cu}_4\text{P}_4\text{L}_{\text{lin}}\mathbf{3}_4)_2(\text{Cu}_2\text{P}_2\text{L}_{\text{lin}}\mathbf{3})_2]$ -fragments is formed (yellow squares). Those fragments are connected to each other by linker molecules so that a one-dimensional pipe is formed. These are again connected to each other by a pair of linker molecules (blue ellipsoids), which in turn are part of a neighbouring  $[(\text{Cu}_4\text{P}_4\text{L}_{\text{lin}}\mathbf{3}_4)_2(\text{Cu}_2\text{P}_2\text{L}_{\text{lin}}\mathbf{3})_2]$ -fragment.

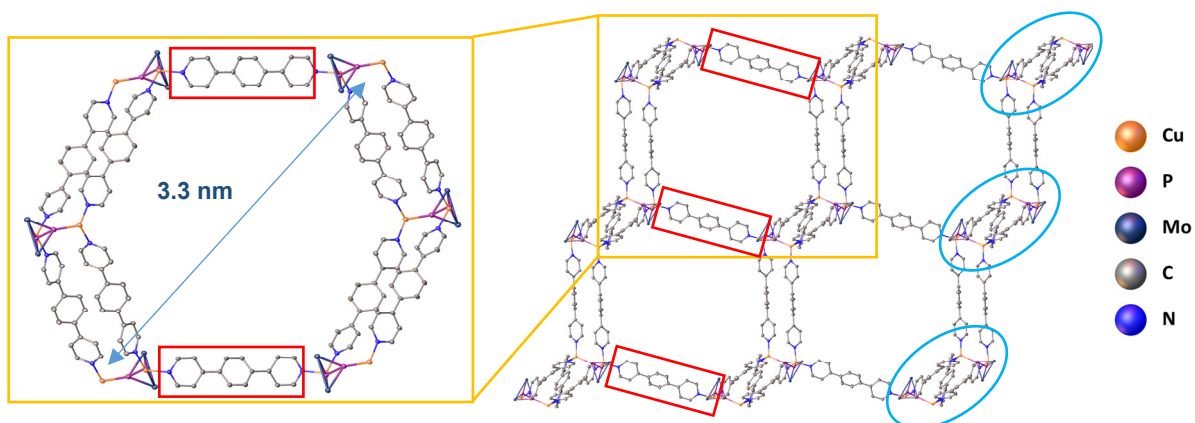


**Figure 8-8.** Different views on the solid-state structure of compound **8-6**. Thermal ellipsoids are shown at 50 % probability level.<sup>[1]</sup>

The refinement of the X-ray structures of compounds **8-5** and **8-6** further revealed the structure of a new WCA (**Figure 8-9**). This new anion appears to have been formed as a side-product in the synthesis of  $[\text{Cu}(\text{CH}_3\text{CN})_{3.5}][\text{FAI}]$ , which is performed by reacting  $\text{LiFAI}$  with  $[\text{Cu}(\text{CH}_3\text{CN})_4][\text{BF}_4]$  in dichloromethane. The FAI anion consists of a central aluminium atom with one fluorine atom and three  $\{\text{O}(\text{C}_6\text{F}_{10})(\text{C}_6\text{F}_5)\}$ -fragments attached. In the new found WCA, a central boron atom is surrounded by two fluorine atoms and two  $\{\text{O}(\text{C}_6\text{F}_{10})(\text{C}_6\text{F}_5)\}$ -fragments. Negative ion ESI mass spectrometry ( $\text{CH}_3\text{CN}$ , r.t.) could confirm the formation of the Bal ( $\text{Bal} = [\text{F}_2\text{B}\{\text{O}(\text{C}_6\text{F}_{10})(\text{C}_6\text{F}_5)\}_2]^-$ ) anion. In the  $^{11}\text{B}$  NMR spectrum of **8-6**, a triplet at 0.85 ppm with a coupling constant of  $J = 22$  Hz was observed, hinting to B-F coupling. As boron is smaller than fluorine, a third  $\{\text{O}(\text{C}_6\text{F}_{10})(\text{C}_6\text{F}_5)\}$ -fragment might not be possible to bond to the central boron atom due to steric hindrance. Compared to FAI, the new  $[\text{F}_2\text{B}\{\text{O}(\text{C}_6\text{F}_{10})(\text{C}_6\text{F}_5)\}_2]^-$  (= Bal) anion is not as big, but flatter. This appears to have been beneficial for the formation of compounds **8-5** and **8-6**, which makes the direct synthesis of this anion very interesting. A non-spherical but flat anion could lead to a whole new set of coordination polymers and might even facilitate the formation of three-dimensional CPs.

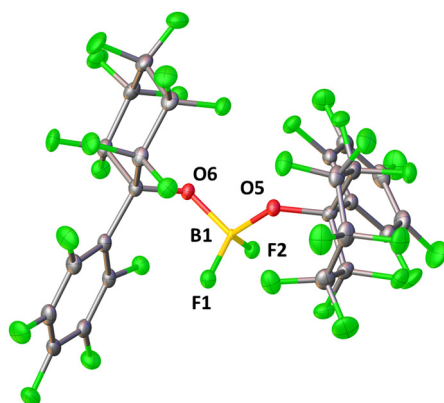
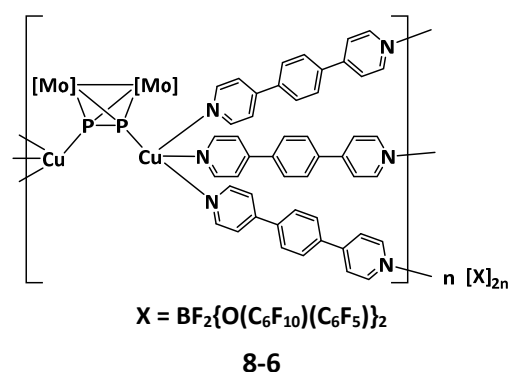
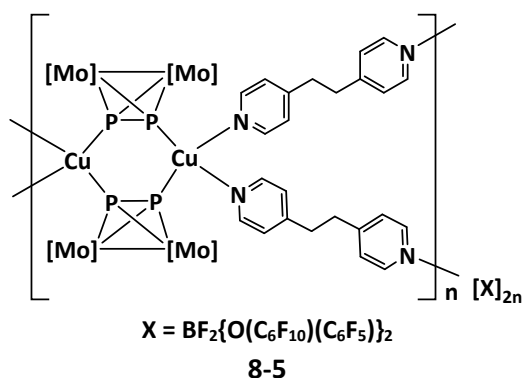


**Figure 8-9.** Molecular structure of the Bal-anion of **8-5** in the solid-state. Thermal ellipsoids are shown at 50 % probability level. Average of selected bond lengths [ $\text{\AA}$ ] and angles [ $^\circ$ ]: B1-F1 1.395(2), B1-F2 1.389(2), B1-O5 1.504(2), B1-O6 1.512(2), F1-B1-O5 109.8(1), F1-B1-O6 110.7(1), F2-B1-F1 111.8(2), F2-B1-O5 111.3(1), F2-B1-O6 107.0(1), O5-B1-O6 106.1(1).

Experimental Procedures:



**8-5:** The P<sub>2</sub> ligand complex **A** (1.2 eq., 30 mg, 0.06 mmol), **CuFAI** (1 eq., 79 mg, 0.05 mmol) and **L<sub>lin</sub>3** (1 eq., 9.2 mg, 0.05 mmol) were dissolved in dichloromethane (5 mL). Acetonitrile (2 mL) was added, the reaction stirred for 3 h, filtrated and layered with *n*-pentane. After a few days, compound **8-5** was obtained as clear orange blocks. The supernatant was decanted off, the remaining crystals washed with *n*-pentane and dried in vacuo. Crystalline Yield: A few crystals (< 5%). <sup>1</sup>H-NMR δ[ppm] = 8.42 (d, CH<sub>pyr.</sub>), 7.22 (d, CH<sub>pyr.</sub>), 5.31 (s, C<sub>5</sub>H<sub>5</sub>), 2.66 (t, *J* = 7.67 Hz, CH<sub>2</sub>). <sup>31</sup>P-NMR δ[ppm] = -45.1 (s).

**8-6:** The P<sub>2</sub> ligand complex **A** (1 eq., 50 mg, 0.1 mmol), **CuFAI** (1 eq., 159 mg, 0.1 mmol) and **L<sub>lin</sub>3** (1 eq., 23 mg, 0.1 mmol) were dissolved in a 1:1 mixture of dichloromethane and acetonitrile (5 mL). The reaction was stirred overnight, filtrated and layered with *n*-pentane. After a few days, compound **8-6** was obtained as orange blocks. The supernatant was decanted off, the remaining crystals washed with *n*-pentane and dried in vacuo. Crystalline Yield: A few crystals (< 5%). <sup>1</sup>H-NMR δ[ppm] = 8.64 (dd, CH<sub>pyr.</sub>), 7.90 (s, CH<sub>arom.</sub>), 7.72 (dd, CH<sub>pyr.</sub>), 5.32 (s, C<sub>5</sub>H<sub>5</sub>). <sup>31</sup>P-NMR δ[ppm] = -50.81 (s). <sup>11</sup>B-NMR δ[ppm] = 0.85 (t, *J* = 22 Hz). Positive ion ESI-MS (CH<sub>3</sub>CN, r.t.): *m/z* (%) = 103.96 (100) [Cu(CH<sub>3</sub>CN)]<sup>+</sup>, 144.98 (100) [Cu(CH<sub>3</sub>CN)<sub>2</sub>]<sup>+</sup>, 233.11 (100) [C<sub>16</sub>H<sub>13</sub>N<sub>2</sub>]<sup>+</sup>, 336.06 (100) [Cu(C<sub>16</sub>H<sub>12</sub>N<sub>2</sub>){CH<sub>3</sub>CN}]<sup>+</sup>, 527.13 (100) [Cu(C<sub>16</sub>H<sub>12</sub>N<sub>2</sub>)<sub>2</sub>]<sup>+</sup>, 599.77 (100) [Cu(CH<sub>3</sub>CN){Cp<sub>2</sub>Mo<sub>2</sub>(CO)<sub>4</sub>P<sub>2</sub>}]<sup>+</sup>, 790.85 (55.5) [Cu(C<sub>16</sub>H<sub>12</sub>N<sub>2</sub>){Cp<sub>2</sub>Mo<sub>2</sub>(CO)<sub>4</sub>P<sub>2</sub>}]<sup>+</sup>, 1056.56 (60) [Cu{Cp<sub>2</sub>Mo<sub>2</sub>(CO)<sub>4</sub>P<sub>2</sub>}]<sup>+</sup>. Negative ion ESI-MS (CH<sub>3</sub>CN, r.t.): *m/z* (%) = 938.95 (100) [F<sub>2</sub>B{O(C<sub>6</sub>F<sub>10</sub>)(C<sub>6</sub>F<sub>5</sub>)<sub>2</sub>}]<sup>-</sup>, 1380.90 (38.9) [FAI{O(C<sub>6</sub>F<sub>10</sub>)(C<sub>6</sub>F<sub>5</sub>)<sub>3</sub>}]<sup>-</sup>.<sup>i</sup> Elemental analysis calculated for B<sub>2</sub>C<sub>110</sub>Cu<sub>2</sub>F<sub>64</sub>H<sub>46</sub>Mo<sub>2</sub>N<sub>6</sub>O<sub>8</sub>P<sub>2</sub> · CH<sub>2</sub>Cl<sub>2</sub> (3283.84 g·mol<sup>-1</sup>): 40.56 %C, 1.47 %H, 2.56 %N; Found: 40.53 %C, 1.60 %H, 2.14 %N.

<sup>i</sup> The presence of the FAI-anion in the negative ion ESI-MS spectrum can be explained by the fact that a different charge of crystals, containing residual [Cu(CH<sub>3</sub>CN)<sub>3.5</sub>][FAI], was used for the analysis.

$[\{\text{Cp}_2\text{Mo}_2(\text{CO})_4(\mu, \eta^{2:2:1:1}\text{-P}_2)_2(\mu, \eta^{1:1}\text{-C}_{22}\text{H}_{16}\text{N}_2)_2\text{Cu}_2\}]_n[\text{FAI}\{\text{O}(\text{C}_6\text{F}_{10})(\text{C}_6\text{F}_5)\}_3]_2$  (**8-7**) and  
 $[\{\text{Cp}_2\text{Mo}_2(\text{CO})_4(\mu, \eta^{2:2:1:1}\text{-P}_2)(\mu, \eta^{1:1}\text{-C}_{22}\text{H}_{16}\text{N}_2)_3\text{Cu}_2\}]_n[\text{FAI}\{\text{O}(\text{C}_6\text{F}_{10})(\text{C}_6\text{F}_5)\}_3]_2$  (**8-8**)

Compound **8-7** was obtained by the reaction of the  $\text{P}_2$  ligand complex  $[\text{Cp}_2\text{Mo}_2(\text{CO})_4(\mu, \eta^{2:2}\text{-P}_2)]$  (**A**) with the Cu(I) salt  $[\text{Cu}(\text{CH}_3\text{CN})_{3.5}][\text{FAI}]$  (**CuFAI**,  $\text{FAI} = \text{FAI}\{\text{O}(\text{C}_6\text{F}_{10})(\text{C}_6\text{F}_5)\}_3$ ) and the organic linker 1,4-di(4-pyridyl)benzene (**L<sub>lin</sub>3**) in dichloromethane (5 mL) and layering of the crude reaction mixture with *n*-pentane. **8-7** crystallises as orange blocks in the triclinic space group  $P\bar{1}$  (Table 8-3). Single crystal X-ray crystallography of **8-7** revealed the formation of a two-dimensional coordination polymer (Figure 8-10). Like in previously discussed structures, a six-membered  $\text{Cu}_2\text{P}_4$ -ring served as a node and the terminal units of **A** are substituted against **L<sub>lin</sub>3**, which connect the nodes, forming a two-dimensional network. The bond lengths and angles are also comparable to the reported complexes **D**<sup>[3]</sup> and similar coordination polymers.<sup>[3,4]</sup> The size of the cavities made up by the network are up to 2.6 nm in diameter.<sup>[1]</sup>

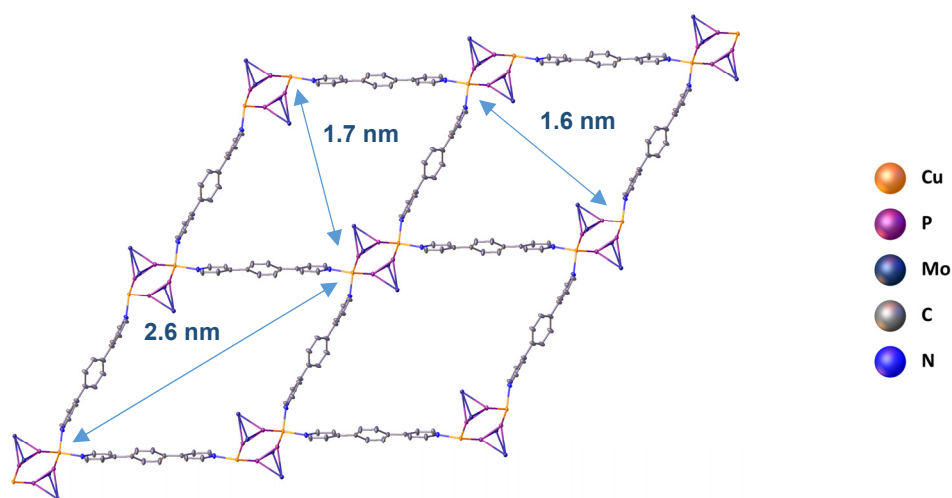


**Figure 8-10.** Molecular structure of the cation of **8-7** in the solid-state along the *a*-axis. Thermal ellipsoids are shown at 50 % probability level. Hydrogen atoms, Cp- and CO-ligands omitted for clarity. Selected bond lengths [Å] and angles [°]: Cu1-P1 2.2740(5), Cu1-P2 2.2635(5), Cu1-N1 2.061(1), Cu1-N2 2.037(1), P1-P2 2.0784(6), P2-Cu1-P1 113.23(2), N1-Cu1-P1 109.67(4), N2-Cu1-P1 109.98(4), N1-Cu1-P2 104.89(4), N2-Cu1-P2 119.80(4), N2-Cu1-N1 97.60(6).<sup>[1]</sup>

Crystals of **8-8** formed by the reaction of the  $\text{P}_2$  ligand complex  $[\text{Cp}_2\text{Mo}_2(\text{CO})_4(\mu, \eta^{2:2}\text{-P}_2)]$  (**A**) with the Cu(I) salt  $[\text{Cu}(\text{CH}_3\text{CN})_{3.5}][\text{FAI}]$  (**CuFAI**,  $\text{FAI} = \text{FAI}\{\text{O}(\text{C}_6\text{F}_{10})(\text{C}_6\text{F}_5)\}_3$ ) and the organic linker 1,4-di(4-pyridyl)benzene (**L<sub>lin</sub>3**) in dichloromethane (5 mL) and acetonitrile (1 mL) and the diffusion of *n*-pentane into the crude reaction mixture. **8-8** crystallises with a yield of 54 %, related to **CuFAI**, as clear light orange blocks in the monoclinic space group  $P2_1/c$  (Table 8-3). The solid-state structure of **8-8** is very similar to compound **8-6**, but the network of **8-8** is not three- but two-dimensional. This is due to the fact that the one-dimensional strands of  $[\text{Cu}_2\text{AL}_{lin}\mathbf{3}]_\infty$  (Figure 8-11), which are connected to each other by linker molecules, are parallel to each other and not twisted by 180°. Thus, a two-dimensional zig-zag sheet is formed with cavities up to 2.06 nm, which are filled with solvent molecules and anions.



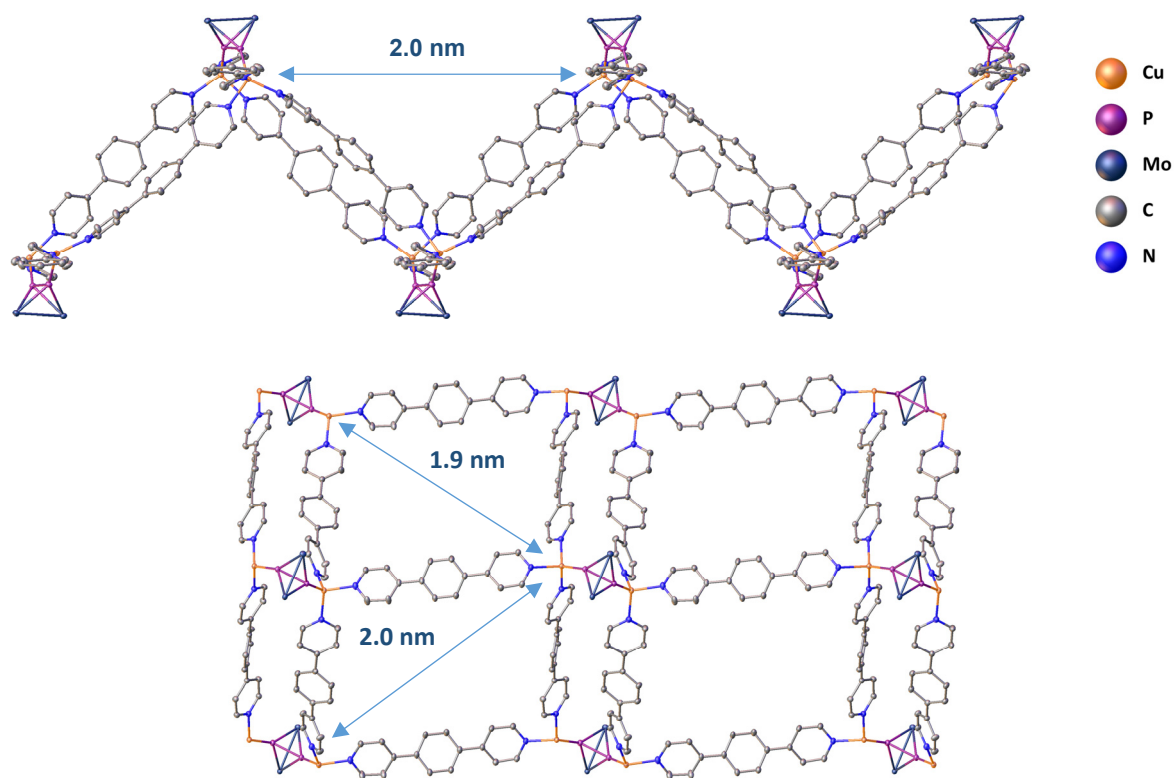
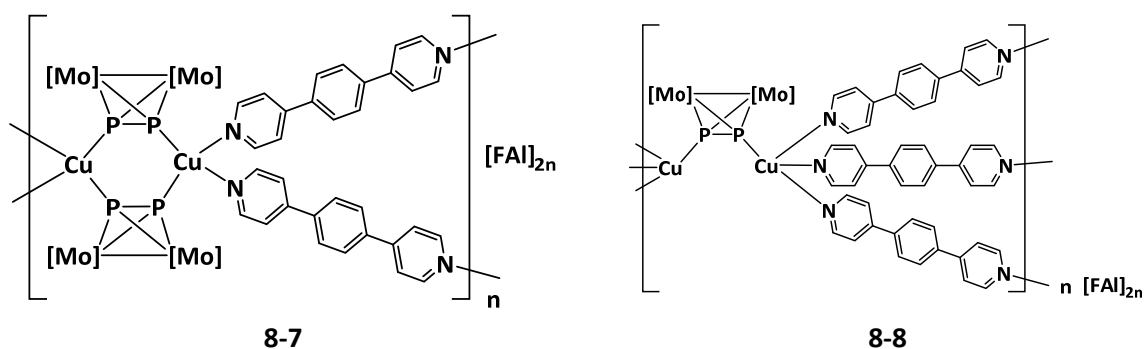


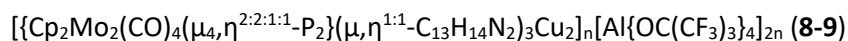
**Figure 8-11.** Molecular structure of the cationic network of **8-8** in the solid-state. Thermal ellipsoids are shown at 50 % probability level. Hydrogen atoms, Cp- and CO-ligands omitted for clarity. Average of selected bond lengths [Å] and angles [°]: Cu1-P2 2.1851(4), Cu2-P1 2.2201(4), P1-P2 2.0925(5), Cu-N 2.043(1)- 2.113(1), P-Cu-N 114.72(4)-120.86(4), N-Cu-N 99.23(5)-103.20(6).<sup>[1]</sup>

## Experimental Procedures:



**8-7:** The P<sub>2</sub> ligand complex **A** (1.2 eq., 30 mg, 0.06 mmol), **CuFAI** (1 eq., 79 mg, 0.05 mmol) and **L<sub>lin</sub>3** (1 eq., 12 mg, 0.05 mmol) were dissolved in dichloromethane (5 mL) and stirred overnight. Acetonitrile (1 mL) was added, the reaction was stirred for 2 h, filtrated and layered with *n*-pentane. After a few days, compound **8-7** was obtained as orange blocks. The supernatant was decanted off, the remaining crystals washed with *n*-pentane and dried in vacuo. Crystalline Yield: 30 mg (28 %, related **CuFAI** and **L<sub>lin</sub>3** equally). <sup>1</sup>H NMR δ[ppm] = 8.64 (dd, 4H, CH<sub>pyr</sub>), 7.90 (s, 4H, CH<sub>arom</sub>), 7.71 (dd, 4H, CH<sub>pyr</sub>), 5.32 (s, 10H, C<sub>5</sub>H<sub>5</sub>). <sup>31</sup>P NMR δ[ppm] = -47.45 (s). <sup>13</sup>C{<sup>1</sup>H} NMR δ[ppm] = 226.58 (s, CO), 148.14 (s, CH<sub>pyr</sub>), 128.76 (s, CH<sub>pyr</sub>), 122.60 (s, CH<sub>pyr</sub>), 87.44 (s, C<sub>5</sub>H<sub>5</sub>). <sup>19</sup>F NMR δ[ppm] = -111.69 (d), -116.12 (d), -121.10 (d), -127.87 (s), -129.78 (d), -136.48 (d), -140.79 (d), -154.00 (m), -164.71 (t), -170.70 (s). Positive ion ESI-MS (CH<sub>3</sub>CN, r.t.): *m/z* (%) = 336.06 (100) [Cu(C<sub>16</sub>H<sub>12</sub>N<sub>2</sub>){CH<sub>3</sub>CN}]<sup>+</sup>, 599.77 (100) [Cu(CH<sub>3</sub>CN){Cp<sub>2</sub>Mo<sub>2</sub>(CO)<sub>4</sub>P<sub>2</sub>}]<sup>+</sup>, 790.85 (55.5) [Cu(C<sub>16</sub>H<sub>12</sub>N<sub>2</sub>){Cp<sub>2</sub>Mo<sub>2</sub>(CO)<sub>4</sub>P<sub>2</sub>}]<sup>+</sup>, 1055.6 (57.7) [Cu{Cp<sub>2</sub>Mo<sub>2</sub>(CO)<sub>4</sub>P<sub>2</sub>}]<sup>+</sup>. Negative ion ESI-MS (CH<sub>3</sub>CN, r.t.): *m/z* (%) = 1380.9 (100) [FAI{O(C<sub>6</sub>F<sub>10</sub>)(C<sub>6</sub>F<sub>5</sub>)}<sub>3</sub>]<sup>-</sup>.

**8-8:** The P<sub>2</sub> ligand complex **A** (1.2 eq., 30 mg, 0.06 mmol), **CuFAI** (1 eq., 79 mg, 0.05 mmol) and **L<sub>lin</sub>3** (2 eq., 23 mg, 0.1 mmol) were dissolved in dichloromethane (5 mL) and stirred overnight. Acetonitrile (1 mL) was added, the reaction was stirred for 2 h, filtrated and layered with *n*-pentane. After a few days, compound **8-8** was obtained as light clear orange blocks. The supernatant was decanted off, the remaining crystals washed with *n*-pentane and dried in vacuo. Crystalline Yield: 37 mg (54 %, related **CuFAI**). IR (solid, CO bands):  $\tilde{\nu}/\text{cm}^{-1}$ : 2012 (ws), 1967 (ws), 1903 (ws). Elemental analysis calculated for C<sub>134</sub>H<sub>46</sub>Al<sub>2</sub>Cu<sub>2</sub>F<sub>92</sub>Mo<sub>2</sub>N<sub>6</sub>O<sub>10</sub>P<sub>2</sub> · C<sub>7</sub>H<sub>8</sub> (4175.82 g·mol<sup>-1</sup>): 40.52 %C, 1.30 %H, 2.01 %N; Found: 40.79 %C, 1.47 %H, 2.18 %N.



Crystals of **8-9** formed after the mother liquor of a three-component reaction of the  $\text{P}_2$  ligand complex  $[\text{Cp}_2\text{Mo}_2(\text{CO})_4(\mu, \eta^{2:2}\text{-P}_2)]$  (**A**), the Cu(I) salt  $[\text{Cu}(\text{CH}_3\text{CN})_4][\text{TEF}]$  (**CuTEF**,  $\text{TEF} = \text{Al}\{\text{OC}(\text{CF}_3)_3\}_4$ ) and the organic linker 1,3-bis(4-pyridyl)propane (**L<sub>flex</sub>1**) was exposed to air, strongly concentrated by evaporation of solvent and stored for one more week at r.t. **8-9** crystallises as orange blocks in the monoclinic space group  $P2_1/c$  (Table 8-3). The solid-state structure of the three-dimensional coordination polymer of **8-9** (Figure 8-12) was analysed by X-ray structure analysis. Like in the previously discussed compound **8-6**, a  $\text{Cu}_2\text{P}_2$  node exists. The nodes are connected to each other via linker molecules and the Cu(I) centres are again tetra-coordinated. Two molecules of **L<sub>flex</sub>1**, which are coordinated to Cu2 (Figure 8-12), connect to the same node. Like this, a  $\text{Cu}_2\text{L}_{\text{flex}1_2}$ -ring with a Cu-Cu distance of 0.8 nm is formed.

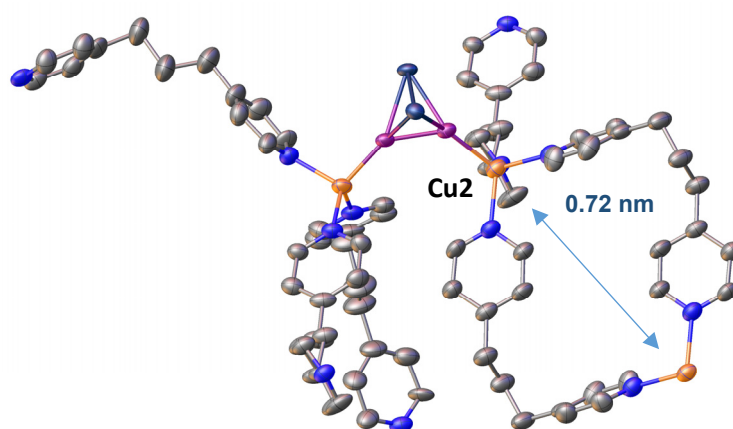


**Figure 8-12.** Detail of the solid-state structure of **8-9** showing the  $\text{Cu}_2\text{P}_2$ -node. Cp- and CO-ligands, hydrogen atoms, anions and solvent molecules are omitted for clarity. Thermal ellipsoids are shown at 50 % probability level. Average of selected bond lengths [Å] and angles [°]: Cu1-P1 2.2066(15), Cu2-P2 2.2196(17), P2-P1 2.081(2), Cu-N 2.037(5)-2.075(6), P-Cu-N 105.94(16)-116.89(18), N-Cu-N 99.4(2)-112.2(2).<sup>[1]</sup>

The other four linker molecules attached to the node connect to four different nodes and thus are not part of a  $\text{Cu}_2\text{L}_{\text{flex}1_2}$ -ring. Those rings however are connected to each other through the nodes and linker molecules, forming a one-dimensional pipe-like  $\text{Cu}_6\text{P}_4\text{L}_{\text{flex}1_6}$ -strand (Figure 8-13).

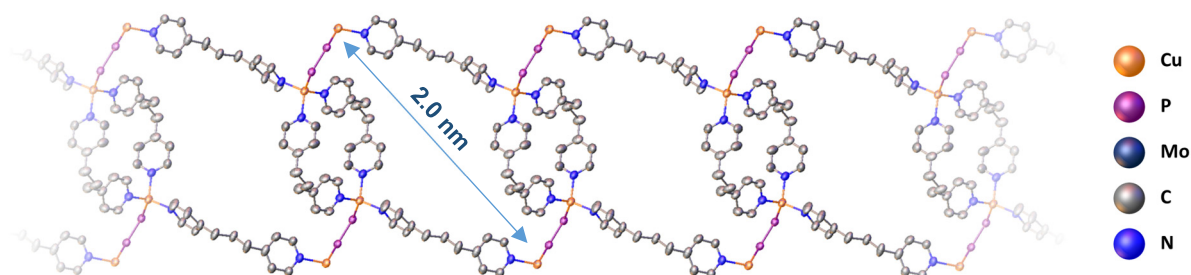


**Figure 8-13.** Sections of the one-dimensional strand of **8-9** in the solid-state. Cp- and CO-ligands, hydrogen atoms, anions and solvent molecules are omitted for clarity. Thermal ellipsoids are shown at 50 % probability level.<sup>[1]</sup>

Based on this 1D strand, there are two positions on one Cu(I) at each  $\text{Cu}_2\text{P}_2$  node not yet occupied. Each of those positions is occupied by linker molecules which each connects to a further one-dimensional pipe-like strand, leading to the three-dimensionality of the CP (**Figure 8-14**).

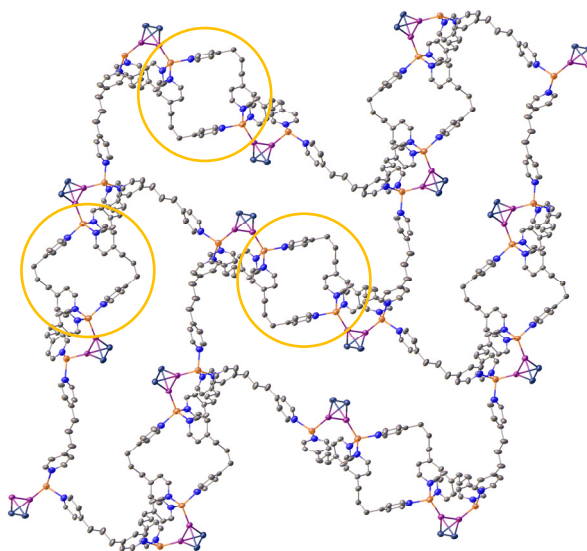
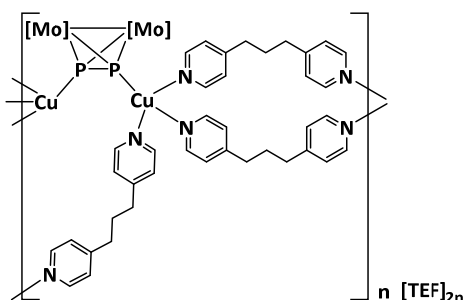


**Figure 8-14.** Sections of the molecular structure of cationic 3D-network of **8-9** in the solid-state, showing the one-dimensional 'pipes' (orange circles) and how they're connected to each other. Cp- and CO-ligands, hydrogen atoms, anions and solvent molecules are omitted for clarity. Thermal ellipsoids are shown at 50 % probability level.

Experimental procedure:



Compound **A** (2 eq., 50 mg, 0.1 mmol), **C** (1 eq., 59 mg, 0.05 mmol) and **L<sub>flex</sub>1** (1 eq., 9.9 mg, 0.05 mmol) were each dissolved in dichloromethane (20, 10 and 10 mL, respectively). The solution of **C** was slowly added to the solution of **A** and the mixture was stirred for 1h. The solution of **L<sub>flex</sub>1** was added slowly, whereupon the reaction turned from a clear red to a turbid orange solution. Acetonitrile (2 mL) was added to clear the mixture and the reaction was stirred overnight. After filtration, the mixture was layered with *n*-pentane. After one day, compound **4-5** was obtained as clear orange blocks. After performing single crystal X-ray analysis of **4-5**, which was accompanied by exposure to air and evaporation of solvent leading to a very concentrated solution, a second sort of crystals (compound **8-9**) formed after storage at r.t. for one week. The supernatant was decanted off, the remaining crystals washed with *n*-pentane and dried in vacuo. Crystalline Yield: A few crystals (< 5%).

## 8.2 Crystallographic Data

**Crystal Structure Analysis:** The crystals were selected and measured on a Gemini Ultra diffractometer equipped with an AtlasS2 CCD detector (**8-1**, **8-2** and **8-4** to **8-8**) or on a GV50 diffractometer equipped with a TitanS2 CCD detector (**8-3** and **8-9**), respectively. The crystals were kept at  $T = 123(1)$  K during data collection. Data collection and reduction were performed with **CrysAlisPro** [Version 171.39.37b, 2017 (**8-3**, **8-4** and **8-6** to **8-9**), 171.40.14a, 2018 (**8-1**, **8-2**, **8-5**, **8-7** and **8-8**)].<sup>[7]</sup> For compounds **8-1**, **8-2** and **8-4** to **8-9**, an analytical numeric absorption correction using a multifaceted crystal model based on expressions derived by R.C. Clark & J.S. Reid<sup>[8]</sup> and an empirical absorption correction using spherical harmonics as implemented in SCALE3 ABSPACK was applied. For compound **8-3**, a numerical absorption correction based on gaussian integration over a multifaceted crystal model and an empirical absorption correction using spherical harmonics as implemented in SCALE3 ABSPACK was applied. Using **Olex2**,<sup>[9]</sup> the structures were solved with **ShelXT**<sup>[10]</sup> and a least-square refinement on  $F^2$  was carried out with **ShelXL**<sup>[11]</sup> for all structures. All non-hydrogen atoms were refined anisotropically. Hydrogen atoms at the carbon atoms were located in idealised positions and refined isotropically according to the riding model.

**Compound 8-1:** The asymmetric unit contains 1 CH<sub>2</sub>Cl<sub>2</sub> solvent molecule, which was heavily disordered. Therefore, a solvent mask was calculated, and 384 electrons were found in a volume of 1856 Å<sup>3</sup> in one void per unit cell. This is consistent with the presence of one CH<sub>2</sub>Cl<sub>2</sub> molecule per asymmetric unit, which account for 336 electrons per unit cell. Further, the asymmetric unit contains a C<sub>16</sub>H<sub>12</sub>N<sub>2</sub> linker molecule, two acetonitrile molecules coordinated to two half occupied Cu atoms located on special positions and one [Al{OC(CF<sub>3</sub>)<sub>3</sub>}<sub>4</sub>] anion. Two of the C(CF<sub>3</sub>)<sub>3</sub> groups of the anion are disordered over two positions (79:21, 77:23). To describe this disorder the restraints SADI and SIMU were applied. Additionally compound **8-1** was refined as a two-component inversion twin.

**Compound 8-2:** The asymmetric unit contains 0.7 CH<sub>2</sub>Cl<sub>2</sub> solvent molecules, two BF<sub>4</sub> anions and the complex  $\{[\text{Cp}_2\text{Mo}_2(\text{CO})_4(\mu_4, \eta^{2:2:2:1}\text{-P}_2)]\{[\text{Cp}_2\text{Mo}_2(\text{CO})_4(\mu_4, \eta^{2:2:1:1}\text{-P}_2)]\{[\text{Cp}_2\text{Mo}_2(\text{CO})_3(\mu_4, \eta^{2:2:2:1}\text{-P}_2)]\}\text{-Cu}_2(\text{NCCH}_3)_2\}$ . One of the BF<sub>4</sub> anions is disordered over two positions (66:34). The SIMU restraint was used to describe this disorder.

**Compound 8-3:** The asymmetric unit contains one CH<sub>3</sub>CN and one CH<sub>2</sub>Cl<sub>2</sub> solvent molecule. The CH<sub>2</sub>Cl<sub>2</sub> molecule is heavily disordered and therefore a solvent mask was calculated, and 168 electrons were found in a volume of 808 Å<sup>3</sup> in 3 voids per unit cell. This is consistent with the presence of 0.2 CH<sub>2</sub>Cl<sub>2</sub> and 0.8 CH<sub>2</sub>Cl<sub>2</sub> per asymmetric unit, which accounts for 168 electrons per unit cell. The asymmetric unit further contains two [FAl{O(C<sub>6</sub>F<sub>10</sub>)(C<sub>6</sub>F<sub>5</sub>)<sub>3</sub>}] anions, two C<sub>13</sub>H<sub>14</sub>N<sub>2</sub> linker molecules, two Cu atoms and two times the complex [Cp<sub>2</sub>Mo<sub>2</sub>(CO)<sub>4</sub>(P<sub>2</sub>)]. The two linker molecules, one Cu atom and one [Cp<sub>2</sub>Mo<sub>2</sub>(CO)<sub>4</sub>(P<sub>2</sub>)] complex are disordered over two positions (76:24, 64:36). Additionally, the CH<sub>3</sub>CN solvent molecule is also disordered over two positions (67:33). To describe the disorder the restraints SADI, ISOR, RIGU and SIMU were applied.

**Compound 8-4:** The asymmetric unit contains one CH<sub>2</sub>Cl<sub>2</sub> solvent molecule, two [FAl{O(C<sub>6</sub>F<sub>10</sub>)(C<sub>6</sub>F<sub>5</sub>)<sub>3</sub>}] anions, one C<sub>13</sub>H<sub>14</sub>N<sub>2</sub> linker molecule, two Cu atoms, two times the complex [Cp<sub>2</sub>Mo<sub>2</sub>(CO)<sub>4</sub>(P<sub>2</sub>)] and two coordinated CH<sub>3</sub>CN molecules.

Compound **8-5**: The asymmetric unit contains in total 0.97 CH<sub>3</sub>CN and 1.03 CH<sub>2</sub>Cl<sub>2</sub> solvent molecules, which occupy the same positions in a ratio of 37:63 and 60:40 respectively. Further the asymmetric unit contains the anion [BF<sub>2</sub>{O(C<sub>6</sub>F<sub>10</sub>)(C<sub>6</sub>F<sub>5</sub>)}<sub>2</sub>], the complex [Cp<sub>2</sub>Mo<sub>2</sub>(CO)<sub>4</sub>(P<sub>2</sub>)] and two times half the linker molecule (C<sub>12</sub>H<sub>12</sub>N<sub>2</sub>). The restraints DFIX, SADI, ISOR and SIMU were applied to describe the mixed positions of the solvent molecules.

Compound **8-6**: The asymmetric unit contains 3.62 CH<sub>3</sub>CN and 4.38 CH<sub>2</sub>Cl<sub>2</sub> solvent molecules. Only 2.63 CH<sub>3</sub>CN and 0.38 CH<sub>2</sub>Cl<sub>2</sub> solvent molecules could be modelled. The other solvent molecules were heavily disordered. Therefore, a solvent mask was calculated, and 385 electrons were found in a volume of 1899 Å<sup>3</sup> in one void per unit cell. This is consistent with the presence of 4 CH<sub>2</sub>Cl<sub>2</sub> and one CH<sub>3</sub>CN molecules per asymmetric unit, which account for 380 electrons per unit cell. The asymmetric unit further contains two Cu atoms, three linker molecules (C<sub>16</sub>H<sub>12</sub>N<sub>2</sub>), two [BF<sub>2</sub>{O(C<sub>6</sub>F<sub>10</sub>)(C<sub>6</sub>F<sub>5</sub>)}<sub>2</sub>] anions and the complex [Cp<sub>2</sub>Mo<sub>2</sub>(CO)<sub>4</sub>(P<sub>2</sub>)]. The DFIX and SIMU restraints were applied to describe the mixed positions of a CH<sub>2</sub>Cl<sub>2</sub> and a CH<sub>3</sub>CN molecule.

Compound **8-7**: The asymmetric unit contains two CH<sub>2</sub>Cl<sub>2</sub> and two toluene solvent molecules. However only one toluene molecule could be modelled with a disorder over two positions (53:47). The other solvent molecules were heavily disordered over several positions. Therefore, a solvent mask was calculated, and 121 electrons were found in a volume of 560 Å<sup>3</sup> in one void per unit cell. This is consistent with the presence of two CH<sub>2</sub>Cl<sub>2</sub> and one toluene molecule per asymmetric unit, which account for 268 electrons per unit cell. Further the asymmetric unit contains a [FAl{O(C<sub>6</sub>F<sub>10</sub>)(C<sub>6</sub>F<sub>5</sub>)}<sub>3</sub>] anion, the linker (C<sub>16</sub>H<sub>12</sub>N<sub>2</sub>), a Cu atom and the complex [Cp<sub>2</sub>Mo<sub>2</sub>(CO)<sub>4</sub>(P<sub>2</sub>)]. The SIMU restraint was used to model the disorder of the toluene molecule.

Compound **8-8**: The asymmetric unit contains 0.5 CH<sub>3</sub>CN, 1.5 CH<sub>2</sub>Cl<sub>2</sub> and 1.5 C<sub>7</sub>H<sub>8</sub> solvent molecules, which are partly disordered over several positions. Further it contains three linker molecules (C<sub>16</sub>H<sub>12</sub>N<sub>2</sub>), two [FAl{O(C<sub>6</sub>F<sub>10</sub>)(C<sub>6</sub>F<sub>5</sub>)}<sub>3</sub>] anions, two Cu atoms and the complex [Cp<sub>2</sub>Mo<sub>2</sub>(CO)<sub>4</sub>(P<sub>2</sub>)]. The DFIX, SADI and SIMU restraints were applied to model the disorder of the solvent molecules.

Compound **8-9**: The asymmetric unit contains 1.5 CH<sub>2</sub>Cl<sub>2</sub> solvent molecules, which were heavily disordered. Therefore, a solvent mask was calculated, and 244 electrons were found in a volume of 996 Å<sup>3</sup> in two voids per unit cell. This is consistent with the presence of 1.5 CH<sub>2</sub>Cl<sub>2</sub> per asymmetric unit, which account for 252 electrons per unit cell. The asymmetric unit further contains three linker molecules (C<sub>13</sub>H<sub>14</sub>N<sub>2</sub>), two Cu atoms, the complex [Cp<sub>2</sub>Mo<sub>2</sub>(CO)<sub>4</sub>(P<sub>2</sub>)] and two [Al{OC(CF<sub>3</sub>)<sub>3</sub>}<sub>4</sub>] anions. Seven OC(CF<sub>3</sub>)<sub>3</sub> groups of these anions are heavily disordered over two or three positions. Additionally two of the linker molecules show minor disorder (54:46; 58:42). The restraints SADI, DANG and SIMU were applied to model these disorders.

**Table 8-1.** Crystallographic data and details of diffraction experiments for compounds **8-1-8-3**.

<b>Compound</b>	<b>8-1 · CH<sub>2</sub>Cl<sub>2</sub></b>	<b>8-2 · 0.7 CH<sub>2</sub>Cl<sub>2</sub></b>	<b>8-3 · 1 CH<sub>3</sub>CN · CH<sub>2</sub>Cl<sub>2</sub></b>
Data set (internal naming)	<b>abs422d</b>	<b>abs444a</b>	<b>abs285</b>
Formula	AlC <sub>37</sub> Cl <sub>2</sub> CuF <sub>36</sub> H <sub>20</sub> N <sub>4</sub> O <sub>4</sub>	C <sub>45.7</sub> H <sub>37.4</sub> B <sub>2</sub> Cl <sub>1.4</sub> Cu <sub>2</sub> F <sub>8</sub> Mo <sub>6</sub> N <sub>2</sub> O <sub>11</sub> P <sub>6</sub>	Al <sub>2</sub> C <sub>129</sub> Cl <sub>2</sub> Cu <sub>2</sub> F <sub>92</sub> H <sub>53</sub> Mo <sub>4</sub> N <sub>5</sub> O <sub>14</sub> P <sub>4</sub>
<i>D</i> <sub>calc.</sub> / g cm <sup>-3</sup>	1.754	2.102	1.958
$\mu$ /mm <sup>-1</sup>	0.684	13.469	5.470
Formula Weight	1429.99	1902.36	4404.34
Colour	clear light yellow	metallic dark black	orange
Shape	block	block	block
Size/mm <sup>3</sup>	0.65×0.51×0.38	0.53×0.33×0.13	0.27×0.16×0.14
<i>T</i> /K	123(1)	123(1)	122.9(2)
Crystal System	tetragonal	triclinic	monoclinic
Space Group	<i>P</i> 4 <sub>2</sub> <i>bc</i>	<i>P</i> $\bar{1}$	<i>P</i> 2 <sub>1</sub> / <i>c</i>
<i>a</i> /Å	23.0858(8)	10.4832(2)	23.37750(10)
<i>b</i> /Å	23.0858(8)	14.0398(3)	18.72780(10)
<i>c</i> /Å	20.3215(10)	21.8696(4)	35.3129(2)
<i>a</i> °	90	96.310(2)	90
<i>b</i> °	90	93.631(2)	104.8700(10)
<i>g</i> °	90	109.103(2)	90
<i>V</i> /Å <sup>3</sup>	10830.4(9)	3006.19(11)	14942.55(15)
<i>Z</i>	8	2	4
<i>Z</i> '	1	1	1
Wavelength/Å	0.71073	1.54184	1.54184
Radiation type	MoK $\alpha$	CuK $\alpha$	CuK $\alpha$
<i>Q</i> <sub>min</sub> /°	3.336	3.364	3.504
<i>Q</i> <sub>max</sub> /°	32.319	72.901	75.173
Measured Refl.	33836	32544	57258
Independent Refl.	13324	11621	29402
Reflections with <i>I</i> > 2( <i>I</i> )	8427	11350	27012
<i>R</i> <sub>int</sub>	0.0369	0.0403	0.0230
Parameters	961	805	2679
Restraints	784	78	949
Largest Peak	0.265	1.200	0.701
Deepest Hole	-0.346	-0.683	-1.720
GooF	1.007	1.048	1.027
<i>wR</i> <sub>2</sub> (all data)	0.1161	0.0776	0.0850
<i>wR</i> <sub>2</sub>	0.1009	0.0769	0.0830
<i>R</i> <sub>1</sub> (all data)	0.0833	0.0318	0.0351
<i>R</i> <sub>1</sub>	0.0457	0.0309	0.0323

**Table 8-2.** Crystallographic data and details of diffraction experiments for compounds **8-4-8-6**.

<b>Compound</b>	<b>8-4 · CH<sub>2</sub>Cl<sub>2</sub></b>	<b>8-5 · 0.97 CH<sub>3</sub>CN · 1.03 CH<sub>2</sub>Cl<sub>2</sub></b>	<b>8-6 · 3.62 CH<sub>3</sub>CN · 4.38 CH<sub>2</sub>Cl<sub>2</sub></b>
Data set (internal naming)	<b>abs408b_1D</b>	<b>abs448b</b>	<b>abs421d</b>
Formula	C <sub>118</sub> H <sub>42</sub> Al <sub>2</sub> Cl <sub>2</sub> Cu <sub>2</sub> F <sub>92</sub> Mo <sub>4</sub> N <sub>4</sub> O <sub>14</sub> P <sub>4</sub>	C <sub>52.97</sub> H <sub>26.97</sub> BCl <sub>2.06</sub> Cu F <sub>32</sub> Mo <sub>2</sub> N <sub>2.97</sub> O <sub>6</sub> P <sub>2</sub>	B <sub>2</sub> C <sub>121.62</sub> Cl <sub>8.76</sub> Cu <sub>2</sub> F <sub>64</sub> H <sub>65.62</sub> Mo <sub>2</sub> N <sub>9.62</sub> O <sub>8</sub> P <sub>2</sub>
<i>D</i> <sub>calc.</sub> / g cm <sup>-3</sup>	2.012	1.955	1.630
<i>μ</i> /mm <sup>-1</sup>	0.927	6.400	0.748
Formula Weight	4247.13	1810.16	3718.99
Colour	clear orange	clear orange	orange
Shape	block	block	block
Size/mm <sup>3</sup>	0.56×0.38×0.20	0.15×0.12×0.08	0.53×0.33×0.26
<i>T</i> /K	123(2)	123(1)	123.15
Crystal System	monoclinic	triclinic	triclinic
Space Group	<i>P</i> <sub>2</sub> <sub>1</sub> / <i>c</i>	<i>P</i> $\bar{1}$	<i>P</i> $\bar{1}$
<i>a</i> /Å	29.5837(6)	13.58200(10)	17.6762(3)
<i>b</i> /Å	18.9240(4)	16.7524(2)	19.8376(3)
<i>c</i> /Å	25.7345(6)	16.89670(10)	22.7687(4)
<i>a</i> <sup>o</sup>	90	116.4840(10)	72.009(2)
<i>b</i> <sup>o</sup>	103.356(2)	95.3410(10)	89.7210(10)
<i>g</i> <sup>o</sup>	90	110.5930(10)	86.4510(10)
<i>V</i> /Å <sup>3</sup>	14017.6(5)	3074.54(6)	7578.1(2)
<i>Z</i>	4	2	2
<i>Z</i> '	1	1	1
Wavelength/Å	0.71073	1.54184	0.71073
Radiation type	MoK <sub>α</sub>	CuK <sub>α</sub>	MoK <sub>α</sub>
<i>Q</i> <sub>min</sub> <sup>o</sup>	3.345	3.284	3.246
<i>Q</i> <sub>max</sub> <sup>o</sup>	29.604	66.027	32.569
Measured Refl.	98438	39186	91203
Independent Refl.	33253	10655	46909
Reflections with <i>I</i> > 2( <i>I</i> )	27191	9983	35669
<i>R</i> <sub>int</sub>	0.0277	0.0261	0.0303
Parameters	2181	1002	1877
Restraints	0	227	71
Largest Peak	1.253	0.876	1.140
Deepest Hole	-0.851	-0.405	-0.593
GooF	1.054	1.016	1.016
<i>wR</i> <sub>2</sub> (all data)	0.1017	0.0554	0.1079
<i>wR</i> <sub>2</sub>	0.0945	0.0543	0.1005
<i>R</i> <sub>1</sub> (all data)	0.0529	0.0244	0.0629
<i>R</i> <sub>1</sub>	0.0396	0.0223	0.0454



**Table 8-3.** Crystallographic data and details of diffraction experiments for compounds **8-8-8-9**.

<b>Compound</b>	<b>8-7</b> · 2 CH <sub>2</sub> Cl <sub>2</sub> · 2 C <sub>7</sub> H <sub>8</sub>	<b>8-8</b> · 0.5 CH <sub>3</sub> CN · 1.5 CH <sub>2</sub> Cl <sub>2</sub> · 1.5 C <sub>7</sub> H <sub>8</sub>	<b>8-9</b> · 1.5 CH <sub>2</sub> Cl <sub>2</sub>
Data set (internal naming)	<b>abs441b</b>	<b>abs441c</b>	<b>abs273_3D</b>
Formula	AlC <sub>82</sub> Cl <sub>4</sub> CuF <sub>46</sub> H <sub>42</sub> Mo <sub>2</sub> N <sub>2</sub> O <sub>7</sub> P <sub>2</sub>	C <sub>147</sub> H <sub>62.8</sub> Al <sub>2</sub> Cl <sub>3</sub> Cu <sub>2</sub> F <sub>92</sub> Mo <sub>2</sub> N <sub>6.5</sub> O <sub>10</sub> P <sub>2</sub>	Al <sub>2</sub> C <sub>86.5</sub> Cl <sub>3</sub> Cu <sub>2</sub> F <sub>72</sub> H <sub>55</sub> Mo <sub>2</sub> N <sub>6</sub> O <sub>12</sub> P <sub>2</sub>
<i>D</i> <sub>calc.</sub> / g cm <sup>-3</sup>	1.785	1.852	1.847
<i>μ</i> /mm <sup>-1</sup>	0.789	0.679	4.727
Formula Weight	2527.31	4369.04	3279.57
Colour	orange	clear light orange	orange
Shape	block	block	block
Size/mm <sup>3</sup>	0.39×0.28×0.26	0.47×0.39×0.28	0.69×0.12×0.07
<i>T</i> /K	123(1)	123.15	172.98(15)
Crystal System	triclinic	monoclinic	monoclinic
Space Group	<i>P</i> $\bar{1}$	<i>P</i> 2 <sub>1</sub> / <i>c</i>	<i>P</i> 2 <sub>1</sub> / <i>c</i>
<i>a</i> /Å	17.9781(4)	19.8140(2)	15.4342(3)
<i>b</i> /Å	18.8054(3)	35.0926(3)	36.9634(5)
<i>c</i> /Å	18.8772(3)	22.5404(2)	21.6999(4)
<i>a</i> <sup>o</sup>	94.654(2)	90	90
<i>b</i> <sup>o</sup>	117.764(2)	91.6640(10)	107.6505(19)
<i>g</i> <sup>o</sup>	116.545(2)	90	90
<i>V</i> /Å <sup>3</sup>	4702.50(18)	15666.3(2)	11797.0(4)
<i>Z</i>	2	4	4
<i>Z</i> '	1	1	1
Wavelength/Å	0.71073	0.71073	1.54184
Radiation type	MoK <sub>α</sub>	MoK <sub>α</sub>	CuK <sub>α</sub>
<i>Q</i> <sub>min</sub> <sup>o</sup>	3.319	3.243	3.337
<i>Q</i> <sub>max</sub> <sup>o</sup>	29.461	32.354	74.161
Measured Refl.	70641	290922	48432
Independent Refl.	22677	52934	22866
Reflections with <i>I</i> > 2( <i>I</i> )	19187	42647	16739
<i>R</i> <sub>int</sub>	0.0279	0.0356	0.0585
Parameters	1273	2644	2684
Restraints	192	360	4205
Largest Peak	0.393	0.504	1.121
Deepest Hole	-0.321	-0.842	-1.270
GooF	1.019	0.935	1.052
<i>wR</i> <sub>2</sub> (all data)	0.0695	0.1303	0.2414
<i>wR</i> <sub>2</sub>	0.0665	0.1172	0.2218
<i>R</i> <sub>1</sub> (all data)	0.0382	0.0517	0.1034
<i>R</i> <sub>1</sub>	0.0297	0.0366	0.0807

### 8.3 References

- [1] The cavity sizes of the CPs are calculated by subtracting the sum of the *van-der-Waals*-radii of Cu (1.7 Å)\* from the Cu-Cu-distances obtained from the X-ray experiment. \*N. Wiberg, A. F. Hollemann *Hollemann, Wiberg – Lehrbuch der Anorganischen Chemie* **2007**, 102<sup>nd</sup> Edition: de Gruyter Berlin.
- [2] P. Pyykkö, M. Atsumi *Chem. Eur. J.* **2009**, *15*, 12770-12779.
- [3] a) M. Scheer, L. J. Gregoriades, M. Zabel, J. Bai, I. Krossing, G. Brunklaus, H. Eckert *Chem. Eur. J.* **2008**, *14*, 282-295; b) M. E. Moussa, M. Piesch, M. Fleischmann, A. Schreiner, M. Seidl, M. Scheer *Dalton Trans.* **2018**, 47, 16031-16035; c) M. E. Moussa, M. Fleischmann, E. V. Peresypkina, L. Dütsch, M. Seidl, G. Balázs, M. Scheer *Eur. J. Inorg. Chem.* **2017**, 3222-3226.
- [4] M. Fleischmann, S. Welsch, E. V. Peresypkina, A. V. Virovets, M. Scheer *Chemistry* **2015**, *21*, 14332-14336.
- [5] B. Attenberger, S. Welsch, M. Zabel, E. Peresypkina, M. Scheer *Angew. Chem. Int. Ed.* **2011**, *50*, 11516-11519.
- [6] B. Attenberger, E. V. Peresypkina, M. Scheer *Inorg. Chem.* **2015**, *54*, 7021-7029.
- [7] CrysAlisPro Software System, Rigaku Oxford Diffraction, (2018).
- [8] Clark, R. C. & Reid, J. S. *Acta Cryst.* **1995**, *A51*, 887-897.
- [9] O.V. Dolomanov, L.J. Bourhis, R.J. Gildea, J.A.K. Howard, H. Puschmann, Olex2: A complete structure solution, refinement and analysis program, *J. Appl. Cryst.* **2009**, *42*, 339-341.
- [10] Sheldrick, G.M., ShelXT-Integrated space-group and crystal-structure determination, *Acta Cryst.* **2015**, *A71*, 3-8.5.G.
- [11] M. Sheldrick, Crystal structure refinement with ShelXL, *Acta Cryst.* **2015**, *C27*, 3-8.

## 9 Appendix

### 9.1 Thematic List of Abbreviations

NMR	
NMR	Nuclear Magnetic Resonance
s	singlet
d	doublet
Hz	Hertz, s <sup>-1</sup>
ppm	parts per million
δ	chemical shift

NMR Mass Spectrometry	
MS	mass spectrometry
[M] <sup>+</sup>	molecular ion peak
m/z	mass to charge ratio
ESI	electron spray ionisation

Weakly Coordinating Anions	
FAI	[FAI{O(C <sub>6</sub> F <sub>10</sub> )(C <sub>6</sub> F <sub>5</sub> ) <sub>3</sub> } <sub>3</sub> ] <sup>-</sup>
TEF	[Al{OC(CF <sub>3</sub> ) <sub>3</sub> } <sub>4</sub> ] <sup>-</sup>

Solvents	
CH <sub>2</sub> Cl <sub>2</sub>	dichloromethane
CH <sub>3</sub> CN	acetonitrile

Organic Linkers	
<b>bipy</b>	4,4'-bipyridine
<b>L<sub>lin</sub>2</b>	1,2-di(pyridin-4-yl)ethyne
<b>L<sub>lin</sub>3</b>	1,4-di(4-pyridyl)benzene
<b>L<sub>lin</sub>4</b>	4,4'-di(4-pyridyl)biphenyl
<b>L<sub>flex</sub>1</b>	1,3-bis(4-pyridyl)propane
<b>L<sub>flex</sub>2</b>	1,2-bis(4-pyridyl)ethane
<b>dpe</b>	trans-1,2-di(pyridine-4-yl)-ethene

Other (in alphabetic order)	
∠	angle
Å	Ångström, 1 Å = 1 · 10 <sup>-10</sup> m
Cp	cyclopentadienyl, η <sup>5</sup> -C <sub>5</sub> H <sub>5</sub>
CP	Coordination Polymer
° C	degree Celsius
DFT	density functional theory
<i>d</i>	distance
eq.	equivalents
mg	milligram
mL	millilitre
MOF	Metal-Organic Framework
r.t.	room temperature
T	temperature
WCA	weakly coordinating anion

## 9.2 Acknowledgements

At the end, I would like to thank the following people for their support:

**Prof. Dr. Manfred Scheer** for the opportunity to work in this group under splendid working conditions, his confidence in my work and the great research topic.

**Dr. Michael Seidl** for supporting the X-ray measurements, the refinement and finalisation of the structures, for proof-reading and his helpfulness in all matters.

**Dr. Gábor Balázs** for performing the DFT calculations and for the fun get-togethers outside of the laboratory.

My cooperation partners **Jana Schiller** and **Mehdi Elsayed Moussa**

The members of the departments of the **central analytics** (NMR, MS, EA and X-ray) and the **workshops** (glassblowers, precision mechanics and electronic technicians).

All other former and current members of the **Scheer group**, especially the following:

**Dani a.k.a.** 'liebste Lieblings-Dani, Herrin des Universums und der ganzen Welt' for her friendship and support. Thank you for all the good times we had and will have watching anime, cooking, eating Sushi, talking, doing Yoga and all the amazing hugs!

**Anna**, who I am happy to be able to call not only a very good colleague but also a dear friend.

**Helena**, who was always there to offer valuable advice.

**Reini** for his support and motivation during the last metres, which made the difference!

**Julian** for being able to insult people though not coming across as rude. *Miststück!*

**Luis**, whose company I very much enjoyed especially during the conference in Potsdam.

**Claudia, Maria, Feli, Martin, Tobi** and **Pieschi** for having an open ear when needed and allowing me to join their lunch breaks from time to time.

(Phosphini)**Lena, Vroni, Rudi, Matze, Christoph, Nase, Kevin, Dominik, Sabrina, Robert** and everyone else who contributed to a comfortable and friendly work atmosphere!

the technical assistants **Martina, Petra, Lukas** and especially **Julian** for the early morning coffee times and **Schotti** for a great teamwork during the laboratory courses.

and last, but not least: **Eva**, whose apology was not necessary but has been accepted!

The legendary '**Mensa Gurrri!**' for the lunch and coffee breaks:

**Frauke** for her non-judgemental attitude and inspiring conversations that made me see things from a different perspective.

**Sina** for being so down to earth, her honest advices and loyalty.

**Franzi**, who changed everything by founding the legen...dary Mädelsabend and who is always great to have around.

**Moni** for simply being there and all the crazy talk: *Wieso? – Ich mag Backfisch! Eier, wir brauchen Eier! Guck ma die Geschenke an, sind die nicht supergeiiii!*

The **Regensburger Mädels** and the **Chemiker-Stammtisch** for all the get-togethers and celebrations. I would not want to have missed them!

My friends **Agnes, Tanja, Marie** and **Tobi**. Thank you for being there and lifting me up whenever I needed it.

And most importantly:

**My parents** for their financial support and unconditional love.

**My sisters** for always taking care of me.

The littlest members of our growing family, for whom I am hoping to be an inspiring role model.

‘So long, and thanks for all the fish’

– Douglas Adams,  
*‘The Ultimate Hitchhiker’s Guide to the Galaxy’*